Drill Cuttings Deposition, Produced Water, and Storage Displacement Water Dispersion Modelling for the Hebron Project

Prepared For

Stantec Consulting Ltd.
607 Torbay Road
St. John's, NL A1A 4Y6
Telephone: (709) 576-1458
Facsimile: (709) 576-2126

Prepared By

AMEC Earth & Environmental
a Division of AMEC Americas Limited
133 Crosbie Road
P.O. Box 13216
St. John's, NL A1B 4A5
Telephone: (709) 722-7023
Facsimile: (709) 722-7353

September 2010

JWSL Job #: 1053484.05 Phase A5304
AMEC Project: TN09243173

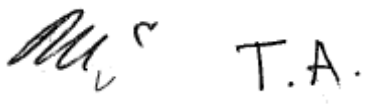
Prepared	Reviewed	Approved
		
J. McClintock, T. Alcinov	S. Donnet	B. Batstone

TABLE OF CONTENTS

1. INTRODUCTION 1
1.1 Project Background 1
1.2 Objectives 2
2. DRILL CUTTINGS DEPOSITION 2
2.1 Methods 2
2.1.1 Primary Sedimentation Model (3D) 2
2.1.1.1 Model Input 4
2.1.1.2 Well Sequences, Well Types and Scenarios 4
2.1.1.3 Cuttings Particle Characterization 6
2.1.1.4 Ocean Currents 7
2.1.1.5 Model Geometry 9
2.1.1.6 Model Algorithm 10
2.1.1.7 Model Output 11
2.1.2 Gravity Base Structure-Considered Model (one-dimensional) 11
2.1.2.1 Model Set-up and Rationale 11
2.1.2.2 Model Testing and Calibration 12
2.2 Results 13
2.2.1 Results of Primary Modelling (three-dimensional) 13
2.2.2 Results of Gravity Base Structure-Considered Modelling (one-dimensional) 17
2.3 Sensitivity Analyses 17
2.3.1 Particle Composition 18
2.3.2 Particle Settling Velocities 18
2.3.3 Ocean Current Sensitivities 19
2.3.4 Observations from the Sensitivity Runs 22
3. PRODUCED WATER DISPERSION MODELLING 25
3.1 Methods 25
3.1.1 Model Theory on Produced Water Mixing 25
3.1.2 Diffuser Configuration and Effect on Dilution 26
3.1.3 Effluent Characteristics and Effect on Dilution 28
3.1.4 Ambient Characteristics and Effect on Dilution 28
3.1.4.1 Stratification and Nascent Density Effect 28
3.1.4.2 Current 29
3.1.5 Visual Plumes and UM3 Models 30
3.1.6 Model Input 31
3.1.7 Diffuser and Effluent Discharge 31
3.1.8 Ambient Characteristics 32

3.1.8.1 Temperature, Salinity Profiles and Oceanic Stratification 32
3.1.8.2 Ocean Currents and Directions 35
3.1.8.3 Other Input Parameters 36
3.1.9 Summary of Model Scenarios and Input 36
3.2 Results 38
4. STORAGE DISPLACEMENT WATER MODELLING 48
4.1 Methods 48
4.1.1 Model Input 49
4.1.2 Diffuser and Effluent Discharge Input 49
4.1.3 Ambient Characteristics 50
4.1.4 Summary of Model Scenarios and Input 50
4.2 Results 51
4.3 Sensitivity Analyses 53
4.4 Storage Displacement Water Modelling Conclusions 55
5. REFERENCES 56
5.1 Personal Communications 56
5.2 Literature Cited 56
6. GLOSSARY / ACRONYMS 58

LIST OF APPENDICES

Appendix A Grand Banks Currents
Appendix B Drill Cuttings Deposition Model Sensitivity Results
Appendix C Grand Banks Temperature and Salinity Profiles
Appendix D Produced Water Dispersion Model Results
Appendix E Storage Displacement Water Dispersion Model Results

LIST OF FIGURES

Page No.

Figure 1-1 Hebron Project Location 1
Figure 2-1 Cuttings Deposition Following Platform Drilling, 8-km View 14
Figure 2-2 Cuttings Deposition Following Platform Drilling, 1-km View 15
Figure 2-3 Cuttings Deposition Following Platform Drilling, Grand Banks View (100 m depth contour is shown) 16
Figure 2-4 Comparison of Hebron Design and Hibernia Time-Series Near-bottom Currents 21
Figure 3-1 Produced Water Mixing Process Illustration 27
Figure 3-2 Seawater Density Diagram 30
Figure 3-3 Summer and Winter Density Profiles 35
Figure 3-4 February, 56,000 m^3/d, 52.9 psu, produced water discharge plume section profile in high (blue), average (red), and low (green) current conditions. 41
Figure 3-5 February, 56,000 m^3/d, 52.9 psu, produced water discharge plume dilution profile in high (blue), average (red), and low (green) current conditions. 42
Figure 3-6 February, 30,000 m^3/d, 32.7 psu, produced water discharge plume section profile in high (blue), average (red), and low (green) current conditions. 43
Figure 3-7 February, 56,000 m^3/d, 52.9 psu, zone of influence estimate, concentration vs. horizontal distance 44
Figure 3-8 February, 56,000 m^3/d, 52.9 psu, zone of influence estimate, concentration vs. depth ... 45
Figure 3-9 February, 56,000 m^3/d, 52.9 psu, zone of influence estimate, plume diameter vs. horizontal distance 45
Figure 4-1 Wet Naturally-pressured Storage System 48
Figure 4-2 Dilution Envelope for Storage Displacement Water Modelling 52
Figure 4-3 Sensitivity Analysis for Discharge Elevation and Temperature: August 54
Figure 4-4 Sensitivity Analysis for Discharge Elevation and Temperature: February 55

LIST OF TABLES

Page No.

Table 2-1 Drill Cuttings Volumes 5
Table 2-2 Drill Cuttings Modelling Scenarios 5
Table 2-3 Cuttings Particle Size Composition 6
Table 2-4 Time Steps for the Hebron Domain 10
Table 2-5 Comparison of Hebron Design and Hibernia Time-Series Currents 20
Table 2-6 Cuttings Deposition Summary 23
Table 3-1 Summer and Winter Ambient Temperature, Salinity and Density Profiles 34
Table 3-2 Hebron Summer and Winter Current Speed (cm/s) and Direction 36
Table 3-3 Produced Water Modelling Scenarios 37
Table 3-4 Produced Water Discharge Summary, Salinity = 52.9 psu 39
Table 3-5 Produced Water Discharge Summary, Salinity = 42, 32.7 psu 40
Table 4-1 Storage Displacement Water Modelling Scenarios 50
Table 4-2 Dilution Variation with Distance for Storage Displacement Water Modelling 51

1. Introduction

1.1 Project Background

ExxonMobil Canada Properties, on behalf of the Hebron Project Proponents, ExxonMobil Canada Properties, Chevron Canada Limited, Petro-Canada, StatoilHydro Canada Limited, and Nalcor Energy - Oil and Gas Inc., is leading the development of the Hebron Field on the Grand Banks of Newfoundland, which will be with a stand-alone concrete gravity base structure (GBS). The Hebron Asset is located in the Jeanne d'Arc Basin, 350 km southeast of St. John's, approximately 9 km north of the Terra Nova development, approximately 32 km southeast of the Hibernia development, and approximately 46 km southwest of the White Rose development (Figure 1-1). Hebron development includes seabed installation of the GBS and production drilling operations of up to approximately 52 wells to be drilled by the GBS platform rig. The productive life of the Project is currently estimated at 30 years. Additional details are presented in the *Hebron Project Description* (ExxonMobil Canada Properties, 2009).

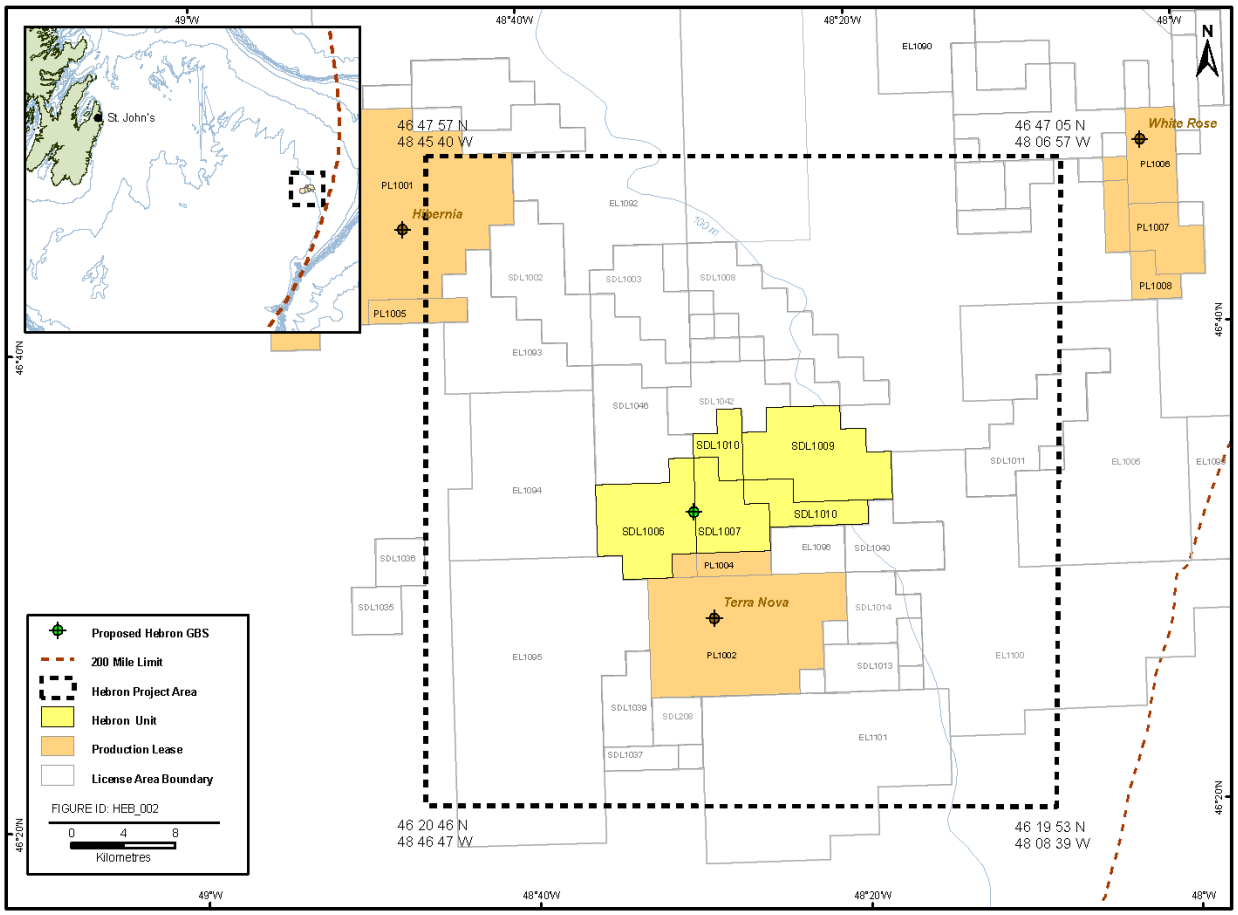


Figure 1-1 Hebron Project Location

1.2 Objectives

This report presents the results of drilling discharge dispersion fate modelling for the Hebron Project. The objectives were:

- to determine the deposition pattern of drill cuttings for life-of-Project
- to determine the seasonal pattern of produced water associated with production operations on the platform
- to determine the seasonal pattern of storage displacement water associated with production operations on the platform

It is noted that these studies are preliminary and the information will be updated as design progresses through FEED and detailed engineering.

2. Drill Cuttings Deposition

Two modelling treatments of drill cuttings deposition were considered. The primary model (Section 2.1.1) considered proposed sequences of wells to be drilled for the Project and the associated time history of cuttings discharges. The subsequent path of the discharged cuttings (with advection as a result of the ambient ocean current) to their ultimate fate on the seabed was predicted with a three-dimensional (3D) sedimentation computer model. A second one-dimensional (1D) model (Section 2.1.2) was employed to address considerations related to the presence of the Hebron GBS.

The design basis of 52 wells was selected for the modelling. For each well, cuttings from the first, conductor, section drilled with water-based muds (WBM) will be deposited inside the GBS (approximately 91 m^3 per well). Cuttings from the second, surface, section (approximately 171 m^3 per well) also drilled with water-based muds (WBM) will be discharged from one of two shale chutes in the GBS to the sea. The remaining well sections will be drilled with synthetic-based muds (SBM): associated cuttings will not be released to the sea (see Section 2.1.1.2). Associated with each well is a cuttings characteristic and discharge rate.

2.1 Methods

2.1.1 Primary Sedimentation Model (3D)

The analysis of the drill cuttings discharges was accomplished by making use of a numerical computer model developed by AMEC to determine cuttings depositions. The AMEC software ADM is written in Visual Fortran and developed based on previous corporate experience and modelling algorithms including those from the Hibernia cuttings fate modelling study (Hodgins, 1993).

To accompany the delivery of the deposition model results, a description of the model and techniques used, and observations based on the modelling activity are presented.

In the model, a transport computation was employed to simulate the advection of the dispersed drill cuttings materials in three dimensions through the water column, following release into the sea, until the particles come to rest on the sea bottom. For the purposes of predicting their physical deposition on the seabed, the cuttings were considered as a composition of four particle types or sizes: pebbles, coarse sand, medium sand, and fines. These particle sizes were generally representative of the materials encountered drilling on the Grand Banks. A key element of the modelling was knowledge of the relative proportions of these amounts for the cuttings volumes to be discharged, as well as the physical settling velocity of each. These are discussed below.

At any given time, a particle was assumed to be subject to independent displacing forces due to the ocean current and to a fall velocity that was constant for a given particle type. A term to model turbulent diffusion was added to the displacements. Over the time-step of the available ocean current data, the displacements were calculated and added to yield a new particle position. Sequential vector additions were computed over each successive time-step until the simulation terminated with deposition on the sea bottom (which may be some time after well drilling had terminated).

A model grid was selected to encompass the study area and possible domain for the deposition of the cuttings. The model tracked the fate and deposition of the particles. In addition to each particle's path, the weight of material was tracked. This was the primary particle attribute. After completion of a model run, when all particles were settled, or had reached the model grid boundaries (in which case, they were taken to have drifted outside the domain and are tabulated as 'lost'), each particle was binned in one of the model grid cells and the total weight, W was calculated. In addition, the following other parameters were calculated for each grid cell:

$$C = W \times 1000 / A \quad (1)$$

$$T = C / \gamma \quad (2)$$

where W = cuttings weight (kg)
C = cuttings density (g/m^2)
T = cuttings thickness (mm)
A = area of one grid cell (m^2)
γ = in situ bulk density (1,850 kg/m^3)

Since WBM cuttings alone, no SBM cuttings, were considered, there was no requirement for estimating oil concentrations (although this is a feature available in the software). Grid cells were given a size of 8 and 32 m for the platform drilling operations. These values were set to resolve the spatial areas

potentially to be affected (e.g., through the larger 32 m) and to provide increased resolution (e.g., 8 m) for near the platform. Therefore, A=64 and 1024 m^2 respectively.

2.1.1.1 Model Input

The basic model input was a characterization of the cuttings in terms of the following components which were assembled as digital data files for the software:

- a well sequence, defining the sequence of wells to be drilled for the given scenarios being modelled
- a well type and well duration. One generic well and associated well casing design was used. The casing design defines the depths and size of each well section to be drilled which in turn allows estimation of the associated drill cuttings anticipated to be generated, over that well duration.
- drill cuttings particle composition, which characterized the proportion of the different cuttings materials, as a function of depth, for the well type noted above
- ocean current. A time-series of representative ambient currents for predicting the advection of the particles as they are discharged to sea during drilling

The drilling and cuttings discharge for each well within the well sequence were treated as a separate model run. An option was implemented for each well to add the cuttings deposition results for that model run to those yielded following the completion of the previous well in the sequence. In this way, a cumulative cuttings deposition pattern was built up.

2.1.1.2 Well Sequences, Well Types and Scenarios

The design basis of 52 wells was selected and it was assumed that each well requiring 75 days to drill would be drilled sequentially: this corresponds to a time period of approximately 10 years and nine months.

One generic well type was considered. Table 2-1 presents the section hole size, depth (relative to GBS platform rig, i.e., first section is to depth 165 m below sea surface), length and volume of drill cuttings for the top conductor and surface well sections. For each well, cuttings from the first, 838-mm, conductor section, drilled with WBM, will be deposited inside the GBS. The second, 660-mm, surface section will also be drilled with WBM and 100% of the cuttings will be discharged from one of two shale chutes to the sea. These are the cuttings modeled in this study. This translates into approximately 4,453 m^3 of cuttings per chute following completion of 52 wells. The remaining intermediate and main deeper well sections (not detailed here) will be drilled with synthetic-based muds (SBM): associated cuttings will not be released to the sea. The Project proponents in compliance with regulatory agencies will evaluate best available cuttings management technology and practices to identify a waste

management strategy for spent Non-Aqueous Fluids (NAFs) and NAF cuttings (ExxonMobil Canada Properties, 2009).

Table 2-1 Drill Cuttings Volumes

Hole Size		Start Depth	End Depth	Hole Length	Volume per Well
Imperial (inches)	Metric (m)	(m)	(m)	(m)	(m3)
33	0.838	135	300	165	91
26	0.660	300	800	500	171

The discharge of cuttings (171 m^3 per well) was simulated to occur uniformly over a three day period at the beginning of each well, corresponding to drilling of the surface section. Discharge was assumed at approximately 20 m above sea bottom from one of two shale chutes. To provide a worst case estimate of cuttings deposition near the platform, the presence of the GBS was not considered in the primary modelling exercise (see Section 2.1.2). A total of seven modelling scenarios were considered with the key parameters for each run summarized in Table 2-2. The runs numbered 2 through 7 are sensitivity runs, discussed in Section 2.3.

Table 2-2 Drill Cuttings Modelling Scenarios

Run #	Scenario ID [1]	Drilling Platform	Drilling Sequence	Mud Type [2]	Discharge Location	Cuttings Particle Composition	Particle Settling Velocties	% Cuttings Released	Currents	dxy (m) [3]	500-m View	8-km View	Grand Banks View
1	He0	Platform	52 wells [2]	WBM	Two shale chutes of GBS: 20 m above seabed	near-surface for Surface est. from Hibernia K-18	Sleath (1984)	100%	Hibernia Time-Series (HTS)	8, 32	X	X	X
2	HeMF					more fines					X	X	
3	HeLF					less fines					X	X	
4	HeC67								HTS * 0.67 ("Hebron Design") 4		X	X	
5	HeC133								HTS * 1.33		X	X	
6	HeFF						Fast settling velocity for fines				X	X	
7	He90d		52 wells @ 90 day well duration								X	X	

Notes: 1. Sensitivity runs, 2 to 7 use same model input as in the original base case run 1 except where noted.
2. From Platform, 52 wells (WBM-drilled surface sections are only cuttings released to sea), 75 day well duration
3. Model domain for grid cell size, dxy, of 8 and 32 m is +/-2 and +/-8 km respectively.
4. See Section 2.3.3 Ocean Current Sensitivities.

2.1.1.3 Cuttings Particle Characterization

No cuttings particle size distributions that would quantify the composition of different mineral materials as a function of depth are available from the Hebron exploratory wells. Information for the nearby Hibernia K-18 well is available (from a sieve analysis performed by AGAT Laboratories, 1993) though this details depths of 1000 m and greater.

For the present application and the surface well section to be drilled at depths of approximately 165 to 665 m, a particle composition as presented in Table 2-3 was assumed. Two additional percentage compositions were estimated, as presented in Table 2-3 and discussed in Section 2.3.1.

Table 2-3 Cuttings Particle Size Composition

Well Type/Section	Measured Weight Percent Mineral			
	Pebble	Coarse Sand	Medium Sand	Fines
Surface Section drilled with WBM				
Base Case	7	4	1	88
Less Fines Sensitivity	14	8	2	76
More Fines Sensitivity	3	2	1	94

It is assumed that the cuttings will enter the sea in a disaggregated form. The model considered the pebble and sand materials to remain disaggregated in their fall to the seabed. Fines were assumed to aggregate into flocs of size on the order of about 0.1 mm and settle with a constant speed.

Particle fall velocities, *w*, were estimated from the particle diameter using the following relationships from Sleath (1984):

$$w = 4.2\sqrt{D}, D > 0.0001m \quad (4)$$

$$w = 12x10^{4} D^{2}, D \leq 0.0001m \quad (5)$$

where w is the fall velocity in m/s and *D* is the diameter in m.

For the four particle types considered, this yields the following values:

	Cuttings Material			
	pebbles	coarse sand	medium sand	fines
particle diameter (mm)	7	1	0.25	0.1
particle fall velocity (m/s)	0.351	0.133	0.066	0.0012

2.1.1.4 Ocean Currents

Together with particle settling velocities, horizontal current was the other key factor in determining how far cuttings may potentially be dispersed, so it was important to employ a good characterization of the local current behaviour as a driving force for the model. It was essential that any current information be representative of the drilling location site and its surroundings, and that the data be available in the form of long time-series (ideally, several years to span the scenario well sequences) of current speed and direction pairs, and regularly spaced in time (hourly, three-hourly, six-hourly, etc.). Since the cuttings will settle through the water column, a characterization of the currents as a function of depth was also required.

The temporal coverage of the current data record was important in allowing application of the drilling well sequences and it also dictated the statistical reliability of conclusions drawn from analysis of the current data. The regularity of time spacing was essential due to the structure of the advection calculations in the model.

Hibernia Five-Year Time-Series

The Hibernia five-year time-series of wind, wave, and currents (Dal Santo, 1986) was assembled for the Hibernia region. These time-series incorporate both measured and estimated data. The ocean current time-series was assembled separately for each of three depths, near-surface (approximately 20 m), mid-depth (approximately 40 m), and near-bottom (approximately 60 m). Hourly speed and direction values were extracted from available well-site measurements and gaps were filled with estimates of three current components to yield a complete five-year (1980 to 1984) time-series at each depth. The three components are the tidal component, the inertial component, and the low frequency component.

In a comparison of currents at Hibernia (including measurements from the five-year time-series) with those at Terra Nova during compilation of the *Physical Environmental Data for Production Systems at Terra Nova* report (Seaconsult, 1988), the authors concluded that:

1) *"Directional distributions will be altered somewhat from the true distributions, but not to a great extent since directional flow preferences are weak;*
2) *current speed distributions for near-surface flows will be unbiased by incorporating Hibernia data; and*
3) *current speed distributions at mid-depth and near-bottom levels will be biased high by incorporating Hibernia data.*

   Use of the composite data set is justified in terms of providing increased reliability for modelling the current variability, and for providing extreme speed estimates on the safe side at all depths."

While it is acknowledged the Hibernia currents may not be the most representative for this application, e.g., point 3) noted above, since at 20 m it is the near-bottom currents that will be employed, the proximity of Hebron to Terra Nova, and Hibernia, and the utility of the five-year duration and its' one-hour spacing of the time-series are positive attributes to consider. Together with the recognition that current speed sensitivities are employed in this modelling, and the absence of any readily accessible alternative data sources, the Hibernia time-series is an appropriate selection for use in the cuttings deposition model.

Grand Banks Current Summary

Monthly statistics for near-surface, mid-depth, and near-bottom current speed, from the Hibernia time-series are presented in tabular format in Appendix A. Near-surface currents range, on average, from 14 cm/s in May through July to 20 to 21 cm/s in the winter. Maximum currents of 114 cm/s in April and 127 cm/s in September are reported. The 95 percent upper limit current is 37 cm/s annually, ranging from 27 cm/s in May to 45 cm/s in November.

Mid-depth currents range, on average, from 11 cm/s in June to 20 cm/s in December. Maximum currents range from highs of 119 cm/s in November and 78 cm/s in December, to a low of 38 cm/s in May. The 95 percent upper limit current is 29 cm/s annually, and ranges from 22 cm/s in May to 37 cm/s in December.

Near-bottom currents range on average, from 11 cm/s in May through August, to 14 to 15 cm/s in winter. Maximum currents range from highs of 72 cm/s in November and 57 cm/s in December and February, to a low of 30 cm/s in April. The 95 percent upper limit current is 24 cm/s annually, and ranges from 20 to 21 cm/s in spring and summer to 26 to 29 cm/s in winter.

Monthly bivariate current speed vs. current direction tables are also provided in Appendix A. These illustrate the distribution of current speed with direction. On an annual basis, approximately 1 percent of currents exceed 50 cm/s at near-surface, 1 percent exceed approximately 38 cm/s at mid-depth, and 1 percent exceed approximately 32 cm/s near-bottom. At all depths, and for most months, the predominant current direction is to the southwest (frequently 20 percent of the time or greater). Currents to the southeast through west are also common (approximately 10 to 20 percent of the time): directions to the north and northwest and generally least frequent (typically less than 10 percent of the time). These observations from the Hibernia data source should be generally consistent with that presented for Hebron (CSR Oceanography Section 3.1).

Model Application of Currents

In the model algorithm, as each day of drilling and possible discharge is followed, a corresponding day of current data is input from the five-year time-series file and is used to advect the particles as per

equations (6) and (7) in Section 2.1.1.6. It was assumed that drilling would commence in summertime following GBS towout and seabed installation and so a July 1 start date was selected for the modelling of the first well. Thus, the first calendar year of drilling was assigned to the 1980 current data. Currents for wells drilled in the next year were taken from 1981 and so on. The five years of current were recycled, so that the first five years of drilling used 1980 to 1984, the next five repeated use of 1980 to 1984, and so on. As noted above, an assumed 75 day well duration translates into a period of approximately 10 years and nine months. A scenario considering a 90 day well duration (and hence a total of 12 years and eight months for 52 wells) was employed as a sensitivity as described in Section 2.3.4.

2.1.1.5 Model Geometry

The transport (and spatial extent) and fate of the cuttings was modelled as a function of time. A given well sequence as a number of days drilling was employed. For each day, and for each different size class of material (i.e., the pebbles, coarse sand, medium sand, and fines in Table 2-3), a collection of particles were discharged. Particles were assigned a weight apportioned on the number of days drilling and the volume of cuttings associated with the particular well section. A time step was assigned appropriate for the geographic scale and model grid of the study area and the ambient current conditions. It was also necessary to choose time steps appropriate for each of the different particle types which exhibit a range of fall velocities. At each time step in the model, a new location for a given particle was calculated. Selection of too large a time step may yield inaccurate results. Too small a time step makes for overly intensive computations in the model. For the given Hebron domain, the time steps employed are provided in Table 2-4.

Table 2-4 Time Steps for the Hebron Domain

Modelling Scenario	Cuttings Material			
	Pebbles	Coarse Sand	Medium Sand	Fines
Platform				
time step, Δt (s)	20	40	60	300
# particles per Δt	1	2	3	15
# steps per day	4,320	2,160	1,440	288

It is instructive to consider these time steps together with the particle settling velocities presented in Section 2.1.1.3. Their application in the model has a direct bearing on the deposition predictions. For platform discharge 20 m above the surface, the particles will settle to the seabed in times that range from one minute for pebbles and three minutes for the coarse sand, to five minutes for the medium sand, and as long as five hours for the fines. This is further evidence of the large influence of the particle size composition assumptions. The essential observation is that the pebbles and sand will settle quickly and have short times to drift away in the horizontal plane from the discharge point, while for the fines, the length of time is considerable and so deposition at a far-field distance from the origin is possible.

A grid was employed in the model to track the spatial extent of the deposition. The model grid was a Cartesian grid centred on the Hebron location (46°32'50" N latitude, 48°30'12" W longitude) and extending out a finite distance both in X (or East) and Y (or North) directions. For the platform scenarios a grid consisting of a 500x500 array of grid cells each of size 32 m was selected. This covers the Hebron location ±8 km. An additional grid cell size of 8 m was also employed to characterize the Hebron location ±2 km to a higher resolution. A uniform depth of 94 m is assumed for the model grids.

2.1.1.6 Model Algorithm

The path of each particle released is tracked by calculating at each new time step, n+1, its position (*x,y,z*) based on its position at the previous time step, *n*, as given by equations (6) to (8):

$$x_{n+1} = x_n + u \times \Delta t + x' \times R_x \quad (6)$$

$$y_{n+1} = y_n + v \times \Delta t + y' \times R_y \quad (7)$$

$$z_{n+1} = z_n + w \times \Delta t + z' \times R_z \quad (8)$$

where x = the particle position in the east-west horizontal distance (m)
y = the particle position in the north-south horizontal distance (m)

z = the particle position, or depth, in the vertical distance (m) (depth positive downwards)
u = east-west component of the ocean current (m/s)
v = north-south component of the ocean current (m/s)
Δt = time step for the given particle type (s)
w = fall velocity for the given particle type (m/s)
R_x, R_y, R_z= random numbers in the range (-1,1)

and where the x'R_x terms, and similarly for y and z, are included to simulate some element of turbulence in the current drift of the particles. The x' and y' are assigned the values 3.5, 6.0, 8.5 and 45.0 m for the pebble, coarse sand, medium sand and fines particles, respectively. The z' are assigned the values 0.35, 0.4, 0.4, and 0.22 m for the pebble, coarse sand, medium sand and fines particles, respectively.

2.1.1.7 Model Output

Following each well run, an output file was generated containing an x,y grid of the model domain with the following variables calculated for each grid cell:

- x, y, origin of cell, relative to discharge (x,y,z) origin = (0,0,74) for the platform (km)
- range (km) and bearing (degT) from origin
- total weight of cuttings (kg)
- cuttings density (g/m^2)
- cuttings thickness(mm)
- number of particles of each of four types (pebble, coarse sand, medium sand, fines)

A run log file was also generated that echoes key model inputs and reports the total weight of cuttings deposited on the seabed and the amount of cuttings which drift outside the model grid. There were no such losses for the 32 m grid cell size scenarios employed. For the 8 m scenario runs, where the domain covers ±2 km, typically less than a small fraction of one percent of the cuttings total mass might drift outside the domain for each well. These particles would be exclusively fines.

2.1.2 Gravity Base Structure-Considered Model (one-dimensional)

As an additional consideration of cuttings discharge from the platform, a simple cuttings model was also formulated and is summarized below.

2.1.2.1 Model Set-up and Rationale

The mud and cutting discharge modelling conducted for Hibernia (Hodgins, 1993) was referenced for the Hebron modelling study. The Hibernia modelling study considered the hydrodynamics and

turbulences caused by the GBS and the subsequent potential interference with the current flow field. The modelling results for Hibernia indicated that the effects of the GBS on the flow field diminished with distance from the GBS. The Hibernia modelling study showed that the sediment deposition with distance from the GBS is symmetrical. This is due to the fact that the current in the area is generally evenly distributed in all directions (based on the input current speed-direction distribution applied in the model), with no prevailing current in any particular directions.

For the Hebron Project, a 1D model was established considering the symmetrical characteristics of the sediment deposition distribution. The model can readily consider variation in current patterns in each of the 16 quadrants where current data are available. The model adopted a radial modelling grid system, with the origin at the sediment discharge point. The model considered sedimentation by gravity in the vertical direction and movement with the current in the horizontal direction. Hydrodynamics and turbulences caused by the GBS were not considered. However, the Hibernia model was used to calibrate the 1D model with respect to the effects of hydrodynamics and turbulences generated by the GBS (see Section 2.1.2.2).

The 1D model was established on the basis that the particle size settling at a distance is a function of the current velocity and settling depth. Any portion of the cuttings sediment with sizes finer than the particle sizes established for the model are not considered but will be farther down current.

2.1.2.2 Model Testing and Calibration

Assuming a Hebron GBS concept considered to be similar in size to the Hibernia GBS, the 1D model was applied to the Hebron case using the same input data as presented in the Hibernia Effluent Fate and Effects Modelling report (Hodgins, 1993). The results on sediment deposition obtained from the 1D model were compared with the original modelling results presented in that report, which was obtained by considering hydrodynamics and turbulence about the platform. The results obtained from the 1D and original modelling exercises were comparable. It appears that the hydrodynamics and turbulences generated by the GBS have little effect on sediment deposition around the GBS. Several factors may have contributed to this observation. The current in the Project area generally has a low velocity, which causes the turbulences generated by the GBS to be low. The particles deposited around the GBS are typically coarse materials, which are less influenced by turbulences than fine particles. With distance from the GBS, where finer particles tend to settle, the turbulence generated by the GBS diminishes. Also, since the flow field employed for the Hibernia area was virtually symmetrical in all direction, without a prevailing current direction, the effect of the GBS on sedimentation tended to average out in all directions.

2.2 Results

2.2.1 Results of Primary Modelling (three-dimensional)

For ease of reference, all runs of the 3D model are given scenario identifiers as listed in Table 2-2. Graphical presentations of cuttings deposition thickness on the seabed following completion of different stages of well drilling at Hebron are the main model output data product presented. Thicknesses of 1 mm, 1 and 2 cm, 10 and 20 cm, and 1 m are shown. Each graph shows a plan view of the seabed, the grid is oriented with the Hebron GBS at origin, North pointing up, East pointing to the right and so on. The scenario identifier is included in the upper left corner of each graph. Several spatial scales or views are used to present the results, also as noted in Table 2-2.

Figure 2-1 presents a far-field view out to 8-km. The cuttings deposition is predicted to extend in thicknesses up to 1 mm (shown in grey) as far as about 5.5 km to the southwest and 6 km to the northeast. Northern, western, and southeastern extents are generally limited to about 2 to 4 km. Small pockets of cuttings deposition between 1 and 10 mm (shown in dark blue) are within about 1 km of the GBS and as far as 3 km to the southeast. The cuttings deposition near the GBS, out to 1-km, is shown in Figure 2-2. Maximum thicknesses in the grid squares over a radius of about 50 m from the GBS range from 2.4 m directly at the GBS, to 1.6 to 1.9 m in the neighbouring grid squares to about 50 cm within 16 m away and about 15 cm within 24 m. At 32 m away thicknesses are on the order of 5 to 7 cm height and at 40 to 60 m thicknesses may be on the order of 1 cm. The heights accumulating directly at the GBS (e.g., the 2.4 m value) do not account for slumping of this 'pile' (the absence of the GBS was also assumed for this modelling). Assuming a likely angle of repose of about 30 degrees, one might estimate from these thicknesses, a maximum height more likely on the order of 1.5 to 2 m. Therefore, thicknesses of 1 to 2 m within 10 m distance and 10 to 20 cm within 25 m are predicted. Thicknesses of at least 1 cm (shown in cyan) are generally confined to within about 50 to 60 m of the GBS. These cuttings near the GBS are almost exclusively the fast-settling pebbles and sand (a very small percentage of the fines will drift for a time and ultimately settle near the GBS) whereas at distances greater than about 50 to 200 m, the deposits will be exclusively fines. Finally, a third view is shown in Figure 2-3, where the cuttings deposition are shown in relation to the other oil developments on the Grand Banks. The southern extent of the first 1 mm thickness contour remains about 4 km from Terra Nova.

The following assumptions should also be noted regarding the cuttings deposition fate on the seabed:

1) in addition to the currents being taken as representative of the Hebron location, they are also assumed to be uniform over the deposition grids modelled
2) the modelling predicts the initial deposition of the cuttings only. The subsequent weathering, fate, and obliteration of the material accumulated on the seabed is a separate, less-readily predicted process

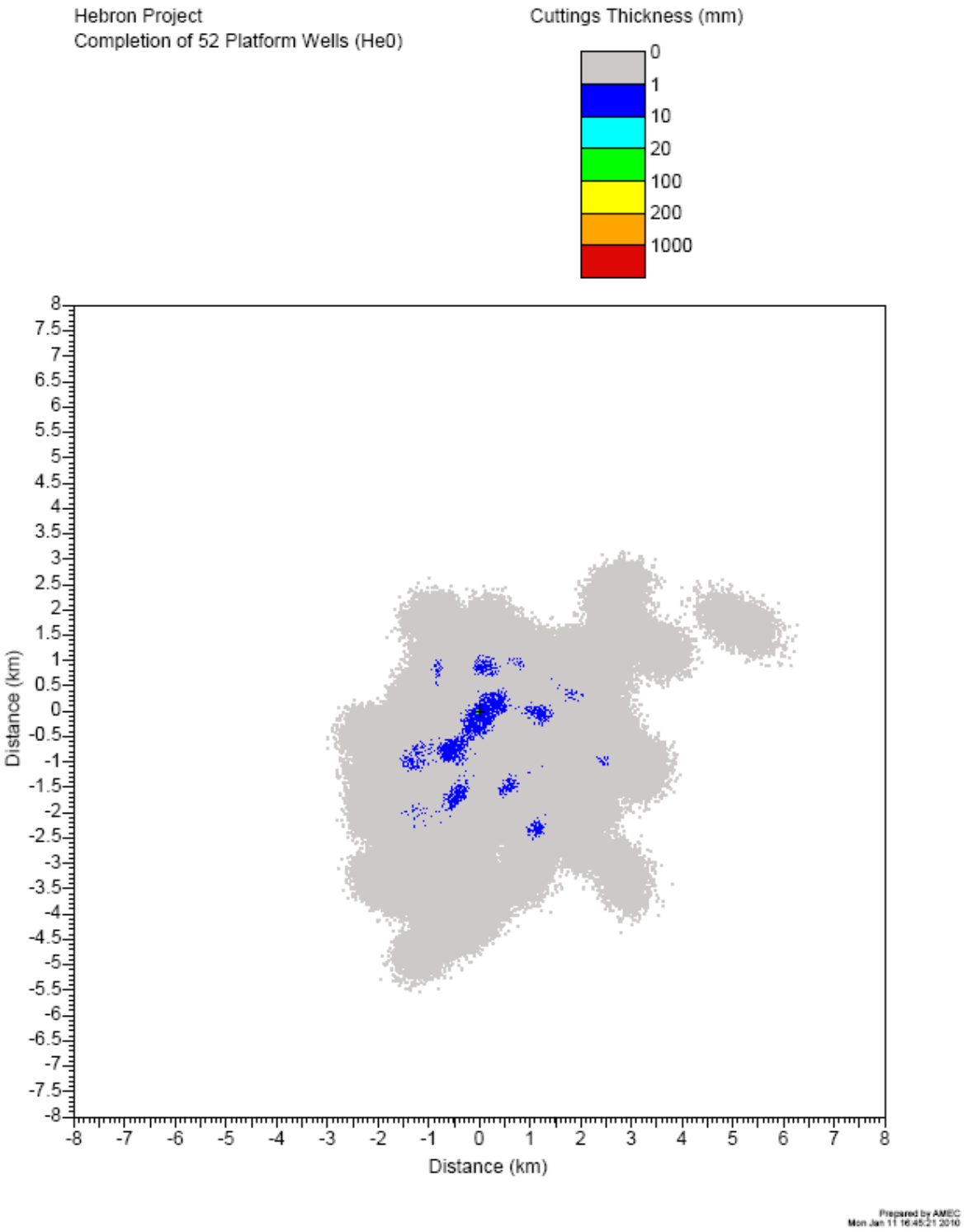


Figure 2-1 Cuttings Deposition Following Platform Drilling, 8-km View

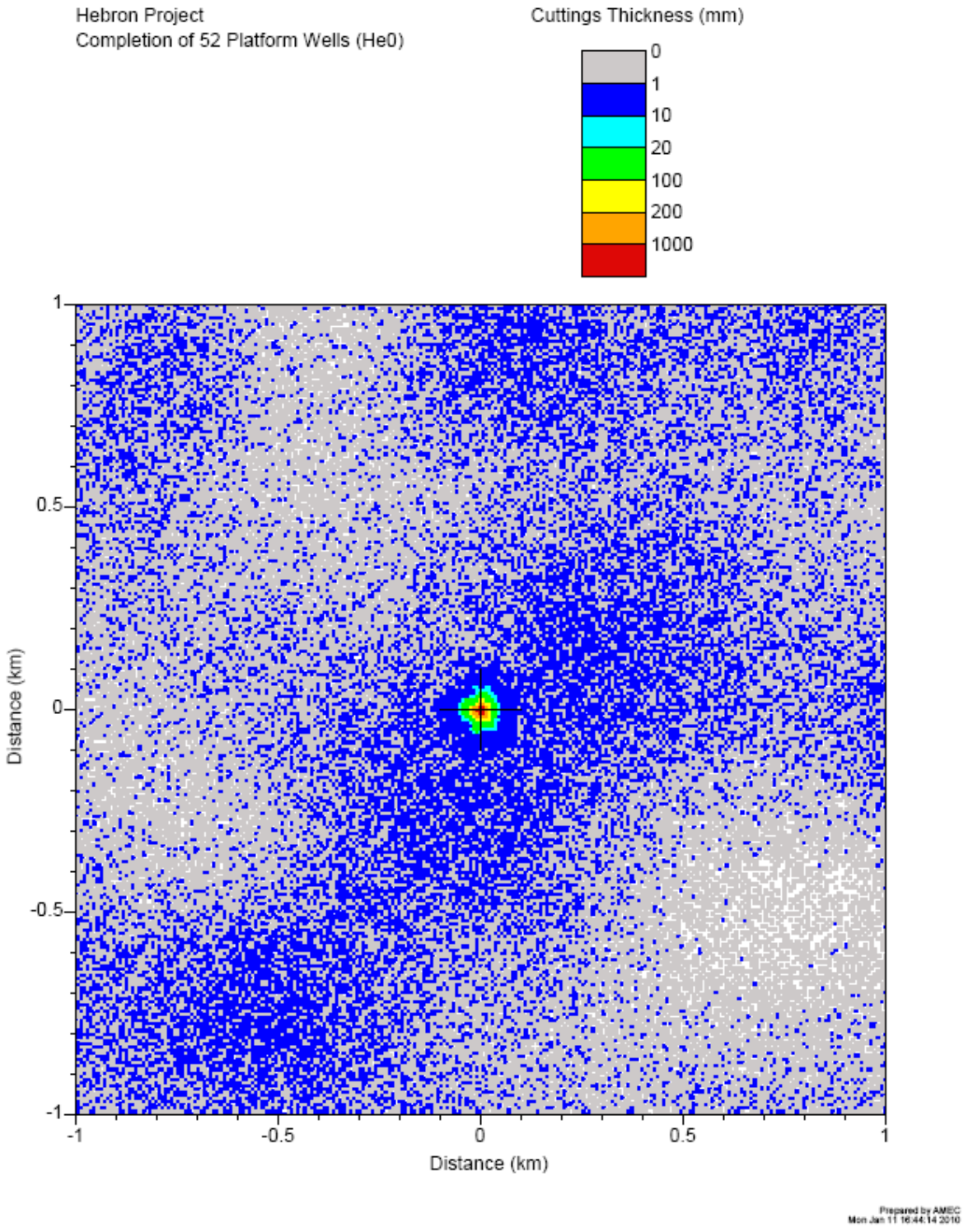


Figure 2-2 Cuttings Deposition Following Platform Drilling, 1-km View

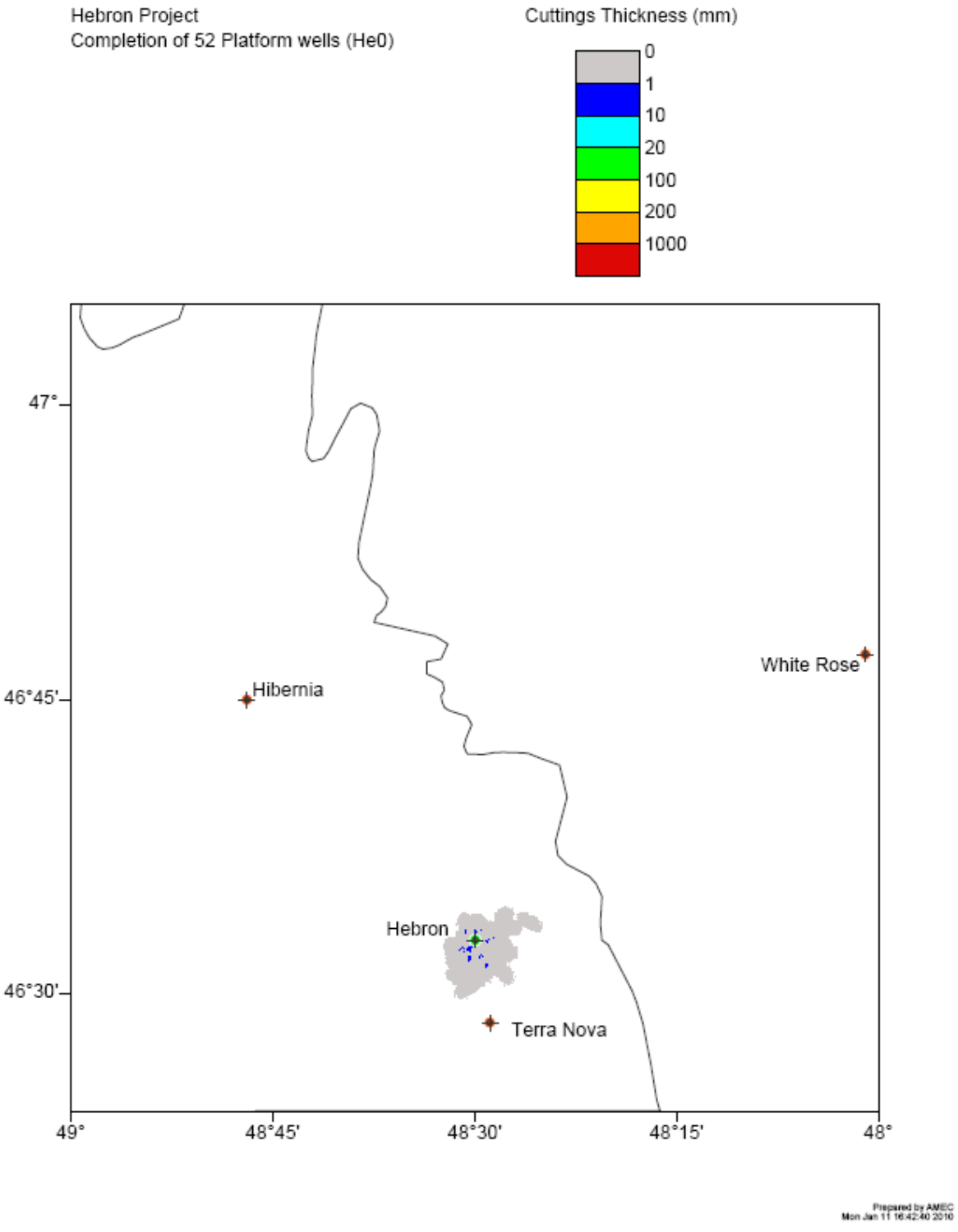


Figure 2-3 Cuttings Deposition Following Platform Drilling, Grand Banks View (100 m depth contour is shown)

2.2.2 Results of Gravity Base Structure-Considered Modelling (one-dimensional)

From the 1D exercise, it was seen that settling and transport by the current of sediment particles is the primary mechanism in determining sediment deposition. For the Project area, the effect of turbulences generated by a GBS on sediment deposition is not substantive. It is observed that particle size distribution is by far the most substantive in determining sedimentation in any particular area. The available particle size distribution data groups all the particle sizes into four classes: pebble, coarse sand, medium sand and fines. The fines category consists of between 60 to greater than 80 percent of the total cuttings. There are no data to further break down this class of material. It was evaluated that the sediment deposition predicted near the GBS, as obtained from the 1D modelling study, is more reliable than results at a distance from the GBS. This is because the sediment settling near the GBS is typically coarse material, for which available grain size distribution data are generally better. With distance from the GBS, the modelling results become less reliable due to uncertainty regarding the grain size distribution for the fine portion of the sediment.

2.3 Sensitivity Analyses

It is instructive in interpreting the predictions of the model to understand how sensitive those predictions are to changes in the cuttings characterization and in the ocean current input to the model. In order to assess the effects of perturbations or alterations to these parameters, a number of sensitivity scenarios were developed. In each scenario, one aspect of model input was altered while all others were held constant.

The fate of drill cuttings deposition is affected by the following key factors:

- particle composition
- particle settling velocities
- ocean current velocities
- drill cuttings volumes

A 90-day, rather than 75-day, well duration was also assumed as a sensitivity to consider what effect that parameter may have. One base case (Run ID #1) as well as six additional modelling scenarios as noted in Table 2-2 were completed. The sensitivities are each of one of the above four types and are described in Sections 2.3.1 to 2.3.4. Deposition thickness graphs associated with the runs are presented in Appendix B, with two graphs per page to facilitate comparison. Observations of the sensitivity run results are noted in Section 2.3.4.

2.3.1 Particle Composition

The most variable parameter associated with the cuttings characterizations is the amount of fines material, which settle to the seabed at much slower rates than the pebbles and sands, which comprise the remainder of the cuttings. This amount is dependent on the stratigraphy of the wells drilled, the type of drilling mud used and the nature of the cuttings treatment applied on the platform prior to discharge. Deposition is most sensitive to particle size distribution: more fines means greater deposition farther away from the point of discharge; less fines means greater deposition close to the origin.

As presented in Table 2-3, two cuttings particle size sensitivities are considered. A sensitivity of 'more fines' composition was estimated by increasing the fines by 6 percent and reducing the percentage of pebble and sands proportionally by a total of 6 percent. For 'less fines' the fines were decreased by twice this amount, 12 percent, and the additional material added proportionally to the pebble and two sand classifications. These were professional judgements only on two possible sensitivities to consider.

2.3.2 Particle Settling Velocities

As already noted, the pebble and sand elements of the cuttings tend to fall much closer to their discharge origin compared with the slower settling fines. A sensitivity was required to consider the possible effect of faster settling of the fines, which frequently make up a large percentage of the cuttings volumes modelled.

In the study of drift and dispersion of suspended drill muds from the Hibernia platform, Tedford et al. (2003) approximate the processes of flocculation and floc breakup by making the settling velocity a function of the bottom stress. Three velocities were employed. A fast-settling velocity of 0.005 m/s was selected for the early stages of the discharge plume and used until the bottom stress exceeded a critical threshold. The flocs were then modelled to break up into their individual components and assume a low settling velocity of 0.0001 m/s. This settling velocity was employed until the bottom stress then fell back below that critical threshold at which point the material was modelled to flocculate into the background of marine flocs with a larger settling velocity of 0.001 m/s, almost equal to the fines settling velocity of 0.0012 m/s estimated in Section 2.1.1.3. These latter two settling velocities were alternately employed depending on the bottom stress.

For the present modelling, one settling velocity is employed for each particle type. For a faster fines settling velocity sensitivity, the value of 0.005 m/s from Tedford et al. (2003) was selected and applied as a sensitivity for each of the three base case scenarios.

2.3.3 Ocean Current Sensitivities

The Hibernia time-series of ocean currents provided a useful means of modelling the currents at Hebron. An alternative source of current information is contained in the Hebron Site Meteorological and Oceanographic Design Criteria (ExxonMobil Upstream Research Company, 2009). This alternative source is limited though for the cuttings modelling since no time-series information is presented. Nevertheless, given the importance of the Hebron Site Meteorological and Oceanographic Design Criteria as a source of current estimates to be used in Project design at the Hebron site, a sensitivity for the cuttings deposition needed to be considered which would attempt to employ these Hebron design currents in some fashion. The time-series nature of the Hibernia data still needed to be employed; however, a comparison was made to estimate an adjustment to the speeds that would yield currents with similar magnitudes to the Hebron design values. A comparison of August and February current statistics is presented in Table 2-5, and a comparison of annual near-bottom currents is provided in Figure 2-4. Near-bottom currents are reported since for cuttings discharge modeled at 20 m above the seabed, these are the currents of primary interest in determining their fate. The annual directional distributions are similar, with as much as 5% more currents to the southwest for Hibernia and 5% more currents to the north for Hebron; otherwise the differences are within less than 1% to 3% of each other in each of the cardinal direction sectors. This comparison of directional distributions therefore suggests the directional information contained in the 2009 URC current update would have little change to the modelled cuttings deposition results. In terms of current speeds, values are less for Hebron: 55% of speeds are 10 cm/s or less compared with 32% for Hibernia. Conversely for Hibernia 55% of speeds are in the 10-20 cm/s range (40% for Hebron). Based on the Hibernia measurements, 87% of speeds are 20 cm/s or less compared with 94% for Hebron. About 1% of Hebron (consistent with 99% upper limit from URC design is 28 cm/s), and 2% of Hibernia near-bottom currents are reported above 30 cm/s.

A uniform scaling of speeds in the Hibernia time-series by 0.67 (a reduction of 33 percent) is estimated to yield currents ‘comparable’ to the Hebron Design currents. A companion scaling of 1.33 (an increase of 33 percent) is also considered.

Table 2-5 Comparison of Hebron Design and Hibernia Time-Series Currents

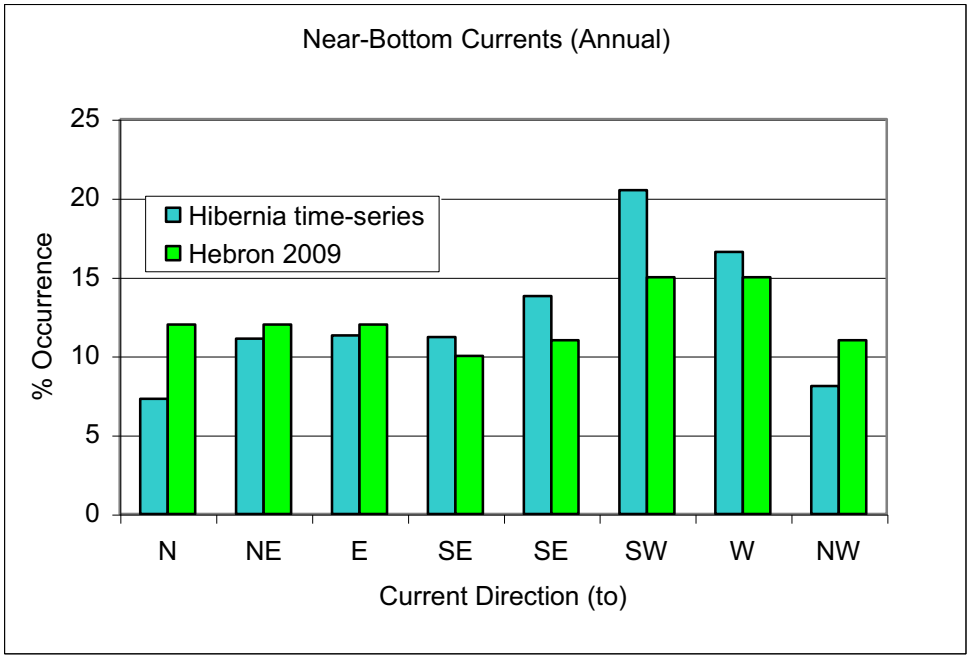
Month [1]		Current Speed Condition [2,3] High (Hibernia)	High (2009) [a]	Average	Average (2009) [b]	Low	Low (2009) [c]	Current Direction (to) [4]	Current Direction (to) (2009) [d]
August									
Near-Surface	(20 m)	74.0	64.0	15.4	13.0	3.0	~5.0	S	SW or SE
Mid-Depth	(45 m)	40.0	34.0	12.7	9.0	4.0	~5.0	SW	W
Near-Bottom	(70 m)	33.0	26.0	11.0	9.0	3.0	~5.0	SW	W
February									
Near-Surface	(20 m)	59.0	53.0	18.1	13.0	3.0	~5.0	SW	S
Mid-Depth	(45 m)	61.0	46.0	15.8	9.0	4.0	~5.0	SW	SW
Near-Bottom	(70 m)	57.0	42.0	14.3	9.0	4.0	~5.0	SW	SW

Source: HTS (Hibernia time-series)

Notes:
1. Month of observation
2. High currents are the maximum value in the time-series
3. Low and Average currents are the 95% lower limit and mean values respectively
4. Directions are those with the largest percent occurrence for the given month

Source: ExxonMobil URC (2009).

Notes:
a. Table 9 seasonal current extremes from Terra Nova measurements
b. Table 7 estimates of current extremes: 50% non-exceedance value (annual): seasonal values would need to be estimated from monthly speed vs. direction bivariate tables; however, no large difference from annual statistics anticipated
c. values can be estimated from monthly speed vs. direction bivariate tables; however, values are expected to be low ~O(5 cm/s)
d. Directions are those with the largest percent occurrence (Tables 103-105 and 85-87 resp. for Aug, Feb)



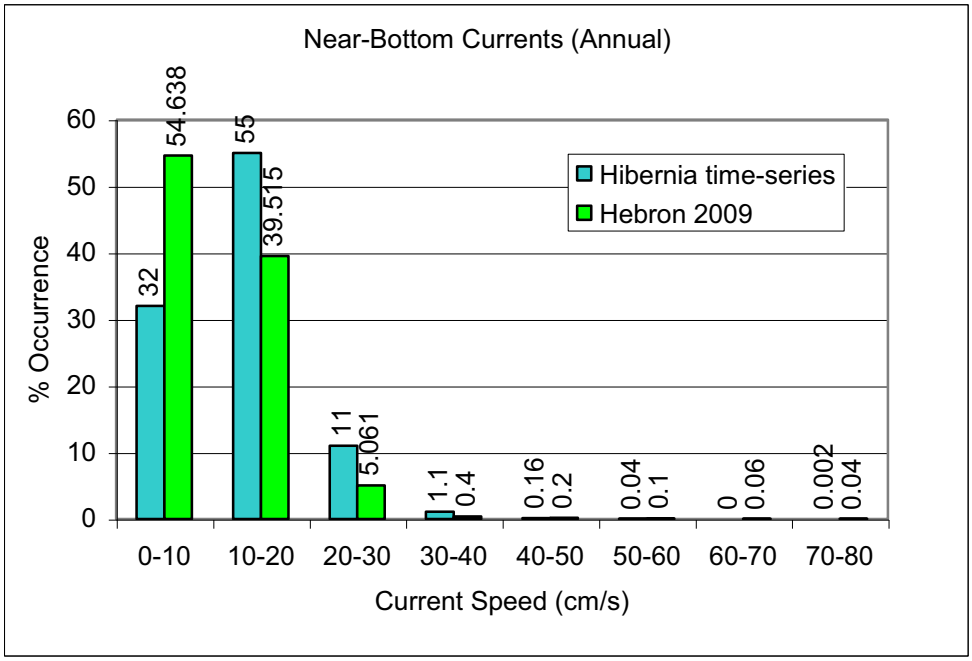


Figure 2-4 Comparison of Hebron Design and Hibernia Time-Series Near-bottom Currents

2.3.4 Observations from the Sensitivity Runs

One base case (scenario id He0) as well as six additional modelling scenarios are identified in Table 2-6. Figures of the associated cuttings deposition predictions are presented in Appendix B.

For the first two sensitivities where the amount of fines are increased or decreased, there are virtually identical deposition patterns to the base case due to the high proportion of fines to begin with. The sensitivity increase/decrease of the amount of fines results in a corresponding decrease/increase in proportion of pebble and sand material and hence slightly lesser/greater accumulations near the GBS, respectively.

For the increased ocean current sensitivity, the deposition extents are about 1 km or so farther than in the base case due to the increased scaling of the ambient currents. At the same time, few small pockets of cuttings deposition between 1 and 10 mm remain compared with the base case since the fines (exclusively the cuttings particles at distances from the GBS) are now distributed over a larger area due to the increased currents. For the decreased ocean current sensitivity, cuttings depositions up to 1 mm thickness extend out to about 4 km to the south and northeast from the GBS, the general deposition pattern shape being similar to the base case though not as far (5.5 to 6 km for the base case). Whereas in the base case a dozen or so small pockets of cuttings deposition between 1 and 10 mm were located in the area within about 1 km of the GBS and as far as 3 km to the southeast, this same area out to about 1 to 2 km from the GBS is now consistently between 1 and 10 mm. Due to the reduced ocean current velocities considered, the fines particles will experience less horizontal distribution.

The sensitivity to consider a faster vertical settling velocity for the fines results in the most dramatic changes to the predicted cuttings deposition pattern near the GBS. All cuttings deposition is limited to within about 2 km of the GBS. Out to 100 m, the mean thickness is about 8 mm and maximum 3 cm, slightly greater than for the base case due to the sooner, and hence increased amount of, settling fines.

The sensitivity to consider a slightly longer well duration resulted in the least difference from the base case: the same basic deposition pattern is seen, with small alteration to the location of the small dark blue pockets of cuttings deposition between 1 and 10 mm thickness. This is not unexpected given the sensitivity had the effect of separating the dates that the wells were drilled and hence further randomizing the associated ambient ocean currents to be encountered.

Further discussion is presented in Table 2-6.

Table 2-6 Cuttings Deposition Summary

Scenarios	Sensitivity	Results
He0	base case	▪ cuttings deposition up to 1 mm thickness out to about 5.5 km to the southwest and 6 km to the northeast from the GBS. Northern, western, and southeastern extents are generally limited to about 2 to 4 km. Small pockets of cuttings deposition between 1 and 10 mm (shown in dark blue) are generally within about 1 km of the GBS and as far as 3 km to the southeast ▪ near the GBS, out to 1-km, a maximum thickness of 1.5 to 2 m is predicted to accumulate directly at the GBS, with a mean thicknesses of 17 cm within 50 m distance. Out to 100 m, the mean thickness is about 4 mm and maximum 2.7 cm. ▪ at distances greater than 100 m from the GBS, thicknesses are generally 1 mm or less on average and no greater than 4 mm.
HeMF	more fines	▪ virtually identical deposition pattern to the base case due to high proportion of fines to begin with: slightly increased extent of the small pockets of 1 and 10 mm thickness (in dark blue) within about 1 to 3 km of the GBS. ▪ near the GBS, out to 1-km, a maximum thickness of about 60 to 80 cm is predicted to accumulate directly at the GBS, with a mean thicknesses of 8 cm within 50 m distance. Out to 100 m, the mean thickness is about 3 mm and maximum 2.0 cm. The sensitivity increase of the amount of fines results in a corresponding decrease in proportion of pebble and sand material and hence less (not as high) accumulation near the GBS
HeLF	less fines	▪ virtually identical deposition pattern to the base case due to high proportion of fines to begin with: slightly decreased extent and density of the small pockets of 1 and 10 mm thickness (in dark blue) within about 1 to 3 km of the GBS. ▪ near the GBS, out to 1-km, a maximum thickness of about 2.5 to 3.5 m is predicted to accumulate directly at the GBS, with a mean thicknesses of 33 cm within 50 m distance. Out to 100 m, the mean thickness is about 6 mm and maximum about 5 cm. The sensitivity decrease of the amount of fines results in a corresponding increase in proportion of pebble and sand material and hence slightly greater accumulations near the GBS
HeC67	reduced ocean currents	▪ cuttings deposition up to 1 mm thickness out to about 4 km to the south and northeast from the GBS, the general deposition pattern shape being similar to the base case. Whereas in the base case a dozen or so small pockets of cuttings deposition between 1 and 10 mm were located in the area within about 1 km of the GBS and as far as 3 km to the southeast, this same area out to about 1 to 2 km from the GBS is now consistently between 1 and 10 mm (dark blue). Due to the reduced ocean current velocities considered, the fines particles will experience less horizontal distribution. This increased presence of fines settling nearer the GBS is also evident in the 1-km view figure which shows (again) a much greater prevalence of dark blue compared with grey for increased thickness. ▪ near the GBS, out to 1-km, a maximum thickness of about 2.5 to 3 m is predicted to accumulate directly at the GBS, with a mean thicknesses of

		16 cm within 50 m distance. Out to 100 m, the mean thickness is about 3 mm and maximum about 1 cm. Due to the sensitivity decrease of current speed, there is an increase in the amount of pebble and sand materials accumulating nearer the GBS as they experience less horizontal drift.
HeC133	increased ocean currents	▪ cuttings deposition up to 1 mm thickness occurs out to about 7 km to the south and northeast from the GBS. Northern, western, and southeastern extents are generally out to about 4 to 5 km. This is a greater extent due to the increased scaling of the ambient currents. At the same time, few small pockets of cuttings deposition between 1 and 10 mm (dark blue) remain compared with the base case. This makes sense given the fines (exclusively the cuttings particles at distances from the GBS) are now distributed over a larger area due to the increased currents. The increased presence of fines settling nearer the GBS is evident in the 1-km view figure which shows less areas of dark blue compared with grey and hence decreased thicknesses in general outside of about 100 m from the GBS. ▪ near the GBS, out to 1-km, a maximum thickness of about 80 cm to 1 m is predicted to accumulate directly at the GBS, with a mean thicknesses of 16 cm within 50 m distance. Out to 100 m, the mean thickness is about 6 mm and maximum about 4 cm.
HeFF	fast settling velocity for fines	▪ the sensitivity to consider a faster vertical settling velocity for the fines results in the most dramatic changes to the predicted cuttings deposition pattern near the GBS. All cuttings deposition is limited to within about 2 km of the GBS. Cuttings thicknesses up to 10 mm occur out to about 1 to 1.5 km and a patch of about 30 to 50 m diameter of thickness 1 to 2 cm is present about 30 m west of the GBS. ▪ near the GBS, out to 1-km, similar to the base case, a maximum thickness of about 1.5 to 2 m is predicted to accumulate directly at the GBS, with a mean thicknesses of 17 cm within 50 m distance. Out to 100 m, the mean thickness is about 8 mm and maximum 3 cm, slightly greater than for the base case due to the sooner, and hence increased amount of, settling fines. ▪ at distances greater than 100 m and out to 1 km from the GBS, thicknesses are generally about 2 to 6 mm on average and no greater than about 15 mm.
He90d	90 day well duration	▪ the sensitivity to consider a slightly longer well duration resulted in the least difference from the base case: the same basic deposition pattern is seen, with small alteration to the location of the small dark blue pockets of cuttings deposition between 1 and 10 mm thickness. This is not unexpected given the sensitivity had the effect of separating the dates that the wells were drilled and hence further randomizing the associated ambient ocean currents to be encountered. ▪ near the GBS, out to 1-km, statistics on the thicknesses are virtually identical to those reported for the base case

3. PRODUCED WATER DISPERSION Modelling

3.1 Methods

3.1.1 Model Theory on Produced Water Mixing

When produced water is discharged from a diffuser into the ambient seawater, it becomes mixed with the ambient seawater and diluted by a process termed entrainment. Entrainment is essentially the result of relative movement between the effluent plume and the ambient seawater. The produced water discharge typically possesses a velocity momentum relative to the ambient current, which causes the effluent plume to initially follow a trajectory consistent with the discharge direction. This initial momentum diminishes with distance, and the plume eventually takes on the trajectory of the ambient current.

Depending on its salinity and temperature, the produced water can have densities higher or lower than the ambient seawater after its discharge. This density difference will cause the effluent plume to rise, if it is lighter than the ambient (buoyant), or fall if it is denser than the ambient. The effluent plume will eventually stop its rise or fall as it is cooled and diluted by the ambient seawater such that their densities are at comparable levels.

Both velocity momentum and the buoyancy force (or gravity force in the case of denser effluent than ambient) will cause the produced water discharge to have velocities different from the ambient current, both in terms of direction and magnitude. This velocity difference will cause the ambient seawater to be "pulled or entrained" into the effluent plume around the interface and become part of the plume due to water viscosity. The turbulence generated by the velocity difference along the interface will further accelerate the entrainment process, and is typically a more dominant force than the viscous shear force.

As the ambient seawater becomes entrained into the produced water plume, the plume grows in diameter, becoming diluted by the ambient seawater in the process. Concurrently, the plume loses its momentum relative to the ambient current due to the momentum exchange between the plume and the seawater. At the end of this process, the plume becomes indistinguishable in terms of its physical properties (velocity and density), and essentially becomes part of the ambient current.

After the initial entrainment process is complete, the plume will undergo further dilution by ambient turbulence and diffusion. Typical ambient turbulence includes wave action and current turbulence, which will cause the plume to be diluted around the interface similar to the initial mixing process. However, due to the absence of relative movement between the ambient water and the plume, this dilution process occurs at a slower rate than the initial mixing. The diffusion process occurs as a result

of the tendency of contaminant (oil) to migrate from high concentration zones to low concentration ambient water.

The produced water mixing process is partially depicted in Figure 3-1. The initial mixing region is termed near-field in discharge modelling. The region beyond the initial mixing is termed far-field. The depth or elevation at which the plume density becomes equal to the ambient water is termed trap lines.

3.1.2 Diffuser Configuration and Effect on Dilution

Diffuser configuration typically includes diameter, orientation and depth. As the diffuser diameter increases or decreases, the momentum of the effluent discharge varies inversely, which would affect the trajectory of the effluent plume, plume diameter at the end of near-field and, ultimately, the dilution factor at a given distance from the discharge. When the diffuser port is oriented toward the surface for a plume with lower density than the ambient, the plume approaches the trap line or surface at an accelerated rate. The same is true if the diffuser port is oriented downward toward the bottom for a plume with density higher than the ambient. In both cases, there is less time for the plume to develop and, as a result, the plume diameter is reduced, as is the near-field dilution. When the diffuser port is oriented in the direction of the ambient current, the relative movement between the plume and ambient is reduced, which minimizes entrainment mixing. Often, the discharge angle of the diffuser port is selected as large as possible from horizontal to slow or prevent the plume from rising to the surface, or sinking to the bottom.

As the diffuser diameter increases for a given discharge, the discharge velocity decreases. Under conditions of effluent density lower than the ambient, the effluent discharge tends to rise to the top of the diffuser port as its discharge velocity decreases. This could lead to salt water intrusion into the diffuser port, which is a documented problem for diffuser design. The Densimetric Froude Number (DFN) is the scaling factor commonly used to describe the momentum of the diffuser discharge relative to its buoyancy. As the DFN is reduced to less than unity, salt water intrusion into the diffuser port may occur. This problem is unlikely to occur for effluent discharge with densities higher than the ambient.

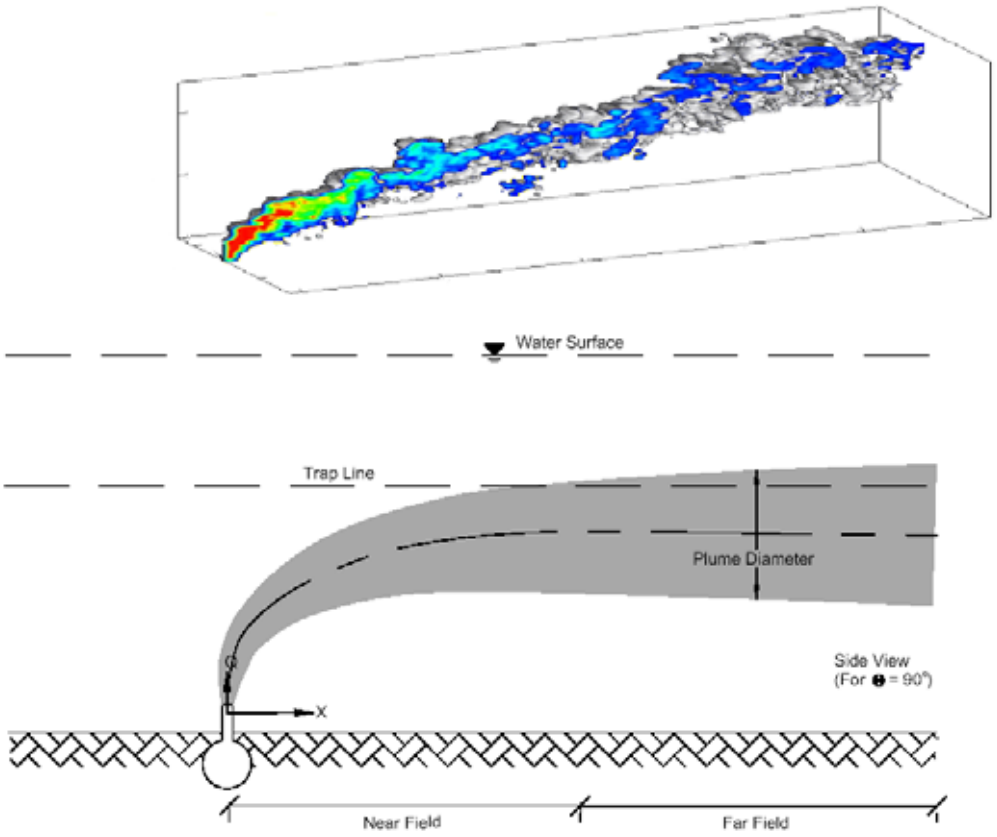


Figure 3-1 Produced Water Mixing Process Illustration

The depth of the diffuser may affect the total plume rise or fall and dilution. In general, the deeper the diffuser, the higher the total potential rise of the plume if the effluent is lighter than the ambient, and the higher the depth of the water column available for dilution. The opposite may be true for conditions where the effluent is denser than the ambient. As discussed in Section 4.2, the shallow depth of the marine environment in the Project area is typically stratified in the summer, which can limit the rise for plumes with densities less than the ambient. Placing the diffuser as far below the stratified layer as possible in such cases will have added importance to improve dilution. For plumes denser than the ambient, it may be advantageous to place the diffuser close to the surface to maximize the use of the water column depth. The determination of the diffuser depth may need to take into consideration other factors. For possible locating of the diffuser near the seabed, the thickness of any drill cuttings deposition in the near-field, may be a factor.

3.1.3 Effluent Characteristics and Effect on Dilution

The effluent characteristics affecting dilution include its temperature, salinity and discharge rate. The temperature and salinity of the effluent discharge will determine its initial density. This, in combination with the discharge direction, will determine the initial trajectory of the plume. The initial trajectory of the plume, together with the ambient conditions, will determine the plume path and total dilution achieved at a given distance. For given effluent characteristics, the higher the discharge rate, the lower the dilution rate achieved.

3.1.4 Ambient Characteristics and Effect on Dilution

The ambient conditions can have profound and complex effects on the produced water dilution. The ambient characteristics affecting the dilution of produced water discharge include primarily the temperature and salinity stratification, which in turn determines the density stratification, and the ambient current velocity and direction.

3.1.4.1 Stratification and Nascent Density Effect

If produced water with lower density than the ambient is discharged into a stable non-stratified ambient, the produced water plume will continuously rise until it reaches the same density as the ambient, or the ambient surface. However, in a stable stratified ambient, the density of the ambient decreases toward the surface. As the produced water plume rises toward the surface, it encounters increasingly less dense ambient, which causes the plume to lose its buoyancy at an accelerated rate. Therefore, the stratification of the ambient has the effect of reducing the plume rise and, consequently, the water column depth available for dilution.

Due to its residual rising momentum, the produced water plume will not stop its rise at the trap line, where its density is similar to the ambient density, and will continue along its path for a distance. In stratified ambient, the plume density when it stops rising may be higher than the ambient, which may cause the plume to sink again following its initial rise. This oscillating process will terminate when the plume momentum as it crosses the trap line is exhausted. However, stratification will not result in a similar effect for a plume with densities higher than the ambient.

When produced water with relatively high temperature is discharged into an ambient with low temperature, it may first rise and then fall when the temperature of the plume is continuously cooled to the ambient level. This phenomenon is called the nascent density effect, which can be understood by considering discharging hot water into a freshwater ambient with a temperature near 0°C. It is understood that freshwater reaches maximum density near 4°C, above and below which freshwater will expand to lower densities. As the hot water discharge is cooled, its density will first increase. As the

temperature is cooled to about 8°C, the discharge plume will have similar density as the ambient water, and will slow down and eventually stop its rising. However, the discharge plume will continue to be cooled by the ambient at this point, and will become denser than the ambient. This will cause the effluent plume to sink. The rate of sinking is highest as the temperature of the discharge plume reaches 4°C, at which temperature the density difference between the effluent plume and the ambient is the highest. This sinking of the plume will terminate when the discharge plume is eventually cooled to the ambient temperature, and the density of the plume reaches equilibrium with the ambient.

The density of saline seawater and produced water is determined not only by temperature, but also by its salinity, and the nascent density effect in a saline environment is somewhat more complex than for freshwater conditions. The density diagram for seawater as a function of salinity and temperature is shown in Figure 3-2. The mixing line for produced water discharged at 70°C temperature and 52.9 psu salinity into the ambient seawater at 0°C temperature and 33 psu salinity is plotted in blue in Figure 3-2. For non-stratified ambient seawater at near 0°C, typical of the winter stratification of the Hebron marine environment, the produced water will initially rise (Figure 3-2). However, as the plume is cooled by the ambient to approximately 30°C, the plume will have a comparable density as the ambient (sigma equal to 26.5). As the plume is continually cooled by the ambient sea water, its density becomes higher than the ambient, and the plume will start to sink. The sinking of the plume will continue until the plume density reaches ambient level (sigma of 26.5) or the ocean bottom is reached. In cases when the produced water salinity value is closer to or equal to the ambient seawater salinity (cyan and green mixing lines in Figure 3-2), the produced water will initially rise at a relatively higher rate due to the higher density contrast with the ambient seawater. In these cases, the plume may rise to the surface before the plume density reaches the value of the ambient seawater. Additionally, the plume density may exceed that of the ambient seawater only briefly (in the case of 42 psu) or not at all (in the case of 33 psu). See Section 3.1.7 for rationale for considering these two additional salinities. Thus, in these cases the plume may not sink below the diffuser depth and the water column available for dilution may be limited.

3.1.4.2 Current

If no ambient current is present, the produced water discharge will simply rise to the surface or the trap line if the produced water has a lower salinity, or sink to the bottom or trap line if the effluent has a higher salinity. The effluent plume will form a pool when it stops its rise or fall, from where the effluent plume will spread out in all directions. With the increase in current velocity, the effect on mixing and dilution is somewhat complex. High current conditions tend to provide high dilution in the near-field as a result of high turbulence. However, the plume migrates quickly under high current conditions, and the time of travel by the plume to a given location is reduced. As a result, the mixing and dilution experienced by the plume at a given location in the far-field is also reduced.

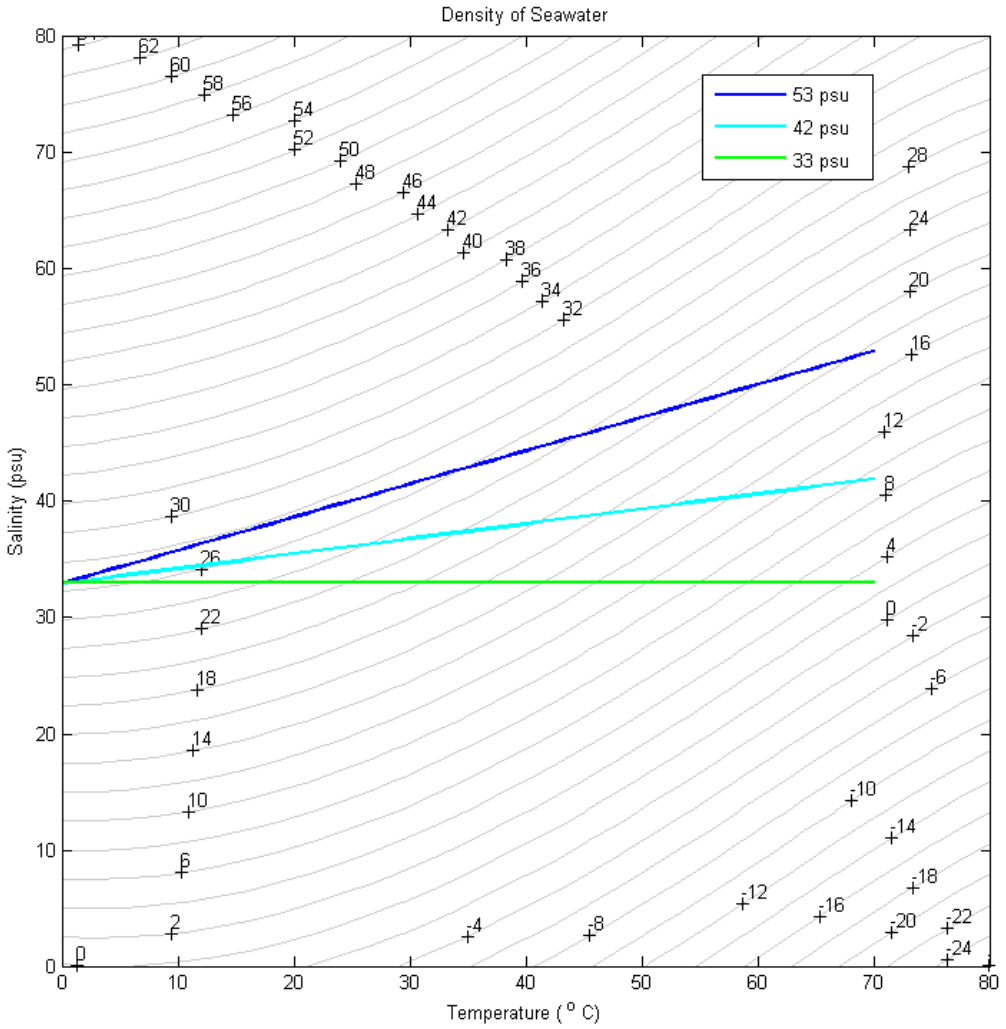


Figure 3-2 Seawater Density Diagram

3.1.5 Visual Plumes and UM3 Models

Visual Plumes (VP) is the software used for simulating the produced water plume for the Hebron Project. VP is a Windows-based program for predicting the behaviours of submerged jets and plumes in surface water environments. It is a public domain program developed by the Ecosystems Research Division of the U.S. Environmental Protection Agency. VP is essentially a modelling platform supporting multiple near- and far-field dilution models that simulate submerged plumes in stratified ambient flow field. The near-field simulation models supported by VP include DKHV, NRFIELD, and Updated Merge 3 (UM3). The Brooks algorithm is used for predicting far-field centreline dilution and

plume width. VP also supports the surface discharge model PDS, which simulates effluent discharge at the surface of the ambient flow field.

The UM3 model is used for simulating produced water plume for the Hebron project. UM3 is a three-dimensional Updated Merge (UM) model for simulating single and multiple-port submerged discharge. UM3 uses a coordinate system termed Lagrangian formulation, which moves along the plume trajectory. The model element (basic modelling unit) consists of a slice of the plume which has a bent cone shape. The properties within the slice are assumed constant, but vary along the trajectory with time. The properties simulated by UM3 represent the average contaminant concentration for each slice.

3.1.6 Model Input

VP requires the input of the following two groups of parameters, which are categorized in separate input tabs, for simulating submerged plume as a result of discharge from diffuser port(s):

- diffuser and effluent discharge characteristics
- ambient characteristics

3.1.7 Diffuser and Effluent Discharge

Simulation of the produced water plume using VP requires the input of a produced water discharge rate. The produced water system for Hebron will be designed to treat roughly 30,000 to 56,000 m^3/d of produced water for overboard disposal as per regulations or possibly re-injection into the subsurface if feasible (ExxonMobil Canada Properties, 2009). These two discharge rates were therefore selected as bounds for the produced water modelling.

Salinity of the produced water effluent is another important input parameter, which will have a measurable effect on the rise or fall of the plume and its trajectory.

Previous modelling exercises for produced water discharge for offshore drilling projects on the Grand Banks have considered effluent densities ranging from measurably higher than the ambient to measurably lower than the ambient. The salinities determined from these densities also vary from measurably higher than the ambient to measurably lower than the ambient. Produced water characteristics including salinity and density can vary widely between oil fields and even within the same field. As noted by the Canadian Association of Petroleum Producers (2001) most produced waters have salinities greater than that of seawater. In the Gulf of Mexico, salinities in the range 50 to 150 psu are common: offshore Canadian produced waters are also in this range. Therefore, it is expected that a produced water plume will typically sink when discharged into the marine environment.

Laboratory analysis of water samples from the Ben Nevis horizon of the Hebron M-04 field, shows that the source water has a density of 1,037 kg/m^3 at 25°C. Produced water will be essentially source water with some minor contamination no greater than 30 mg/L of hydrocarbons. The salinity calculated from the density and temperature provided is 52.9 psu. For this modelling exercise, a salinity value of 52.9 psu is used as model input. A discharge temperature of 70°C was selected.

Other parameters selected for the diffuser and effluent water discharge input include the following:

- discharge port diameter: 0.61 m (24")
- discharge vertical angle: 0 degrees to horizontal
- discharge horizontal angle: 270 degrees from north
- discharge elevation: 45 m from sea bottom
- water depth: 94 m
- oil concentration at discharge: 30 ppm

It is noted that over time, as more and more seawater is injected into the reservoirs, the salt content of the produced water will be reduced and will eventually approximate the concentration of seawater. To that end, two additional salinity values were selected for the modelling: 42 psu as a midpoint value between the source 52.9 psu value and ambient, and 32.7 psu to be representative of ambient conditions. The exact timing of when these salinity values might be reached is not known or predicted; however, these additional values enable modelling sensitivity to bracket the potential trajectory of the discharged produced water plume.

3.1.8 Ambient Characteristics

Input on ambient characteristics required by VP includes temperature and salinity profiles, which in turn, determines the density profile. Current profiles and directions are also required for ambient characteristics.

3.1.8.1 Temperature, Salinity Profiles and Oceanic Stratification

A summary of the monthly temperature, salinity and density data for the Hebron region obtained from the Ocean Science hydrographic database is presented in Appendix C. This includes average monthly temperature and salinity profiles and tables based on these data.

On an average, the seawater temperature of the project area is highest in August, when the temperature stratification is also the highest. The seawater temperature and stratification is at a minimum in January and February. It appears that, on an average, the temperature stratification is primarily limited to within 50 m depth below the water surface. Below the 50 m depth, the seawater temperature remains near zero on average all year round.

Salinity typically increases with depth. The salinity data for the Project area appear to suggest that the seawater is slightly less saline near the water surface in the summer than in the winter (see Appendix C).

Seawater density is a function of temperature and salinity (Figure 3-2). Consistent with the temperature stratification, seawater density stratification in the Project area is also highest in August, becoming less dense toward the surface. The seawater density stratification is the lowest in January and February.

The available seawater temperature, salinity, and density data suggest that the typical August and February seawater conditions would provide an envelope of the conditions that can be encountered in an average year. In this modelling exercise, the average August and February temperature and salinity profiles are considered in the identification of modelling scenarios. It should be noted that VP does not require the input of density profiles, which the model calculates automatically based on temperature and salinity input.

The August and February temperature and salinity profiles used as input for the ambient conditions in this modelling exercise are summarized in Table 3-1 and illustrated in Figure 3-3.

Table 3-1 Summer and Winter Ambient Temperature, Salinity and Density Profiles

Depth (m)	Temperature		Salinity		Sigmat	
	Mean (°C)	Standard Deviation (°C)	Mean (psu)	Standard Deviation (psu)	Mean	Standard Deviation
Summer Profile (August)						
0	11.99	2.24	31.94	0.44	24.18	0.53
10	10.83	2.88	32.05	0.40	24.43	0.51
20	6.88	3.84	32.46	0.27	25.30	0.59
30	3.49	3.22	32.70	0.26	25.92	0.47
40	0.96	2.09	32.89	0.25	26.36	0.25
50	-0.16	1.22	33.00	0.20	26.50	0.17
60	-0.39	1.06	33.04	0.26	26.54	0.19
70	-0.71	0.95	33.11	0.17	26.62	0.13
80	-0.81	0.99	33.17	0.18	26.67	0.14
90	-0.62	1.13	33.24	0.20	26.73	0.15
100	-0.55	1.03	33.28	0.18	26.75	0.13
Winter Profile (February)						
0	-0.53	0.67	32.99	0.20	26.51	0.16
10	-0.56	0.65	33.06	0.26	26.57	0.21
20	-0.50	0.64	32.99	0.23	26.51	0.20
30	-0.47	0.62	33.03	0.22	26.54	0.18
40	-0.37	0.58	33.18	0.28	26.65	0.23
50	-0.40	0.65	33.12	0.23	26.61	0.19
60	-0.28	0.55	33.21	0.31	26.67	0.25
70	-0.32	0.58	33.23	0.23	26.70	0.17
80	-0.34	0.60	33.24	0.27	26.71	0.20
90	-0.18	0.43	33.45	0.23	26.86	0.17
100	-0.13	0.71	33.36	0.28	26.79	0.20

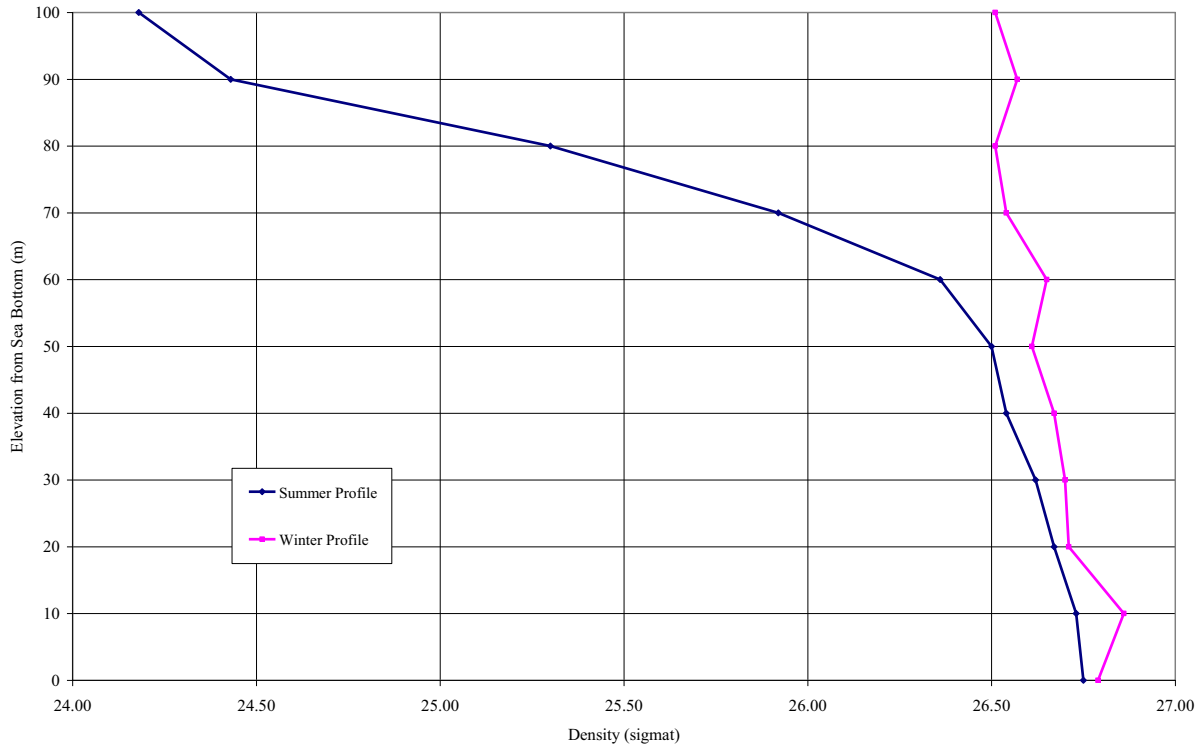


Figure 3-3 Summer and Winter Density Profiles

3.1.8.2 Ocean Currents and Directions

The representative current velocity profiles used in the modelling are summarized in Table 3-2. Current values were derived from the September 2009 ExxonMobil Upstream Research Company (URC) design report values (ExxonMobil Upstream Research Company 2009).

The current profiles used are based on current measurements collected at the Terra Nova FPSO. Current measurements were collected at three depth levels, covering the period from July 1999 to October 2008 with intermittent gaps (ExxonMobil Upstream Research Company 2009). The location of the Terra Nova site is 6.4 km south of the Hebron GBS site at a similar depth with similarly trending bathymetry.

Table 3-2 Hebron Summer and Winter Current Speed (cm/s) and Direction

Month [1]		Current Speed Condition (cm/s) High[2]	Average[3]	Low	Current Direction (to) [4]
August					
Near-Surface	(20 m)	64.0	13.0	5.0	SW
Mid-Depth	(45 m)	34.0	9.0	5.0	W
Near-Bottom	(70 m)	26.0	9.0	5.0	W
February					
Near-Surface	(20 m)	53.0	13.0	5.0	S
Mid-Depth	(45 m)	46.0	9.0	5.0	SW
Near-Bottom	(70 m)	42.0	9.0	5.0	SW

Source: Exxon Mobil URC (2009).

Notes:
1. August (February) currents are those employed to represent summer (winter) conditions.
2. Source: Table 9 (seasonal current extremes) from Terra Nova measurements.
3. Source: Table 7 (estimates of current extremes): 50% annual non-exceedance value.
4. Directions are those with the largest percent occurrence for August and February.

3.1.8.3 Other Input Parameters

Other ambient input parameters required by VP include background concentration, contaminant decay rate, and far-field dilution coefficient. In this modelling exercise, the contaminant (oil) is assumed to be a conservative chemical and does not decay within the modelling time domain. The background concentration was assumed to be zero. It should be noted that, as the ambient current shifts directions, the background concentration may be somewhat higher than zero under certain conditions; however, it is considered that this condition is short-lived.

The far-field dilution coefficient is used in simulating the far-field plume dilution. A value of 0.0003 $m^{2/3}S^2$ was adopted in the far-field plume simulation based on standard methods.

3.1.9 Summary of Model Scenarios and Input

In summary, two discharge rates, and three produced water salinities, were considered which encompass the range of the produced water discharge rates that can be expected during the Project life. Two ambient temperature and salinity profiles were considered, one for August when maximum stratification

typically occurs, and one for February, when minimum stratification typically occurs. The two ambient profiles represent the envelope of conditions that can typically be expected for an average year. Three velocity profiles were also considered, representing the high, average and low velocities that can be expected in the project area for summer and winter seasons. In combination, a total of 44 scenarios (including eight additional sensitivities for discharge elevation and discharge orientation) were considered. These scenarios encompass all the conditions, including discharge and ambient conditions, that can typically be expected during the Project life. A summary of modelling scenarios considered is presented in Table 3-3.

Table 3-3 Produced Water Modelling Scenarios

Scenario ID	Month [1]	Discharge Rate (m^3/d) [2]	Current Speed	Discharge Elevation (m above sea bottom)	Discharge Orientatation (to)
Effluent salinities = 52.9 psu, 42 psu, 32.7 psu					
Aug F30 Low	August	30,000	low	45	W
Aug F30 Avg	"	"	average	"	"
Aug F30 High	"	"	high	"	"
Aug F56 Low	"	56,000	low	"	"
Aug F56 Avg	"	"	average	"	"
Aug F56 High	"	"	high	"	"
Feb F30 Low	February	30,000	low	"	"
Feb F30 Avg	"	"	average	"	"
Feb F30 High	"	"	high	"	"
Feb F56 Low	"	56,000	low	"	"
Feb F56 Avg	"	"	average	"	"
Feb F56 High	"	"	high	"	"
Effluent salinity = 52.9 psu					
Discharge elevation = 35 m					
Aug F56 Avg [3]	August	56,000	average	35	W
Feb F56 Avg	February	"	"	35	"
Discharge elevation = 55 m					
Aug F56 Avg	August	"	"	55	"
Feb F56 Avg	February	"	"	55	"
Discharge orientation = SW					
Aug F56 Avg	August	"	"	45	SW
Feb F56 Avg	February	"	"	"	SW
Discharge orientation = S					
Aug F56 Avg	August	"	"	"	S
Feb F56 Avg	February	"	"	"	S

Notes:
1. Month determines current, and temperature and salinity profiles used
2. Two discharge rates selected corresponding to Hebron produced water system
3. The final eight scenarios are sensitivities for discharge elevation and discharge orientation (for the 52.9 psu salinity, higher discharge rate, and average ambient current conditions)

3.2 Results

A summary of effluent discharge and near-field plume characteristics for all the scenarios considered is provided in Table 3-44 and Table 3-5. For each scenario, a number of model output parameters are tabulated as follows:

- Maximum Rise Depth for Centreline: this is the centreline depth corresponding to the maximum rise of the plume
- Maximum Fall Depth for Centreline: this is the centreline depth corresponding to the maximum fall of the plume
- End of Near-Field Distance: this is the horizontal distance at which the initial turbulent mixing of the plume is completed and the plume has reached its level of neutral buoyancy
- Maximum Near-Field Plume Diameter: this is the maximum plume diameter within the near-field
- Target Dilution Factor Distance: this is the horizontal distance at which a target dilution of 300 is achieved for the centreline of the plume. An oil concentration criteria of 0.1 ppm will require a minimum dilution factor of 300. The threshold of 0.1 ppm was selected based on 96-h LC50 toxicity tests on larvae of selected commercial fish and invertebrate species that may be sensitive to soluble aromatic hydrocarbons as low as 0.1 to 0.14 ppm (Moore and Dwyer, 1974; Hurlbut et al. 1991; Booman and Foyn 1996).
- Target Dilution Factor Depth: this is the plume centreline depth at which the target dilution of 300 is achieved. Note that for some scenarios this value is not achieved by the end of the near-field mixing and dilution process. In these situations, the end of near-field depth is assumed and reported.

The graphic model outputs for all identified modelling scenarios are presented in Appendix D. For each scenario run, four plot panels are presented:

- plume elevation section view: produced water plume depth vs. horizontal distance
- plume plan view: produced water plume south-north vs. east-west distance
- ambient properties section view: depth vs. produced water plume density
- plumes dilution prediction: produced water dilution factor vs. horizontal distance

The plume centerline and boundary limits are shown in solid and dashed lines respectively. All three of the current speed conditions are included in each plot, high current speed in blue, average current speed in red, and low current speed in green.

Additional section view presentations are presented following the four VPlumes plot panels. Three panels are presented, each showing the three current speed scenarios. The first panel shows oil concentration as a function of horizontal distance from the GBS. A concentration of 0.1 ppm corresponds to -1 on the log10 scale shown. This point corresponds to a dilution factor of 300. This concentration is again shown in the second panel, this time as a function of depth. In the third panel. plume diameter as a function of horizontal distance from the GBS is shown.

Table 3-4 Produced Water Discharge Summary, Salinity = 52.9 psu

Scenario ID	Effluent Discharge Rate	Current Velocity Profile	Max Rise Depth for Centreline	Max Fall Depth for Centreline	End of Near-Field Distance	Max Near-Field Plume Diameter	Target Dilution Factor Distance	Target Dilution Factor Depth
Effluent salinity = 52.9 psu	(m^3/d)		(m)	(m)	(m)	(m)	(m)	(m)
Summer Profile (August)								
Aug F30 Low	30,000	Low	48.9	94.0	45.6	44.9	183	94
Aug F30 Avg	30,000	Average	48.9	94.0	58.8	41.3	42	90
Aug F30 High	30,000	High	48.9	70.8	124.2	30.8	70	66
Aug F56 Low	56,000	Low	49.0	94.0	58.3	52.8	352	94
Aug F56 Avg	56,000	Average	49.0	94.0	73.9	50.5	74	94
Aug F56 High	56,000	High	49.0	75.8	133.5	37.9	75	70
Winter Profile (February)								
Feb F30 Low	30,000	Low	48.9	94.0	27.5	29.9	280	94
Feb F30 Avg	30,000	Average	48.9	89.4	42.6	37.9	41	89
Feb F30 High	30,000	High	49.0	67.0	291.7	31.3	86	60
Feb F56 Low	56,000	Low	49.0	94.0	32.5	25.9	676	94
Feb F56 Avg	56,000	Average	49.0	94.0	53.0	44.3	379	94
Feb F56 High	56,000	High	49.0	71.5	326.0	41.9	101	63
Discharge elevation = 35 m								
Aug F56 Avg	56,000	Average	59.0	94.0	38.2	33.5	611	94
Feb F56 Avg	56,000	Average	59.0	94.0	77.9	54.1	59	94
Discharge elevation = 55 m								
Aug F56 Avg	56,000	Average	39.0	87.5	67.4	44.0	377	88
Feb F56 Avg	56,000	Average	39.0	90.5	52.5	48.2	230	91
Discharge orientation = SW								
Aug F56 Avg	56,000	Average	49.0	94.0	60.4	49.9	156	94
Feb F56 Avg	56,000	Average	49.0	94.0	50.5	36.3	495	94
Discharge orientation = S								
Aug F56 Avg	56,000	Average	49.0	93.2	47.1	51.0	167	93
Feb F56 Avg	56,000	Average	49.0	94.0	53.0	44.3	379	94

Table 3-5 Produced Water Discharge Summary, Salinity = 42, 32.7 psu

Scenario ID	Effluent Discharge Rate	Current Velocity Profile	Max Rise Depth for Centreline	Max Fall Depth for Centreline	End of Near-Field Distance	Max Near-Field Plume Diameter	Target Dilution Factor Distance	Target Dilution Factor Depth
Effluent salinity = 42 psu	(m^3/d)		(m)	(m)	(m)	(m)	(m)	(m)
Summer Profile (August)								
Aug F30 Low	30,000	Low	43.0	63.3	54.8	27.4	992	63
Aug F30 Avg	30,000	Average	44.2	59.9	74.8	26.9	711	60
Aug F30 High	30,000	High	46.6	57.4	176.8	21.1	367	57
Aug F56 Low	56,000	Low	46.5	70.3	68.2	30.8	1576	70
Aug F56 Avg	56,000	Average	46.8	66.4	83.1	32.4	1149	66
Aug F56 High	56,000	High	47.5	61.1	185.2	27.4	628	61
Winter Profile (February)								
Feb F30 Low	30,000	Low	45.0	72.6	54.5	40.7	299	73
Feb F30 Avg	30,000	Average	46.5	62.7	59.7	33.3	305	63
Feb F30 High	30,000	High	48.6	56.8	200.6	19.8	189	57
Feb F56 Low	56,000	Low	47.2	77.7	73.5	53.2	383	78
Feb F56 Avg	56,000	Average	47.7	65.3	73.2	42.4	476	65
Feb F56 High	56,000	High	48.7	57.2	202.4	25.6	202	57
Effluent salinity = 32.7 psu								
Summer Profile (August)								
Aug F30 Low	30,000	Low	27.1	49.0	31.3	20.8	>1600	N/A
Aug F30 Avg	30,000	Average	31.0	49.0	42.6	22.1	1308	36
Aug F30 High	30,000	High	38.5	49.0	139.8	18.6	540	41
Aug F56 Low	56,000	Low	27.2	49.0	46.1	23.4	>1600	N/A
Aug F56 Avg	56,000	Average	30.2	49.0	55.7	25.4	>1600	N/A
Aug F56 High	56,000	High	37.4	49.0	136.9	22.1	1145	41
Winter Profile (February)								
Feb F30 Low	30,000	Low	14.9	49.0	29.8	34.0	435	15
Feb F30 Avg	30,000	Average	27.8	49.0	66.9	37.2	67	34
Feb F30 High	30,000	High	35.1	49.0	325.6	30.1	101	39
Feb F56 Low	56,000	Low	13.3	49.0	37.8	34.5	895	13
Feb F56 Avg	56,000	Average	25.3	49.0	86.3	49.9	86	33
Feb F56 High	56,000	High	34.4	49.0	326.0	36.9	121	37

The modelling results indicate that for the base case salinity value of 52.9 psu, the produced water plume may rise slightly (less than about 1 m) due to the initial high temperature and resulting low density relative to the ambient; however, the plume will be cooled quickly to levels when its density becomes higher than the ambient. From there the plume will start to sink as it continues to be cooled. The plume will eventually sink to the trap line or the ocean bottom. It is also observed that because the discharge elevation selected is near the boundary of the typical stratification limit in the summer, the effect of ocean stratification on the plume trajectory and dilution is minimal. The plume section view and dilution plots for the February, high discharge rate are presented in Figure 3-4 and Figure 3-5. The plots include results from model runs with high (blue), average (red), and low (green) ambient current conditions. The

solid lines represent the values for the plume centerline, while the dotted curves represent the values at the outer bounds of the plume.

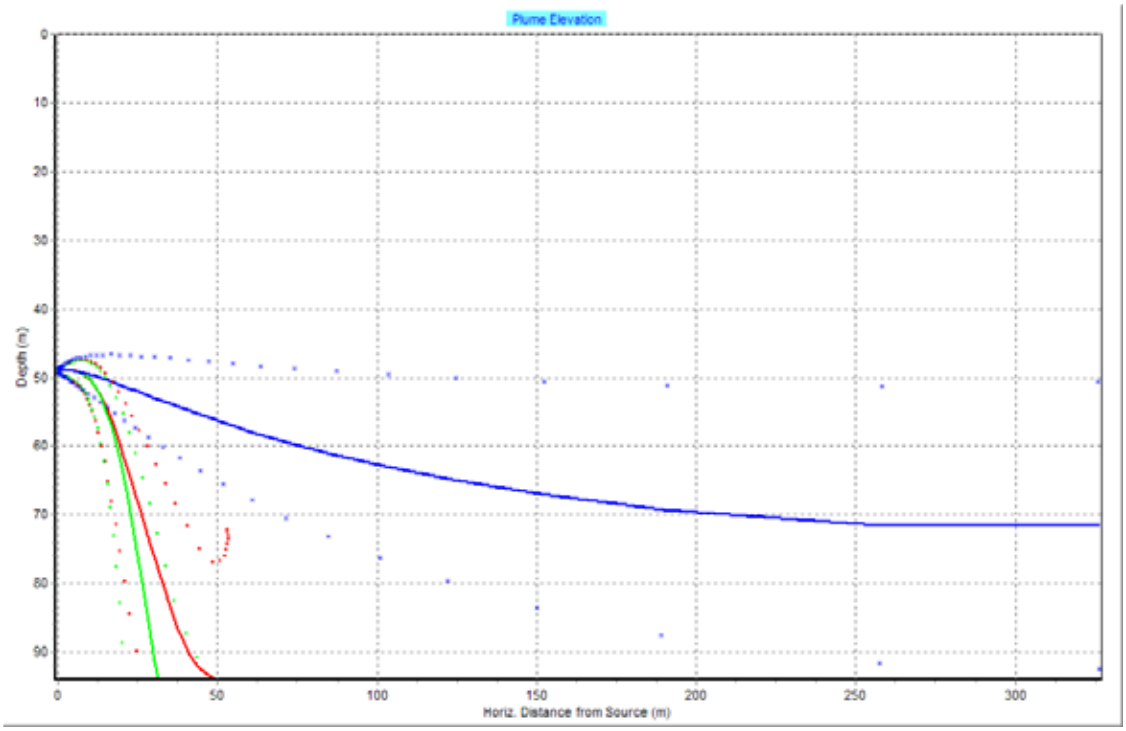


Figure 3-4 February, 56,000 m^3/d, 52.9 psu, produced water discharge plume section profile in high (blue), average (red), and low (green) current conditions.

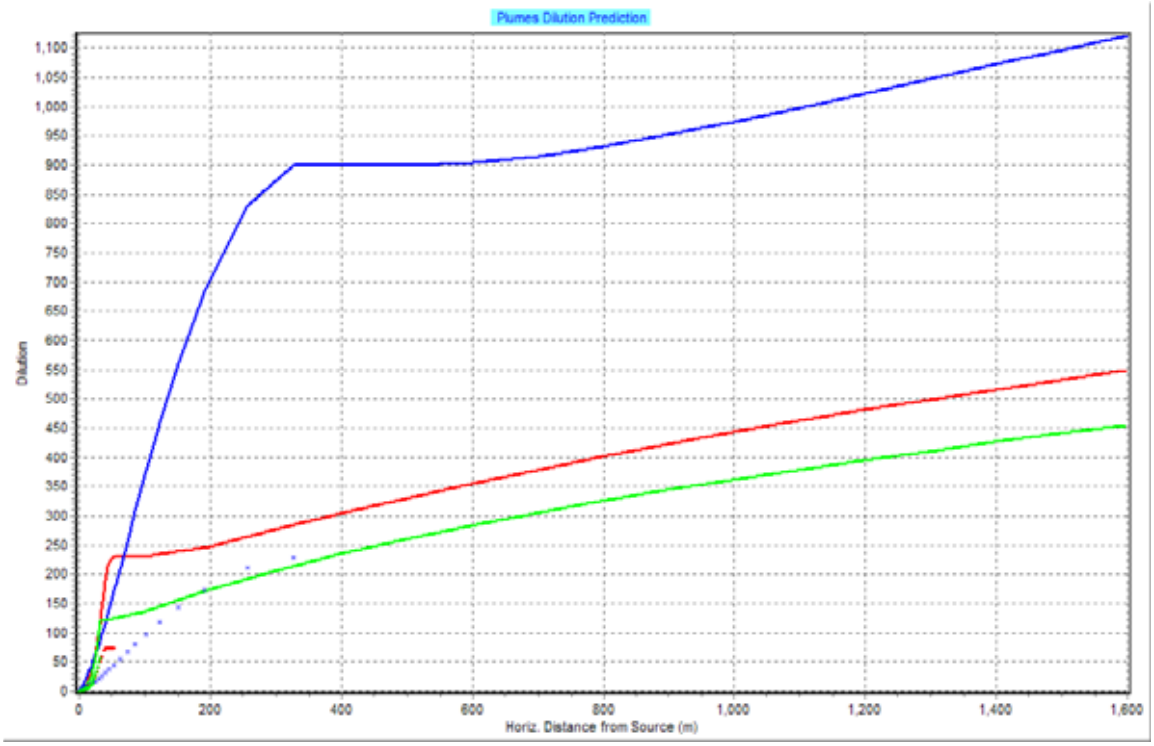


Figure 3-5 February, 56,000 m^3/d, 52.9 psu, produced water discharge plume dilution profile in high (blue), average (red), and low (green) current conditions.

For salinity of 42 psu, the produced water plume exhibits a greater initial rise due to the reduced salinity and density compared with the base case. The plume centerline rises about 3 m for low and average current conditions and slightly less for the high current speed. The amount of rise is greater (up to 6 m) for the low discharge rate. The plume diameters within about 50 m from the discharge are as large as about 20 to 40 m. As for the base case, after these initial rises the plumes all fall back to depths below the discharge elevation. This generally occurs within about 30 m for the low and average currents and within about 50 m for the high current.

For salinity of 32.7 psu, the produced water plume exhibits a still greater rise initially due to the reduced salinity and density. A slightly greater rise is exhibited in February compared with August though the general pattern is the same. The plume centerline in February rises up to about 15 m above the discharge point under high current conditions, rises about 24 m for average current conditions, and rises about 35 m for low currents. Under these (low current) conditions, the plume boundaries are predicted to reach the sea surface within a horizontal distance of about 30 m from the point of discharge (Figure 3-6). Under all modelled conditions for the 32.7 psu (near-ambient) discharge, the plumes remain above the discharge elevation, i.e., in the upper water column (Table 3-5).

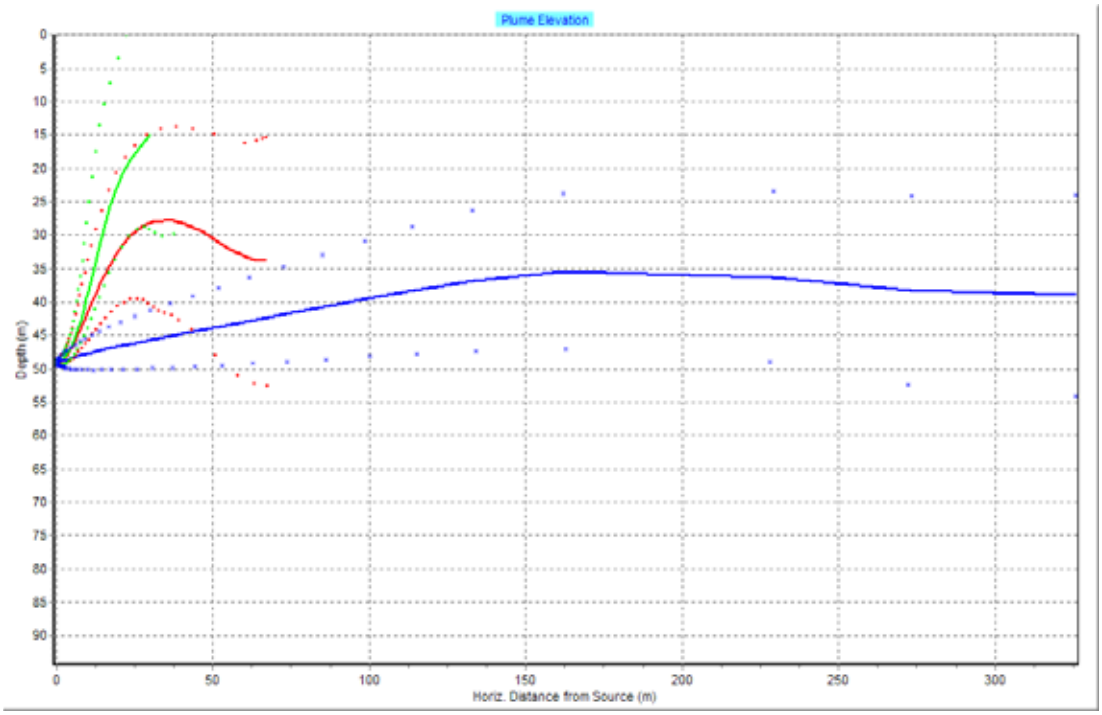


Figure 3-6 February, 30,000 m^3/d, 32.7 psu, produced water discharge plume section profile in high (blue), average (red), and low (green) current conditions.

Only under the salinity of 52.9 psu base case is the produced water plume predicted to reach the sea bottom. The modelling results show that the current velocity has a measurable effect on the near-field dilution and trajectory of the plume. With increasing current velocity, the near field distance increases, and the plume diameter at the end of near-field generally decreases. The plume will typically sink to the ocean bottom for low and average current conditions; however, it is simulated that under high current conditions, the plume will not sink to the ocean bottom.

The bottom is reached in both summer and winter, under low and average current conditions. The bottom is also reached for the discharge elevations of 35 and 55 m, both in winter and summer, and for both orientation sensitivities under summer conditions.

As reported in Table 3-44, for the produced water salinity of 52.9 psu, under the higher effluent discharge rate (56,000 m^3/d), the dilution factor of 300 is reached within a horizontal distance of 379 m in February under average current conditions, within a distance of 676 m under low ambient current conditions. In August, the dilution factor of 300 is reached at distances of 74 m under average current speeds and out to 352 m under low current speeds. The target dilution distances are comparatively smaller for the lower effluent discharge rate (30,000 m^3/d).

As noted above, under August and February low and average current conditions, the plume reaches the sea bottom (before a dilution factor of 300 is reached). The VPlumes primary UM3 model used to predict the near-field plume behaviour does not predict the plume fate once it encounters the bottom. The plume will remain at the bottom and advect with the ambient bottom currents and passively diffuse. In cases when the target dilution is not reached at the end of the near-field zone, the horizontal distances for target dilution are interpolated using the VPlumes far-field dispersion model. Figure 3-7 to Figure 3-9 (also contained in Appendix D) illustrate, for the February, high rate, base case, the distances and depth required to achieve the dilution factor of 300, resulting in 0.1 ppm (-1 on the log10 y-axis scale), as well as the associated plume diameter.

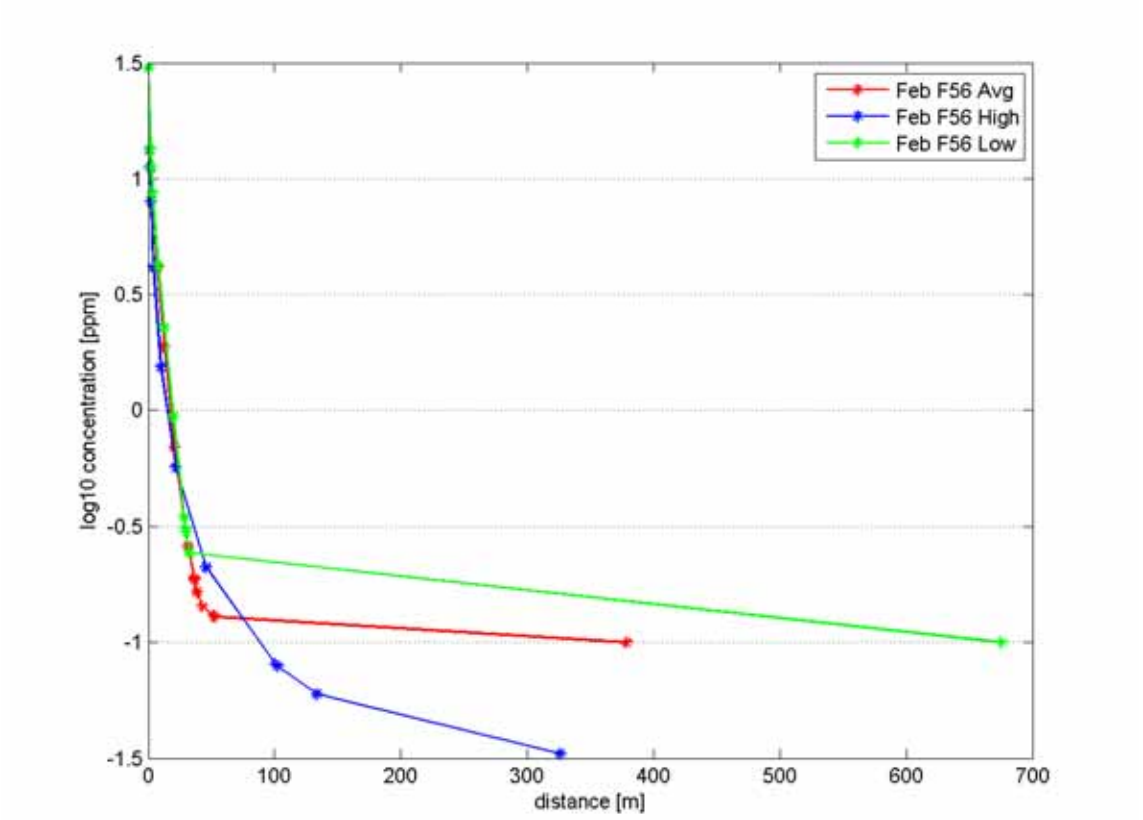


Figure 3-7 February, 56,000 m^3/d, 52.9 psu, zone of influence estimate, concentration vs. horizontal distance

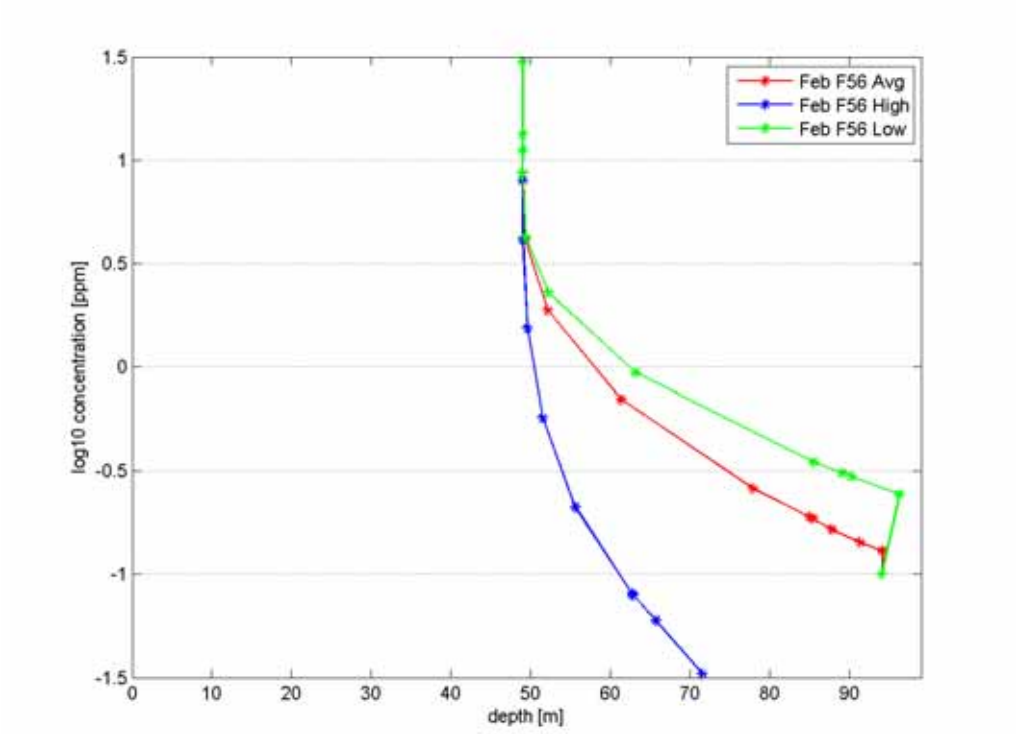


Figure 3-8 February, 56,000 m^3/d, 52.9 psu, zone of influence estimate, concentration vs. depth

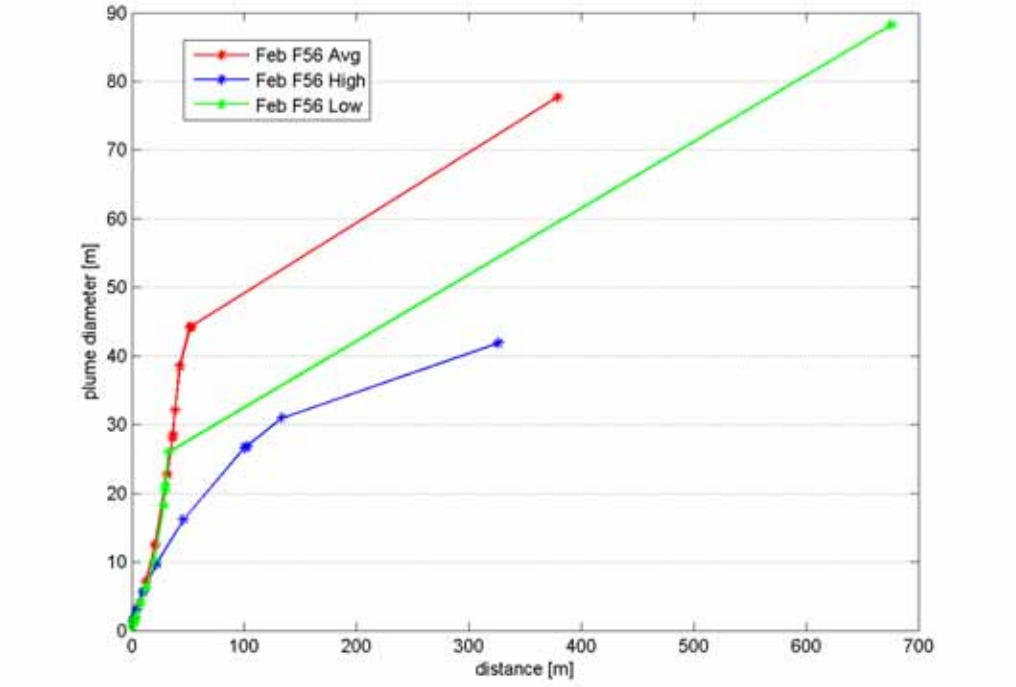


Figure 3-9 February, 56,000 m^3/d, 52.9 psu, zone of influence estimate, plume diameter vs. horizontal distance

Under high current conditions both in August and February the plume centreline is at a depth of about 60-70 m when a dilution factor of 300 is reached.

For the 'discharge closer to the seabed' sensitivity, at elevation of 35 m, the plume reaches the bottom: a dilution factor of 300 is achieved within a horizontal distance of 59 m (in February) to 611 m (in August) (Table 3-4). For the greater discharge elevation of 55 m sensitivity, the plume centerline remains above the bottom at depths of about 91 m in February and 88 m in August, although given the plume diameters are on the order of 30 to 40 m in diameter, seabed contact is predicted. A dilution factor of 300 is achieved within a horizontal distance of 230 m in February, and 377 m in August. For the discharge orientation sensitivities, the plume still encounters the bottom within about 30 to 50 m of discharge. A dilution factor of 300 is obtained within 156 m (August) to 495 m (February) for the southwest orientation, and within 167 m (August) to 379 m (February) for the south orientation.

Under the reduced salinity discharge scenarios, the plume centrelines do not encounter the sea bottom. Under low current conditions the boundaries of the plume are predicted to reach the sea surface within a horizontal distance of about 30 m (e.g., see the plume elevation view plot for "Salinity = 32.7 psu, Discharge Rate = 30,000 m3/d" 4th last page in Appendix D). Target dilution factors of 300 are reached at a wide range of horizontal distances depending on the scenario (Table 3-5). This distance varies from about 50 to 80 m in February under average current conditions to distances greater than 1600 m under low and average current speed conditions in August. Under these conditions, the target dilution was not reached within the acute mixing zone of 1600 m, and the model did not resolve the exact distance at which the target is reached. In these cases, due to the reduced salinity contrast and hence lower density compared with the base case, the plume encounters smaller depth ranges in which to dilute, hence less dilution is achieved over comparable horizontal distances. Greater horizontal distances are necessary to achieve the target dilution of 300 for these reduced salinity scenarios, but generally the higher discharge rate results in longer target dilution distances compared to the lower discharge rate scenarios.

The modelling results illustrate that a high current may provide a high initial dilution, especially under high discharge rate conditions. This is due to high turbulence and entrainment mixing typically associated with high current; however, with increasing distance from the discharge, the effect of high turbulence on dilution is offset by the reduced migration time. As a result, the contaminant concentration at a given location in the far field may be higher under high current conditions than under low current conditions. Another major factor controlling the time, and subsequently distance, within which the target dilution is achieved, is the effluent discharge rate. Depending on the relative orientation of the discharge direction and the ambient currents, these two factors can combine to prolong even further the target dilution distance by transporting the plume away from the source at a higher rate.

Therefore, the effect of current velocity on dilution is not always immediately apparent. The modelling results also show that the dilutions provided by the ambient under summer and winter temperature and salinity profiles in the project area are generally comparable.

Sensitivity analysis for discharge elevation and orientation relative to the ambient current indicates that an increase in the discharge elevation will result in an increased effluent dilution in the winter season, but decreased dilution rate in the summer season for the base case salinity scenario. Changing the discharge orientation of the diffuser port relative to the ambient current did not appear to improve dilution for the orientations considered. For the orientations considered to date, the best dilution is achieved for the base case orientation to the west.

Additional modelling was conducted to confirm the dilution envelope developed would encompass the typical ambient conditions experienced in the Project area. For this purpose, the May and October ambient temperature and salinity profiles as reported in the Hebron Metocean Design Basis (Chevron Energy Technology Company, 2005) report were used. The corresponding high, average and low currents for each month as reported in the document were used in the evaluation. In total, six additional scenarios were considered. The resulting dilutions simulated were compared with the envelope developed, and it was determined that the dilution for these scenarios fall within the envelope. As noted previously, seasonal ambient variation and stratification in terms of salinity and temperature profiles is typically limited to within 50 m from the surface of the ocean in the project area. Below the 50 m depth, where the interaction between the ambient and discharge plume primarily takes place, the ambient salinity and temperature profiles remain relatively constant. For this reason, the seasonal effect of the ambient conditions on dilution is expected to be limited.

4. Storage Displacement Water modelling

4.1 Methods

Oil will be stored in the GBS using Oil Storage/Ballast Systems with displaced water returned to the sea. When oil is pumped out of storage, seawater will be allowed to flow back into a buffer compartment and oil storage compartment under the natural hydrostatic head. A schematic of how such a system like this may be configured is shown in Figure 4-1.

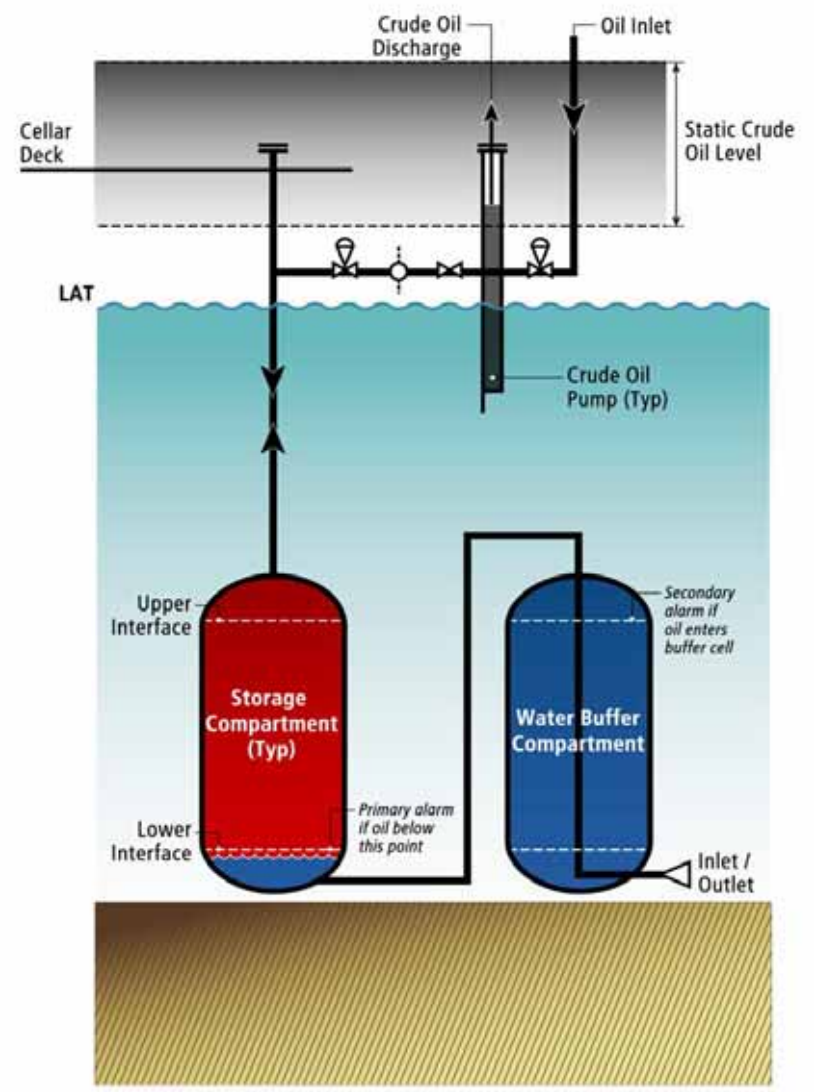


Figure 4-1 Wet Naturally-pressured Storage System

An objective of the modelling was to determine the seasonal pattern of this storage displacement water associated with production operations.

The dilution processes for storage displacement water are very similar to that for produced water discharge, which have been discussed in Section 3. The VP software was again selected for modelling storage displacement water discharge.

4.1.1 Model Input

VP requires the input of the following two groups of parameters, which are categorized in separate input tabs, for simulating a submerged plume as a result of discharge from diffuser port(s):

- diffuser and effluent discharge characteristics
- ambient characteristics

4.1.2 Diffuser and Effluent Discharge Input

For storage displacement water discharge modelling, a discharge rate of 26,000 m^3/d was used. Storage displacement water consists essentially of seawater and is expected to have salinities similar to that of the ambient at the depth of the water intake. The seawater salinity at a given location and depth experiences seasonal fluctuations; however, this fluctuation decreases with depth. The seasonal salinity fluctuation near the ocean bottom in the Project area, where water intake for the oil storage compartments will be located, is considerably less than the seasonal salinity fluctuation near the surface. In this modelling exercise, the salinity value near the ocean bottom of the Project area is used as a model input, and is adjusted for the ambient profiles (February and August) being modelled.

The crude oil stored in the oil storage compartments has an initial temperature measurably higher than that of the ambient seawater. It is expected that the oil will gradually be cooled by the ambient over time. When the oil is removed from the oil storage compartment ambient seawater is withdrawn via the water buffer compartment into the oil storage compartment. This seawater will be warmed up by the remaining oil in the storage compartment and its temperature will rise. The final temperature of the storage displacement water is dependent on the heat transfer between the oil and storage displacement water, and the length of time that the seawater is stored in the oil storage compartments. In this modelling exercise, the final temperature of the storage displacement water prior to its discharge is assumed to be 30°C. However, a sensitivity analysis was conducted to evaluate the effect of temperature on dilution of discharged storage displacement water.

Other parameters for the diffuser and storage water discharge input include the following:

- discharge port diameter: 0.42 m

- discharge vertical angle: 0° to horizontal
- discharge horizontal angle: 180° from east
- discharge elevation: 5 m from sea bottom
- oil concentration at discharge: 15 ppm based on the OWTG (NEB et al. 2002)

4.1.3 Ambient Characteristics

The ambient seawater characteristics required as input in the modelling include ambient temperature and salinity profiles, current velocity profiles and directions, background contaminant concentration and decay rate, and far-field dilution coefficient. These parameters used in the storage displacement water modelling are the same as those used in the produced water modelling, which have been discussed in Section 3.1.8.

4.1.4 Summary of Model Scenarios and Input

In summary, two ambient temperature and salinity profiles were considered, one for August, when maximum stratification typically occurs, and one for February, when minimum stratification typically occurs. The two ambient profiles represent the envelope of conditions that can typically be expected for an average year. Three velocity profiles were also considered, representing the high, average and low velocities that can be expected in the project area for summer and winter seasons. In combination, a total of six base case scenarios were considered. A summary of the scenarios is provided in Table 4-1.

Table 4-1 Storage Displacement Water Modelling Scenarios

	Scenario ID	Month [1]	Discharge Rate (m^3/d) [2]	Current Speed	Current Direction (to)	Discharge Elevation (m above sea bottom)	Discharge Temperature (°C)	Discharge Orientatation (to)	Discharge / Current Offset (deg) [3]
1	AL	August	26,000	low	S	5	30	W	90
2	AA	"	"	average	"	"	30	"	"
3	AH	"	"	high	"	"	30	"	"
4	FL	February	26,000	low	SW	"	30	"	45
5	FA	"	"	average	"	"	30	"	"
6	FH	"	"	high	"	"	30	"	"
7	SAE10 [4]	August	26,000	average	S	10	30	W	90
8	SAT10	"	"	"	"	5	10	"	"
9	SFE10	February	"	"	"	10	30	"	45
10	SFT10	"	"	"	"	5	10	"	"

Notes:
1. Month determines current, and temperature and salinity profiles used (A or F in Scenario ID).
2. The discharge orientation offset is the difference between current direction and discharge orientation direction.
3. The final four scenarios are sensitivities for discharge elevation and discharge temperature.

4.2 Results

A summary of effluent dilution with distance for the six scenarios simulated is presented in Table 4-2. The maximum and minimum dilution envelope that can typically be expected for the production life of the Hebron Project is presented in Figure 4-2, based on the maximum and minimum dilution values simulated for all the scenarios. The direct text and graphic model output for all identified modelling scenarios are presented in Appendix E.

The modelling results indicate that in all cases, the storage displacement water plume will rise as a result of its initial higher temperature than the ambient. The rise is the highest under low current conditions, when the plume is cooled the slowest. The rise is the smallest under high current conditions, when the plume is cooled the fastest. Under all conditions, the plume will not rise to within the 50 m depth from the ocean surface, where seasonal temperature and salinity stratification is expected. Therefore, seasonal stratification of the ocean environment will unlikely have a measurable effect on plume dilution. Under all cases, the storage displacement water plume will not rise to the surface

The modelling results show that the current velocity has a measurable effect on dilution. High currents tend to provide high initial dilution as a result of high turbulence. However, with increasing distance, the effect of turbulence associated with high current is offset by the high migration rate of the plume. As a result, the dilution achieved at a given distance is reduced. The reverse is true for low current conditions.

Table 4-2 Dilution Variation with Distance for Storage Displacement Water Modelling

Distance from Discharge (m)	Dilution Factor							
	AL	AA	AH	FL	FA	FH	Max	Min
0	1	1	1	1	1	1	1	1
10	16	26	36	17	22	22	36	16
20	38	71	60	37	50	41	71	37
30	64	139	82	68	81	58	139	58
40	73	160	103	72	101	73	160	72
50	80	162	124	75	102	87	162	75
60	87	165	145	78	103	102	165	78
70	94	167	167	81	104	117	167	81
80	101	169	188	84	105	131	188	84
90	108	171	209	87	106	143	209	87
100	115	173	227	91	107	156	227	91
300	390	337	341	237	200	210	390	200
500	758	547	374	427	319	228	758	228
700	1,201	790	436	651	457	262	1,201	262
900	1,707	1,060	510	904	610	301	1,707	301
1,100	2,269	1,356	590	1,184	778	345	2,269	345
1,300	2,881	1,675	676	1,488	958	390	2,881	390
1,500	3,541	2,015	765	1,814	1,150	439	3,541	439

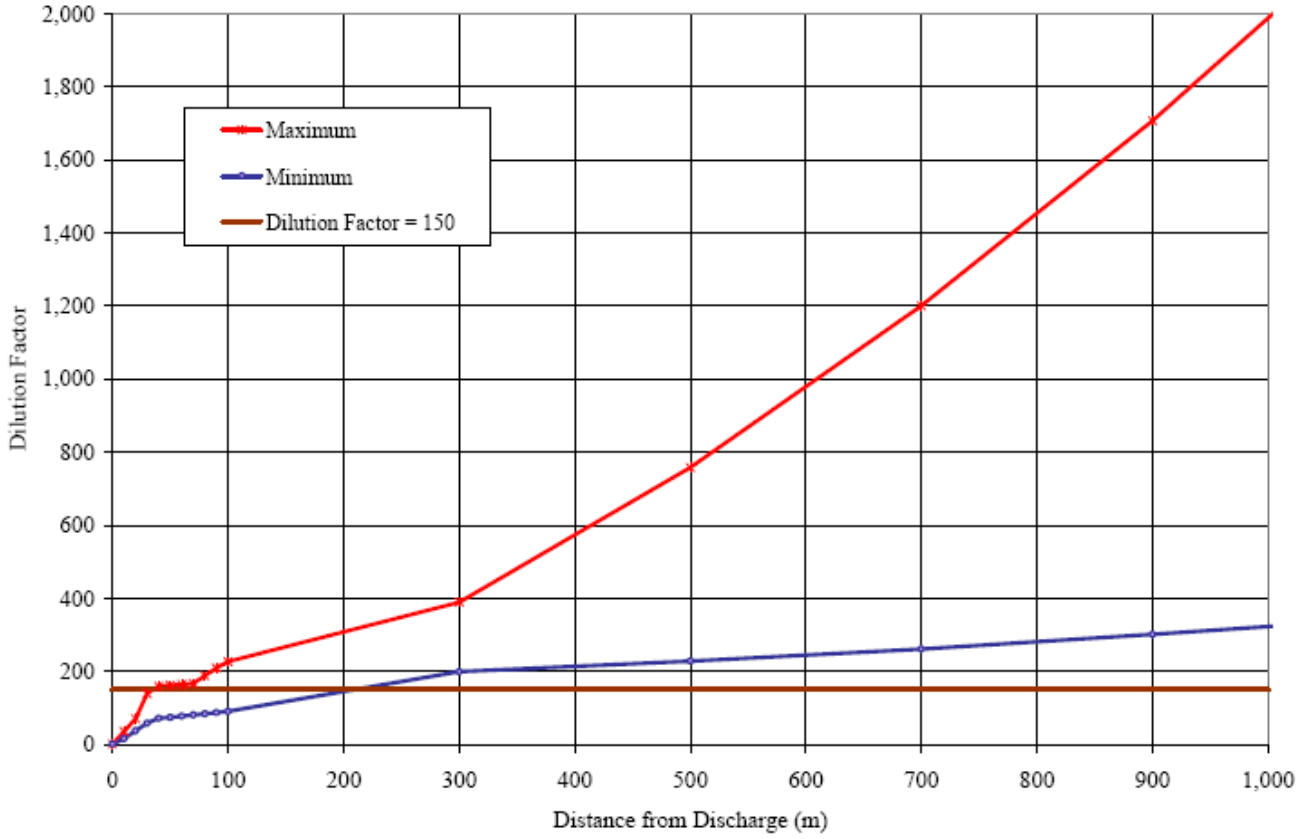


Figure 4-2 Dilution Envelope for Storage Displacement Water Modelling

As per the Offshore Waste Treatment Guidelines (NEB et al. 2002), the oil in water concentration discharge limit is 15 ppm. Using a 0.1 ppm oil concentration in evaluating the mixing zone distance, a dilution factor of 150 for the storage water displacement water discharge will be required to meet the oil concentration criteria. This dilution factor can be achieved within a distance of approximately 200 m for all scenarios modelled (Figure 4-2).

4.3 Sensitivity Analyses

Sensitivity analyses were conducted to evaluate the effect raising the discharge elevation might have on dilution. For this sensitivity, an alternate discharge elevation of 10 m from the sea bottom was considered for both August and February profiles under average current conditions. There is also some uncertainty regarding the temperature of the storage displacement water discharge. To evaluate the effect of discharge temperature on dilution, an alternative discharge temperature of 10°C was simulated for both the August and February ambient profiles. These four sensitivity scenarios are listed in Table 4-1.

A summary of results from the sensitivity analyses is provided in Table 4-3. Comparisons of the dilution factors for the August and February profiles for the selected elevation and temperature inputs are presented in Figure 4-3 and Figure 4-4 respectively. The figures show that increasing discharge elevation will have little effect on dilution. This is likely due to the fact that the discharge plume rises, and the increased elevation would have little effect on the plume dimension. Reducing the discharge temperature has limited effect on dilution. This is likely due to the fact that the plume will be cooled very quickly upon discharge, and the effect of discharge temperature diminishes within a short distance.

Table 4-3 Sensitivity Analyses for Storage Displacement Water Modelling

Distance from Discharge (m)	Dilution Factor					
	AA	SAE10	SAT10	FA	SFE10	SFT10
0	1	1	1	1	1	1
10	26	26	21	22	22	20
20	71	69	61	50	49	45
30	139	130	112	81	80	71
40	160	153	143	101	104	91
50	162	155	145	102	105	92
60	165	157	147	103	106	94
70	167	159	149	104	107	95
80	169	162	151	105	108	96
90	171	164	153	106	109	97
100	173	166	155	107	111	98
300	337	326	308	200	204	185
500	547	531	505	319	326	299
700	790	767	734	457	466	431
900	1,060	1,031	988	610	621	577
1,100	1,356	1,320	1,267	778	791	737
1,300	1,675	1,631	1,568	958	975	909
1,500	2,015	1,964	1,890	1,150	1,170	1,093

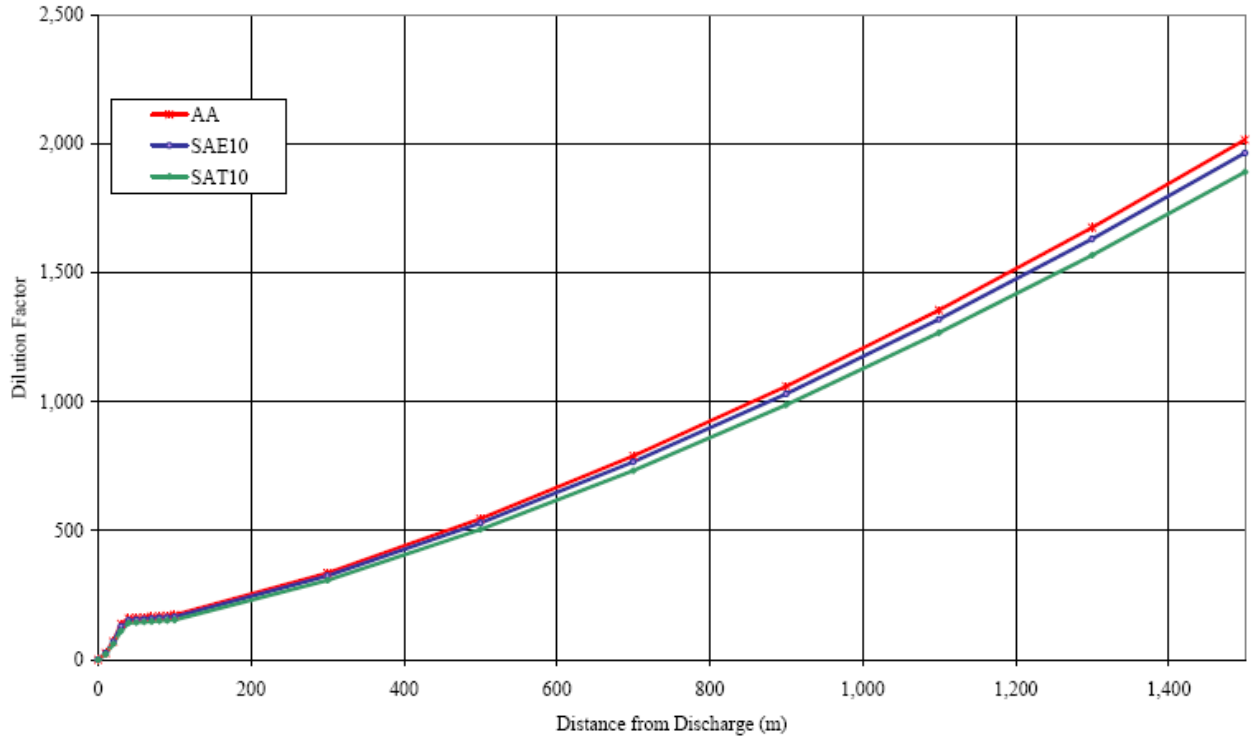


Figure 4-3 Sensitivity Analysis for Discharge Elevation and Temperature: August

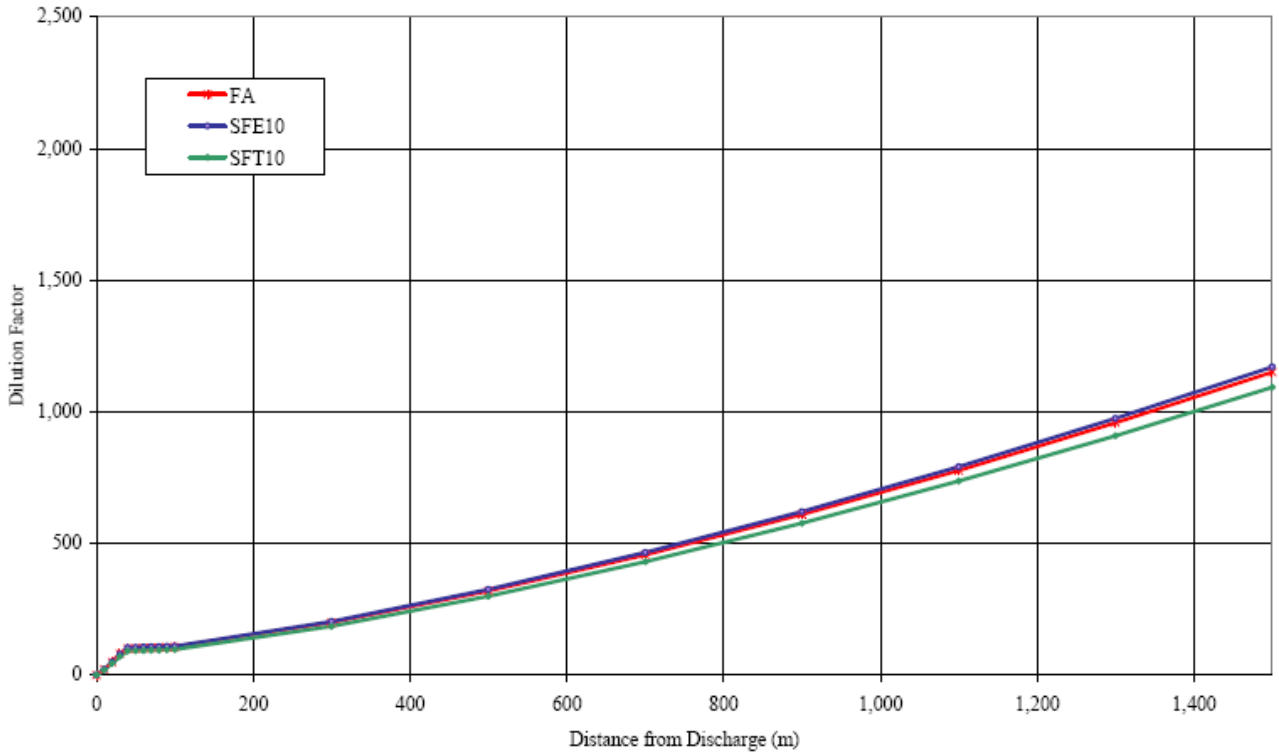


Figure 4-4 Sensitivity Analysis for Discharge Elevation and Temperature: February

4.4 Storage Displacement Water Modelling Conclusions

The modelling study shows that under all ambient conditions that can typically be expected in the Project area, an oil concentration criteria of 0.1 ppm can be achieved within a distance of 200 m.

Due to its high temperature relative to the ambient, the storage displacement water plume will rise in all cases. The distance will be greater under high current conditions than under low current conditions. In all cases, the plume will be unlikely to rise near the ocean surface.

Sensitivity analyses indicate that increasing the discharge elevation has little effect on dilution, and reducing the discharge temperature has only limited effect on dilution.

5. REFERENCES

5.1 Personal Communications

5.2 Literature Cited

AGAT Laboratories. *Hibernia Particle Size Distribution: Mobil et al. Hibernia K-18*. Prepared for Hibernia Management and Development Company Ltd., 1993.

Booman, C. and L. Foyn. Effects of the Water Soluble Fraction of Crude Oil on Marine Fish Larvae and Crustaceans. In: *Produced Water 2: Environmental Issues and Mitigation Technologies*. Environmental Science Research 52, Plenum Press, New York, NY., 1996.

Brandsma, M.G.. Computer Simulations of Oil-based Mud Cuttings Discharges in the North Sea. In: *The Physical and Biological Effects of Processed Oily Drill Cuttings*. E&P Forum Report No. 2.61/202, London, UK., 1996.

Canadian Association of Petroleum Producers. *Produced Water Waste Management*. Report 2001-030 prepared by Canadian Association of Petroleum Producers, 2001.

Chevron Energy Technology Company. *Metocean Design Criteria, Hebron Field, Grand Banks, East Coast Canada: Version: 2.1,* September 9, 2005.

ExxonMobil Canada Properties. *Hebron Project Description*. March 2009

ExxonMobil Upstream Research Company. *Hebron Metocean Criteria,*. Memo dated 2 September 2009, 91 p

Dal-Santo, R. *Development of a Continuous Five-Year Time-Series of Winds, Waves and Currents at Hibernia*. Report prepared for Mobil Oil Canada Ltd. Report prepared by Seaconsult Limited. 1996.

Hodgins, D.O.. Hibernia Effluent Fate and Effects Modelling. Report prepared for Hibernia Management and Development Company Ltd., 1993.

Hodgins, D.O. and S.L.M. Hodgins. *Distribution of Well Cuttings and Produced Water for the Terra Nova Development*. Report prepared for Terra Nova Alliance, 1998

Hodgins, D.O. and S.L.M. Hodgins. *Modelled Predictions of Well Cuttings Deposition and Produced Water Dispersion for the Proposed White Rose Development*. Report prepared for Husky Oil Operations Limited, 2000.

Hurlbut, S.E., S.E. French and B.J. Taylor. *Evaluation of Potential Effects of Major Oil Spills on Grand Banks Commerical Fish Species as a Result of Impacts on Eggs and Larvae*. Environmental Studies Research Funds Report No. 110, Calgary, AB. 53 pp., 1991.

Moore S.F. and R.L. Dwyer. *Effects of Oil on Marine Organisms: A Critical Assessment of Published Data*. Water Research, 8: 819-827, 1974.

NEB, C-NOPB and C-NSOPB (National Energy Board, Canada-Newfoundland Offshore Petroleum Board, and Canada-Nova Scotia Offshore Petroleum Board). *Offshore Waste Treatment Guidelines*, 2002.

Seaconsult Limited. *Physical Environment Data for Production Systems at Terra Nova*. Report prepared for Petro-Canada Inc., 1988.

Sleath, J.F.A.. Sea Bed Mechanics. Published by John Wiley & Sons, 1984.

T. Tedford, A. Drozdowski and C.G. Hannah, 2003. Suspended Sediment Drift and Dispersion at Hibernia. Report prepared by Ocean Sciences Division, Maritimes Region, Fisheries and Oceans Canada.

6. Glossary / Acronyms

1D. one-dimensional.

3D. three-dimensional.

ADM. Drill cuttings deposition modelling software.

advection. The process of, or referring to the transport of one fluid mass (air, water) by the movement of another.

bathymetry. The measurement of depths of water in oceans, seas and lakes; also the information derived from such measurements.

bentonite. A clay formed from volcanic ash decomposition.

borehole. The hole in the earth made by the drill; the uncased drill hole from the surface to the bottom of the well.

casing. Steel pipe used in oil and gas wells to seal off fluids from the *borehole* and to prevent the walls of the hole from sloughing or caving. There may be several strings of casing in a well, one inside the other.

C-NOPB. Canada-Newfoundland Offshore Petroleum Board. Now, the C-NLOPB (Canada-Newfoundland and Labrador Offshore Petroleum Board).

C-NSOPB. Canada-Nova Scotia Offshore Petroleum Board.

clay. A mineral fragment or detrital particle of any composition (often a crystalline fragment of a clay mineral), smaller than a very fine silt grain, having a diameter less than 4 microns.

crude oil. Unrefined petroleum.

CTD. Conductivity-temperature-depth.

DFN. Densimetric Froude Number.

development drilling. Drilling and bringing into production additional wells on a lease following project the drilling of the discovery and appraisal wells.

development well. A well drilled in an area already proved to be productive.

drill string. The column or string of drill pipe.

drill water. Water used as the liquid phase in water-based mud; usually denoting non-saline water.

drilling mud. A special mixture of clay, water and chemical additives pumped down the wellbore through the drill pipe and drill bit to cool the rapidly rotating bit, lubricate the drill pipe as it turns in the wellbore, and carry rock cuttings to the surface; may have a water base or oil base.

fines. Very fine silt and clay mineral sediment particles.

floc. A flocculent mass formed in a fluid through precipitation or aggregation of suspended particles

flocculation. Formation into flocculent masses.

flocculent. Having a fluffy or woolly appearance.

formation water. See *produced wate*r.

FEED. Front End Engineering and Design.

g. The abbreviation for gram.

gravity base structure (GBS). The base of an offshore drilling and production platform, usually made of concrete, and of such weight that it is held securely on the ocean bottom without the need for piling or anchors.

injection water. Water pumped into the formation to maintain reservoir pressure (secondary recovery technique); offshore, injection water is filtered seawater treated with biocides, oxygen scavenger and scale inhibitor.

kg. The abbreviation for kilogram.

km. The abbreviation for kilometre.

L. The abbreviation for litre.

LC50. The concentration of a toxicant necessary to kill 50 percent of the test organisms in a standard time period.

larva. The first immature phases of many animals after hatching of eggs and before assuming the adult form and habit.

m. The abbreviation for metre.

m^2. The abbreviation for square metre.

m^3. The abbreviation for cubic metre.

mg. The abbreviation for milligram.

mm. The abbreviation for millimetre.

micron. One millionth of a metre.

NEB. National Energy Board.

OWTG. Offshore Waste Treatment Guidelines.

pebbles. Smooth rounded stones ranging in diameter from 2 to 64 mm.

platform. A large structure used during the development and production phases to support such facilities as the drilling rigs, living quarters, production equipment and helipads.

plume. A trail of effluent, in this report, either produced water or storage displacement water.

porosity. The volume of the pore space expressed as a percentage of the total volume of the rock mass.

ppm. Parts per million.

produced water. Water brought up from hydrocarbon bearing strata during the extraction of oil and/or gas and can include formation water, injection water, small volumes of condensed water, and trace amounts of treatment chemicals.

psu. Practical salinity unit.

reservoir. A subsurface, porous, permeable rock body in which oil or gas has accumulated; most reservoir rocks are limestones, dolomites, sandstones, or a combination of these.

rig. Refers to the combination of equipment used to drill wells.

sand. A detrital particle smaller than a granule and larger than a coarse silt grain, having a diameter in the range of 0.0625 mm to 2 mm.

SBM. Synthetic-based mud.

shale. Sedimentary rock consisting dominantly of clay-sized particles, an appreciable amount of which are clay minerals.

silt. A mineral sediment particle, smaller than a very fine sand grain, having a diameter less than 62 microns.

sigma. Density of seawater

stratification. Division of the water column into layers, or strata, because of differences in water density, structure or temperature.

t. The abbreviation for tonne (a metric ton).

thermocline. A temperature gradient as in a layer of sea water, in which the temperature decrease with depth is greater than that of the overlying and underlying water.

topside facilities (or topsides). The oil- and gas-producing and support equipment located on the top of an offshore structure.

transport (or transportation). A phase of sedimentation that includes the movement by natural agents (such as flowing water, ice, wind or gravity) of sediment or of any loose material, either as solid particles or in solution, from one place to another on or near the Earth's surface (e.g., the drifting of sand along a seashore under the influence of currents, the creeping movement of rocks on a glacier or the conveyance of silt, clay and dissolved salts by a stream).

VP. Visual Plumes modelling software.

water column. The vertical dimension of a body of water (i.e., the water between a reference point or area on the surface and one located directly below it on the bottom).

WBM. Water-based mud. A drilling mud in which the continuous phase is water. See *drilling mu*d.

well casing. See *casin*g.

Appendix A
Grand Banks Currents
(Source: Dal-Santo 1986)

Site: Hibernia Time-Series
Sampling Interval (DT): 1 h
Observation Period: 1980/ 1/ 1 0: 0 to 1984/12/31 23: 0 GMT

		Mean	Std Dev	Median	Max	Min	95% Upper Limit	95% Lower Limit	# Points
Near-Surface	Jan	21.05	12.69	19.00	67.00	0.00	44.00	4.00	3720
Current Speed (cm/s)	Feb	18.05	10.62	16.00	59.00	0.00	38.00	3.00	3408
	Mar	14.63	8.22	14.00	47.00	0.00	30.00	3.00	3720
	Apr	14.55	8.20	14.00	114.00	0.00	29.00	3.00	3600
	May	13.54	7.37	13.00	44.00	0.00	27.00	3.00	3720
	Jun	13.90	8.64	13.00	59.00	0.00	29.00	2.00	3600
	Jul	13.78	7.82	13.00	50.00	0.00	28.00	3.00	3720
	Aug	15.36	10.14	13.00	74.00	0.00	33.00	3.00	3720
	Sep	15.91	11.51	14.00	127.00	0.00	36.00	3.00	3600
	Oct	18.58	11.32	16.00	68.00	0.00	39.00	4.00	3720
	Nov	21.33	12.38	19.00	74.00	1.00	45.00	5.00	3600
	Dec	20.28	11.67	18.00	59.00	0.00	41.00	4.00	3720
	Total	16.74	10.59	15.00	127.00	0.00	37.00	3.00	43848
Mid-Depth	Jan	18.04	8.39	17.00	48.00	0.00	32.00	5.00	3720
Current Speed (cm/s)	Feb	15.75	8.51	15.00	61.00	1.00	31.00	4.00	3408
	Mar	13.17	6.74	13.00	54.00	0.00	25.00	4.00	3720
	Apr	13.59	6.71	13.00	54.00	0.00	26.00	4.00	3600
	May	11.89	5.83	12.00	38.00	0.00	22.00	2.00	3720
	Jun	10.91	6.89	11.00	75.00	0.00	23.00	2.00	3600
	Jul	12.80	6.07	12.00	44.00	0.00	24.00	4.00	3720
	Aug	12.66	5.65	12.00	40.00	0.00	23.00	4.00	3720
	Sep	14.83	8.36	13.00	59.00	0.00	32.00	4.00	3600
	Oct	16.54	7.32	16.00	57.00	0.00	29.00	6.00	3720
	Nov	19.01	8.16	18.00	119.00	1.00	33.00	7.00	3600
	Dec	20.24	9.06	19.00	78.00	0.00	37.00	7.00	3720
	Total	14.95	7.91	14.00	119.00	0.00	29.00	4.00	43848
Near-Bottom	Jan	14.17	6.25	14.00	39.00	0.00	26.00	5.00	3720
Current Speed (cm/s)	Feb	14.33	7.47	13.00	57.00	0.00	28.00	4.00	3408
	Mar	12.79	6.55	12.00	46.00	0.00	25.00	4.00	3720
	Apr	11.88	5.35	12.00	30.00	0.00	21.00	4.00	3600
	May	11.02	4.94	11.00	32.00	0.00	20.00	4.00	3720
	Jun	11.32	5.17	11.00	36.00	1.00	21.00	4.00	3600
	Jul	11.12	5.20	10.00	36.00	0.00	21.00	4.00	3720
	Aug	11.00	5.24	11.00	33.00	0.00	20.00	3.00	3720
	Sep	11.65	5.63	11.00	56.00	0.00	22.00	3.00	3600
	Oct	13.06	5.79	13.00	36.00	0.00	24.00	4.00	3720
	Nov	15.25	6.39	15.00	72.00	0.00	26.00	6.00	3600
	Dec	15.18	7.37	14.00	57.00	0.00	29.00	5.00	3720
	Total	12.72	6.19	12.00	72.00	0.00	24.00	4.00	43848

Site: Hibernia Current Time-Series
Sampling Interval: 60 min
Observation Period: January

Near-Surface Current Speed vs. Current Direction

	Speed (cm/s)														
Dir (to)	0 to 5	5 to 10	10 to 15	15 to 20	20 to 25	25 to 30	30 to 35	35 to 40	40 to 45	45 to 50	50 to 55	55 to 60	60 to 65	65 to 70	# of Obs.	% Total
N	16	52	53	28	21	24	30	19	12	10		1			266	7.2
NE	26	67	53	52	44	49	35	31	14	3	3				377	10.1
E	34	55	74	43	31	30	30	26	26	4	5	1			359	9.7
SE	28	67	80	62	45	40	44	38	20	9	6	1			440	11.8
S	28	81	113	115	87	113	101	40	39	23	10	5	1	3	759	20.4
SW	45	124	141	111	98	100	66	67	30	24	6	6	2		820	22.0
W	21	73	82	57	25	46	38	34	15	15	4	4	2	1	417	11.2
NW	26	44	44	30	19	30	26	34	12	10	2	2	1		280	7.5
Calm	2														2	0.1
Sum	226	563	640	498	370	432	370	289	168	98	36	20	6	4	3720	
% Exceed	93.9	78.8	61.6	48.2	38.3	26.6	16.7	8.9	4.4	1.8	0.8	0.3	0.1	0.0		

Site: Hibernia Current Time-Series
Sampling Interval: 60 min
Observation Period: February

Near-Surface Current Speed vs. Current Direction

	Speed (cm/s)													
Dir (to)	0 to 5	5 to 10	10 to 15	15 to 20	20 to 25	25 to 30	30 to 35	35 to 40	40 to 45	45 to 50	50 to 55	55 to 60	# of Obs.	% Total
N	30	62	65	65	42	33	15	7	7	2	1		329	9.7
NE	36	88	123	104	44	30	26	9	2				462	13.6
E	33	55	61	50	35	33	12	3	1	1	1		285	8.4
SE	36	66	69	71	43	36	23	5	7	8	3		367	10.8
S	29	87	116	106	99	66	40	38	22	12	2	6	623	18.3
SW	38	86	124	130	126	91	57	37	28	16	7	1	741	21.7
W	30	46	58	63	51	43	36	15	10	4			356	10.4
NW	25	40	56	35	31	21	12	12	7	1	2		242	7.1
Calm	3												3	0.1
Sum	260	530	672	624	471	353	221	126	84	44	16	7	3408	
% Exceed	92.4	76.8	57.1	38.8	25.0	14.6	8.1	4.4	2.0	0.7	0.2	0.0		

Site: Hibernia Current Time-Series
Sampling Interval: 60 min
Observation Period: March

Near-Surface Current Speed vs. Current Direction

Speed (cm/s)

Dir (to)	0 to 5	5 to 10	10 to 15	15 to 20	20 to 25	25 to 30	30 to 35	35 to 40	40 to 45	45 to 50	# of Obs.	% Total
N	21	74	77	89	74	24	17	14	9		399	10.7
NE	40	76	126	150	79	41	23	25	6		566	15.2
E	45	107	103	96	53	15	7	3			429	11.5
SE	42	95	68	62	40	14	10	7			338	9.1
S	46	121	164	94	75	45	15	7	2		569	15.3
SW	43	145	145	153	95	46	23	13	1		664	17.8
W	40	119	122	96	43	19	7		2	1	449	12.1
NW	31	81	71	56	29	16	9	3	4	1	301	8.1
Calm	5										5	0.1
Sum	313	818	876	796	488	220	111	72	24	2	3720	
% Exceed	91.6	69.6	46.0	24.7	11.5	5.6	2.6	0.7	0.1	0.0		

Observation Period: April

Near-Surface Current Speed vs. Current Direction

Speed (cm/s)

Dir (to)	0 to 5	5 to 10	10 to 15	15 to 20	20 to 25	25 to 30	30 to 35	35 to 40	40 to 45	45 to 50	50 to 55	55 to 60	60 to 65	65 to 70	70 to 75	75 to 80	80 to 85	85 to 90	90 to 95	95 to 100	100 to 105	105 to 110	110 to 115	# of Obs.	% Total
N	38	101	115	126	88	35	16	12	4															535	14.9
NE	37	101	155	133	106	43	19	3	3															600	16.7
E	35	115	100	71	41	24	7	1																394	10.9
SE	43	70	94	73	49	45	14	3	2															393	10.9
S	28	110	83	68	63	47	27		2	3														431	12.0
SW	48	97	114	118	81	48	9	7	1															523	14.5
W	45	100	120	86	39	17	4	3	2	1		2											1	420	11.7
NW	29	89	87	44	33	12	3	1		1														299	8.3
Calm	5																							5	0.1
Sum	308	783	868	719	500	271	99	30	14	5	0	2	0	0	0	0	0	0	0	0	0	0	1	3600	
% Exceed	91.4	69.7	45.6	25.6	11.7	4.2	1.4	0.6	0.2	0.1	0.1	0.0	0.0	0.0	0.0	0.0	0.0	0.0	0.0	0.0	0.0	0.0	0.0		

Site: Hibernia Current Time-Series
Sampling Interval: 60 min
Observation Period: May

Near-Surface Current Speed vs. Current Direction

Speed (cm/s)

Dir (to)	0 to 5	5 to 10	10 to 15	15 to 20	20 to 25	25 to 30	30 to 35	35 to 40	40 to 45	# of Obs.	% Total
N	58	107	90	84	47	9	5	1		401	10.8
NE	70	115	124	114	47	15	7	1		493	13.3
E	42	121	116	88	44	14	11	4	1	441	11.9
SE	45	110	105	110	51	20	11	2	2	456	12.3
S	50	99	151	126	102	47	24	8	1	608	16.3
SW	39	102	149	147	83	53	18	1		592	15.9
W	38	88	123	104	49	16	9	1		428	11.5
NW	39	78	79	48	33	8	2	1	1	289	7.8
Calm	12									12	0.3
Sum	393	820	937	821	456	182	87	19	5	3720	
% Exceed	89.4	67.4	42.2	20.1	7.9	3.0	0.6	0.1	0.0		

Site: Hibernia Current Time-Series
Sampling Interval: 60 min
Observation Period: June

Near-Surface Current Speed vs. Current Direction

Speed (cm/s)

Dir (to)	0 to 5	5 to 10	10 to 15	15 to 20	20 to 25	25 to 30	30 to 35	35 to 40	40 to 45	45 to 50	50 to 55	55 to 60	# of Obs.	% Total
N	48	70	69	33	32	5	7	2		1			267	7.4
NE	70	89	79	60	36	7	4		1				346	9.6
E	54	82	90	70	43	19	5	2	1	2			368	10.2
SE	65	110	115	109	69	44	18	8	4	2		1	545	15.1
S	111	150	133	151	105	75	26	7	2	1			761	21.1
SW	75	144	133	151	105	59	30	9	2	3	2	1	714	19.8
W	41	81	68	80	52	25	10	5	3	1	1	1	368	10.2
NW	37	54	40	34	27	13	8	5	1				219	6.1
Calm	12												12	0.3
Sum	513	780	727	688	469	247	108	38	14	10	3	3	3600	
% Exceed	85.8	64.1	43.9	24.8	11.7	4.9	1.9	0.8	0.4	0.2	0.1	0.0		

Site: Hibernia Current Time-Series
Sampling Interval: 60 min
Observation Period: July

Near-Surface Current Speed vs. Current Direction

	Speed (cm/s)												
Dir (to)	0 to 5	5 to 10	10 to 15	15 to 20	20 to 25	25 to 30	30 to 35	35 to 40	40 to 45	45 to 50	50 to 55	# of Obs.	% Total
N	24	42	49	56	29	13	3	1				217	5.8
NE	40	50	62	61	36	15	5	3	1			273	7.3
E	50	78	74	87	46	13	8		1	1	1	359	9.7
SE	84	164	140	140	71	42	16	2	3	1	1	664	17.8
S	93	199	222	211	110	65	32	6	2	3		943	25.3
SW	67	172	183	163	89	45	15	8	2			744	20.0
W	35	74	79	80	42	18	6	4	2			340	9.1
NW	15	35	42	43	23	7	1					166	4.5
Calm	14											14	0.4
Sum	422	814	851	841	446	218	86	24	11	5	2	3720	
% Exceed	88.7	66.8	43.9	21.3	9.3	3.4	1.1	0.5	0.2	0.1	0.0		

Site: Hibernia Current Time-Series
Sampling Interval: 60 min
Observation Period: August

Near-Surface Current Speed vs. Current Direction

	Speed (cm/s)																
Dir (to)	0 to 5	5 to 10	10 to 15	15 to 20	20 to 25	25 to 30	30 to 35	35 to 40	40 to 45	45 to 50	50 to 55	55 to 60	60 to 65	65 to 70	70 to 75	# of Obs.	% Total
N	35	64	60	46	21	19	14	3			1	2	1		1	267	7.2
NE	33	80	82	50	41	14	7	5	2			1	1			316	8.5
E	37	85	104	63	40	23	6	3	3	2	2	2		1		371	10.0
SE	51	130	160	116	96	49	15	12	7	2	2	4				644	17.3
S	61	189	174	149	116	59	35	12	7	7	5	3	2			819	22.0
SW	51	115	164	120	91	49	39	14	3	4	3	2	1	2		658	17.7
W	33	90	97	58	31	25	21	13	5			5	2	1		381	10.2
NW	32	72	58	36	18	17	12	3	1	2	1		2	2	2	258	6.9
Calm	6															6	0.2
Sum	339	825	899	638	454	255	149	65	28	17	14	19	9	6	3	3720	
% Exceed	90.9	68.7	44.5	27.4	15.2	8.3	4.3	2.6	1.8	1.4	1.0	0.5	0.2	0.1	0.0		

Site: Hibernia Current Time-Series
Sampling Interval: 60 min
Observation Period: September

Near-Surface Current Speed vs. Current Direction

Speed (cm/s)

Dir (to)	0 to 5	5 to 10	10 to 15	15 to 20	20 to 25	25 to 30	30 to 35	35 to 40	40 to 45	45 to 50	50 to 55	55 to 60	60 to 65	65 to 70	70 to 75	75 to 80	80 to 85	85 to 90	90 to 95	95 to 100	100 to 105	105 to 110	110 to 115	115 to 120	120 to 125	125 to 130	# of Obs.	% Total
N	40	62	87	48	47	24	23	17	7	5	2		1	1													364	10.1
NE	43	86	94	65	50	18	9	7	4	1	2				1	1		1									382	10.6
E	44	101	86	47	36	17	11	4	2	1	1		1	1	1		1										354	9.8
SE	42	102	117	92	57	31	18	13		5	2					2				1	1						483	13.4
S	61	126	118	107	74	71	47	26	22	11	4			1	1				1	1							671	18.6
SW	50	134	155	119	103	42	29	14	12	8	3	1		1				1		1						1	674	18.7
W	41	102	93	80	52	28	4	3	6	2	2	1	1				1								1		417	11.6
NW	36	66	55	49	21	8	5	2	2		1		1			1		1									248	6.9
Calm	7																										7	0.2
Sum	364	779	805	607	440	239	146	86	55	33	17	2	4	4	3	4	2	3	1	3	1	0	0	1	0	1	3600	
% Exceed	89.9	68.3	45.9	29.0	16.8	10.2	6.1	3.7	2.2	1.3	0.8	0.7	0.6	0.5	0.4	0.3	0.3	0.2	0.2	0.1	0.1	0.1	0.1	0.0	0.0	0.0		

Observation Period: October

Near-Surface Current Speed vs. Current Direction

Speed (cm/s)

Dir (to)	0 to 5	5 to 10	10 to 15	15 to 20	20 to 25	25 to 30	30 to 35	35 to 40	40 to 45	45 to 50	50 to 55	55 to 60	60 to 65	65 to 70	# of Obs.	% Total
N	32	63	74	54	39	32	21	18	6	10	3	1			353	9.5
NE	31	75	81	74	51	35	22	15	11	2	4			1	402	10.8
E	24	69	74	54	40	43	21	12	10	2	4	1			354	9.5
SE	38	74	80	71	64	50	40	19	15	7	3	1	1		463	12.4
S	40	91	124	130	100	80	65	35	16	6	2				689	18.5
SW	48	99	115	121	111	71	70	39	26	4	3	4	1	2	714	19.2
W	43	81	114	60	45	44	39	22	9	6	3	3	2	1	472	12.7
NW	14	55	70	42	20	23	22	11	7	3	3	1		1	272	7.3
Calm	1														1	0.0
Sum	271	607	732	606	470	378	300	171	100	40	25	11	4	5	3720	
% Exceed	92.7	76.4	56.7	40.4	27.8	17.6	9.6	5.0	2.3	1.2	0.5	0.2	0.1	0.0		

Site: Hibernia Current Time-Series
Sampling Interval: 60 min
Observation Period: November

Near-Surface Current Speed vs. Current Direction

	Speed (cm/s)																
Dir (to)	0 to 5	5 to 10	10 to 15	15 to 20	20 to 25	25 to 30	30 to 35	35 to 40	40 to 45	45 to 50	50 to 55	55 to 60	60 to 65	65 to 70	70 to 75	# of Obs.	% Total
N	13	44	43	30	32	41	41	19	9	4	5	2				283	7.9
NE	18	55	53	55	41	51	44	25	10	9	5	2				368	10.2
E	21	58	54	56	28	40	27	17	13	8	10					332	9.2
SE	19	60	101	66	60	38	28	25	12	13	5	3		1		431	12.0
S	22	78	118	133	101	83	48	40	24	17	10	2	1	4	1	682	18.9
SW	30	89	120	117	123	100	79	57	36	22	11	6	2	2	2	796	22.1
W	17	71	76	64	71	52	37	23	20	12	8	1	2	2		456	12.7
NW	16	39	32	44	27	37	21	16	9	8		1	2			252	7.0
Calm																	
Sum	156	494	597	565	483	442	325	222	133	93	54	17	7	9	3	3600	
% Exceed	95.7	81.9	65.4	49.7	36.3	24.0	14.9	8.8	5.1	2.5	1.0	0.5	0.3	0.1	0.0		

Site: Hibernia Current Time-Series
Sampling Interval: 60 min
Observation Period: December

Near-Surface Current Speed vs. Current Direction

	Speed (cm/s)													
Dir (to)	0 to 5	5 to 10	10 to 15	15 to 20	20 to 25	25 to 30	30 to 35	35 to 40	40 to 45	45 to 50	50 to 55	55 to 60	# of Obs.	% Total
N	27	64	48	24	14	19	28	21	6	1	1		253	6.8
NE	32	72	65	49	38	34	34	14	11	1	1		351	9.4
E	28	66	75	34	30	38	18	21	13	5	3		331	8.9
SE	25	69	70	61	32	41	37	28	19	4	10	6	402	10.8
S	19	87	125	159	141	107	103	60	26	16	5	4	852	22.9
SW	28	87	133	142	134	128	126	66	32	9	10	5	900	24.2
W	22	72	86	47	38	44	45	23	20	6			403	10.8
NW	24	55	35	26	12	15	27	22	5	5			226	6.1
Calm	2												2	0.1
Sum	207	572	637	542	439	426	418	255	132	47	30	15	3720	
% Exceed	94.4	79.1	61.9	47.4	35.6	24.1	12.9	6.0	2.5	1.2	0.4	0.0		

Site: Hibernia Current Time-Series
Sampling Interval: 60 min
Observation Period: 1980/ 1/ 1 0: 0 to 1984/12/31 23: 0 GMT

Near-Surface Current Speed vs. Current Direction

Speed (cm/s)

Dir (to)	0 to 5	5 to 10	10 to 15	15 to 20	20 to 25	25 to 30	30 to 35	35 to 40	40 to 45	45 to 50	50 to 55	55 to 60	60 to 65	65 to 70	70 to 75	75 to 80	80 to 85	85 to 90	90 to 95	95 to 100	100 to 105	105 to 110	110 to 115	115 to 120	120 to 125	125 to 130	# of Obs.	% Total
N	382	805	830	683	486	278	220	134	60	33	13	6	2	1	1												3934	9.0
NE	476	954	1097	967	613	352	235	138	65	16	15	3	1	1	1	1		1									4936	11.3
E	447	992	1011	759	467	309	163	96	71	26	27	4	1	2	1		1										4377	10.0
SE	518	1117	1199	1033	677	450	274	162	91	51	32	16	1	1		2				1	1						5626	12.8
S	588	1418	1641	1549	1173	858	563	279	165	99	38	20	4	8	2				1	1							8407	19.2
SW	562	1394	1676	1592	1239	832	561	332	173	90	45	26	6	7	2			1		1						1	8540	19.5
W	406	997	1118	875	538	377	256	146	94	48	18	17	9	5			1						1	1			4907	11.2
NW	324	708	669	487	293	207	148	110	49	31	9	4	6	3	2	1		1									3052	7.0
Calm	69																										69	0.2
Sum	3772	8385	9241	7945	5486	3663	2420	1397	768	394	197	96	30	28	9	4	2	3	1	3	1	0	1	1	0	1	43848	
% Exceed	91.4	72.3	51.2	33.1	20.6	12.2	6.7	3.5	1.8	0.9	0.4	0.2	0.1	0.1	0.0	0.0	0.0	0.0	0.0	0.0	0.0	0.0	0.0	0.0	0.0	0.0		

Observation Period: January
Mid-Depth Current Speed vs. Current Direction

Speed (cm/s)

Dir (to)	0 to 5	5 to 10	10 to 15	15 to 20	20 to 25	25 to 30	30 to 35	35 to 40	40 to 45	45 to 50	# of Obs.	% Total
N	17	44	61	49	44	40	13	3	2		273	7.3
NE	11	38	83	103	59	39	18	7	2		360	9.7
E	8	58	102	90	56	58	17	7	2	1	399	10.7
SE	16	65	107	95	72	62	21	8	6	1	453	12.2
S	24	59	129	122	131	99	51	20	9	3	647	17.4
SW	19	84	151	175	163	129	58	24	6	1	810	21.8
W	17	79	105	103	97	78	21	10	1	1	512	13.8
NW	15	58	55	39	34	48	13	2		1	265	7.1
Calm	1										1	0.0
Sum	128	485	793	776	656	553	212	81	28	8	3720	
% Exceed	96.6	83.5	62.2	41.3	23.7	8.8	3.1	1.0	0.2	0.0		

Site: Hibernia Current Time-Series
Sampling Interval: 60 min
Observation Period: February

Mid-Depth Current Speed vs. Current Direction

	Speed (cm/s)														
Dir (to)	0 to 5	5 to 10	10 to 15	15 to 20	20 to 25	25 to 30	30 to 35	35 to 40	40 to 45	45 to 50	50 to 55	55 to 60	60 to 65	# of Obs.	% Total
N	24	67	82	63	24	11	2	6	5	1	1			286	8.4
NE	30	101	133	104	49	11	3	2	1					434	12.7
E	24	72	111	89	37	16	5	3						357	10.5
SE	20	82	103	97	47	19	9	5	1	2				385	11.3
S	25	71	130	119	106	43	16	15	3	3	1	1		533	15.6
SW	30	83	146	158	129	88	61	16	8	2	1	1		723	21.2
W	24	87	90	79	68	48	18	5	2	2	1			424	12.4
NW	26	73	52	42	48	5	6	4	2	2	2	2	2	266	7.8
Calm															
Sum	203	636	847	751	508	241	120	56	22	12	6	4	2	3408	
% Exceed	94.0	75.4	50.5	28.5	13.6	6.5	3.0	1.3	0.7	0.4	0.2	0.1	0.0		

Site: Hibernia Current Time-Series
Sampling Interval: 60 min
Observation Period: March

Mid-Depth Current Speed vs. Current Direction

	Speed (cm/s)												
Dir (to)	0 to 5	5 to 10	10 to 15	15 to 20	20 to 25	25 to 30	30 to 35	35 to 40	40 to 45	45 to 50	50 to 55	# of Obs.	% Total
N	37	68	99	73	43	11	6	3	2			342	9.2
NE	33	92	129	166	83	31	7	4				545	14.7
E	39	120	177	114	18	5	1	1				475	12.8
SE	38	115	139	57	28	6	1	2	1			387	10.4
S	19	137	143	92	31	20	7	5	2			456	12.3
SW	33	135	191	182	71	16	18	7	3	3	2	661	17.8
W	36	112	175	134	40	15	3	1		4		520	14.0
NW	32	111	103	63	14	3	4	2	1			333	9.0
Calm	1											1	0.0
Sum	268	890	1156	881	328	107	47	25	9	7	2	3720	
% Exceed	92.8	68.9	37.8	14.1	5.3	2.4	1.2	0.5	0.2	0.1	0.0		

Site: Hibernia Current Time-Series
Sampling Interval: 60 min
Observation Period: April

Mid-Depth Current Speed vs. Current Direction

	Speed (cm/s)												
Dir (to)	0 to 5	5 to 10	10 to 15	15 to 20	20 to 25	25 to 30	30 to 35	35 to 40	40 to 45	45 to 50	50 to 55	# of Obs.	% Total
N	28	120	119	98	83	28	13	5	2			496	13.8
NE	25	115	166	136	98	55	11	7	3			616	17.1
E	25	108	172	105	32	10	2		1			455	12.6
SE	29	112	137	72	28	12	1	1	1			393	10.9
S	23	98	130	83	42	9	6	2	2		1	396	11.0
SW	20	99	154	119	59	25	6	1	2		1	486	13.5
W	28	78	149	125	28	9	1	3				421	11.7
NW	27	108	113	63	15	4	3	1	1			335	9.3
Calm	2											2	0.1
Sum	207	838	1140	801	385	152	43	20	12	0	2	3600	
% Exceed	94.3	71.0	39.3	17.1	6.4	2.1	0.9	0.4	0.1	0.1	0.0		

Site: Hibernia Current Time-Series
Sampling Interval: 60 min
Observation Period: May

Mid-Depth Current Speed vs. Current Direction

	Speed (cm/s)									
Dir (to)	0 to 5	5 to 10	10 to 15	15 to 20	20 to 25	25 to 30	30 to 35	35 to 40	# of Obs.	% Total
N	34	129	105	48	25	6			347	9.3
NE	58	149	192	94	30	7	5		535	14.4
E	67	107	182	92	23	3	1		475	12.8
SE	56	92	155	103	26	5	2		439	11.8
S	54	102	175	114	47	18	2	1	513	13.8
SW	63	110	202	149	72	25	4		625	16.8
W	48	87	159	124	50	8			476	12.8
NW	35	81	126	54	13				309	8.3
Calm	1								1	0.0
Sum	416	857	1296	778	286	72	14	1	3720	
% Exceed	88.8	65.8	30.9	10.0	2.3	0.4	0.0	0.0		

Site: Hibernia Current Time-Series
Sampling Interval: 60 min
Observation Period: June

Mid-Depth Current Speed vs. Current Direction

	Speed (cm/s)																	
Dir (to)	0 to 5	5 to 10	10 to 15	15 to 20	20 to 25	25 to 30	30 to 35	35 to 40	40 to 45	45 to 50	50 to 55	55 to 60	60 to 65	65 to 70	70 to 75	75 to 80	# of Obs.	% Total
N	34	80	63	39	10												226	6.3
NE	55	87	112	53	20	7											334	9.3
E	66	94	138	69	21	5	2										395	11.0
SE	123	94	147	94	39	11	3									1	512	14.2
S	134	109	185	129	49	13	4										623	17.3
SW	147	132	199	136	74	17	15	5									725	20.1
W	70	98	124	91	43	14	5	4									449	12.5
NW	50	61	79	26	12	2	1										231	6.4
Calm	105																105	2.9
Sum	784	755	1047	637	268	69	30	9	0	0	0	0	0	0	0	1	3600	
% Exceed	78.2	57.3	28.2	10.5	3.0	1.1	0.3	0.0	0.0	0.0	0.0	0.0	0.0	0.0	0.0	0.0		

Site: Hibernia Current Time-Series
Sampling Interval: 60 min
Observation Period: July

Mid-Depth Current Speed vs. Current Direction

	Speed (cm/s)										
Dir (to)	0 to 5	5 to 10	10 to 15	15 to 20	20 to 25	25 to 30	30 to 35	35 to 40	40 to 45	# of Obs.	% Total
N	23	46	50	34	8	2	1			164	4.4
NE	33	70	82	41	17	5		1		249	6.7
E	31	94	120	58	23	7	3			336	9.0
SE	26	128	116	81	27	6	3			387	10.4
S	22	140	166	109	43	8	4	1		493	13.3
SW	31	213	318	241	141	55	15	3	1	1018	27.4
W	39	196	262	232	68	27	8	2	1	835	22.4
NW	24	66	94	35	11	4	1			235	6.3
Calm	3									3	0.1
Sum	232	953	1208	831	338	114	35	7	2	3720	
% Exceed	93.8	68.1	35.7	13.3	4.2	1.2	0.2	0.1	0.0		

Site: Hibernia Current Time-Series
Sampling Interval: 60 min
Observation Period: August

Mid-Depth Current Speed vs. Current Direction

Speed (cm/s)

Dir (to)	0 to 5	5 to 10	10 to 15	15 to 20	20 to 25	25 to 30	30 to 35	35 to 40	40 to 45	# of Obs.	% Total
N	11	54	87	40	15	8	1	2		218	5.9
NE	21	91	127	90	31	12	3	1		376	10.1
E	27	125	144	80	24	7	1			408	11.0
SE	37	118	120	85	28	1				389	10.5
S	32	126	159	105	24	1	2			449	12.1
SW	30	185	309	222	109	34	3	1	1	894	24.0
W	27	172	275	159	65	22	3	2		725	19.5
NW	15	75	88	56	21	3	1			259	7.0
Calm	2									2	0.1
Sum	202	946	1309	837	317	88	14	6	1	3720	
% Exceed	94.6	69.1	34.0	11.5	2.9	0.6	0.2	0.0	0.0		

Site: Hibernia Current Time-Series
Sampling Interval: 60 min
Observation Period: September

Mid-Depth Current Speed vs. Current Direction

Speed (cm/s)

Dir (to)	0 to 5	5 to 10	10 to 15	15 to 20	20 to 25	25 to 30	30 to 35	35 to 40	40 to 45	45 to 50	50 to 55	55 to 60	# of Obs.	% Total
N	28	64	70	43	17	10	4	5	2	1			244	6.8
NE	23	87	131	119	46	15	5	7	1				434	12.1
E	32	101	143	97	33	28	13	6	5	1		1	460	12.8
SE	28	118	118	56	36	16	13	7	4	5			401	11.1
S	29	94	123	78	41	21	9	11	6	4	1		417	11.6
SW	23	125	194	186	105	53	20	12	7	2	1	3	731	20.3
W	23	117	182	156	87	29	24	20	3	5	2		648	18.0
NW	26	69	70	47	23	16	5	7	1				264	7.3
Calm	1												1	0.0
Sum	213	775	1031	782	388	188	93	75	29	18	4	4	3600	
% Exceed	94.1	72.6	43.9	22.2	11.4	6.2	3.6	1.5	0.7	0.2	0.1	0.0		

Site: Hibernia Current Time-Series
Sampling Interval: 60 min
Observation Period: October

Mid-Depth Current Speed vs. Current Direction

Speed (cm/s)

Dir (to)	0 to 5	5 to 10	10 to 15	15 to 20	20 to 25	25 to 30	30 to 35	35 to 40	40 to 45	45 to 50	50 to 55	55 to 60	# of Obs.	% Total
N	15	35	91	85	53	20	7	5	1				312	8.4
NE	8	52	106	121	69	29	7	2	2				396	10.6
E	28	68	136	114	57	19	6	2					430	11.6
SE	22	76	120	118	77	41	6	2					462	12.4
S	9	74	135	149	128	67	22	6	2				592	15.9
SW	13	95	149	173	158	95	34	13	2	1	1	2	736	19.8
W	12	65	121	114	108	47	21	5	4	1	1		499	13.4
NW	14	49	76	70	45	28	6	1	1	1			291	7.8
Calm	2												2	0.1
Sum	123	514	934	944	695	346	109	36	12	3	2	2	3720	
% Exceed	96.7	82.9	57.8	32.4	13.7	4.4	1.5	0.5	0.2	0.1	0.1	0.0		

Observation Period: November

Mid-Depth Current Speed vs. Current Direction

Speed (cm/s)

Dir (to)	0 to 5	5 to 10	10 to 15	15 to 20	20 to 25	25 to 30	30 to 35	35 to 40	40 to 45	45 to 50	50 to 55	55 to 60	60 to 65	65 to 70	70 to 75	75 to 80	80 to 85	85 to 90	90 to 95	95 to 100	100 to 105	105 to 110	110 to 115	115 to 120	# of Obs.	% Total
N	6	20	46	79	71	30	10	5		2	1														270	7.5
NE	6	20	64	108	88	57	16	3	1		1														364	10.1
E	7	24	87	106	82	40	9	3		1														1	360	10.0
SE	6	45	113	141	83	39	9	8	2	4															450	12.5
S	8	59	132	170	117	65	25	12	6	5		1													600	16.7
SW	11	51	128	184	191	109	55	21	11	7	2	4	1												775	21.5
W	14	31	85	130	150	57	26	11	11	5	2	1													523	14.5
NW	7	24	64	39	66	39	9	6	3	1															258	7.2
Calm																										
Sum	65	274	719	957	848	436	159	69	34	25	6	6	1	0	0	0	0	0	0	0	0	0	0	1	3600	
% Exceed	98.2	90.6	70.6	44.0	20.5	8.4	3.9	2.0	1.1	0.4	0.2	0.1	0.0	0.0	0.0	0.0	0.0	0.0	0.0	0.0	0.0	0.0	0.0	0.0		

Site: Hibernia Current Time-Series
Sampling Interval: 60 min
Observation Period: December

Mid-Depth Current Speed vs. Current Direction

Speed (cm/s)

Dir (to)	0 to 5	5 to 10	10 to 15	15 to 20	20 to 25	25 to 30	30 to 35	35 to 40	40 to 45	45 to 50	50 to 55	55 to 60	60 to 65	65 to 70	70 to 75	75 to 80	# of Obs.	% Total
N	7	23	47	68	41	19	10	3	2								220	5.9
NE	10	32	68	93	56	41	14	2	1		1						318	8.5
E	7	36	64	83	77	44	31	11			1						354	9.5
SE	7	44	69	107	77	51	38	22	11	3	1						430	11.6
S	8	40	108	181	147	118	54	54	16	2	3		1	1	1	1	735	19.8
SW	5	58	154	230	197	135	81	60	23	1	1	1	1	2		3	952	25.6
W	6	37	87	99	107	79	34	20	1	5	1						476	12.8
NW	11	27	54	42	43	32	13	7	3	2							234	6.3
Calm	1																1	0.0
Sum	62	297	651	903	745	519	275	179	57	13	8	1	2	3	1	4	3720	
% Exceed	98.3	90.3	72.8	48.6	28.5	14.6	7.2	2.4	0.9	0.5	0.3	0.3	0.2	0.1	0.1	0.0		

Observation Period: 1980/ 1/ 1 0: 0 to 1984/12/31 23: 0 GMT

Mid-Depth Current Speed vs. Current Direction

Speed (cm/s)

Dir (to)	0 to 5	5 to 10	10 to 15	15 to 20	20 to 25	25 to 30	30 to 35	35 to 40	40 to 45	45 to 50	50 to 55	55 to 60	60 to 65	65 to 70	70 to 75	75 to 80	80 to 85	85 to 90	90 to 95	95 to 100	100 to 105	105 to 110	110 to 115	115 to 120	# of Obs.	% Total
N	264	750	920	719	434	185	67	37	16	4	2														3398	7.7
NE	313	934	1393	1228	646	309	89	36	11		2														4961	11.3
E	361	1007	1576	1097	483	242	91	33	8	3	1	1												1	4904	11.2
SE	408	1089	1444	1106	568	269	106	55	26	15	1					1									5088	11.6
S	387	1109	1715	1451	906	482	202	127	46	17	6	2	1	1	1	1									6454	14.7
SW	425	1370	2295	2155	1469	781	370	163	64	17	9	11	2	2		3									9136	20.8
W	344	1159	1814	1546	911	433	164	83	23	23	7	1													6508	14.8
NW	282	802	974	576	345	184	62	30	12	7	2	2	2												3280	7.5
Calm	119																								119	0.3
Sum	2903	8220	12131	9878	5762	2885	1151	564	206	86	30	17	5	3	1	5	0	0	0	0	0	0	0	1	43848	
% Exceed	93.4	74.6	47.0	24.4	11.3	4.7	2.1	0.8	0.3	0.1	0.1	0.0	0.0	0.0	0.0	0.0	0.0	0.0	0.0	0.0	0.0	0.0	0.0	0.0		

Site: Hibernia Current Time-Series
Sampling Interval: 60 min
Observation Period: January

Near-Bottom Current Speed vs. Current Direction

	Speed (cm/s)									
Dir (to)	0 to 5	5 to 10	10 to 15	15 to 20	20 to 25	25 to 30	30 to 35	35 to 40	# of Obs.	% Total
N	16	62	91	75	13	7	2		266	7.2
NE	14	95	116	111	24	6	1		367	9.9
E	26	75	106	117	39	8	2		373	10.0
SE	29	81	142	166	47	18	4	1	488	13.1
S	25	118	178	185	96	42	17	1	662	17.8
SW	19	116	222	217	101	53	23	9	760	20.4
W	20	93	162	134	54	31	5	1	500	13.4
NW	17	76	108	70	20	8	3		302	8.1
Calm	2								2	0.1
Sum	168	716	1125	1075	394	173	57	12	3720	
% Exceed	95.5	76.2	46.0	17.1	6.5	1.9	0.3	0.0		

Site: Hibernia Current Time-Series
Sampling Interval: 60 min
Observation Period: February

Near-Bottom Current Speed vs. Current Direction

	Speed (cm/s)													
Dir (to)	0 to 5	5 to 10	10 to 15	15 to 20	20 to 25	25 to 30	30 to 35	35 to 40	40 to 45	45 to 50	50 to 55	55 to 60	# of Obs.	% Total
N	21	88	98	62	14	6		6	4				299	8.8
NE	19	103	161	79	23	4	4	1					394	11.6
E	18	104	122	82	28	4	1						359	10.5
SE	17	69	120	82	53	16	7	1		1			366	10.7
S	21	96	174	125	78	41	10	4	5	2		1	557	16.3
SW	34	119	193	139	127	54	30	13	4	2	2		717	21.0
W	28	69	125	108	57	25	13	3	1		1		430	12.6
NW	17	77	94	57	20	6	2	2	3	2	3	1	284	8.3
Calm	2												2	0.1
Sum	177	725	1087	734	400	156	67	30	17	7	6	2	3408	
% Exceed	94.8	73.5	41.6	20.1	8.4	3.8	1.8	0.9	0.4	0.2	0.1	0.0		

Site: Hibernia Current Time-Series
Sampling Interval: 60 min
Observation Period: March

Near-Bottom Current Speed vs. Current Direction

	Speed (cm/s)											
Dir (to)	0 to 5	5 to 10	10 to 15	15 to 20	20 to 25	25 to 30	30 to 35	35 to 40	40 to 45	45 to 50	# of Obs.	% Total
N	30	81	113	78	30	22	5				359	9.7
NE	23	109	154	110	74	26	3	1			500	13.4
E	26	137	184	93	38	10	4	1	1		494	13.3
SE	29	129	129	77	21	11	3		2		401	10.8
S	41	133	167	90	29	18	6	2	4		490	13.2
SW	29	134	234	114	45	21	10	8	4		599	16.1
W	40	143	179	96	27	17	10	4	1	1	518	13.9
NW	30	121	97	62	31	10	3	2			356	9.6
Calm	3										3	0.1
Sum	251	987	1257	720	295	135	44	18	12	1	3720	
% Exceed	93.3	66.7	32.9	13.6	5.6	2.0	0.8	0.3	0.0	0.0		

Site: Hibernia Current Time-Series
Sampling Interval: 60 min
Observation Period: April

Near-Bottom Current Speed vs. Current Direction

	Speed (cm/s)								
Dir (to)	0 to 5	5 to 10	10 to 15	15 to 20	20 to 25	25 to 30	30 to 35	# of Obs.	% Total
N	42	109	115	46	12	2		326	9.1
NE	44	147	206	128	79	14	1	619	17.2
E	26	140	192	114	37	4		513	14.3
SE	26	122	118	62	16	4		348	9.7
S	33	99	115	48	22	7		324	9.0
SW	35	131	210	140	51	9		576	16.0
W	26	150	215	138	51	8		588	16.3
NW	36	103	97	58	8	1		303	8.4
Calm	3							3	0.1
Sum	271	1001	1268	734	276	49	1	3600	
% Exceed	92.5	64.7	29.4	9.1	1.4	0.0	0.0		

Site: Hibernia Current Time-Series
Sampling Interval: 60 min
Observation Period: May

Near-Bottom Current Speed vs. Current Direction

	Speed (cm/s)								
Dir (to)	0 to 5	5 to 10	10 to 15	15 to 20	20 to 25	25 to 30	30 to 35	# of Obs.	% Total
N	43	130	100	21	5			299	8.0
NE	58	214	164	53	12	2		503	13.5
E	32	166	205	69	23			495	13.3
SE	31	140	167	37	15	5		395	10.6
S	30	123	148	74	13	4		392	10.5
SW	37	170	215	139	57	14	3	635	17.1
W	35	161	233	189	38	5	1	662	17.8
NW	33	115	144	38	6			336	9.0
Calm	3							3	0.1
Sum	302	1219	1376	620	169	30	4	3720	
% Exceed	91.9	59.1	22.1	5.5	0.9	0.1	0.0		

Site: Hibernia Current Time-Series
Sampling Interval: 60 min
Observation Period: June

Near-Bottom Current Speed vs. Current Direction

	Speed (cm/s)									
Dir (to)	0 to 5	5 to 10	10 to 15	15 to 20	20 to 25	25 to 30	30 to 35	35 to 40	# of Obs.	% Total
N	33	110	67	23	6	1			240	6.7
NE	42	151	108	29	5	2	1		338	9.4
E	32	121	149	46	14	5	1		368	10.2
SE	17	112	186	59	15	2	1		392	10.9
S	21	148	180	80	15	1	1		446	12.4
SW	43	252	283	135	63	16	6		798	22.2
W	38	188	259	153	64	17	4	3	726	20.2
NW	14	102	120	40	13	3			292	8.1
Calm										
Sum	240	1184	1352	565	195	47	14	3	3600	
% Exceed	93.3	60.4	22.9	7.2	1.8	0.5	0.1	0.0		

Site: Hibernia Current Time-Series
Sampling Interval: 60 min
Observation Period: July

Near-Bottom Current Speed vs. Current Direction

	Speed (cm/s)									
Dir (to)	0 to 5	5 to 10	10 to 15	15 to 20	20 to 25	25 to 30	30 to 35	35 to 40	# of Obs.	% Total
N	29	97	40	20	6	2			194	5.2
NE	32	86	88	33	3				242	6.5
E	29	95	112	40	21				297	8.0
SE	21	147	151	72	12	1			404	10.9
S	36	181	212	88	17	2			536	14.4
SW	62	296	314	192	82	18	5	2	971	26.1
W	42	267	288	128	50	23	4		802	21.6
NW	33	108	103	24	4	1			273	7.3
Calm	1								1	0.0
Sum	285	1277	1308	597	195	47	9	2	3720	
% Exceed	92.3	58.0	22.8	6.8	1.6	0.3	0.1	0.0		

Site: Hibernia Current Time-Series
Sampling Interval: 60 min
Observation Period: August

Near-Bottom Current Speed vs. Current Direction

	Speed (cm/s)								
Dir (to)	0 to 5	5 to 10	10 to 15	15 to 20	20 to 25	25 to 30	30 to 35	# of Obs.	% Total
N	35	90	56	28	4	1		214	5.8
NE	41	137	148	38	5	1		370	9.9
E	42	129	152	68	6		1	398	10.7
SE	40	118	149	82	6	3		398	10.7
S	55	173	141	83	26	1		479	12.9
SW	66	221	288	168	83	25	3	854	23.0
W	60	203	272	129	44	14	3	725	19.5
NW	38	90	108	33	7	1		277	7.4
Calm	5							5	0.1
Sum	382	1161	1314	629	181	46	7	3720	
% Exceed	89.7	58.5	23.2	6.3	1.4	0.2	0.0		

Site: Hibernia Current Time-Series
Sampling Interval: 60 min
Observation Period: September

Near-Bottom Current Speed vs. Current Direction

	Speed (cm/s)												
Dir (to)	0 to 5	5 to 10	10 to 15	15 to 20	20 to 25	25 to 30	30 to 35	35 to 40	40 to 45	45 to 50	50 to 55	55 to 60	# of Obs.	% Total
N	23	82	58	34	16	2							215	6.0
NE	33	125	172	71	21	4	2						428	11.9
E	43	162	155	80	25	3							468	13.0
SE	32	122	148	70	25	3	3						403	11.2
S	38	136	138	60	27	6	2	2					409	11.4
SW	51	210	223	167	63	19	2	1					736	20.4
W	37	159	218	162	51	16	3	1					647	18.0
NW	31	95	94	48	16	6		1				1	292	8.1
Calm	2												2	0.1
Sum	290	1091	1206	692	244	59	12	5	0	0	0	1	3600	
% Exceed	91.9	61.6	28.1	8.9	2.1	0.5	0.2	0.0	0.0	0.0	0.0	0.0		

Site: Hibernia Current Time-Series
Sampling Interval: 60 min
Observation Period: October

Near-Bottom Current Speed vs. Current Direction

	Speed (cm/s)									
Dir (to)	0 to 5	5 to 10	10 to 15	15 to 20	20 to 25	25 to 30	30 to 35	35 to 40	# of Obs.	% Total
N	29	59	75	50	32	10	1	1	257	6.9
NE	26	114	164	95	41	12	1		453	12.2
E	40	135	176	111	24	12	1		499	13.4
SE	21	100	142	81	31	23			398	10.7
S	28	82	147	104	44	14	2		421	11.3
SW	25	117	266	188	83	30	5		714	19.2
W	29	137	245	171	78	21	2		683	18.4
NW	28	71	88	64	35	5	2		293	7.9
Calm	2								2	0.1
Sum	228	815	1303	864	368	127	14	1	3720	
% Exceed	93.9	72.0	36.9	13.7	3.8	0.4	0.0	0.0		

ite: Hibernia Current Time-Series
Sampling Interval: 60 min
Observation Period: November

Near-Bottom Current Speed vs. Current Direction

	Speed (cm/s)																
Dir (to)	0 to 5	5 to 10	10 to 15	15 to 20	20 to 25	25 to 30	30 to 35	35 to 40	40 to 45	45 to 50	50 to 55	55 to 60	60 to 65	65 to 70	70 to 75	# of Obs.	% Total
N	7	54	81	79	40	13	3	1								278	7.7
NE	13	45	105	101	51	17	6									338	9.4
E	13	62	133	91	46	12	2		1							360	10.0
SE	9	64	164	139	52	24	4	1	1							458	12.7
S	15	92	188	156	89	38	10	3		3	1				1	596	16.6
SW	19	89	218	206	117	47	18	4	3	1						722	20.1
W	16	54	178	163	81	28	11	1	1							533	14.8
NW	14	44	101	85	44	15	7	1								311	8.6
Calm	4															4	0.1
Sum	110	504	1168	1020	520	194	61	11	6	4	1	0	0	0	1	3600	
% Exceed	96.9	82.9	50.5	22.2	7.7	2.3	0.6	0.3	0.2	0.1	0.0	0.0	0.0	0.0	0.0		

Site: Hibernia Current Time-Series
Sampling Interval: 60 min
Observation Period: December

Near-Bottom Current Speed vs. Current Direction

	Speed (cm/s)													
Dir (to)	0 to 5	5 to 10	10 to 15	15 to 20	20 to 25	25 to 30	30 to 35	35 to 40	40 to 45	45 to 50	50 to 55	55 to 60	# of Obs.	% Total
N	18	53	107	42	9	5	1	1	1				237	6.4
NE	15	72	147	63	25	3	3		2		1		331	8.9
E	15	65	121	74	26	7	6	3	2	1		1	321	8.6
SE	12	77	146	117	49	23	18	4	5		1	1	453	12.2
S	18	98	200	183	109	66	31	12	6	2		1	726	19.5
SW	19	125	261	246	154	64	32	19	2	1	2	1	926	24.9
W	9	74	156	140	59	25	9	3		1	1		477	12.8
NW	20	55	87	60	15	7	1	2					247	6.6
Calm	2												2	0.1
Sum	128	619	1225	925	446	200	101	44	18	5	5	4	3720	
% Exceed	96.6	79.9	47.0	22.1	10.1	4.8	2.0	0.9	0.4	0.2	0.1	0.0		

Site: Hibernia Current Time-Series
Sampling Interval: 60 min
Observation Period: 1980/ 1/ 1 0: 0 to 1984/12/31 23: 0 GMT

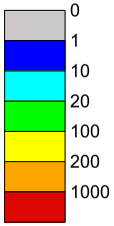
Near-Bottom Current Speed vs. Current Direction

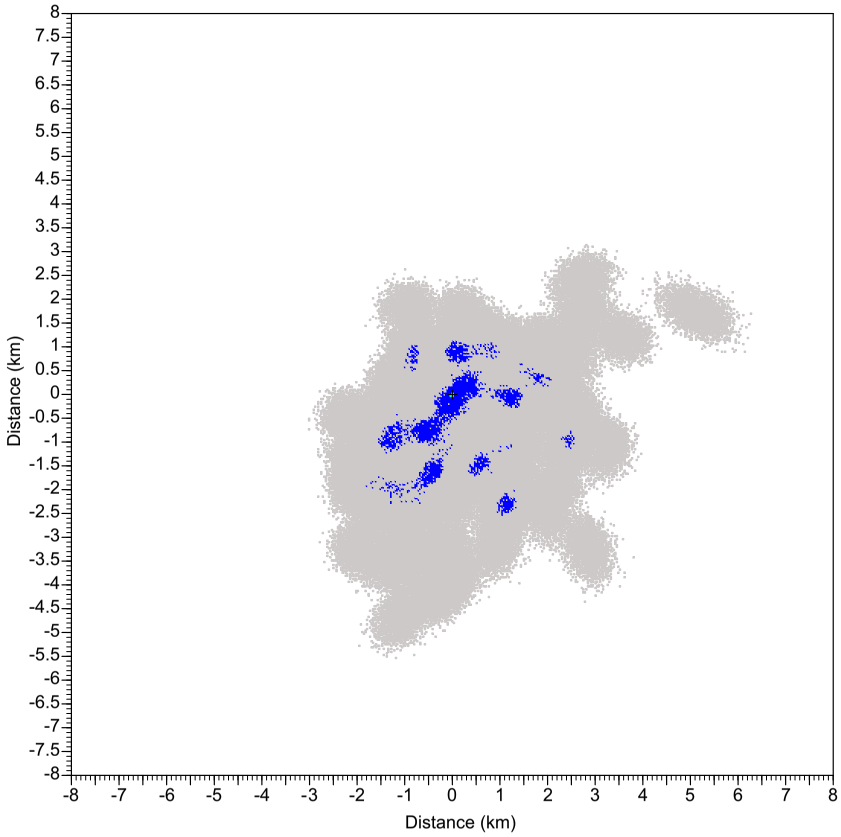
	Speed (cm/s)																
Dir (to)	0 to 5	5 to 10	10 to 15	15 to 20	20 to 25	25 to 30	30 to 35	35 to 40	40 to 45	45 to 50	50 to 55	55 to 60	60 to 65	65 to 70	70 to 75	# of Obs.	% Total
N	326	1015	1001	558	187	71	12	9	5							3184	7.3
NE	360	1398	1733	911	363	91	22	2	2		1					4883	11.1
E	342	1391	1807	985	327	65	18	4	4	1		1				4945	11.3
SE	284	1281	1762	1044	342	133	40	7	8	1	1	1				4904	11.2
S	361	1479	1988	1276	565	240	79	24	15	7	1	2			1	6038	13.8
SW	439	1980	2927	2051	1026	370	137	56	13	4	4	1				9008	20.5
W	380	1698	2530	1711	654	230	65	16	3	2	2					7291	16.6
NW	311	1057	1241	639	219	63	18	8	3	2	3	2				3566	8.1
Calm	29															29	0.1
Sum	2832	1129	914	989	9175	3683	1263	391	126	53	17	12	7	0	0	1	43848
% Exceed	93.5	67.8	33.6	12.7	4.3	1.4	0.5	0.2	0.1	0.0	0.0	0.0	0.0	0.0	0.0		

Appendix B
Drill Cuttings Deposition Model Sensitivity Results

Hebron Project
Completion of 52 Platform Wells (HeMF more fines)

Cuttings Thickness (mm)

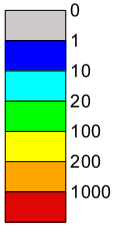


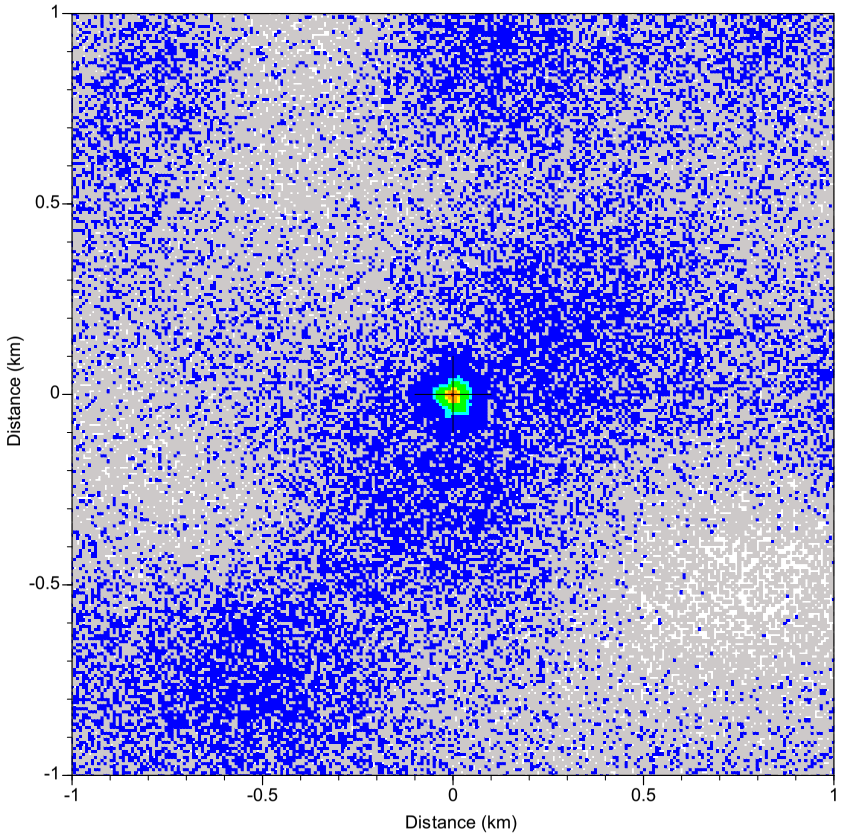


Prepared by AMEC
Mon Jan 11 17:09:50 2010

Hebron Project
Completion of 52 Platform Wells (HeMF more fines)

Cuttings Thickness (mm)

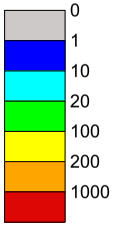


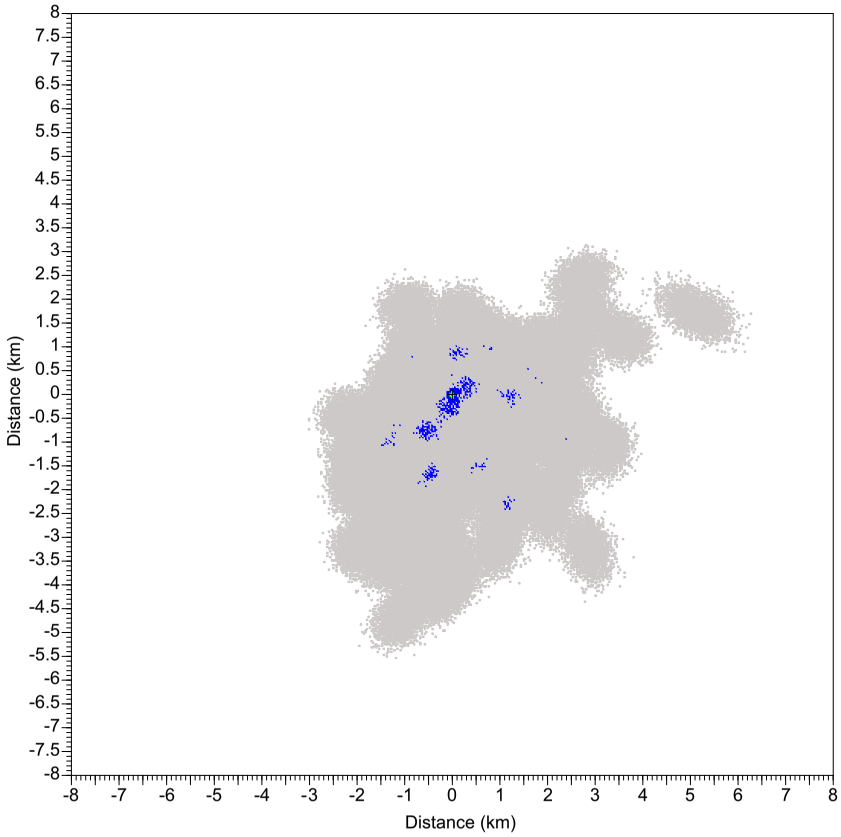


Prepared by AMEC
Mon Jan 11 17:06:01 2010

Hebron Project
Completion of 52 Platform Wells (HeLF less fines)

Cuttings Thickness (mm)

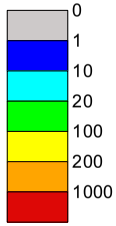


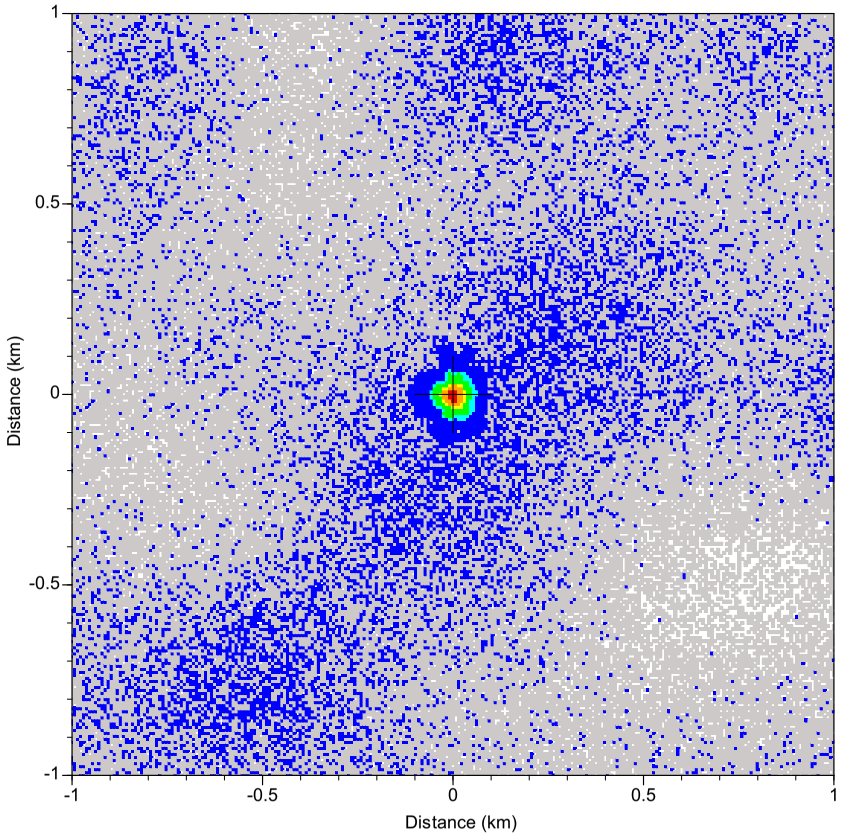


Prepared by AMEC
Mon Jan 11 21:21:25 2010

Hebron Project
Completion of 52 Platform Wells (HeLF less fines)

Cuttings Thickness (mm)

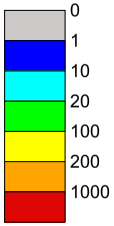


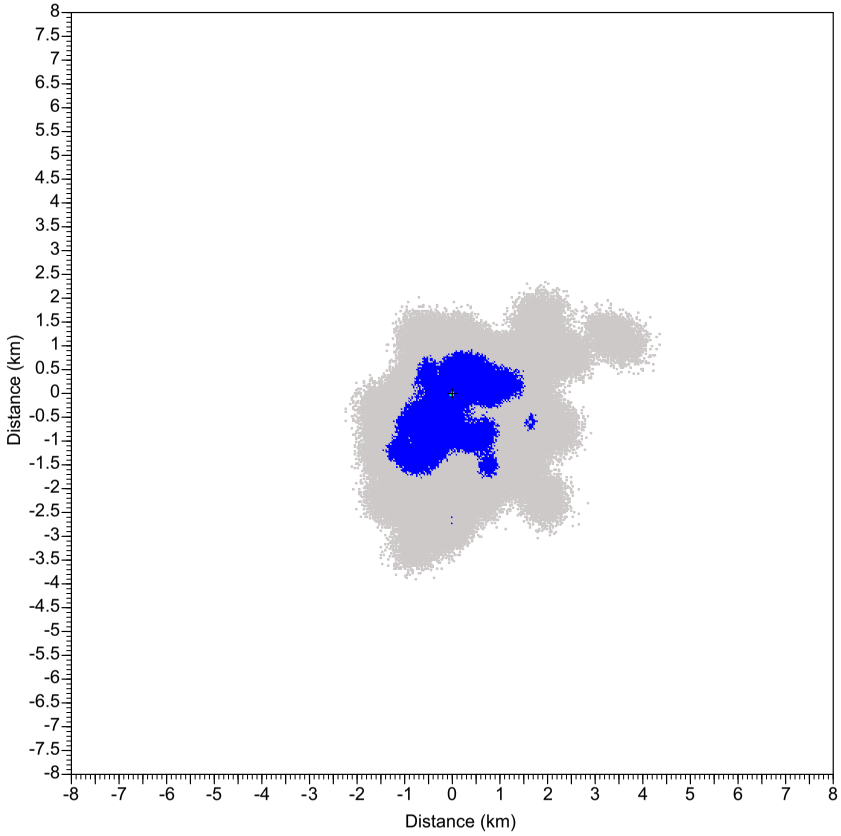


Prepared by AMEC
Mon Jan 11 21:23:26 2010

Hebron Project
Completion of 52 Platform Wells (HeC67 currents x 0.67)

Cuttings Thickness (mm)

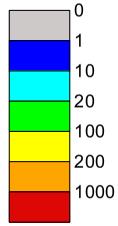


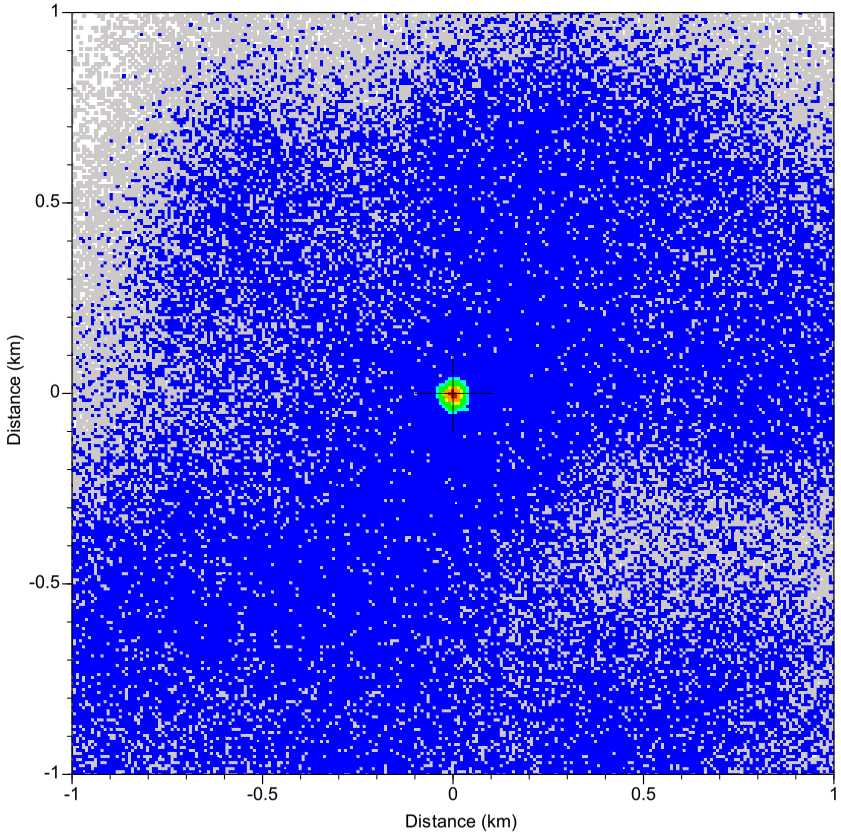


Prepared by AMEC
Mon Jan 11 21:30:21 2010

Hebron Project
Completion of 52 Platform Wells (HeC67 currents x 0.67)

Cuttings Thickness (mm)

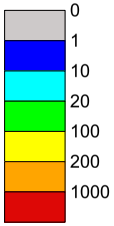


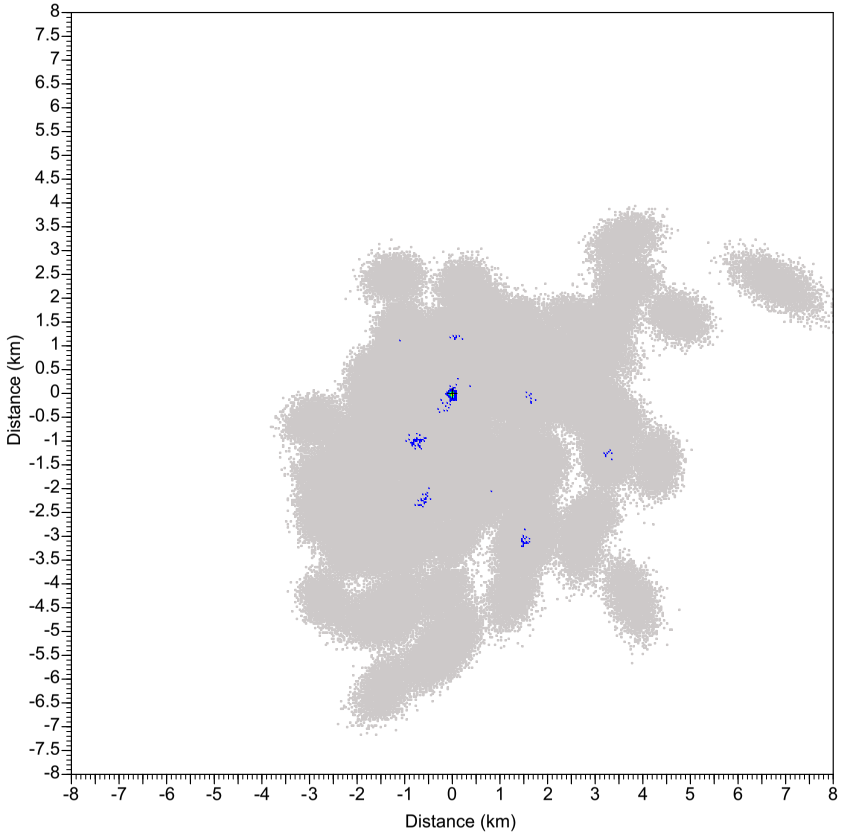


Prepared by AMEC
Mon Jan 11 21:41:14 2010

Hebron Project
Completion of 52 Platform Wells (HeC133 currents x 1.33)

Cuttings Thickness (mm)

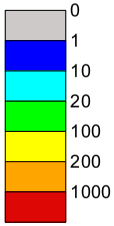


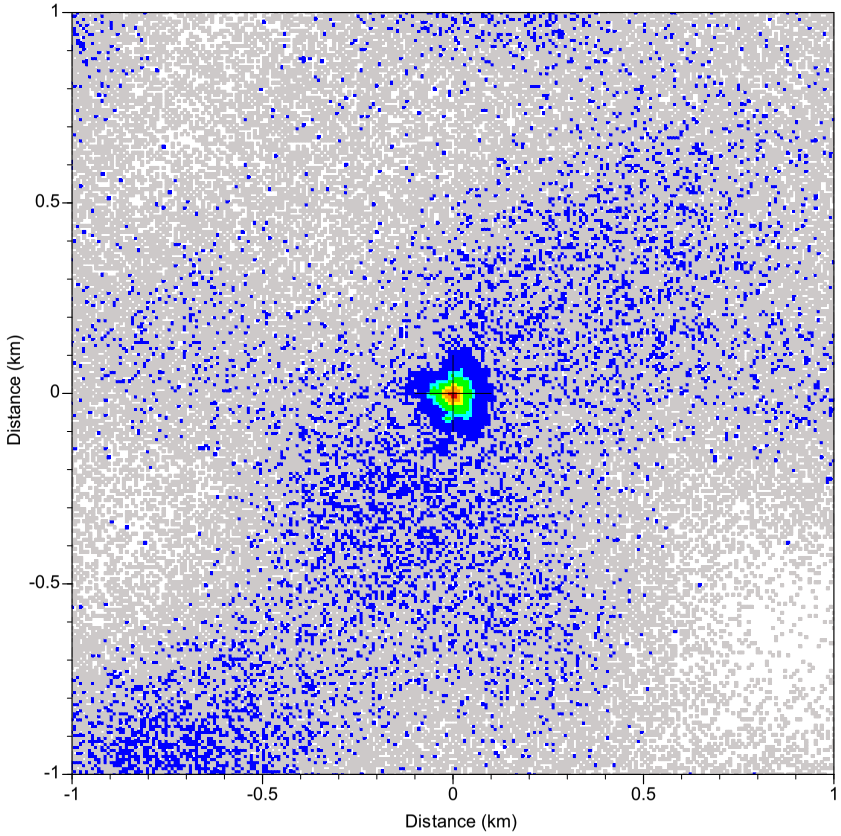


Prepared by AMEC
Mon Jan 11 17:26:42 2010

Hebron Project
Completion of 52 Platform Wells (HeC133 currents x 1.33)

Cuttings Thickness (mm)



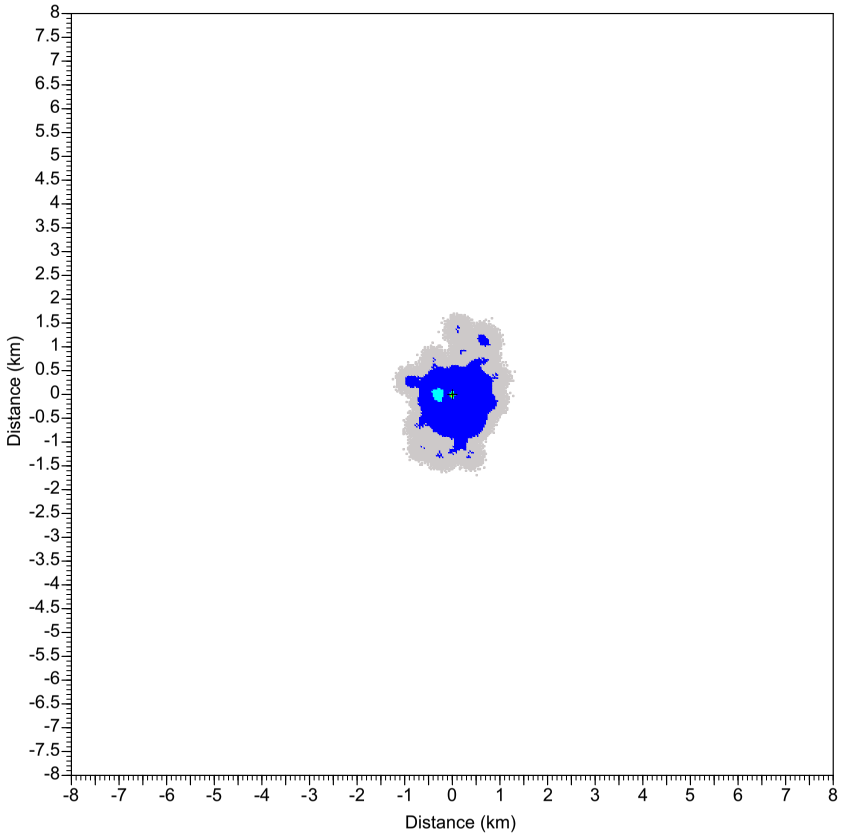


Prepared by AMEC
Mon Jan 11 21:42:06 2010

Hebron Project
Completion of 52 Platform Wells (HeFF fast fines settling)

Cuttings Thickness (mm)

0
1
10
20
100
200
1000

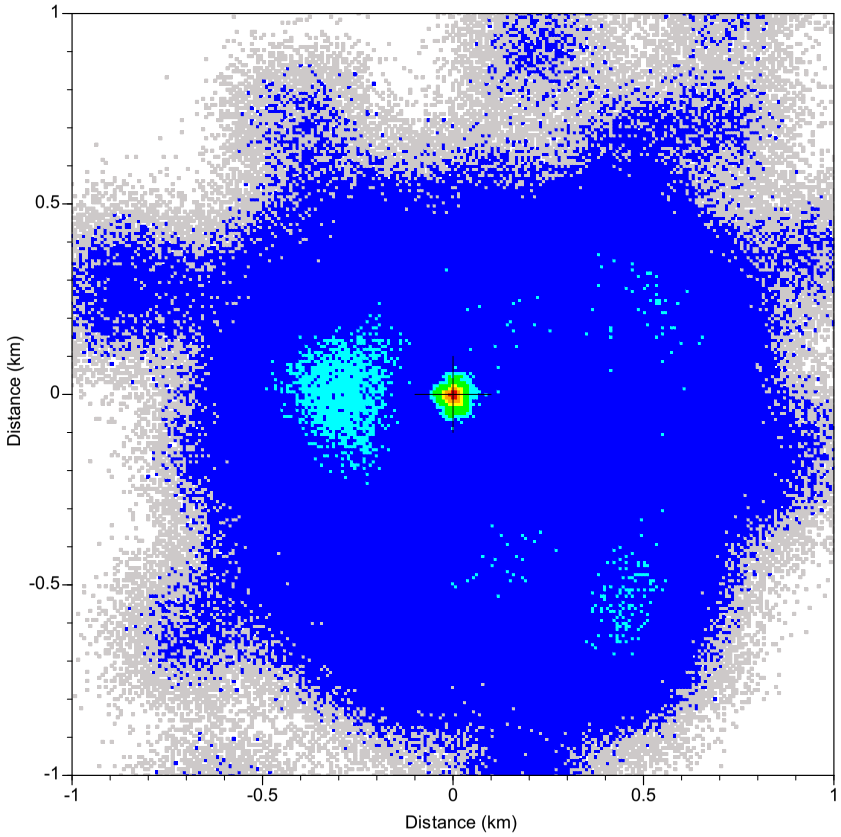


Prepared by AMEC
Mon Jan 11 21:54:10 2010

Hebron Project
Completion of 52 Platform Wells (HeFF fast fines settling)

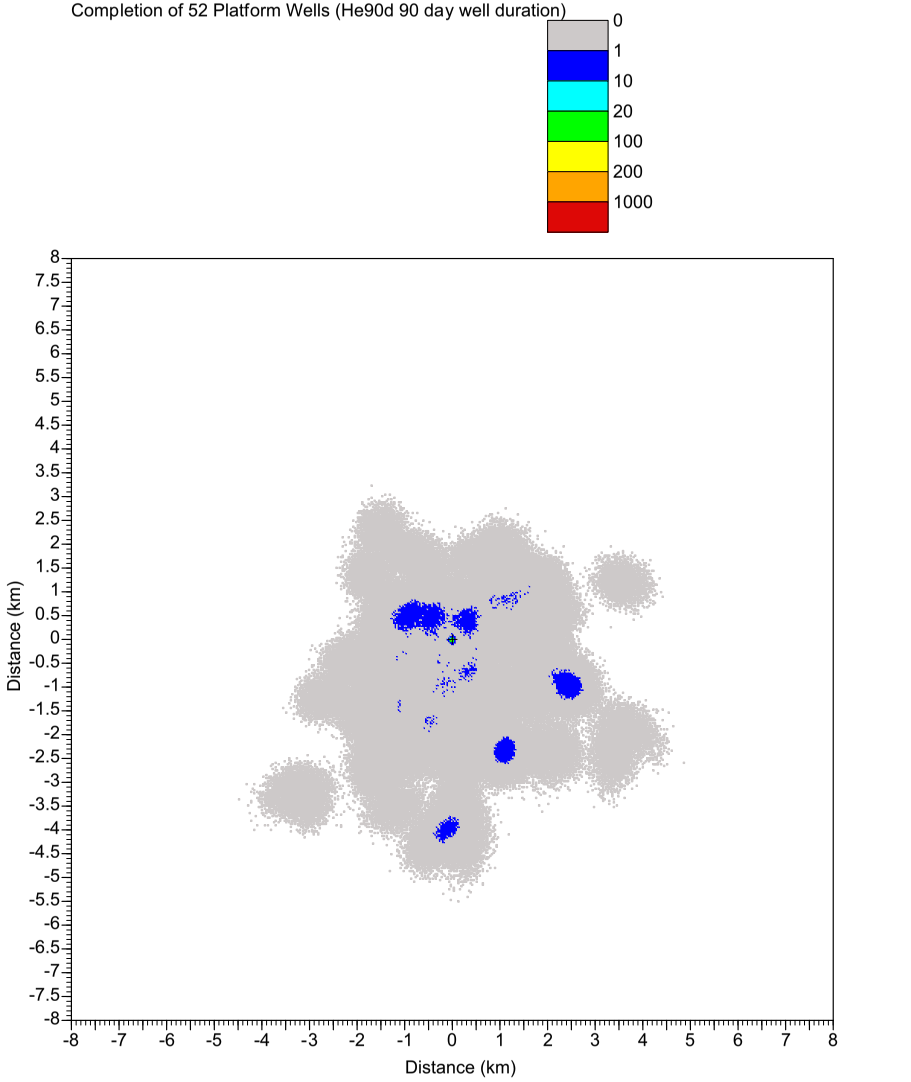
Cuttings Thickness (mm)

0
1
10
20
100
200
1000



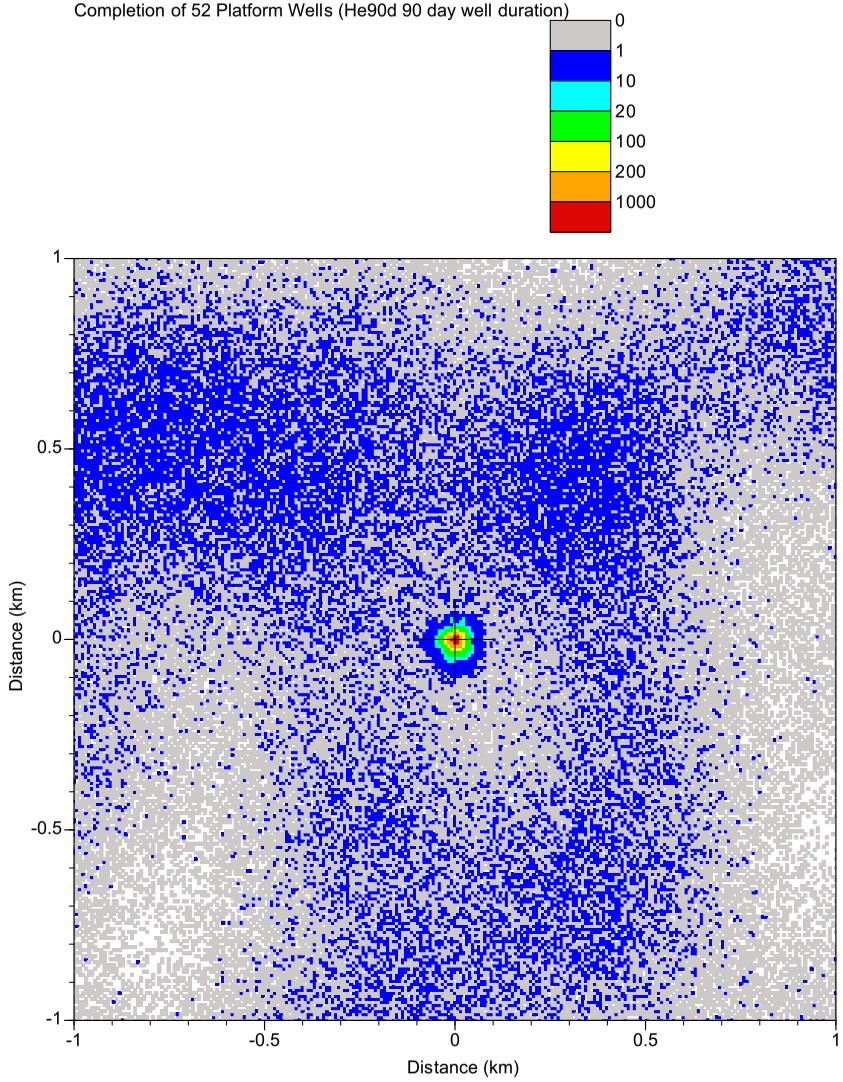
Prepared by AMEC
Mon Jan 11 21:56:12 2010

Hebron Project
Completion of 52 Platform Wells (He90d 90 day well duration)



Prepared by AMEC
Mon Jan 11 21:59:32 2010

Hebron Project
Completion of 52 Platform Wells (He90d 90 day well duration)

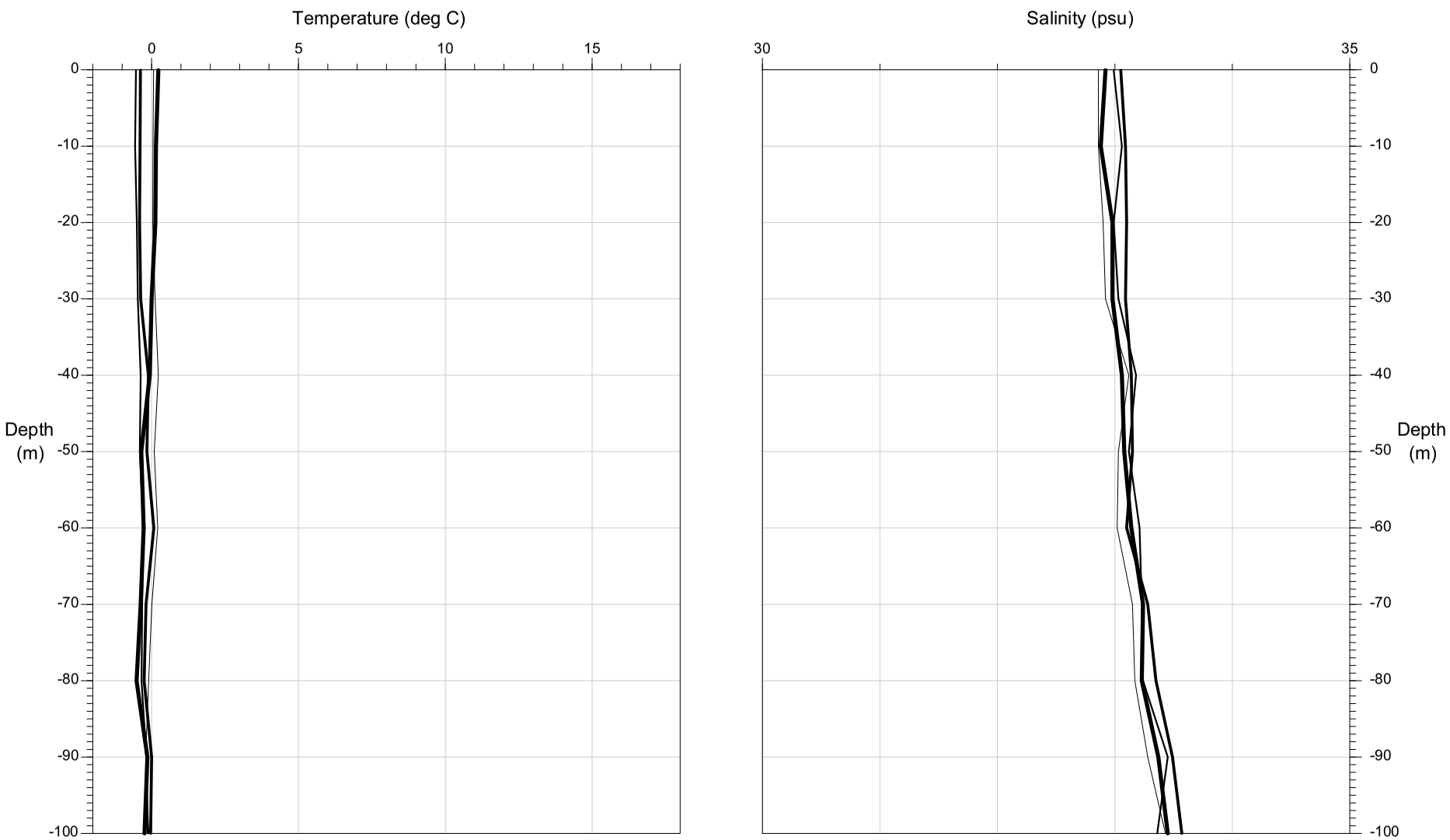


Prepared by AMEC
Mon Jan 11 22:10:37 2010

Appendix C
Grand Banks Temperature and Salinity Profiles
(Source: Ocean Science Hydrographic Database)

HEBRON PROJECT: Temperature and Salinity Profiles, January to April

AMEC Earth & Environmental
Thu Aug 12 15:08:24 2004



Source: Based on the Ocean Science hydrographic database

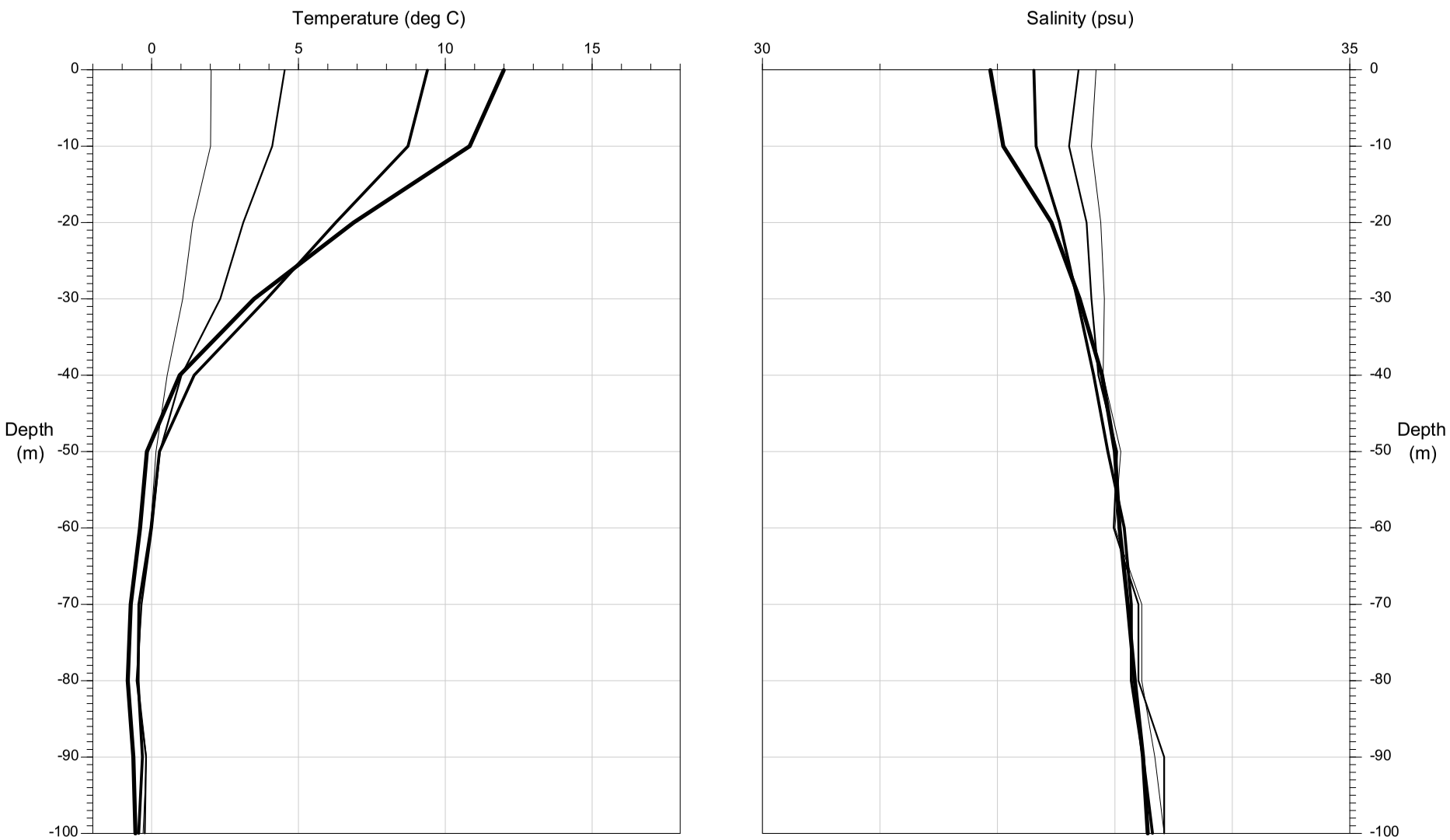
Area 45.5 to 47.5 deg N, 47.5 to 49.5 deg W

Statistics for bin ranges 0+/-5, 10+/-5, ..., 100+/-5m

query completed 11 Aug 2004

HEBRON PROJECT: Temperature and Salinity Profiles, May to August

AMEC Earth & Environmental
Thu Aug 12 15:13:04 2004



Source: Based on the Ocean Science hydrographic database

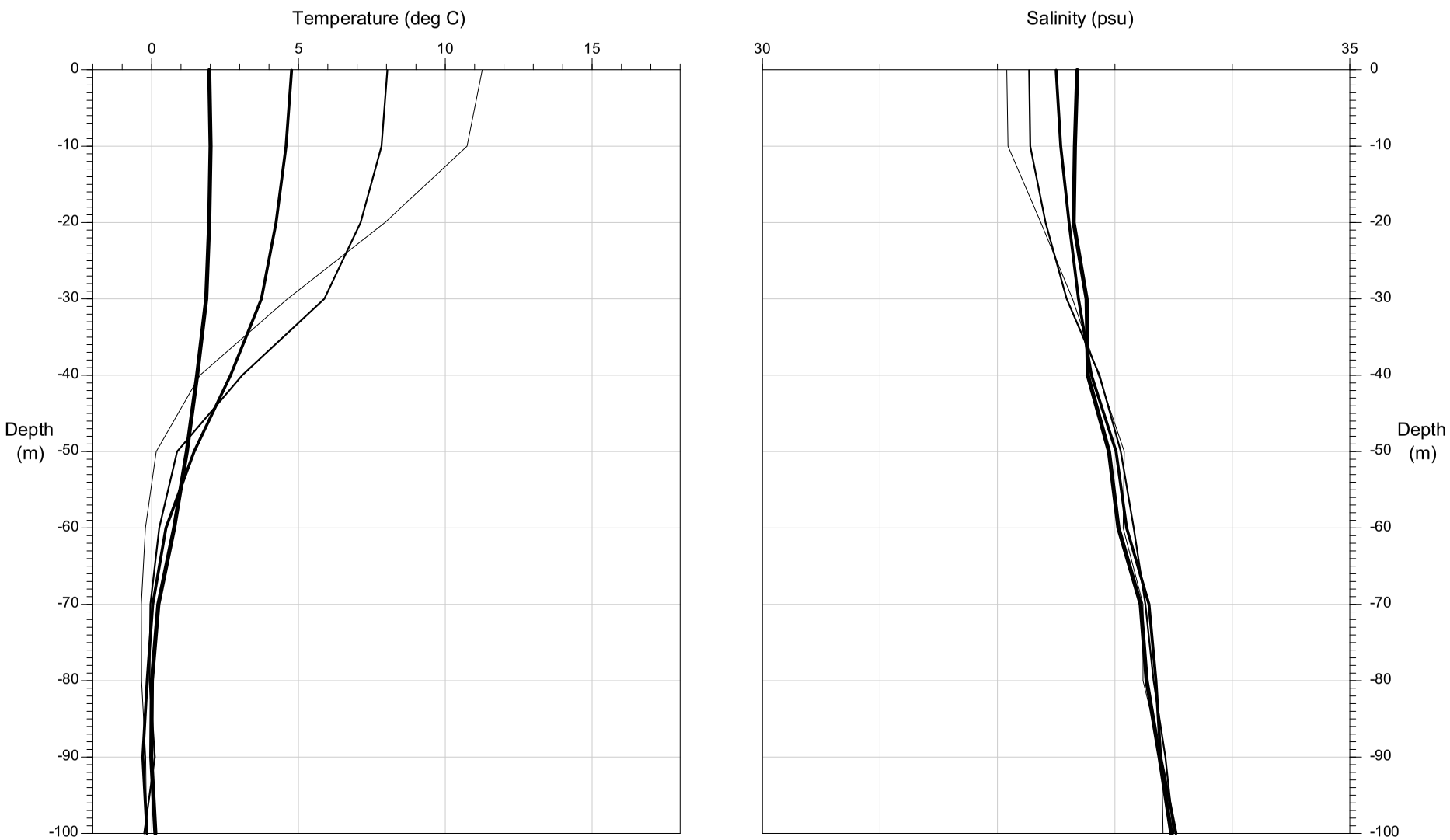
Area 45.5 to 47.5 deg N, 47.5 to 49.5 deg W

Statistics for bin ranges 0+/-5, 10+/-5, ..., 100+/-5m

query completed 11 Aug 2004

HEBRON PROJECT: Temperature and Salinity Profiles, September to December

AMEC Earth & Environmental
Thu Aug 12 15:07:06 2004



Source: Based on the Ocean Science hydrographic database

Area 45.5 to 47.5 deg N, 47.5 to 49.5 deg W

Statistics for bin ranges 0+/-5, 10+/-5, ..., 100+/-5m

query completed 11 Aug 2004

		Temperature (deg C)						Salinity (psu)						Sigmat					
Month	**Depth (m)**	**Min**	**Max**	**Avg**	**Std Dev**	**Count**	**Total**	**Min**	**Max**	**Avg**	**Std Dev**	**Count**	**Total**	**Min**	**Max**	**Avg**	**Std Dev**	**Count**	**Total**
Jan	0	-1.70	3.14	0.07	0.80	20	208	32.19	33.36	32.86	0.29	13	42	25.77	26.77	26.37	0.25	13	42
	10	-1.70	2.21	0.05	0.70	18	244	32.22	33.41	32.86	0.21	11	36	25.82	26.79	26.39	0.17	11	36
	20	-1.70	2.17	0.04	0.80	19	235	32.19	33.45	32.90	0.26	12	37	25.78	26.82	26.42	0.24	12	37
	30	-1.70	3.50	0.12	0.83	19	232	32.19	33.51	32.92	0.31	12	35	25.78	26.87	26.43	0.27	12	35
	40	-1.70	3.80	0.23	0.90	15	162	32.57	33.60	33.12	0.38	3	14	26.18	27.01	26.62	0.32	3	14
	50	-1.71	2.44	0.09	0.68	19	240	32.23	33.83	33.03	0.30	12	39	25.83	27.11	26.52	0.25	12	39
	60	-1.70	2.61	0.21	0.55	17	158	32.38	33.84	33.02	0.61	4	14	25.97	27.18	26.51	0.50	4	14
	70	-1.75	2.69	0.01	0.69	20	218	32.38	34.00	33.15	0.31	13	40	25.97	27.22	26.62	0.25	13	40
	80	-1.75	2.73	-0.10	0.67	20	213	32.69	34.00	33.17	0.29	12	43	26.28	27.22	26.64	0.23	12	43
	90	-1.70	2.73	-0.20	0.80	17	148	32.74	34.00	33.28	0.32	9	31	26.32	27.28	26.73	0.24	9	31
	100	-1.80	2.77	-0.09	0.87	20	167	32.93	34.08	33.43	0.30	13	40	26.47	27.32	26.84	0.22	13	40
Feb	0	-1.82	3.20	-0.53	0.67	27	331	32.36	33.43	32.99	0.20	14	44	25.98	26.87	26.51	0.16	14	44
	10	-1.83	3.30	-0.56	0.65	22	305	32.36	33.79	33.06	0.26	11	33	25.97	27.11	26.57	0.21	11	33
	20	-1.80	3.30	-0.50	0.64	23	266	32.36	33.88	32.99	0.23	11	35	25.97	27.17	26.51	0.20	11	35
	30	-1.80	3.30	-0.47	0.62	26	290	32.37	33.93	33.03	0.22	13	41	25.98	27.20	26.54	0.18	13	41
	40	-1.74	3.30	-0.37	0.58	19	184	32.88	33.95	33.18	0.28	6	15	26.39	27.21	26.65	0.23	6	15
	50	-1.80	3.30	-0.40	0.65	24	289	32.45	33.66	33.12	0.23	13	38	26.05	27.04	26.61	0.19	13	38
	60	-1.75	3.20	-0.28	0.55	22	194	32.75	33.99	33.21	0.31	7	11	26.28	27.24	26.67	0.25	7	11
	70	-1.82	3.40	-0.32	0.58	23	291	32.66	33.79	33.23	0.23	12	30	26.25	27.11	26.70	0.17	12	30
	80	-1.82	1.30	-0.34	0.60	23	250	32.57	34.09	33.24	0.27	13	41	26.17	27.30	26.71	0.20	13	41
	90	-1.79	2.50	-0.18	0.43	19	157	33.19	34.10	33.45	0.23	6	12	26.65	27.31	26.86	0.17	6	12
	100	-1.78	2.90	-0.13	0.71	21	187	32.68	34.15	33.36	0.28	13	37	26.27	27.34	26.79	0.20	13	37
Mar	0	-1.86	3.70	-0.38	0.89	35	246	32.28	33.93	33.05	0.24	22	92	25.97	27.12	26.55	0.18	22	92
	10	-1.86	3.70	-0.39	0.92	29	250	32.50	33.76	33.09	0.27	17	82	26.15	27.10	26.58	0.21	17	82
	20	-1.86	4.90	-0.41	0.94	34	260	32.57	34.04	33.10	0.25	21	102	26.20	27.15	26.58	0.19	21	102
	30	-1.80	4.90	-0.37	1.01	34	259	32.68	34.01	33.09	0.26	22	99	26.20	27.12	26.58	0.19	22	99
	40	-1.80	4.90	-0.11	1.17	25	192	32.70	33.81	33.14	0.33	9	52	26.21	27.02	26.60	0.24	9	52
	50	-1.80	4.90	-0.16	1.34	34	255	32.73	34.24	33.15	0.28	22	106	26.23	27.24	26.62	0.20	22	106
	60	-1.74	4.90	0.08	1.56	24	192	32.75	33.83	33.10	0.34	10	59	26.32	27.11	26.57	0.25	10	59
	70	-1.83	4.13	-0.19	1.09	32	240	32.76	34.44	33.28	0.34	19	96	26.32	27.41	26.72	0.24	19	96
	80	-1.80	4.13	-0.25	0.99	30	235	32.77	34.33	33.35	0.33	17	89	26.27	27.38	26.76	0.20	17	88
	90	-1.81	4.55	0.00	1.47	25	165	32.92	34.34	33.49	0.39	10	40	26.48	27.20	26.86	0.21	10	40
	100	-1.80	4.04	-0.03	1.21	31	203	33.00	34.54	33.57	0.37	19	72	26.45	27.52	26.93	0.24	19	72
Apr	0	-1.60	8.70	0.23	0.74	62	1151	31.47	34.11	32.92	0.21	59	853	25.28	27.31	26.42	0.17	59	850
	10	-1.50	8.70	0.15	0.80	43	1692	32.12	34.08	32.88	0.20	38	1391	25.81	27.23	26.40	0.16	38	1391
	20	-1.70	8.80	0.13	0.95	61	1677	32.19	34.11	32.98	0.25	58	1370	25.83	27.28	26.47	0.18	58	1365
	30	-1.80	8.90	0.00	0.79	62	1805	31.75	34.18	32.98	0.21	59	1473	25.49	27.32	26.48	0.16	59	1472
	40	-1.79	8.90	-0.06	0.99	50	1352	32.03	34.21	33.06	0.34	41	1080	25.72	27.35	26.54	0.25	41	1080
	50	-1.80	8.80	-0.35	0.66	62	1900	32.38	34.26	33.08	0.21	59	1557	25.91	27.36	26.57	0.16	59	1554
	60	-1.80	9.00	-0.27	0.92	50	1312	32.48	34.35	33.14	0.33	43	1052	26.00	27.39	26.61	0.24	43	1052
	70	-1.81	9.30	-0.37	0.95	61	1596	32.48	34.42	33.24	0.27	58	1306	26.00	27.41	26.70	0.18	58	1305
	80	-1.78	9.30	-0.51	0.79	63	1447	32.54	34.55	33.23	0.21	60	1174	26.17	27.47	26.70	0.15	60	1173
	90	-1.80	8.60	-0.14	1.12	50	815	32.56	34.22	33.37	0.31	45	626	26.19	27.31	26.79	0.20	45	626
	100	-1.79	7.70	-0.24	0.92	62	1081	32.68	34.52	33.45	0.26	57	855	26.28	27.53	26.86	0.18	57	851

		Temperature (deg C)						Salinity (psu)						Sigmat					
Month	**Depth (m)**	**Min**	**Max**	**Avg**	**Std Dev**	**Count**	**Total**	**Min**	**Max**	**Avg**	**Std Dev**	**Count**	**Total**	**Min**	**Max**	**Avg**	**Std Dev**	**Count**	**Total**
May	0	-2.00	9.10	2.03	1.35	67	2165	31.84	34.66	32.84	0.23	62	1034	25.13	27.70	26.22	0.23	62	1034
	10	-1.40	8.70	2.01	1.34	45	3003	31.92	34.08	32.80	0.23	40	1429	25.13	27.01	26.19	0.22	40	1429
	20	-1.60	7.00	1.40	1.15	63	3632	31.37	34.48	32.88	0.24	61	1852	25.04	27.09	26.30	0.22	61	1847
	30	-1.80	6.80	1.06	1.01	64	3796	32.22	34.04	32.91	0.21	62	1883	25.59	27.10	26.35	0.17	62	1883
	40	-2.00	6.70	0.53	0.96	48	3010	32.27	34.05	32.90	0.20	31	1317	25.84	27.14	26.38	0.16	31	1317
	50	-2.00	7.04	0.15	0.88	65	3672	32.28	34.48	33.05	0.25	61	1936	25.80	27.42	26.52	0.18	61	1935
	60	-1.90	6.60	-0.03	1.07	51	2635	32.40	34.33	33.00	0.21	43	1298	26.00	27.42	26.50	0.18	43	1298
	70	-2.00	8.02	-0.35	0.96	64	2807	32.41	34.72	33.23	0.27	59	1470	26.01	27.36	26.69	0.18	59	1467
	80	-2.00	6.60	-0.46	1.11	62	2197	32.63	34.46	33.23	0.22	59	1120	26.22	27.44	26.70	0.16	59	1117
	90	-2.00	7.91	-0.17	1.76	55	1300	32.63	34.87	33.34	0.37	47	483	26.24	27.47	26.76	0.20	47	483
	100	-1.88	6.60	-0.29	1.07	63	1650	32.71	34.74	33.42	0.25	60	796	26.30	27.53	26.84	0.17	60	796
June	0	-0.60	14.36	4.53	1.55	68	3080	30.11	33.90	32.69	0.24	59	2457	23.73	26.72	25.88	0.29	59	2457
	10	-0.80	11.08	4.11	1.46	47	5101	31.60	33.36	32.61	0.21	37	4123	24.77	26.66	25.89	0.27	37	4123
	20	-1.70	12.05	3.12	1.25	67	5589	31.61	34.06	32.76	0.23	57	4423	24.77	26.95	26.08	0.24	57	4421
	30	-1.70	12.05	2.34	1.27	67	5774	31.61	34.06	32.80	0.20	56	4574	24.91	27.24	26.17	0.20	56	4570
	40	-1.76	6.90	1.02	1.21	44	5174	31.97	34.64	32.86	0.25	31	4122	25.42	27.63	26.32	0.25	31	4122
	50	-1.79	6.84	0.28	0.84	67	5375	32.17	34.45	33.02	0.26	57	4427	25.62	27.45	26.49	0.21	57	4427
	60	-1.80	4.20	0.02	0.86	48	4549	32.40	34.06	32.99	0.19	38	3762	25.97	27.17	26.48	0.17	38	3761
	70	-1.80	5.80	-0.34	0.72	64	3708	32.48	34.57	33.20	0.28	57	3004	25.99	27.51	26.67	0.21	57	3004
	80	-1.80	5.80	-0.51	0.60	63	2754	32.48	34.56	33.20	0.22	56	2138	25.99	27.47	26.68	0.17	56	2137
	90	-1.73	4.25	-0.19	0.95	51	1880	32.56	34.57	33.42	0.37	38	1366	26.17	27.42	26.84	0.25	38	1366
	100	-1.80	5.80	-0.23	0.79	65	1610	32.56	34.90	33.42	0.33	57	1146	26.17	27.93	26.84	0.24	57	1146
July	0	3.42	14.40	9.39	2.07	59	1080	30.95	33.28	32.31	0.27	53	622	23.47	26.03	24.89	0.40	53	618
	10	-0.70	13.90	8.73	1.93	46	2019	30.97	33.14	32.33	0.26	42	1091	23.50	26.01	24.95	0.39	42	1091
	20	-1.40	12.98	6.27	1.77	58	2450	31.59	33.93	32.53	0.23	52	1245	24.49	26.68	25.46	0.32	51	1244
	30	-1.60	11.40	3.92	1.77	58	2344	31.84	33.32	32.68	0.18	51	1283	24.72	26.69	25.90	0.28	51	1283
	40	-1.80	7.77	1.45	1.08	45	1931	31.96	34.07	32.82	0.24	19	1055	25.36	27.24	26.25	0.17	18	1054
	50	-1.80	7.26	0.27	0.93	57	1952	32.31	34.01	32.94	0.17	52	1265	25.33	27.32	26.42	0.15	51	1264
	60	-1.85	5.77	-0.02	1.15	45	1532	32.57	34.48	33.08	0.36	19	942	26.00	27.32	26.53	0.18	18	940
	70	-1.87	5.90	-0.43	0.82	56	1630	32.61	34.48	33.14	0.16	51	1074	25.91	27.36	26.62	0.12	50	1072
	80	-1.86	5.90	-0.46	0.78	53	1436	32.68	34.00	33.14	0.12	50	951	25.91	27.37	26.63	0.10	50	950
	90	-1.87	5.23	-0.31	0.97	49	1004	32.82	34.52	33.24	0.23	28	613	26.38	27.39	26.70	0.15	28	613
	100	-1.87	6.30	-0.44	0.85	53	1000	32.85	34.54	33.32	0.16	52	656	25.96	27.51	26.76	0.12	51	655
Aug	0	1.10	18.35	11.99	2.24	39	646	30.28	33.07	31.94	0.44	24	201	22.83	25.69	24.18	0.53	24	201
	10	-1.49	18.36	10.83	2.88	35	1971	30.63	33.12	32.05	0.40	21	1193	22.88	26.39	24.43	0.51	21	1193
	20	-1.90	18.23	6.88	3.84	36	2506	30.72	33.52	32.46	0.27	23	1330	23.04	26.55	25.30	0.59	23	1329
	30	-1.90	14.16	3.49	3.22	37	2419	31.29	34.12	32.70	0.26	24	1301	24.02	27.13	25.92	0.47	24	1299
	40	-1.80	9.71	0.96	2.09	32	1830	32.47	34.37	32.89	0.25	14	1009	25.40	27.38	26.36	0.25	14	1009
	50	-1.90	10.86	-0.16	1.22	37	1225	32.55	35.18	33.00	0.20	25	623	25.67	27.42	26.50	0.17	25	622
	60	-1.90	5.40	-0.39	1.06	32	835	32.69	34.40	33.04	0.26	13	399	26.12	27.43	26.54	0.19	13	399
	70	-2.00	4.90	-0.71	0.95	35	737	32.75	34.52	33.11	0.17	23	393	26.33	27.53	26.62	0.13	23	393
	80	-2.00	4.60	-0.81	0.99	33	622	32.75	34.52	33.17	0.18	23	351	26.33	27.53	26.67	0.14	23	351
	90	-2.00	4.40	-0.62	1.13	29	484	32.89	33.84	33.24	0.20	15	278	26.45	27.15	26.73	0.15	15	277
	100	-1.75	10.10	-0.55	1.03	33	566	32.89	35.17	33.28	0.18	24	380	26.45	27.56	26.75	0.13	24	377

		Temperature (deg C)						Salinity (psu)						Sigmat					
Month	**Depth (m)**	**Min**	**Max**	**Avg**	**Std Dev**	**Count**	**Total**	**Min**	**Max**	**Avg**	**Std Dev**	**Count**	**Total**	**Min**	**Max**	**Avg**	**Std Dev**	**Count**	**Total**
Sept	0	0.57	18.20	11.26	2.65	38	630	31.16	33.65	32.08	0.34	21	266	23.19	25.92	24.38	0.68	21	266
	10	0.10	17.20	10.74	2.45	34	898	31.26	33.71	32.09	0.34	17	347	23.26	25.99	24.43	0.64	17	347
	20	-1.30	17.20	7.95	2.85	36	1161	31.48	33.76	32.37	0.26	19	356	23.45	26.50	25.07	0.49	19	356
	30	-1.65	16.40	4.63	2.67	36	1231	31.48	33.85	32.64	0.28	19	401	23.71	26.92	25.72	0.45	19	401
	40	-1.80	10.40	1.65	2.06	31	886	31.86	33.89	32.86	0.28	9	312	24.99	27.04	26.24	0.27	9	312
	50	-1.90	8.84	0.16	1.43	36	723	32.26	34.06	33.08	0.23	20	312	25.48	27.22	26.52	0.19	20	312
	60	-1.96	7.56	-0.21	1.26	28	533	32.52	34.06	33.07	0.21	8	220	25.98	27.11	26.53	0.09	8	220
	70	-1.96	7.30	-0.35	1.15	33	509	32.69	34.33	33.24	0.28	17	228	26.18	27.34	26.71	0.19	17	228
	80	-1.94	7.60	-0.34	1.12	33	415	32.76	34.20	33.24	0.23	17	182	26.31	27.34	26.72	0.17	17	182
	90	-1.74	7.60	-0.20	1.15	29	329	32.89	34.55	33.40	0.42	11	129	26.46	27.47	26.83	0.25	11	129
	100	-1.70	7.30	-0.17	1.11	33	326	32.92	34.42	33.41	0.23	18	133	26.48	27.48	26.85	0.16	18	133
Oct	0	2.90	14.90	8.03	2.09	34	927	30.28	33.86	32.27	0.38	23	480	22.98	26.48	25.13	0.50	23	480
	10	1.27	14.80	7.83	2.05	33	1995	31.30	33.87	32.28	0.39	22	1517	23.80	26.49	25.18	0.51	22	1517
	20	-1.33	14.10	7.12	2.05	34	2112	31.19	33.87	32.41	0.37	24	1497	23.80	26.60	25.39	0.50	24	1497
	30	-1.67	13.78	5.88	2.11	35	2625	31.06	34.43	32.59	0.35	24	1650	23.74	27.14	25.69	0.49	24	1650
	40	-1.70	12.60	3.09	2.37	31	2943	31.87	34.12	32.87	0.26	13	1708	24.46	27.25	26.18	0.34	13	1708
	50	-1.70	11.20	0.87	2.20	35	2698	31.99	34.40	33.05	0.19	25	1757	25.03	27.34	26.50	0.16	25	1756
	60	-1.73	9.40	0.26	2.11	30	2213	32.06	34.39	33.16	0.23	15	1607	25.25	27.42	26.62	0.17	15	1607
	70	-1.74	8.20	-0.04	1.80	34	1924	32.75	34.40	33.26	0.19	23	1418	26.23	27.43	26.72	0.14	23	1418
	80	-1.71	8.07	-0.07	1.77	31	1244	32.81	34.49	33.33	0.22	21	832	26.28	27.43	26.78	0.16	21	832
	90	-1.68	7.20	0.11	1.76	30	872	32.95	34.51	33.43	0.26	15	549	26.51	27.43	26.85	0.17	15	549
	100	-1.68	6.78	-0.25	1.08	29	843	32.93	34.54	33.50	0.26	23	539	26.49	27.50	26.91	0.17	23	539
Nov	0	0.19	11.10	4.77	1.38	36	1241	30.60	33.86	32.50	0.44	29	785	24.11	27.01	25.75	0.46	29	785
	10	-0.02	11.08	4.58	1.30	34	1803	31.62	33.86	32.54	0.41	25	1289	24.50	27.01	25.78	0.43	25	1289
	20	-0.40	11.05	4.24	1.24	36	1801	31.42	34.13	32.61	0.40	29	1226	24.42	27.19	25.88	0.41	29	1224
	30	-1.40	11.02	3.74	1.03	36	2008	31.08	34.46	32.69	0.41	28	1262	24.18	27.46	25.98	0.41	28	1261
	40	-1.40	11.00	2.69	0.97	33	2195	31.41	34.46	32.80	0.35	20	1268	24.39	27.50	26.12	0.32	20	1266
	50	-1.70	9.00	1.45	1.10	36	2284	31.73	34.35	33.01	0.30	29	1321	24.79	27.52	26.42	0.28	29	1319
	60	-1.80	7.52	0.49	1.00	33	1965	31.81	35.16	33.10	0.27	22	1281	24.91	28.26	26.55	0.24	22	1280
	70	-1.50	5.10	0.04	0.77	35	1639	32.11	35.16	33.29	0.28	28	1091	25.64	28.29	26.71	0.21	28	1091
	80	-1.50	5.30	-0.15	0.72	36	1374	32.68	34.18	33.35	0.22	28	944	26.21	27.33	26.76	0.14	28	944
	90	-1.60	4.40	-0.30	0.81	31	1132	32.76	34.37	33.39	0.17	19	832	26.23	27.45	26.81	0.10	19	832
	100	-1.62	5.09	-0.16	0.73	35	1106	32.86	34.45	33.52	0.24	29	827	26.35	27.51	26.91	0.15	29	827
Dec	0	-1.18	6.95	1.96	1.30	24	533	30.05	34.92	32.68	0.42	14	348	24.08	27.77	26.08	0.38	14	348
	10	-1.18	6.95	2.01	1.31	23	946	31.96	34.25	32.66	0.31	14	632	25.16	27.20	26.07	0.31	14	632
	20	-1.17	6.97	1.96	1.23	23	896	31.78	34.24	32.65	0.27	13	578	25.17	27.18	26.07	0.29	13	578
	30	-1.16	6.98	1.86	1.13	23	884	31.78	34.25	32.76	0.30	14	573	25.14	27.18	26.17	0.29	14	573
	40	-1.20	6.86	1.55	0.82	18	853	31.33	34.28	32.77	0.23	10	571	25.00	27.19	26.20	0.23	10	571
	50	-1.60	5.70	1.20	0.96	24	928	31.93	34.31	32.95	0.28	14	587	25.50	27.21	26.37	0.21	14	587
	60	-1.37	5.41	0.77	0.88	21	876	32.15	34.33	33.03	0.22	10	564	25.75	27.22	26.49	0.19	10	564
	70	-1.70	5.25	0.23	0.90	23	858	32.49	34.33	33.22	0.21	14	570	26.09	27.28	26.65	0.14	14	570
	80	-1.59	5.60	0.01	1.01	23	735	32.74	34.42	33.27	0.19	14	496	26.31	27.55	26.70	0.11	14	496
	90	-1.70	5.60	-0.01	1.21	21	425	32.92	34.56	33.38	0.33	14	281	26.46	27.43	26.77	0.20	14	281
	100	-1.80	5.60	0.13	1.76	21	344	33.06	34.65	33.48	0.31	13	225	26.59	27.53	26.86	0.16	13	225

Appendix D
Produced Water Dispersion Model Results

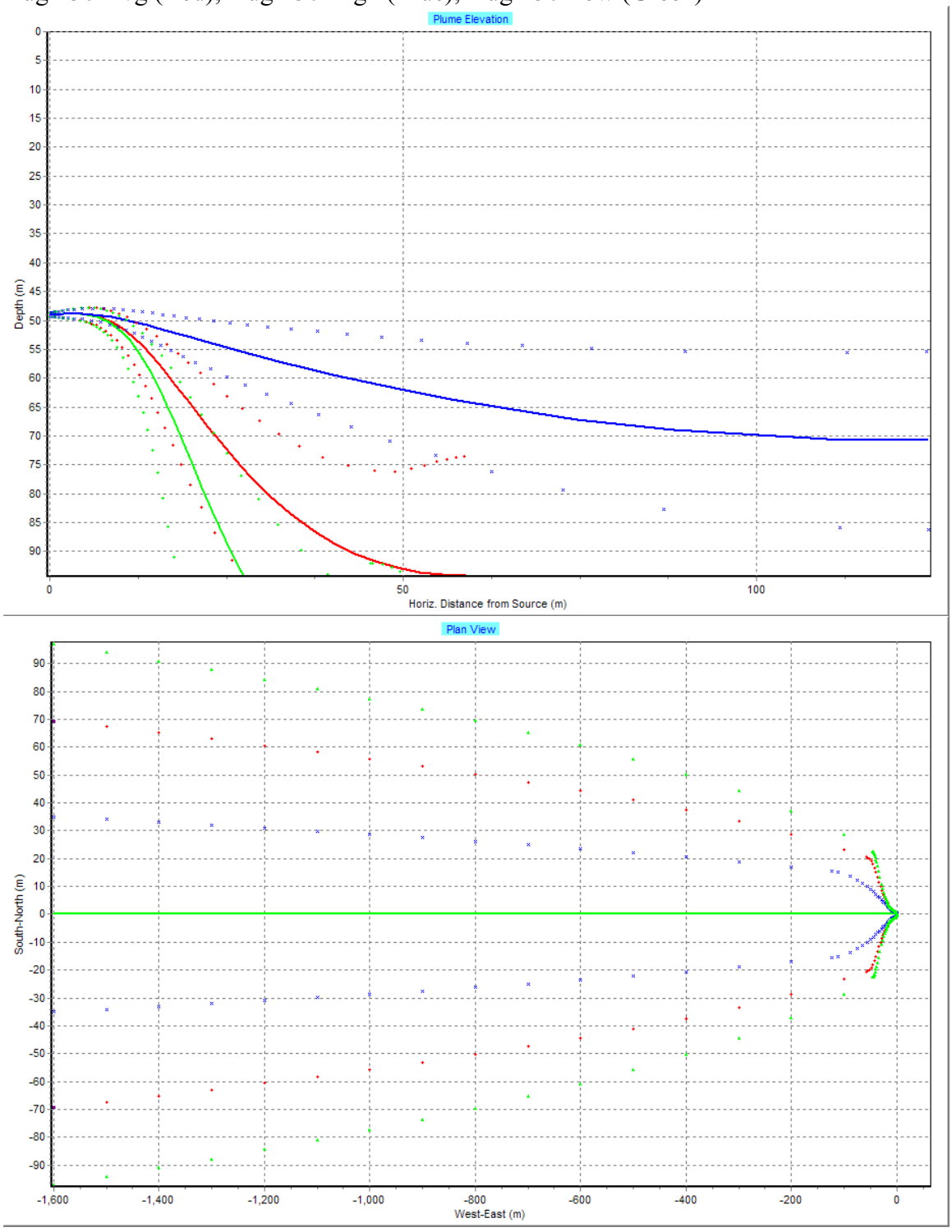
Salinity = 52.9 psu, Discharge Rate = 30,000 m^3/d
Salinity = 52.9 psu, Discharge Rate = 56,000 m^3/d

Salinity = 42 psu, Discharge Rate = 30,000 m^3/d
Salinity = 42 psu, Discharge Rate = 56,000 m^3/d

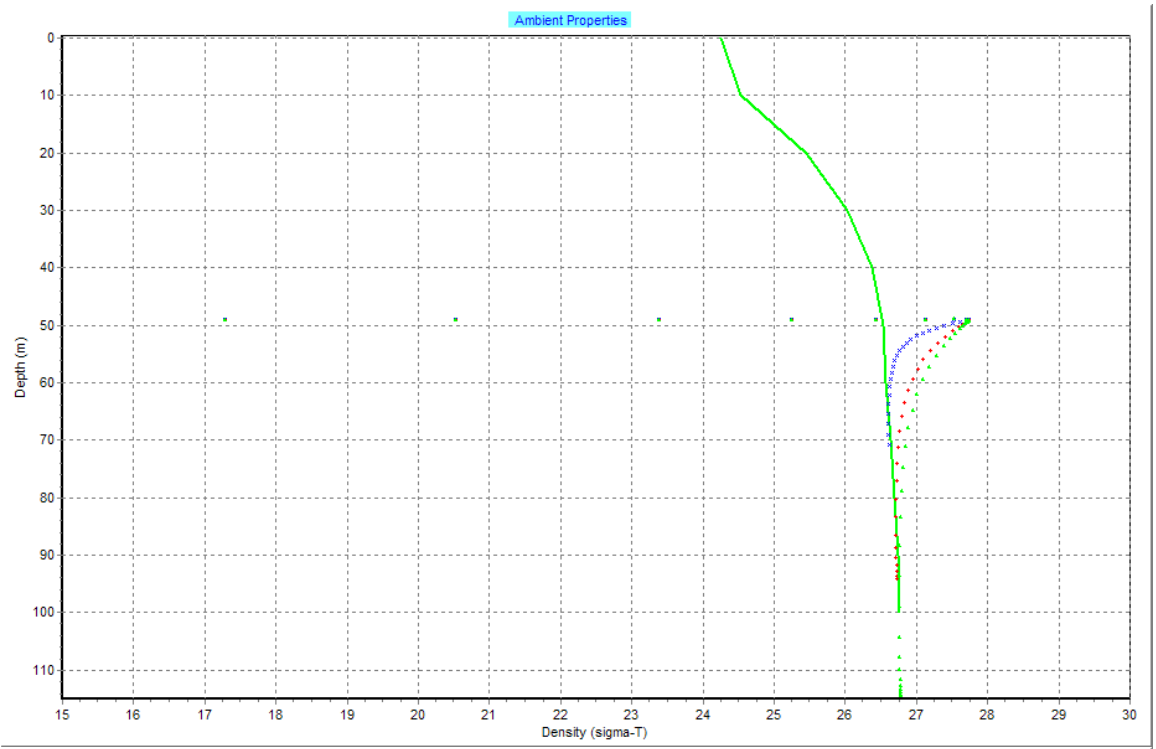
Salinity = 32.7 psu, Discharge Rate = 30,000 m^3/d
Salinity = 32.7 psu, Discharge Rate = 56,000 m^3/d

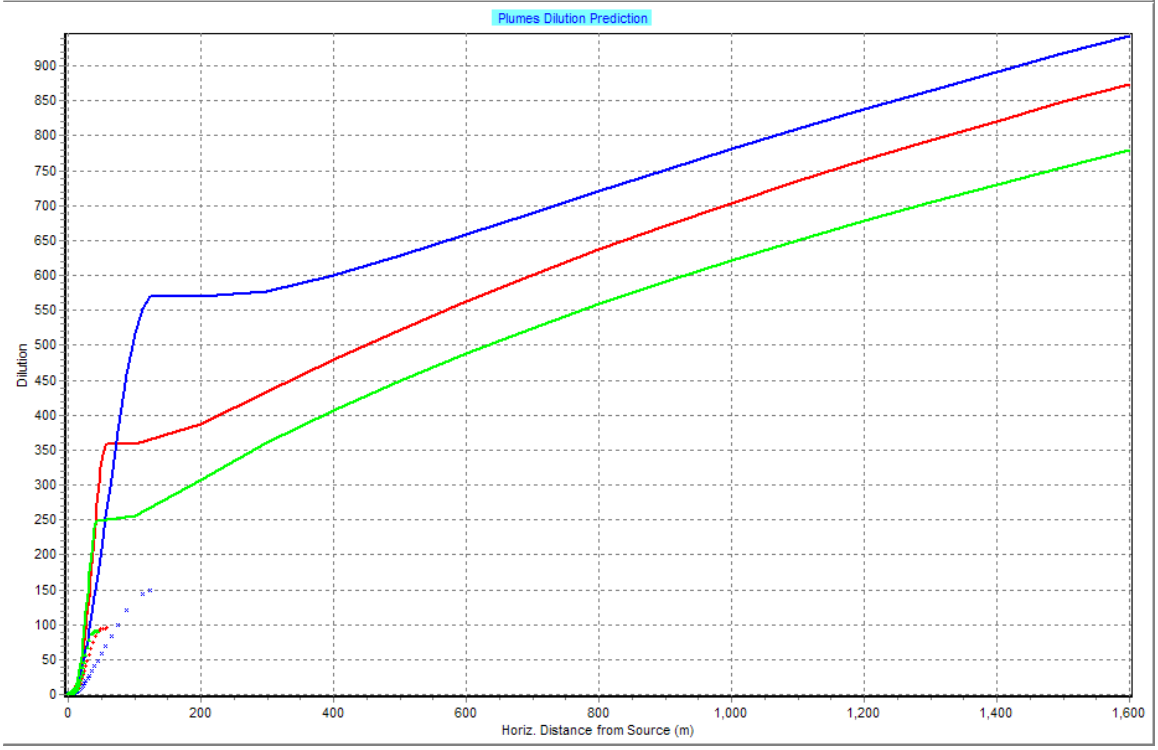
Salinity = 52.9 psu, Discharge Rate = 30,000 m^3/d

Aug F30 Avg (Red); Aug F30 High (Blue); Aug F30 Low (Green)



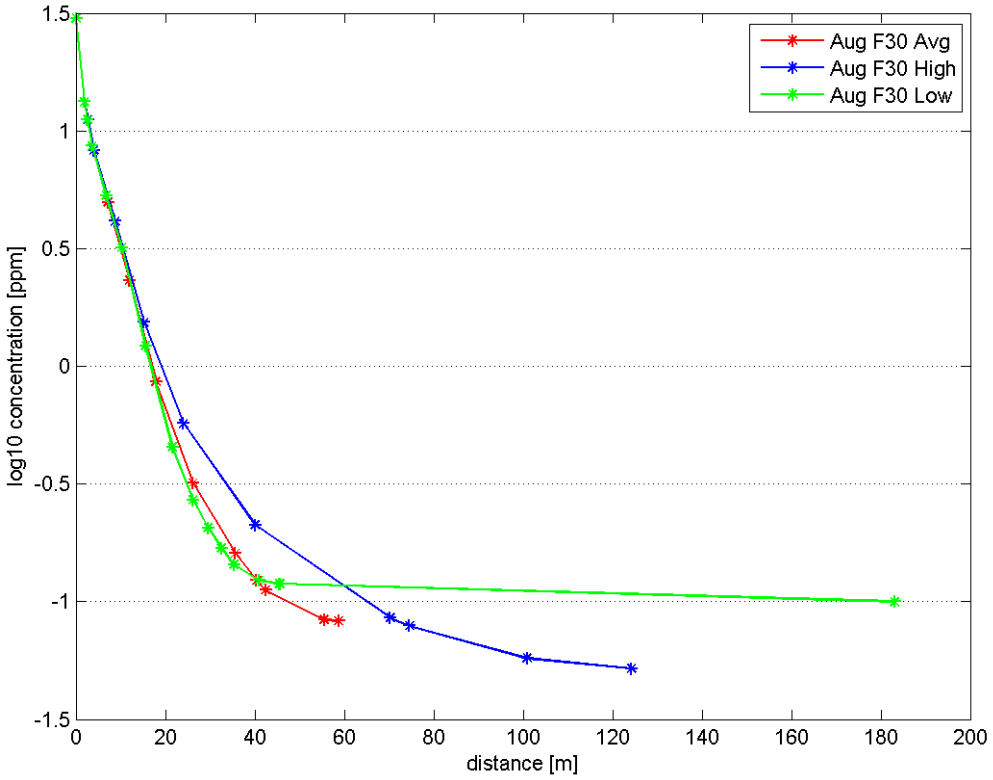
Salinity = 52.9 psu, Discharge Rate = 30,000 m^3/d
Aug F30 Avg (Red); Aug F30 High (Blue); Aug F30 Low (Green)

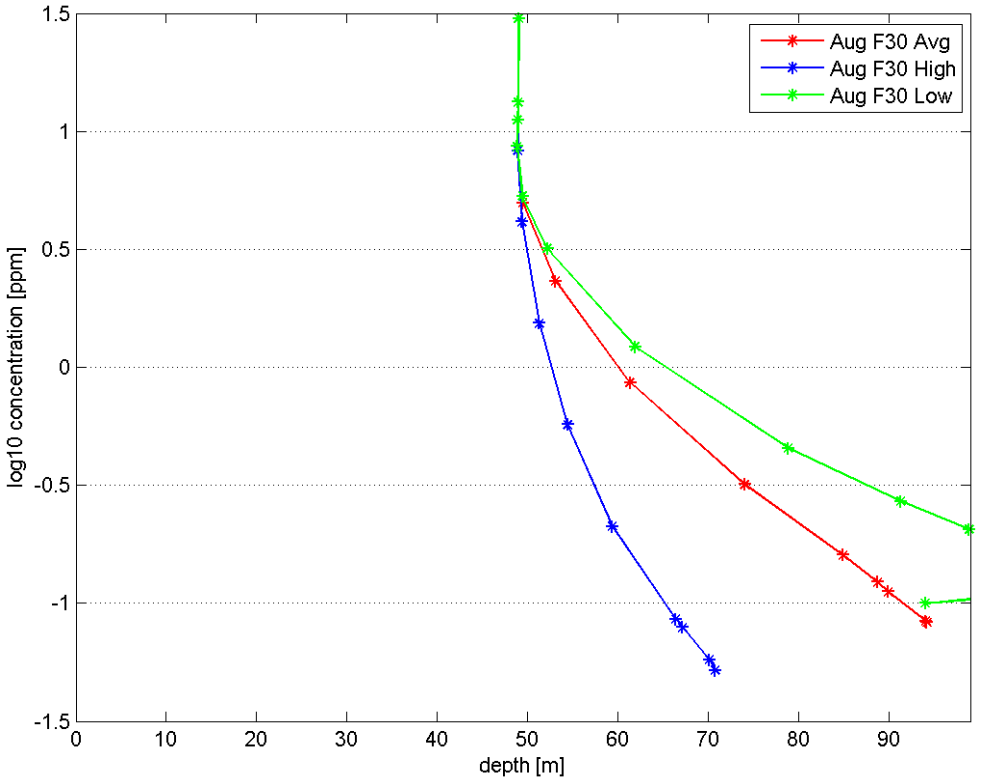




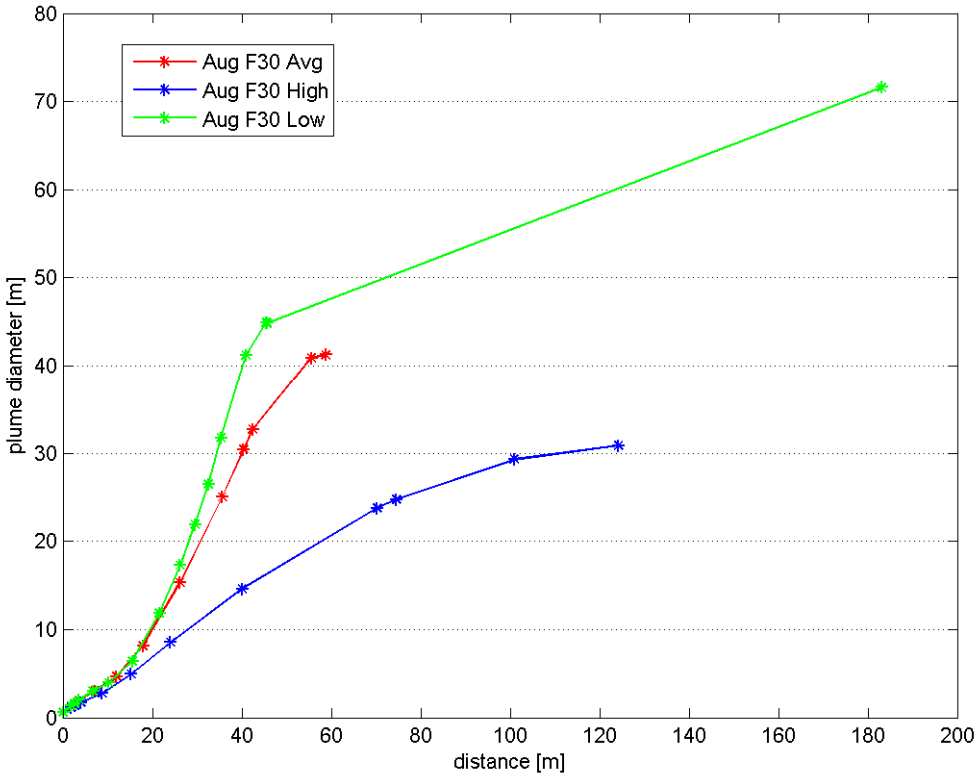
Salinity = 52.9 psu, Discharge Rate = 30,000 m^3/d

Aug F30 Avg (Red); Aug F30 High (Blue); Aug F30 Low (Green)

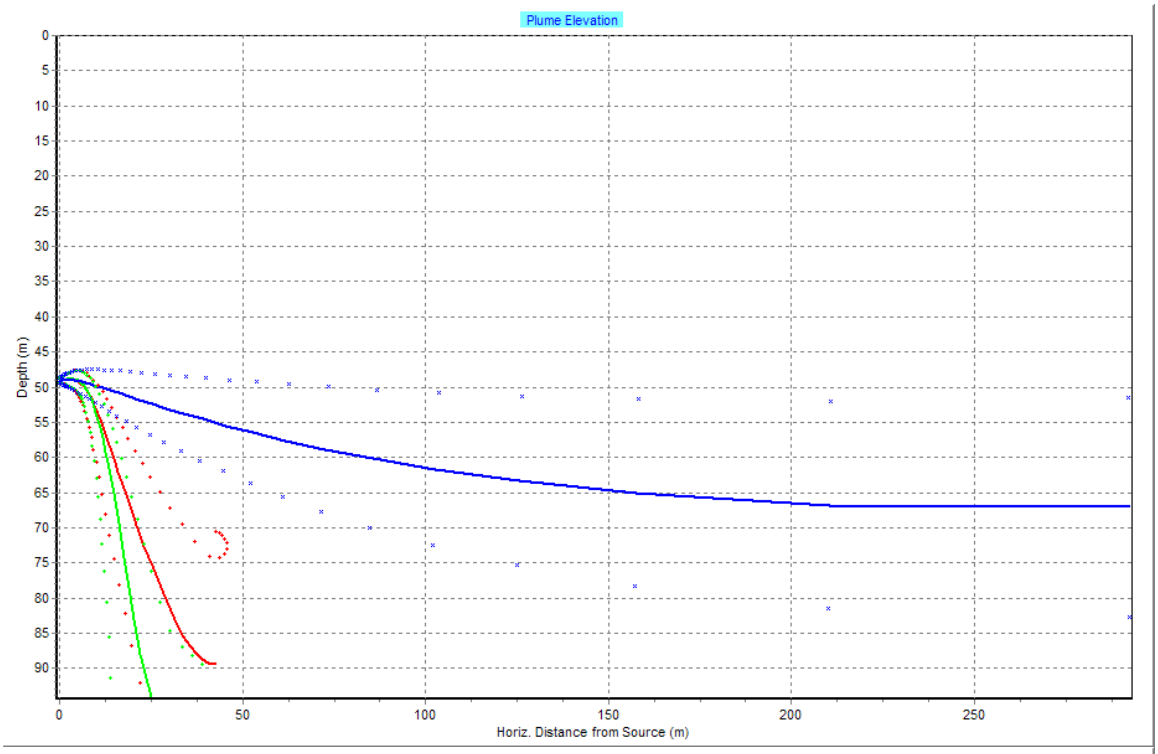


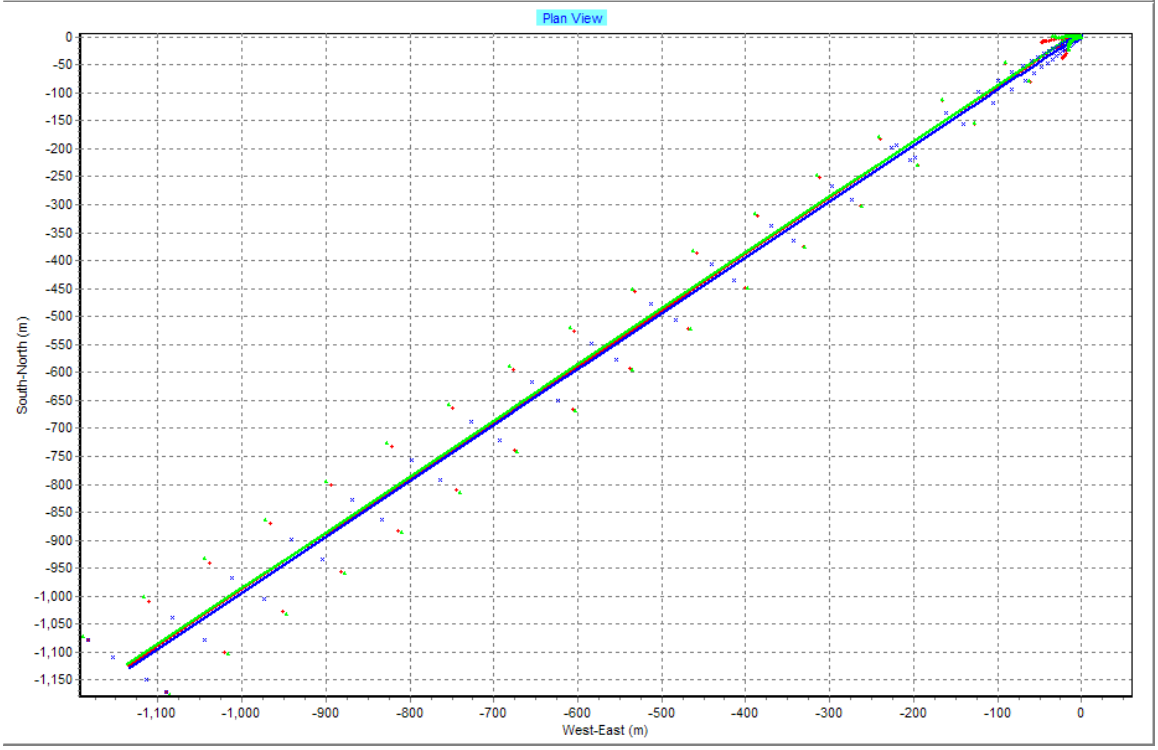


Salinity = 52.9 psu, Discharge Rate = 30,000 m^3/d
Aug F30 Avg (Red); Aug F30 High (Blue); Aug F30 Low (Green)

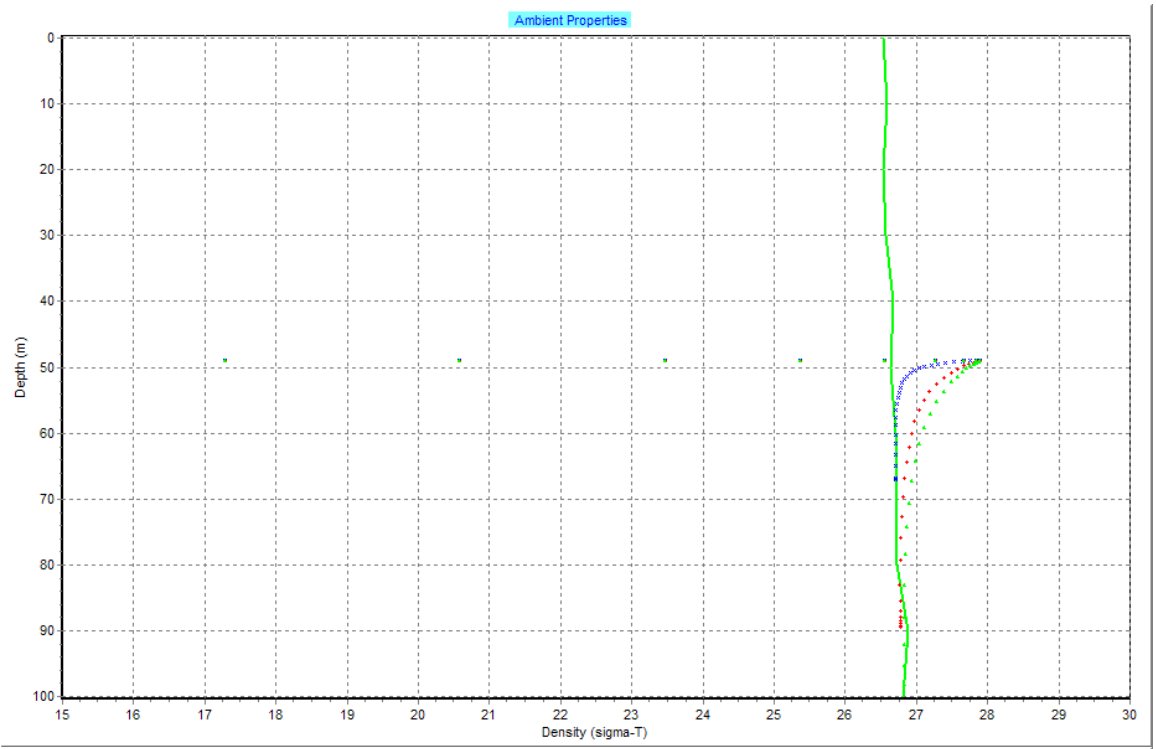


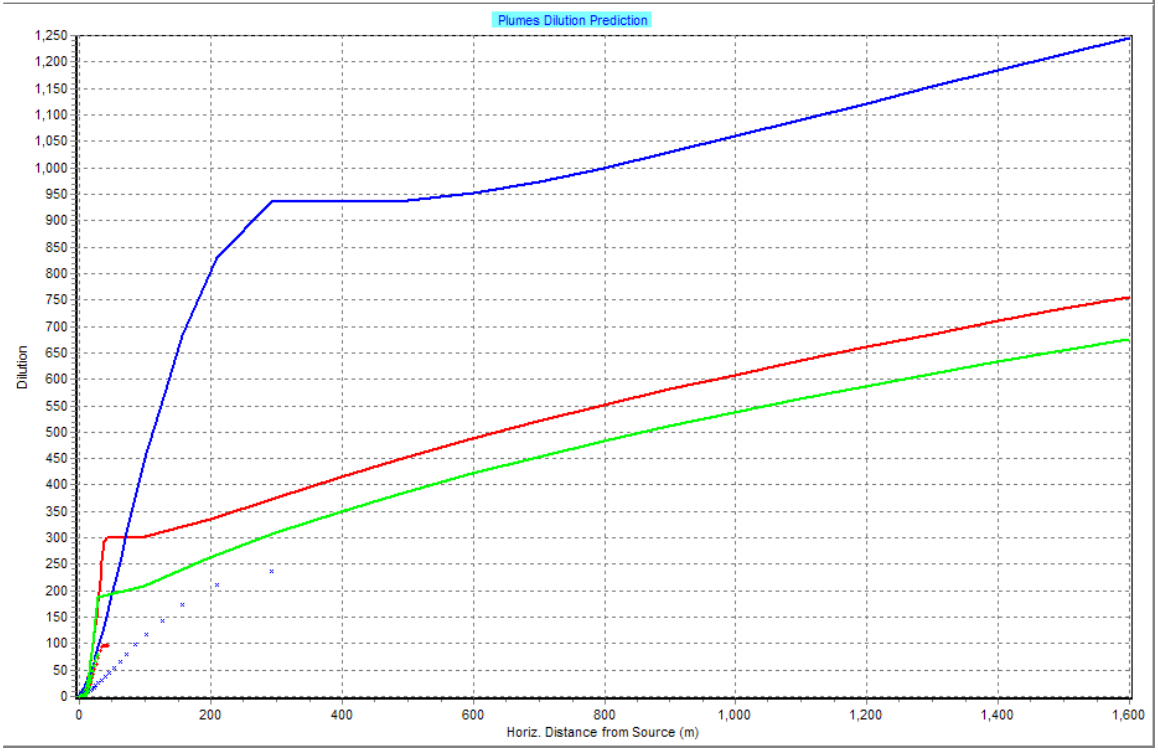
Salinity = 52.9 psu, Discharge Rate = 30,000 m^3/d
Feb F30 Avg (Red); Feb F30 High (Blue); Feb F30 Low (Green)



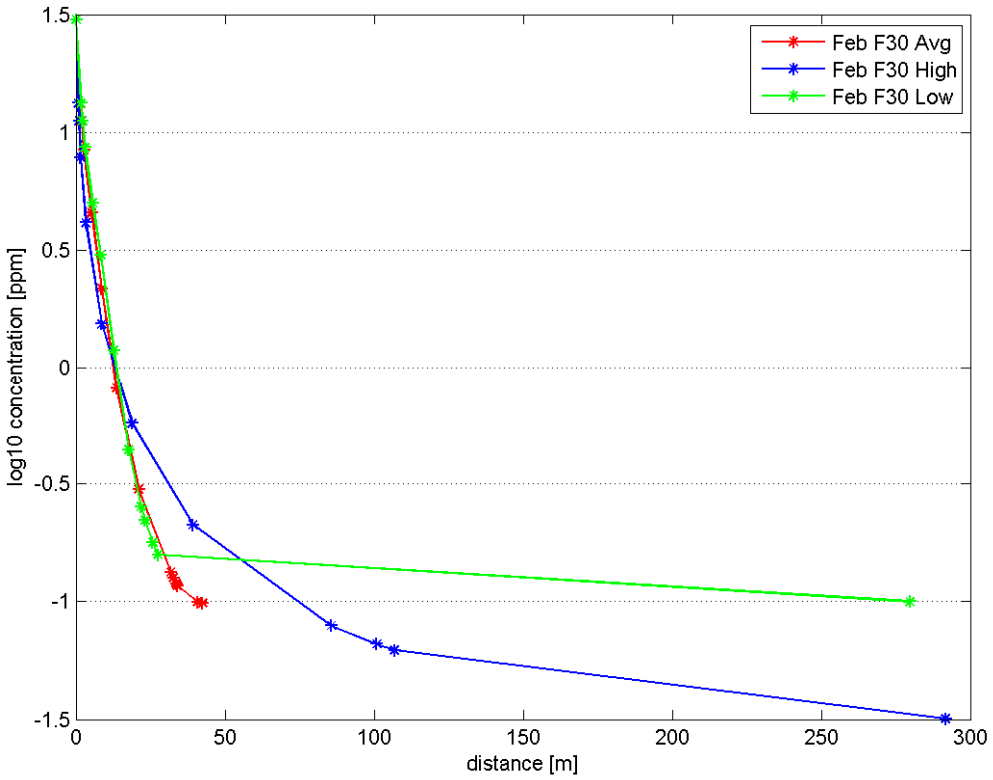


Salinity = 52.9 psu, Discharge Rate = 30,000 m^3/d
Feb F30 Avg (Red); Feb F30 High (Blue); Feb F30 Low (Green)

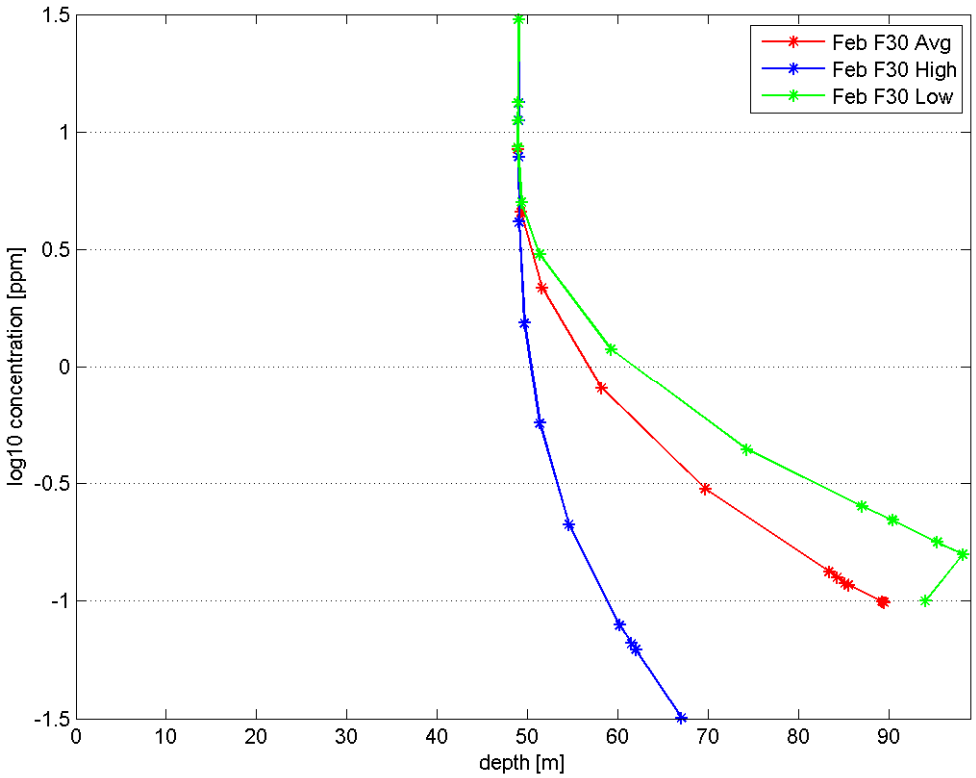




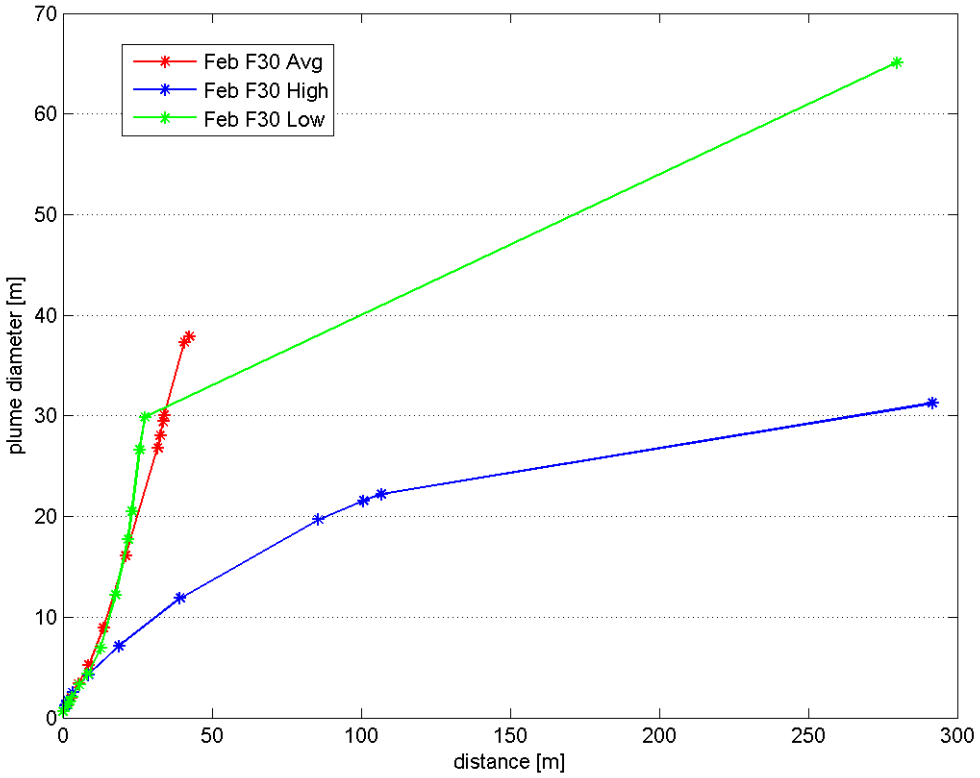
Salinity = 52.9 psu, Discharge Rate = 30,000 m^3/d
Feb F30 Avg (Red); Feb F30 High (Blue); Feb F30 Low (Green)



Salinity = 52.9 psu, Discharge Rate = 30,000 m^3/d
Feb F30 Avg (Red); Feb F30 High (Blue); Feb F30 Low (Green)

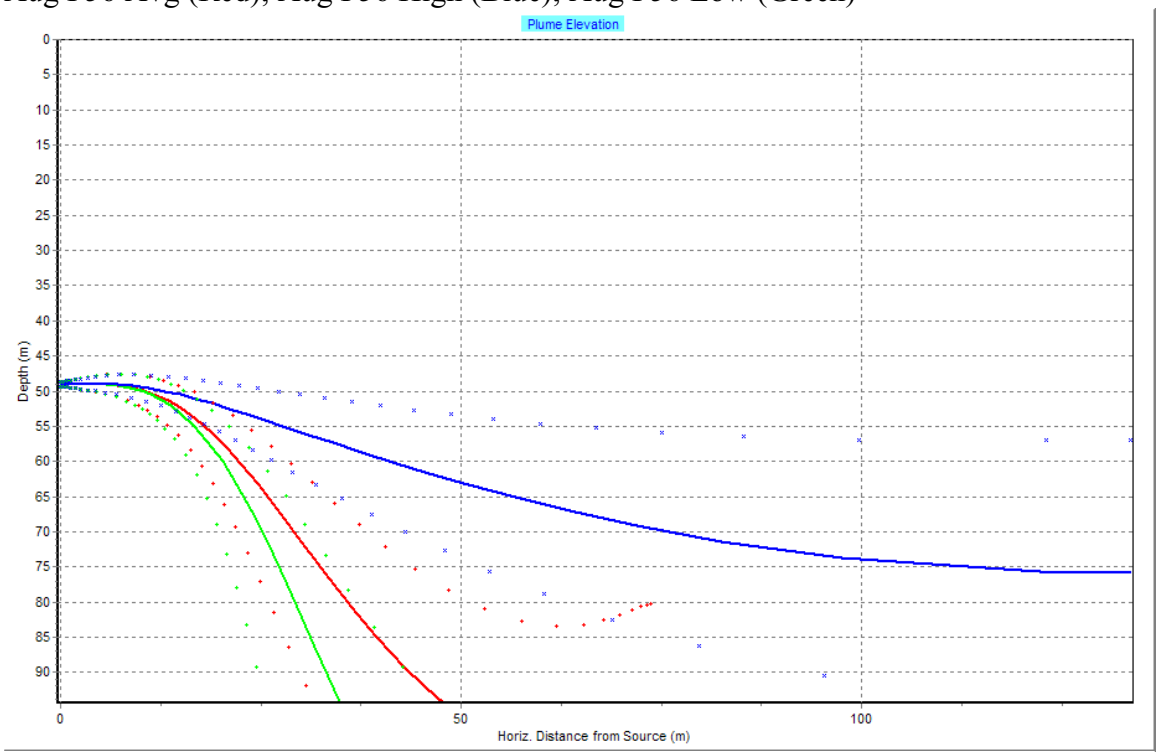


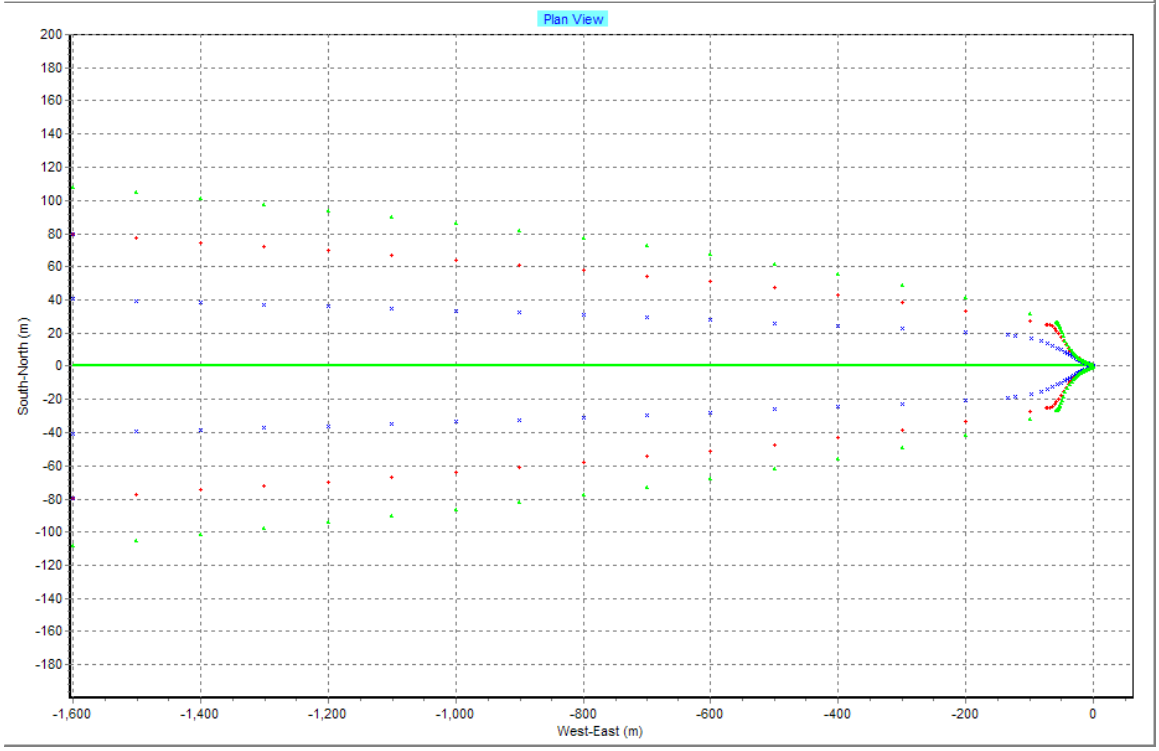
Salinity = 52.9 psu, Discharge Rate = 30,000 m^3/d
Feb F30 Avg (Red); Feb F30 High (Blue); Feb F30 Low (Green)



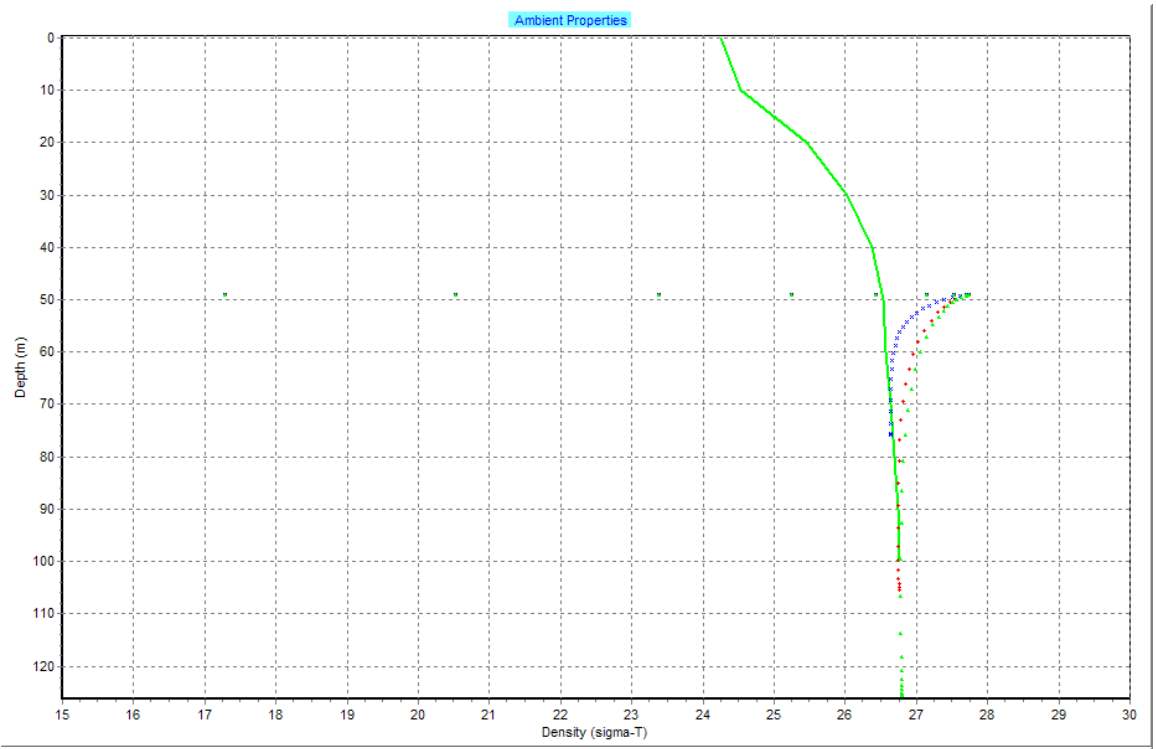
Salinity = 52.9 psu, Discharge Rate = 56,000 m^3/d

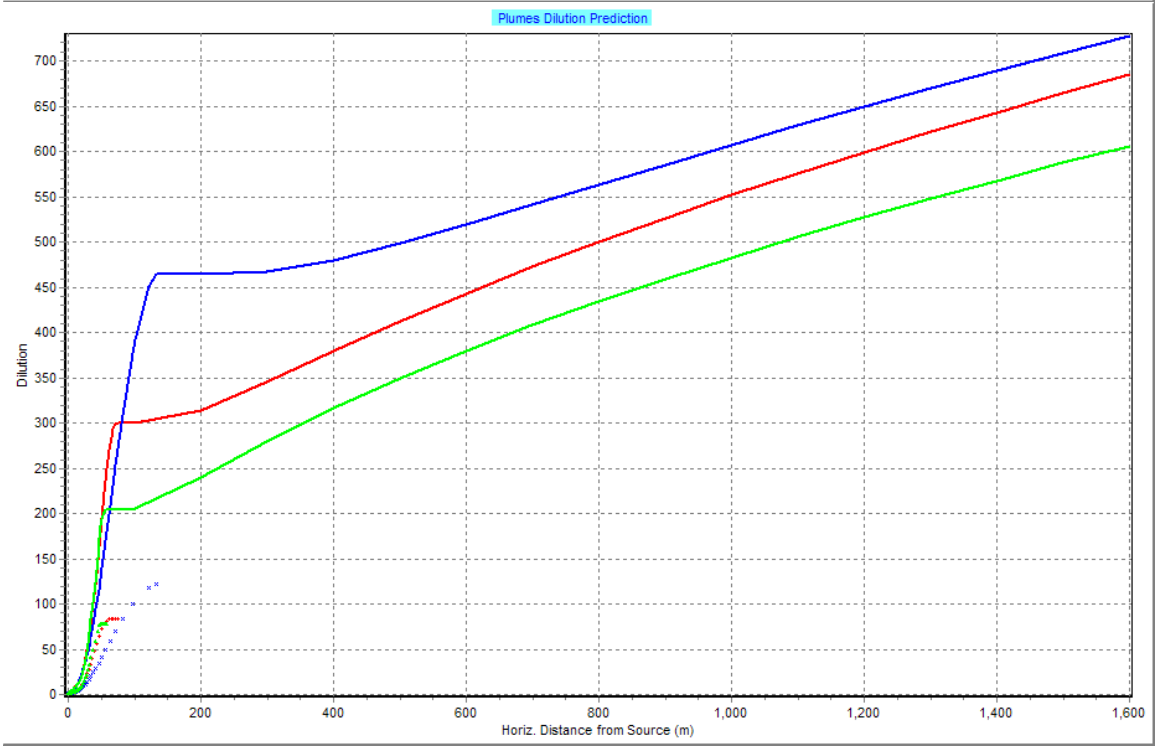
Aug F56 Avg (Red); Aug F56 High (Blue); Aug F56 Low (Green)



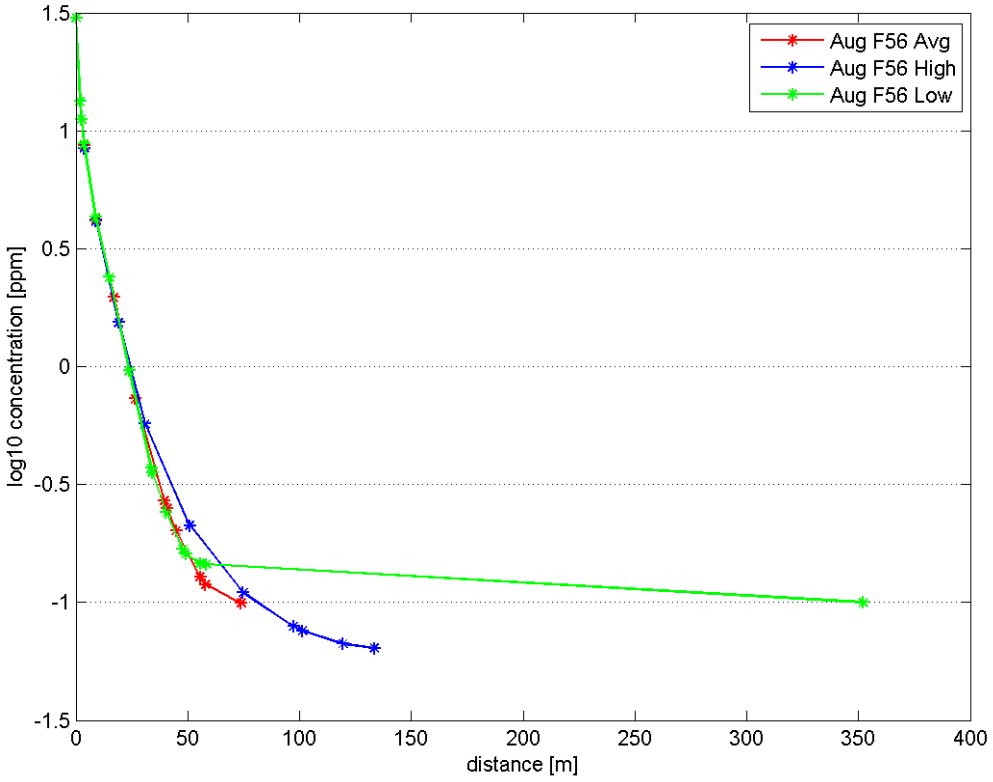


Salinity = 52.9 psu, Discharge Rate = 56,000 m^3/d
Aug F56 Avg (Red); Aug F56 High (Blue); Aug F56 Low (Green)

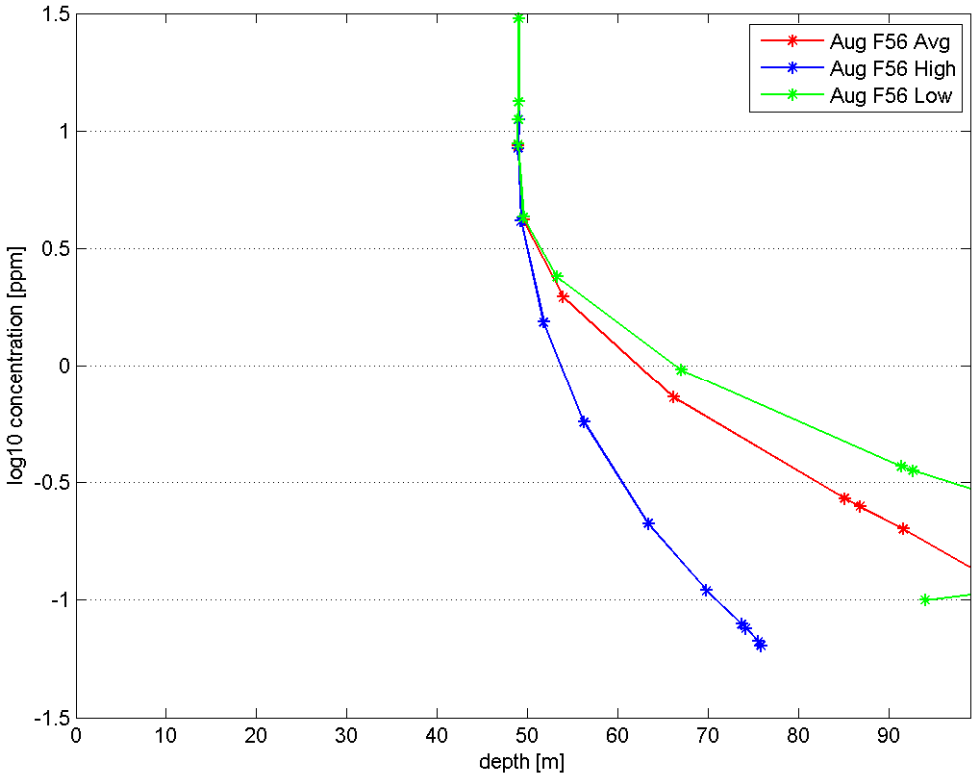




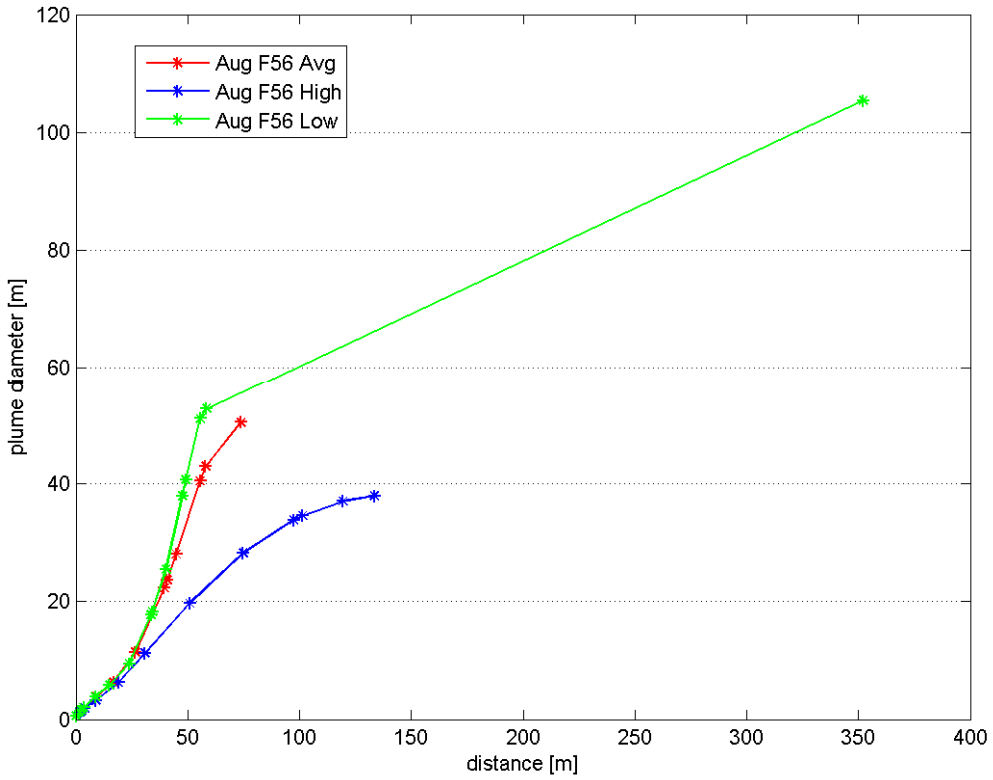
Salinity = 52.9 psu, Discharge Rate = 56,000 m^3/d
Aug F56 Avg (Red); Aug F56 High (Blue); Aug F56 Low (Green)



Salinity = 52.9 psu, Discharge Rate = 56,000 m^3/d
Aug F56 Avg (Red); Aug F56 High (Blue); Aug F56 Low (Green)

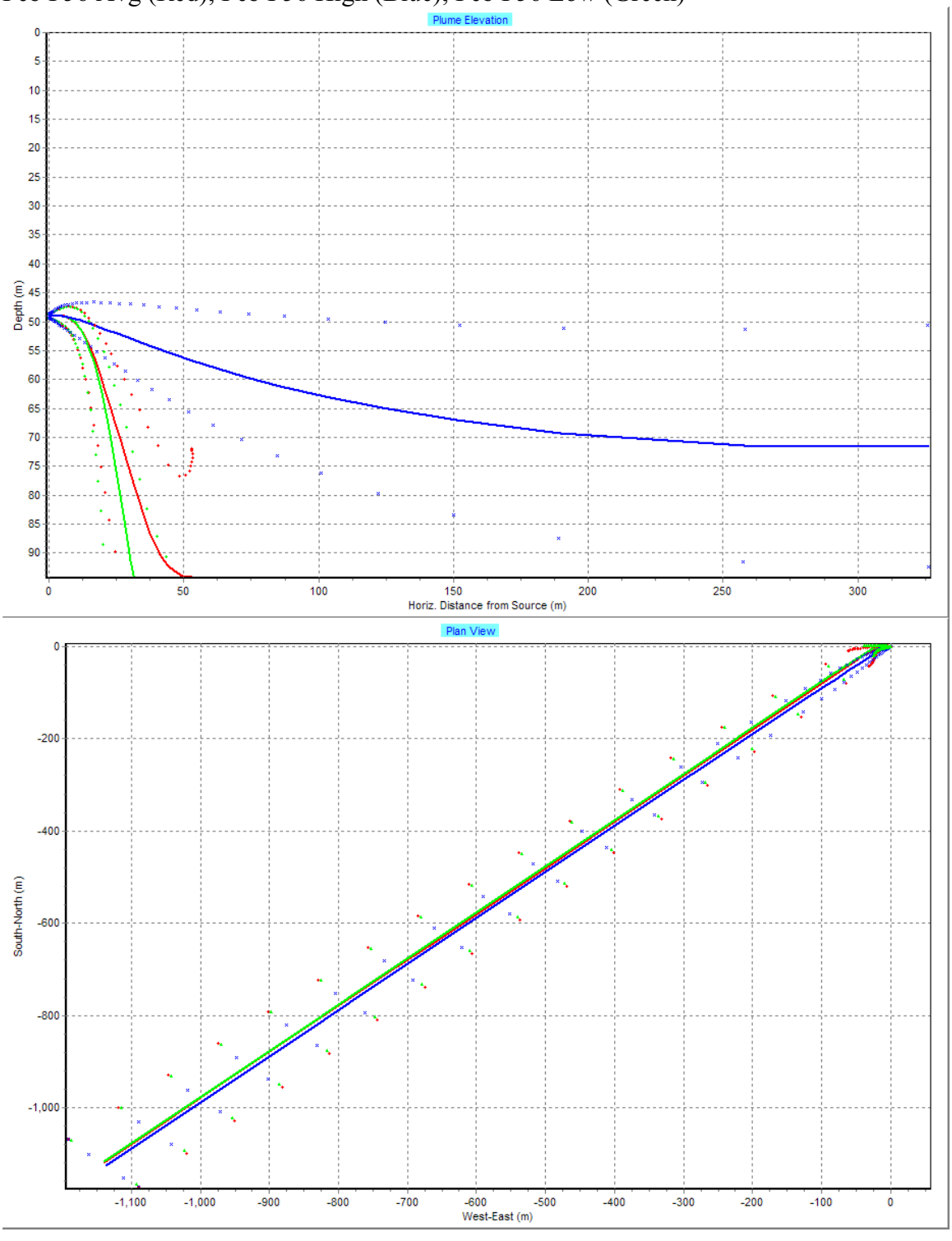


Salinity = 52.9 psu, Discharge Rate = 56,000 m^3/d
Aug F56 Avg (Red); Aug F56 High (Blue); Aug F56 Low (Green)

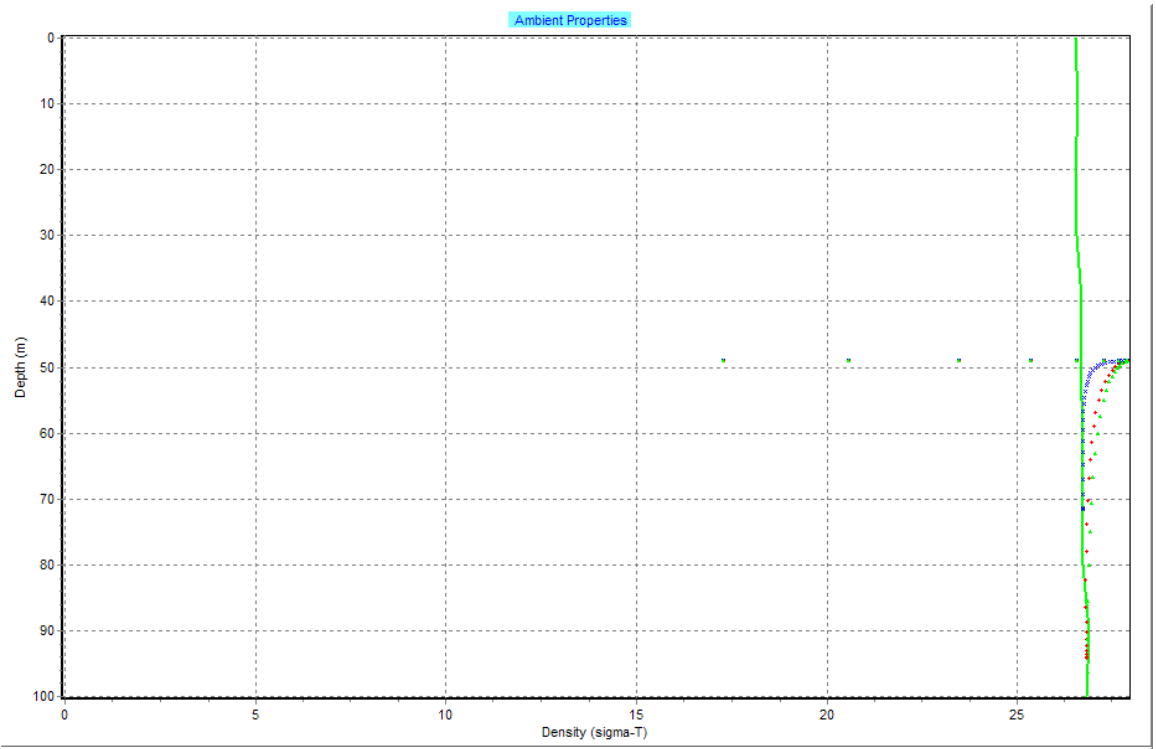


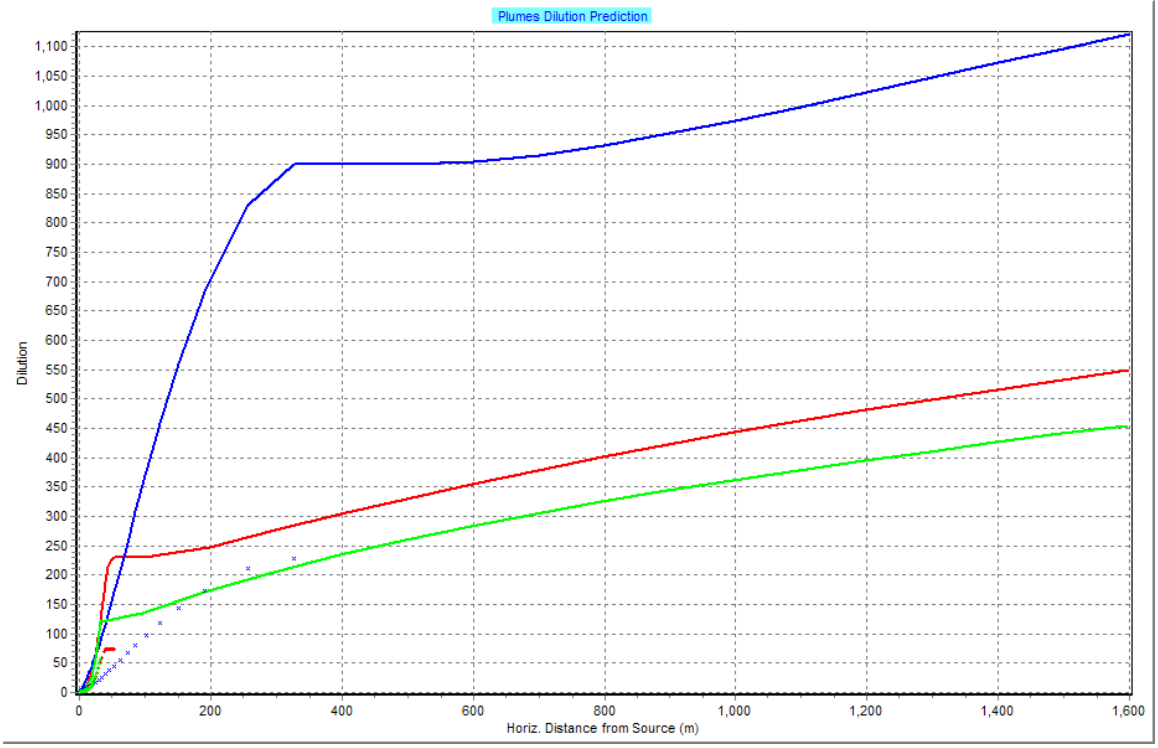
Salinity = 52.9 psu, Discharge Rate = 56,000 m^3/d

Feb F56 Avg (Red); Feb F56 High (Blue); Feb F56 Low (Green)

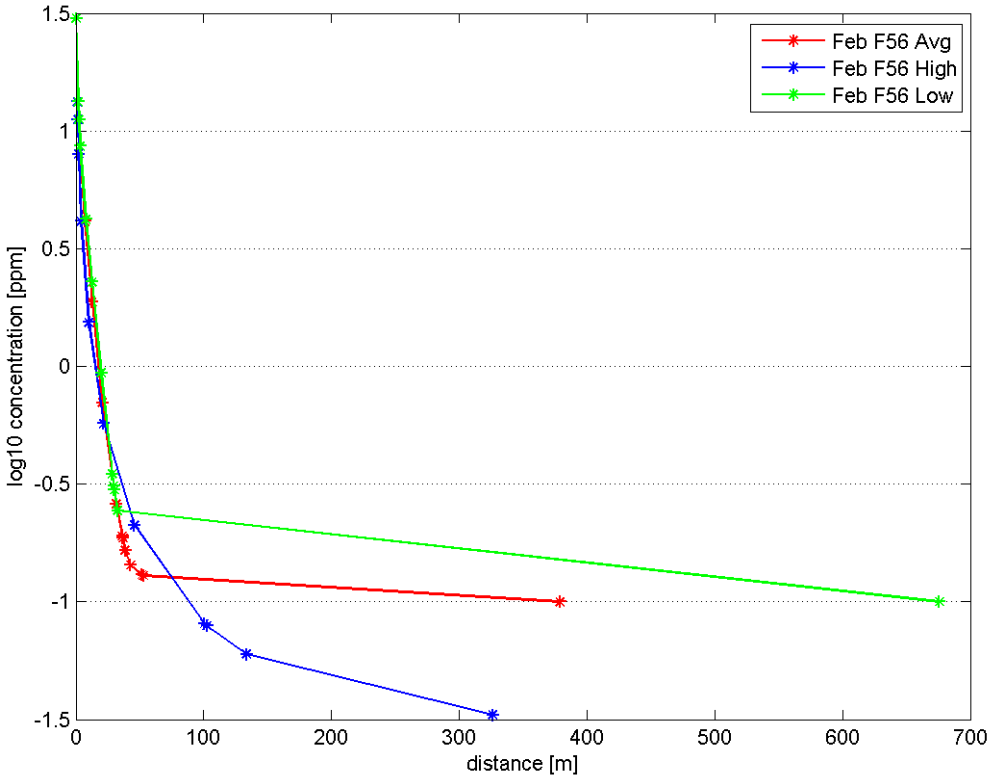


Salinity = 52.9 psu, Discharge Rate = 56,000 m^3/d
Feb F56 Avg (Red); Feb F56 High (Blue); Feb F56 Low (Green)

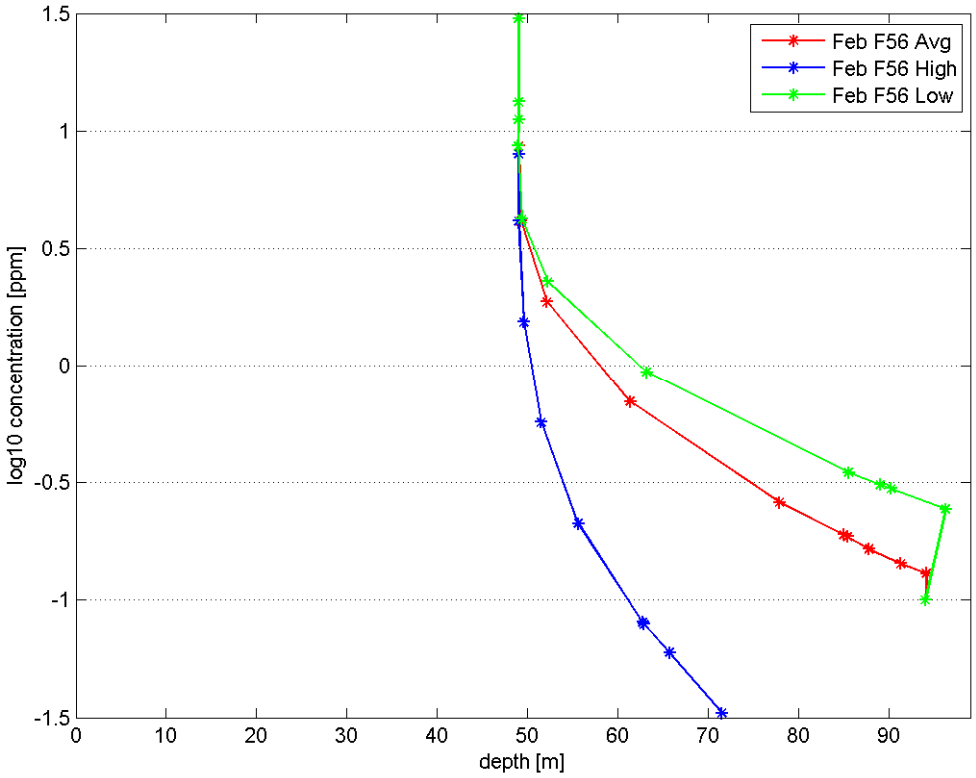




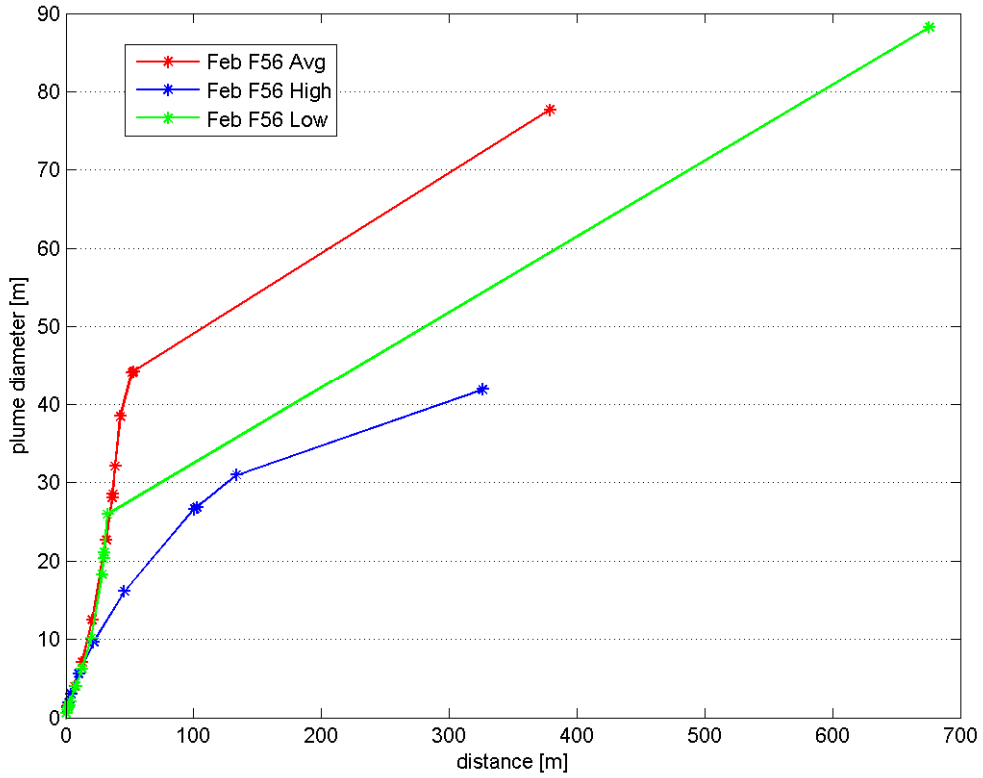
Salinity = 52.9 psu, Discharge Rate = 56,000 m^3/d
Feb F56 Avg (Red); Feb F56 High (Blue); Feb F56 Low (Green)



Salinity = 52.9 psu, Discharge Rate = 56,000 m^3/d
Feb F56 Avg (Red); Feb F56 High (Blue); Feb F56 Low (Green)

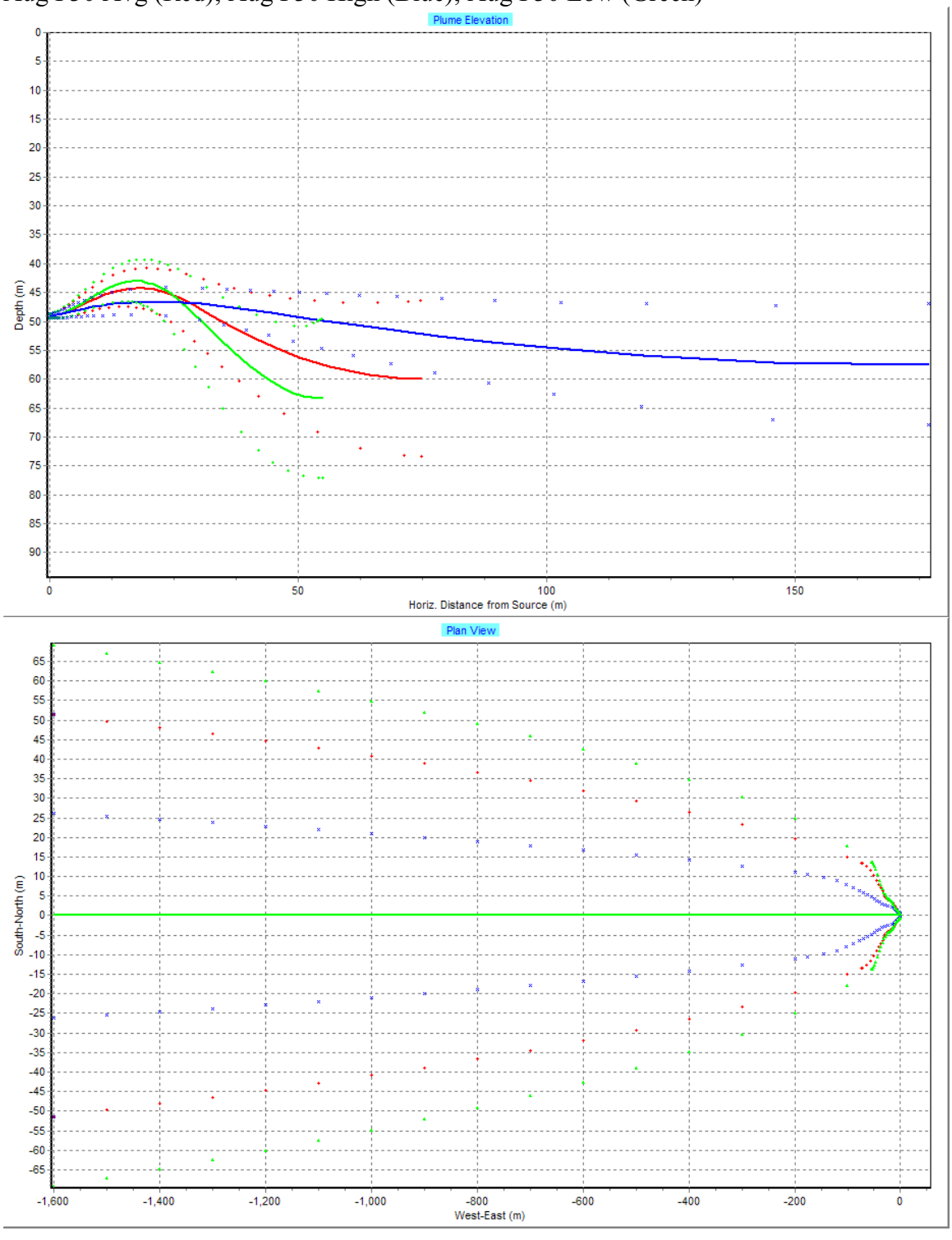


Salinity = 52.9 psu, Discharge Rate = 56,000 m^3/d
Feb F56 Avg (Red); Feb F56 High (Blue); Feb F56 Low (Green)



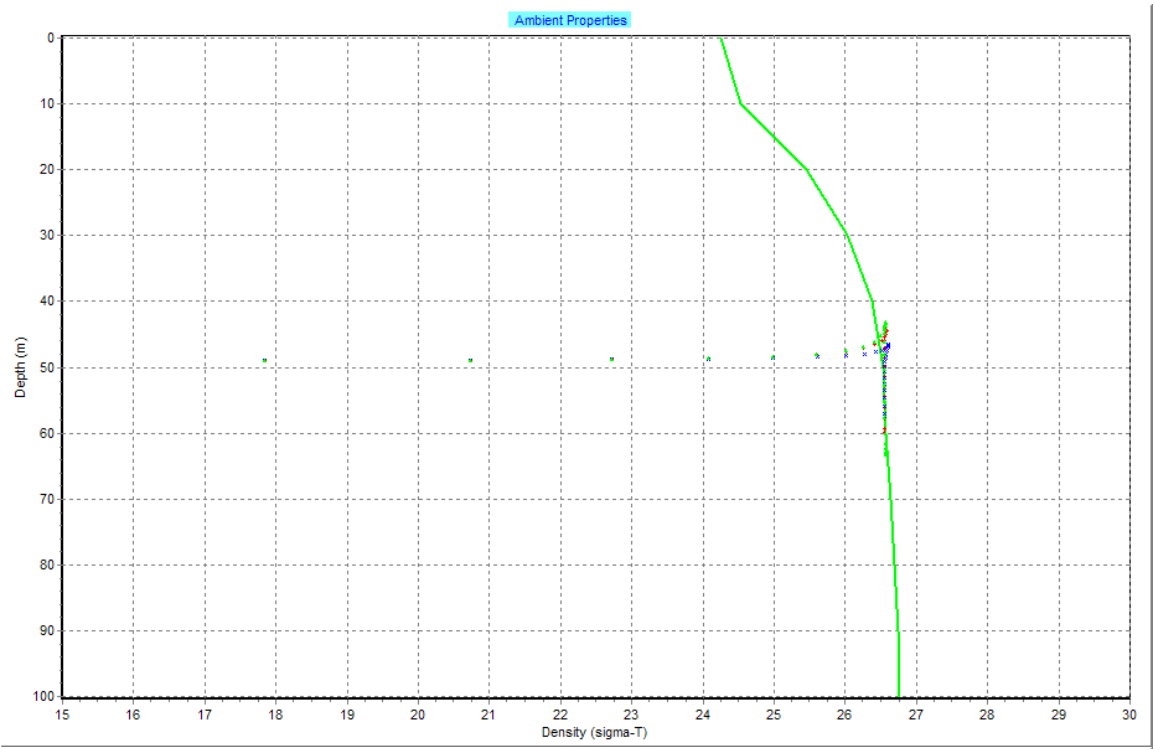
Salinity = 42 psu, Discharge Rate = 30,000 m^3/d

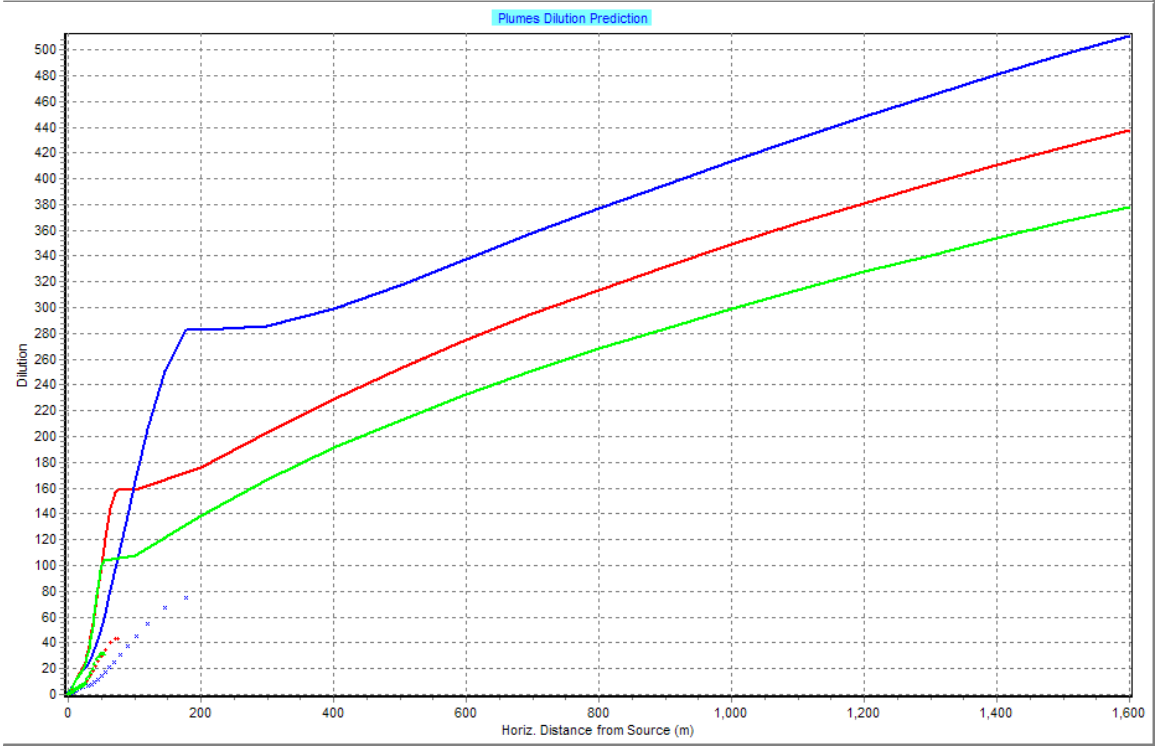
Aug F30 Avg (Red); Aug F30 High (Blue); Aug F30 Low (Green)



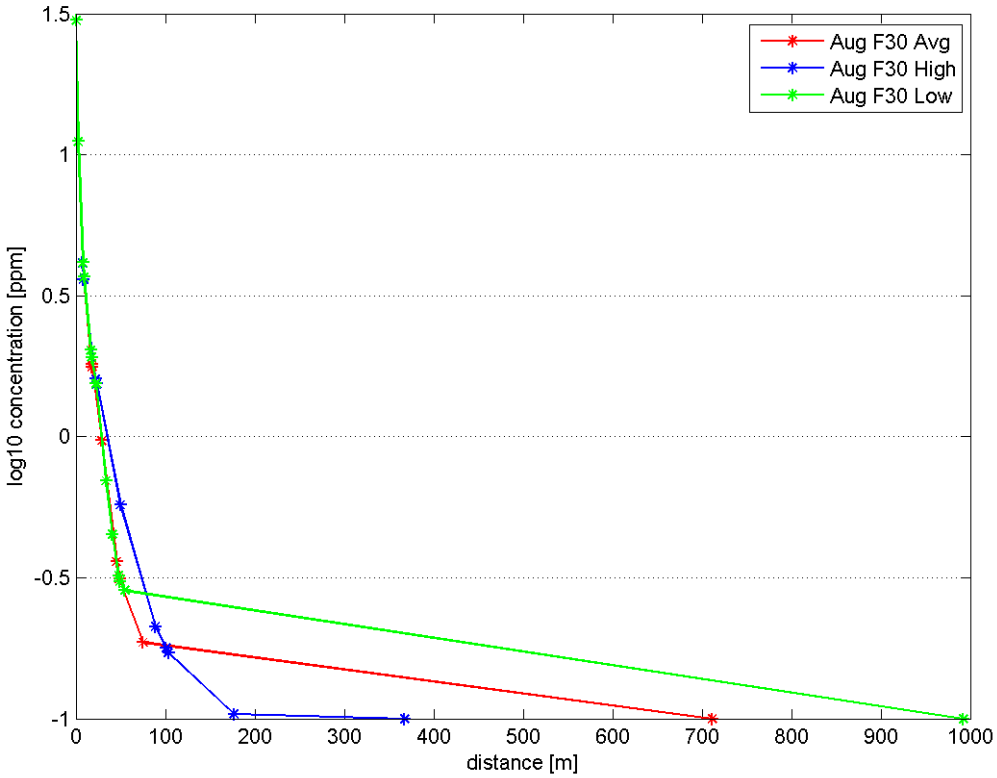
Salinity = 42 psu, Discharge Rate = 30,000 m^3/d

Aug F30 Avg (Red); Aug F30 High (Blue); Aug F30 Low (Green)

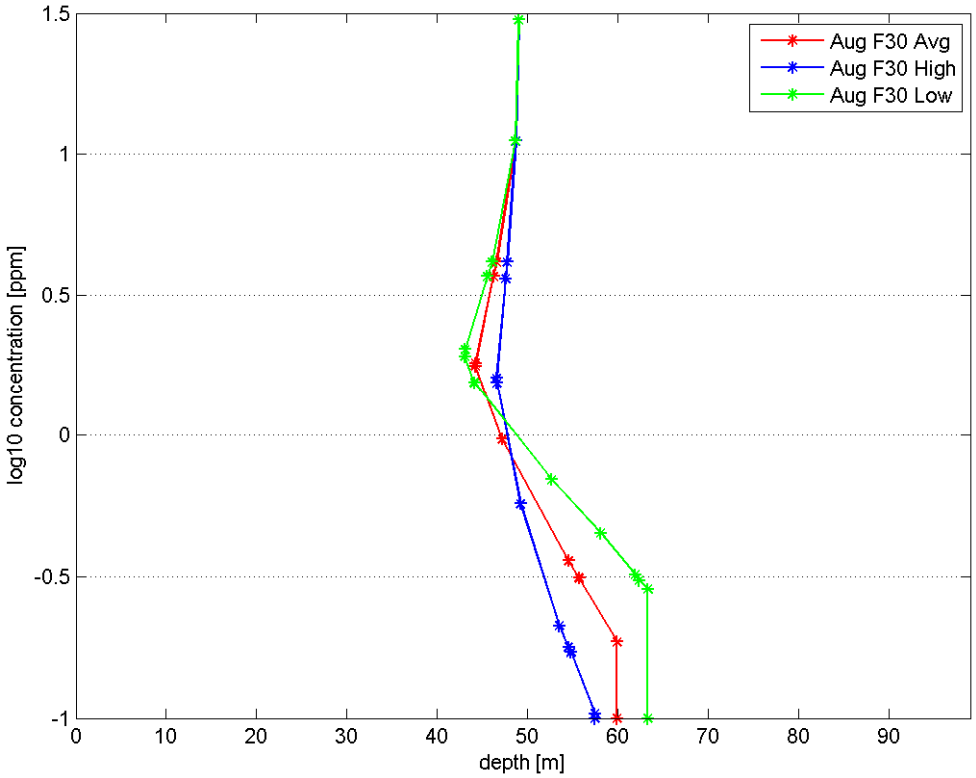




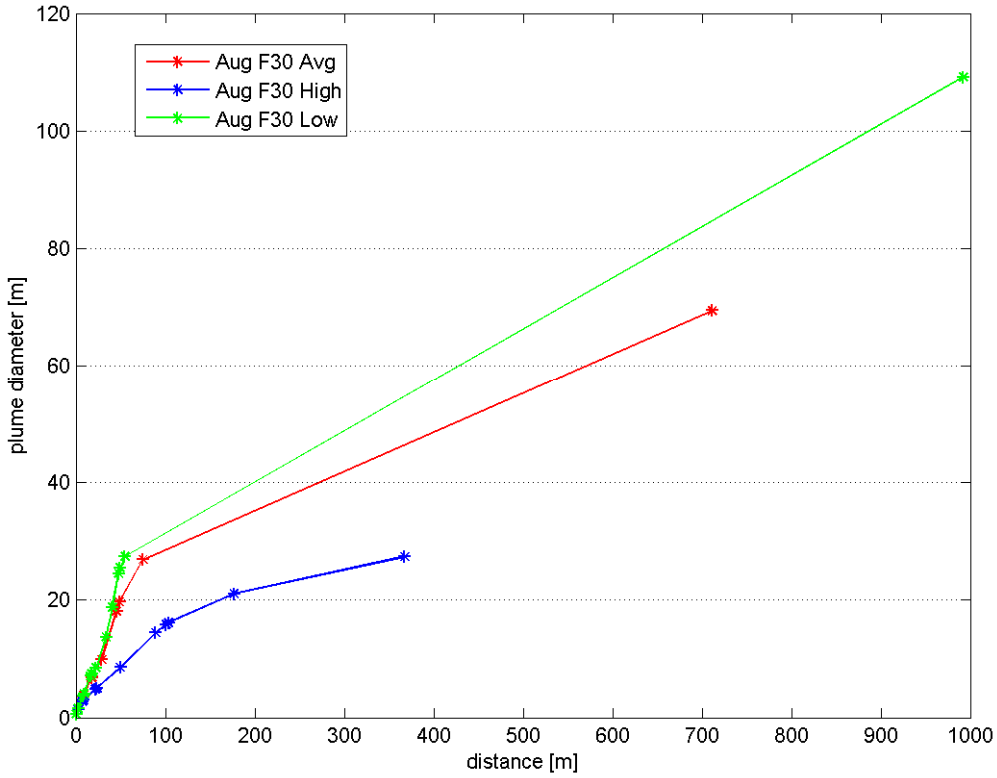
Salinity = 42 psu, Discharge Rate = 30,000 m^3/d
Aug F30 Avg (Red); Aug F30 High (Blue); Aug F30 Low (Green)



Salinity = 42 psu, Discharge Rate = 30,000 m^3/d
Aug F30 Avg (Red); Aug F30 High (Blue); Aug F30 Low (Green)

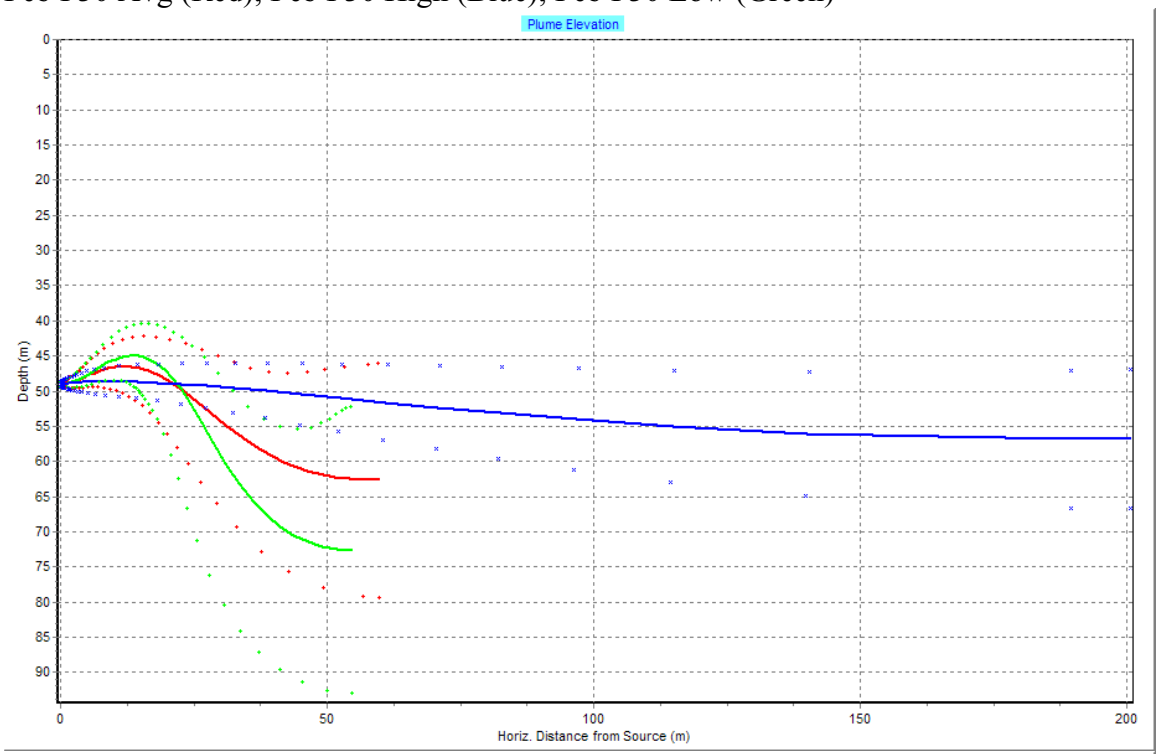


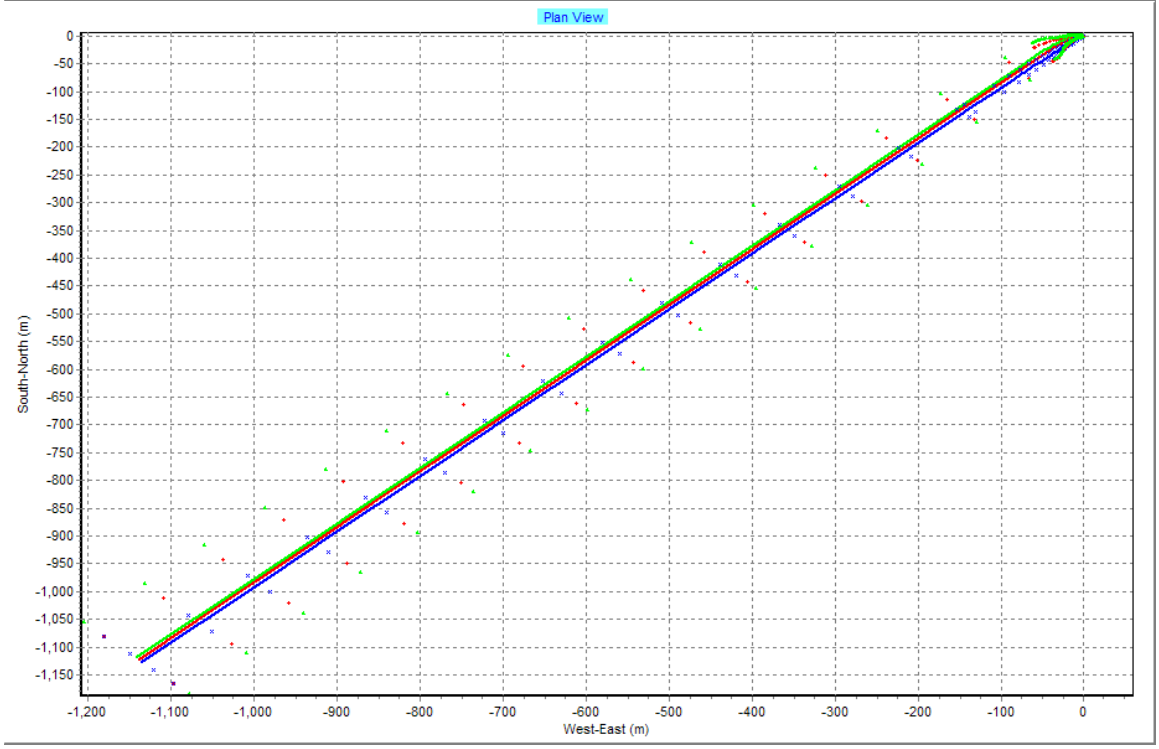
Salinity = 42 psu, Discharge Rate = 30,000 m^3/d
Aug F30 Avg (Red); Aug F30 High (Blue); Aug F30 Low (Green)



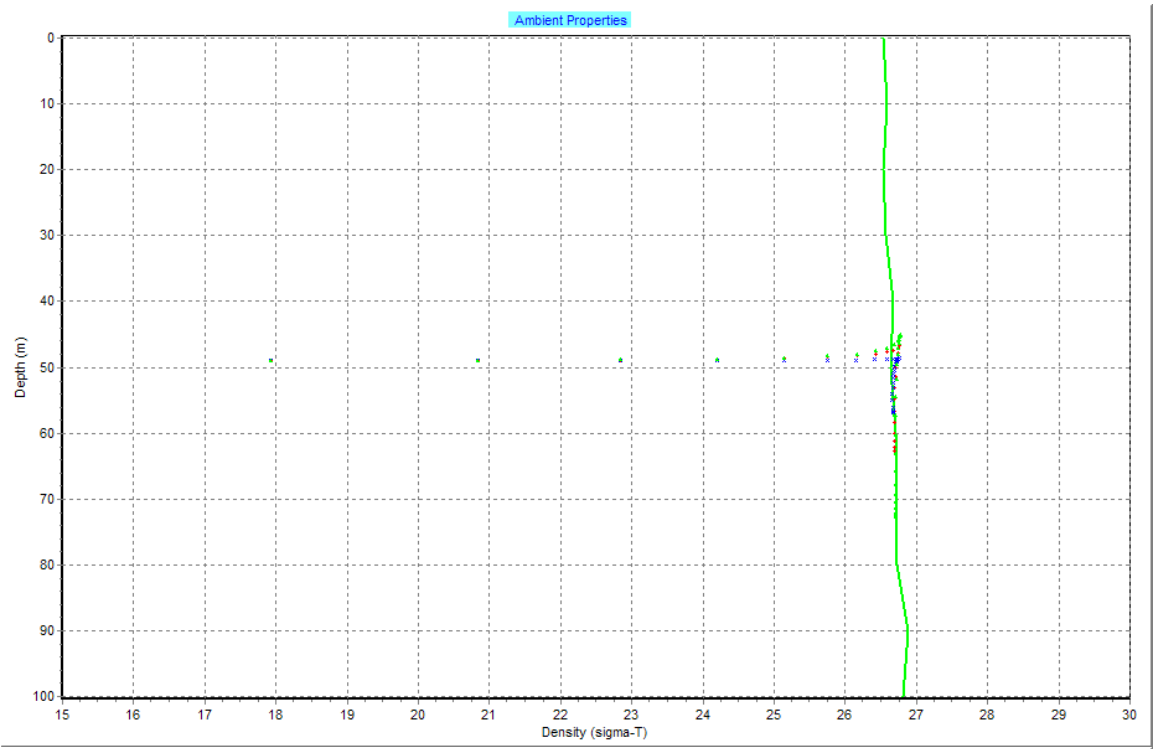
Salinity = 42 psu, Discharge Rate = 30,000 m^3/d

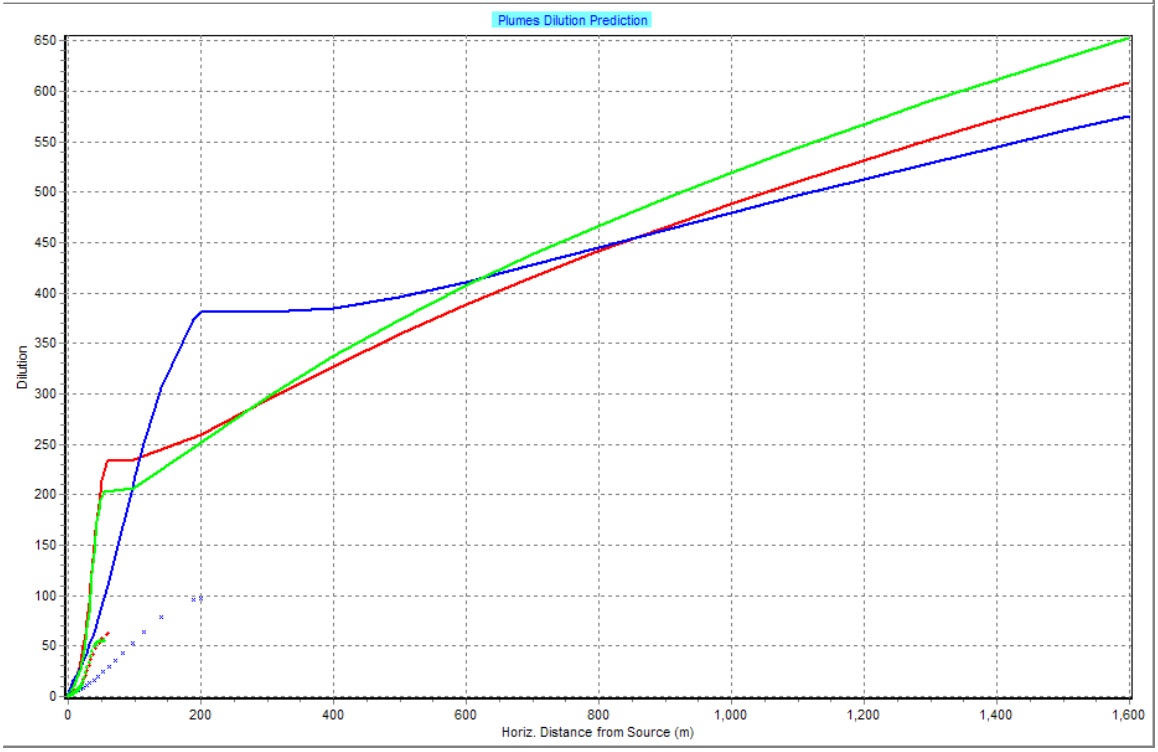
Feb F30 Avg (Red); Feb F30 High (Blue); Feb F30 Low (Green)



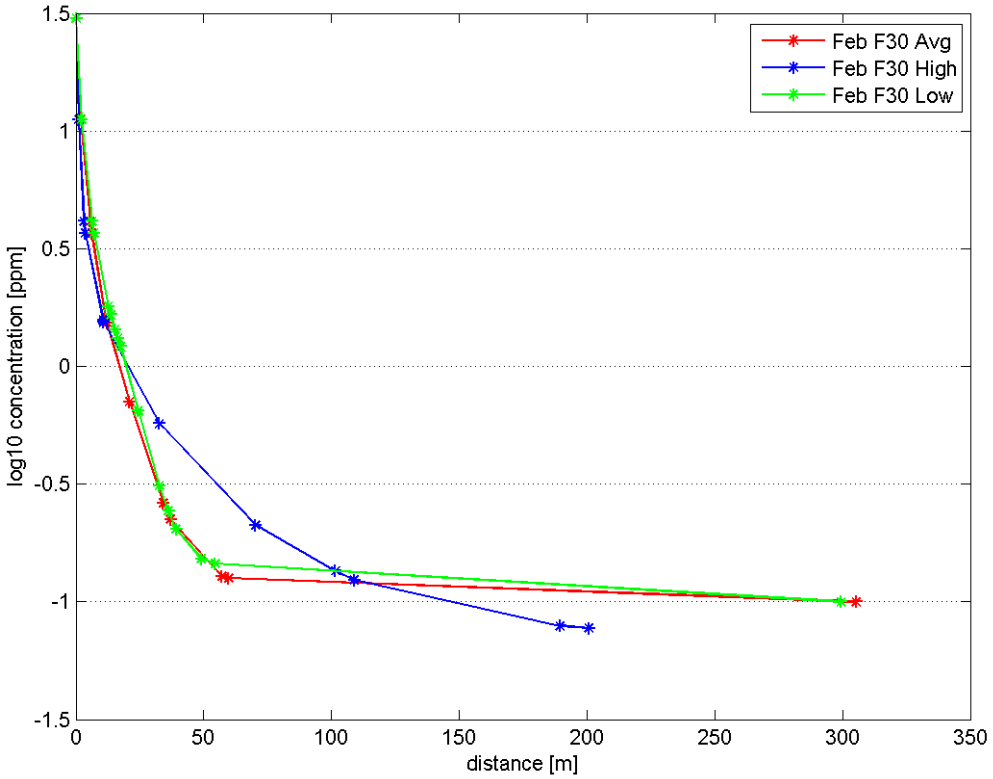


Salinity = 42 psu, Discharge Rate = 30,000 m^3/d
Feb F30 Avg (Red); Feb F30 High (Blue); Feb F30 Low (Green)

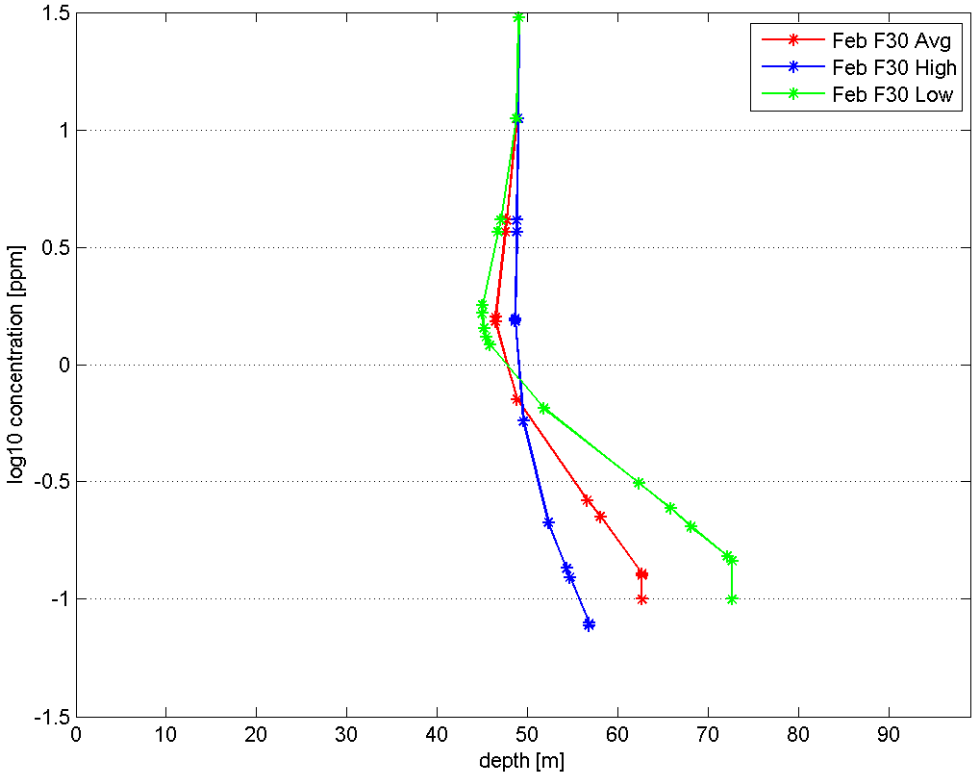




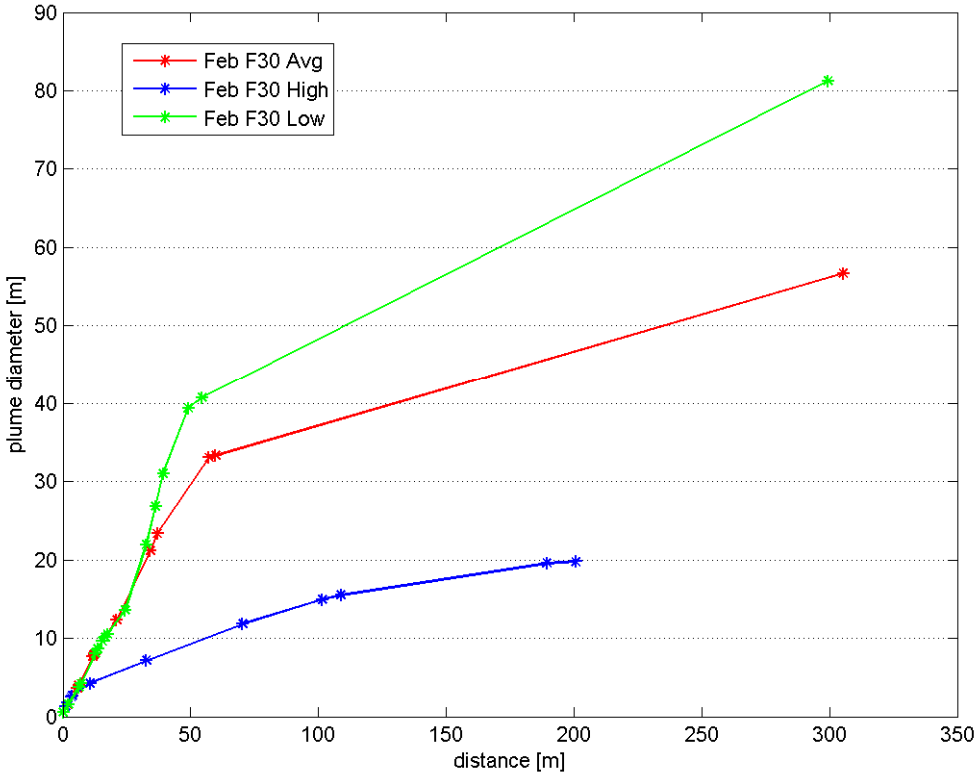
Salinity = 42 psu, Discharge Rate = 30,000 m^3/d
Feb F30 Avg (Red); Feb F30 High (Blue); Feb F30 Low (Green)



Salinity = 42 psu, Discharge Rate = 30,000 m^3/d
Feb F30 Avg (Red); Feb F30 High (Blue); Feb F30 Low (Green)

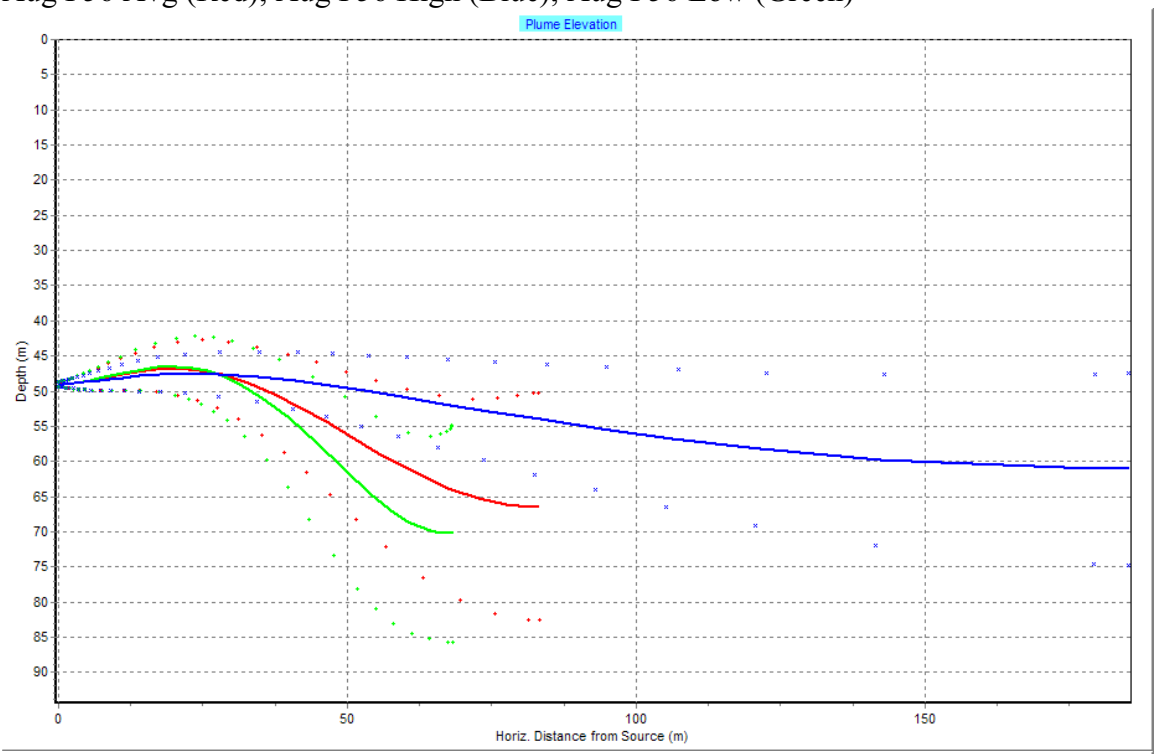


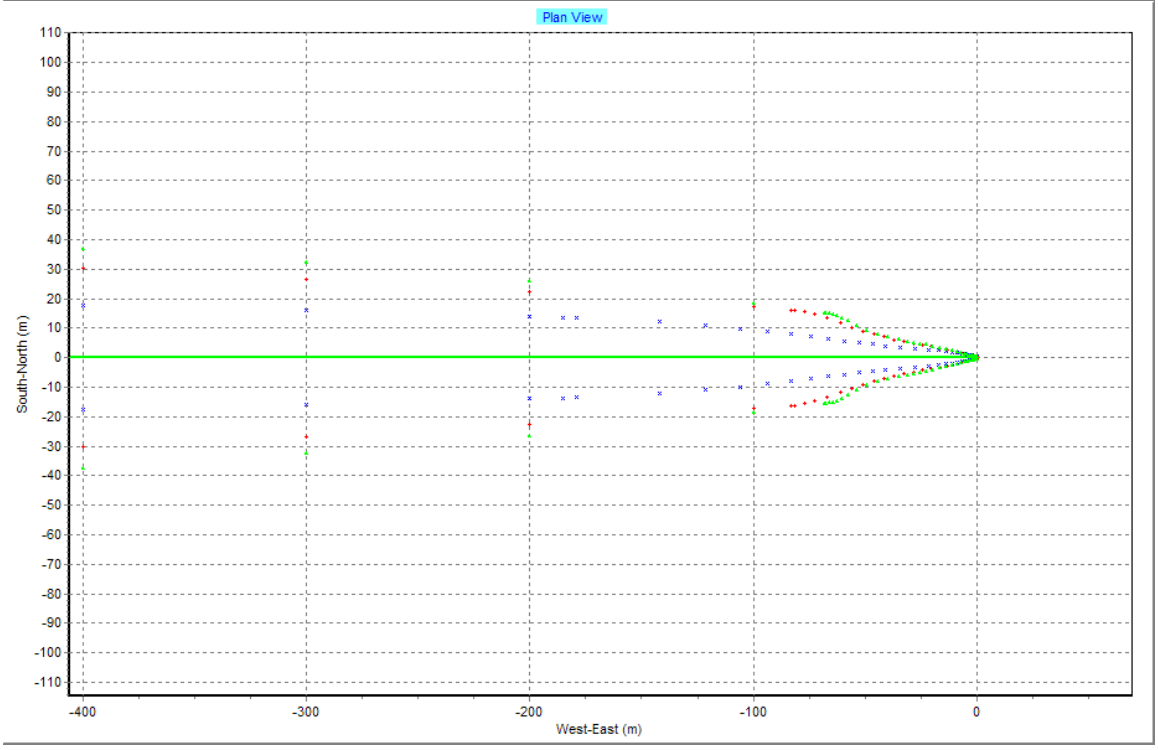
Salinity = 42 psu, Discharge Rate = 30,000 m^3/d
Feb F30 Avg (Red); Feb F30 High (Blue); Feb F30 Low (Green)



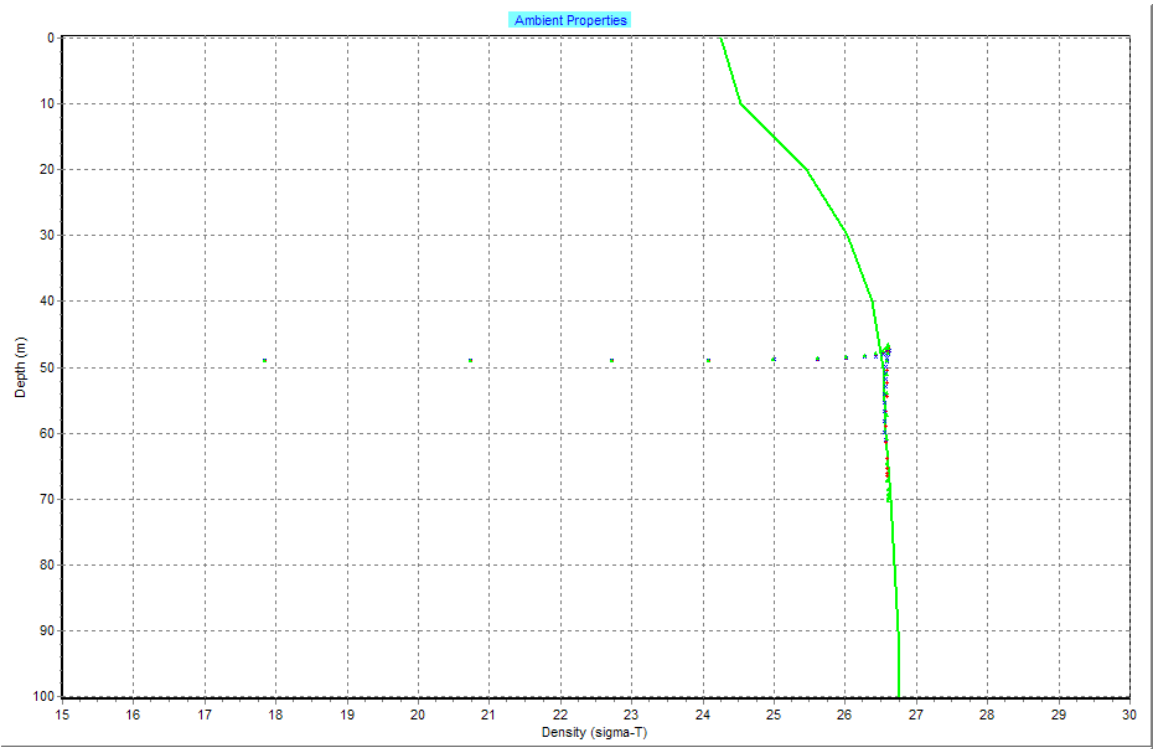
Salinity = 42 psu, Discharge Rate = 56,000 m^3/d

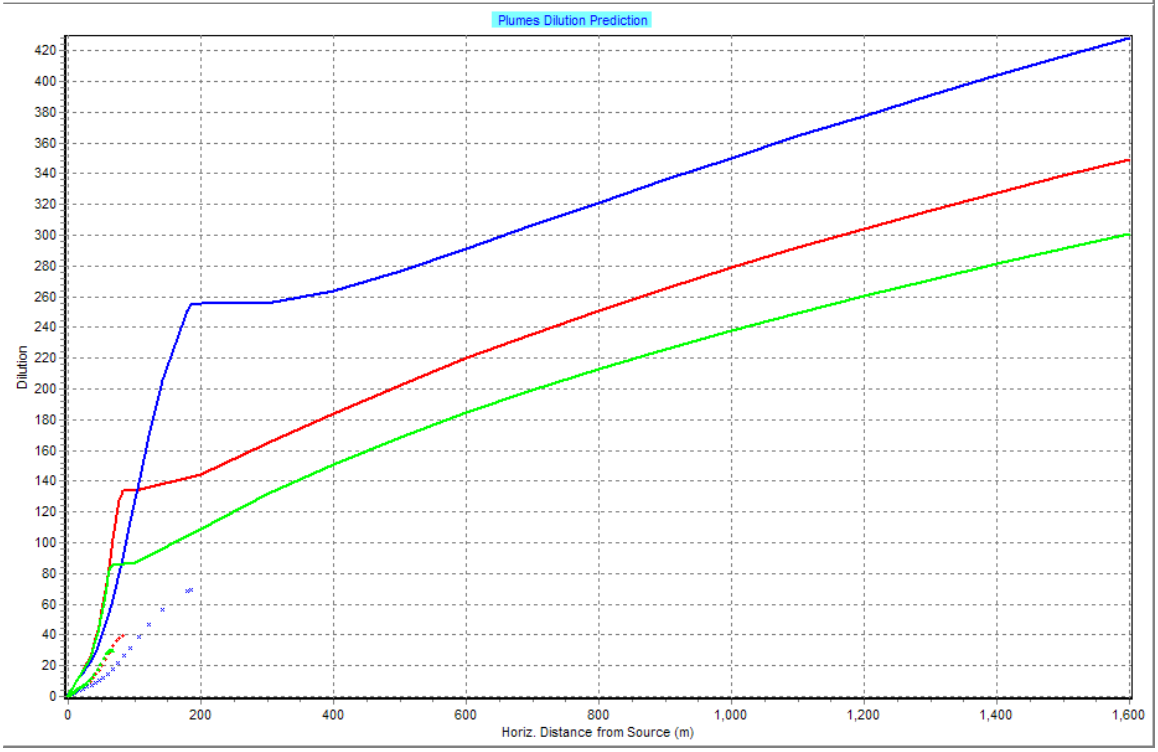
Aug F56 Avg (Red); Aug F56 High (Blue); Aug F56 Low (Green)



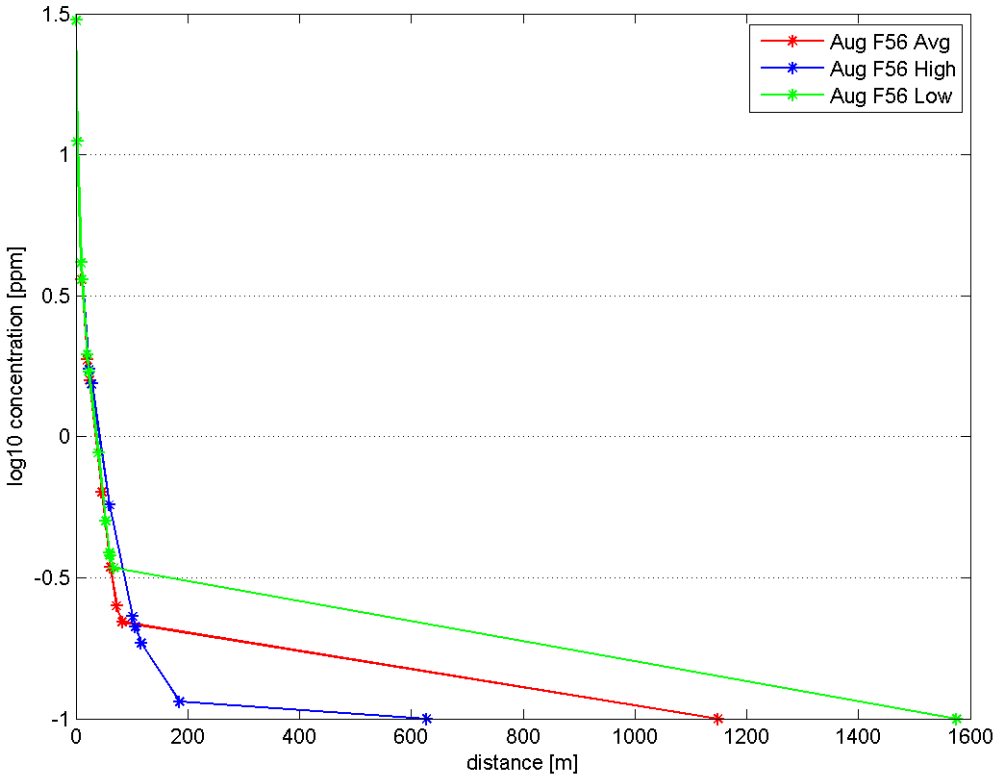


Salinity = 42 psu, Discharge Rate = 56,000 m^3/d
Aug F56 Avg (Red); Aug F56 High (Blue); Aug F56 Low (Green)

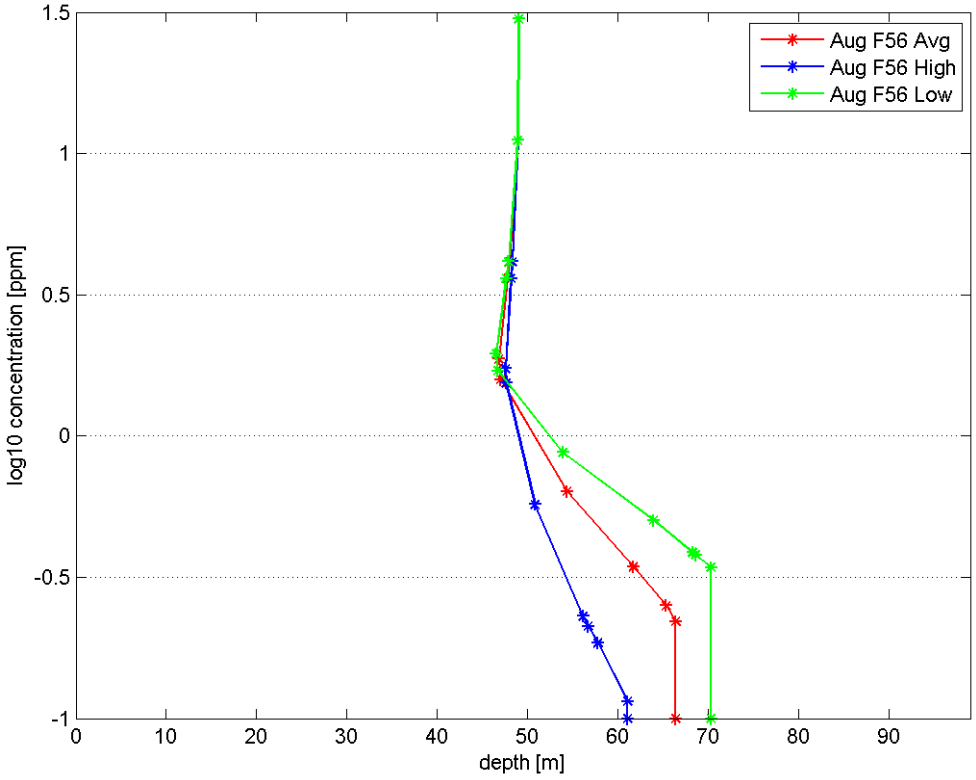




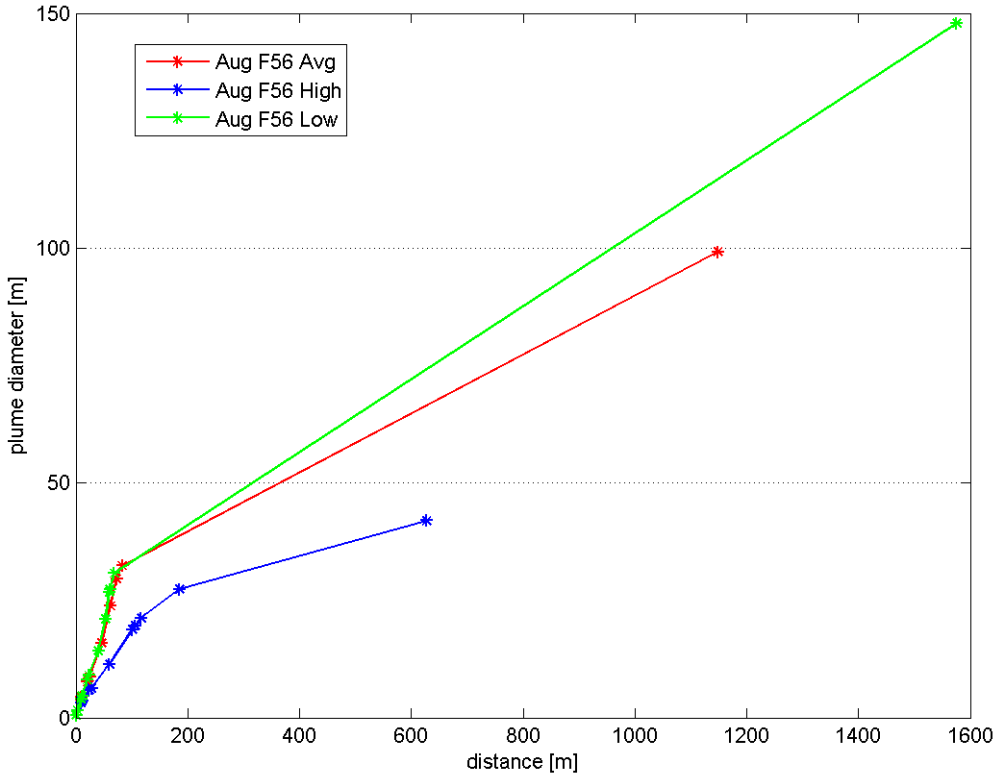
Salinity = 42 psu, Discharge Rate = 56,000 m^3/d
Aug F56 Avg (Red); Aug F56 High (Blue); Aug F56 Low (Green)



Salinity = 42 psu, Discharge Rate = 56,000 m^3/d
Aug F56 Avg (Red); Aug F56 High (Blue); Aug F56 Low (Green)

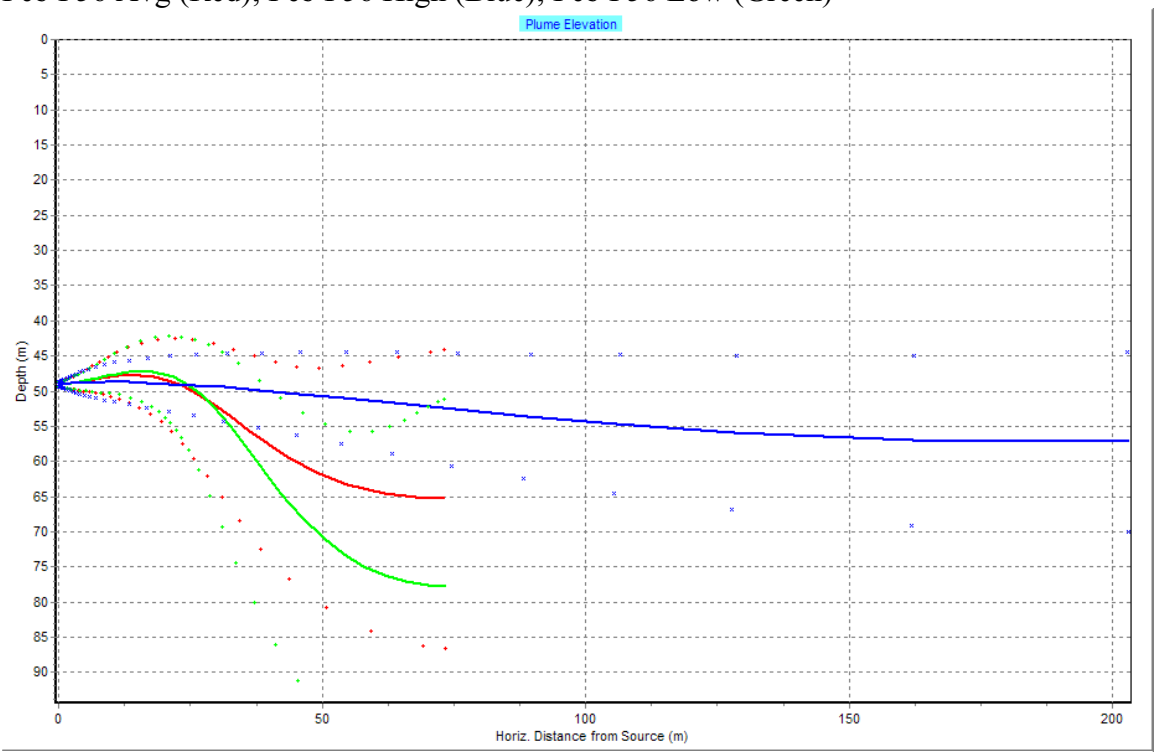


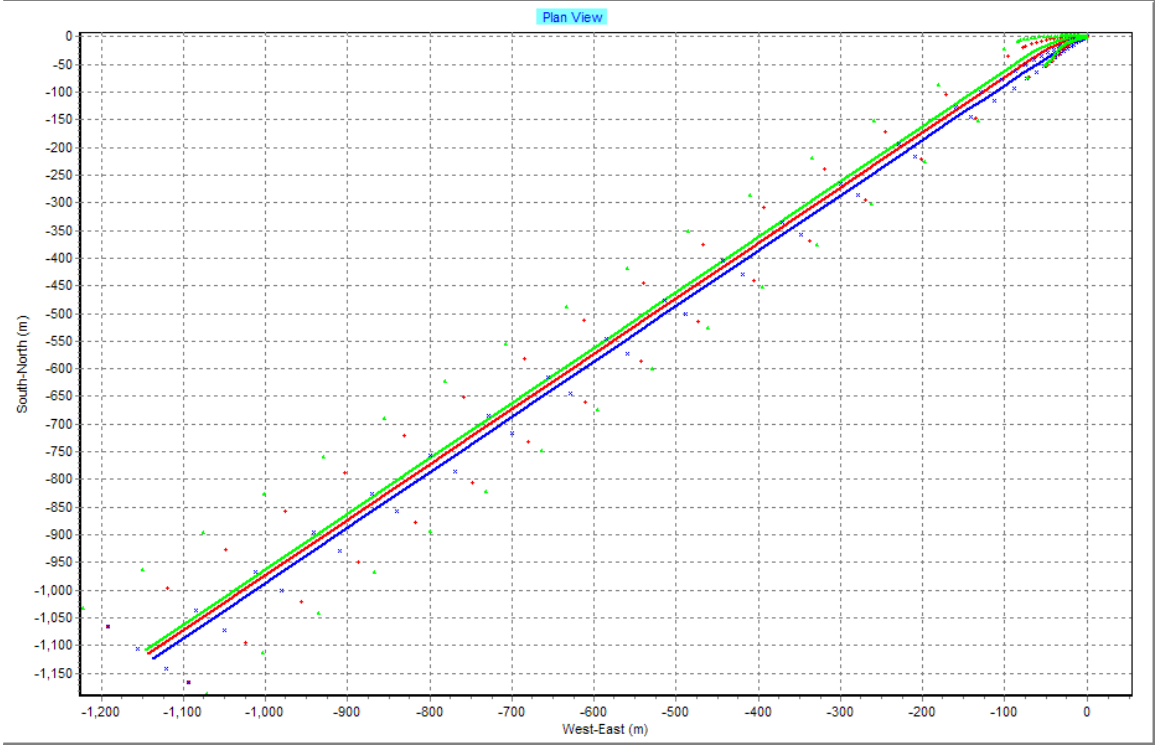
Salinity = 42 psu, Discharge Rate = 56,000 m^3/d
Aug F56 Avg (Red); Aug F56 High (Blue); Aug F56 Low (Green)



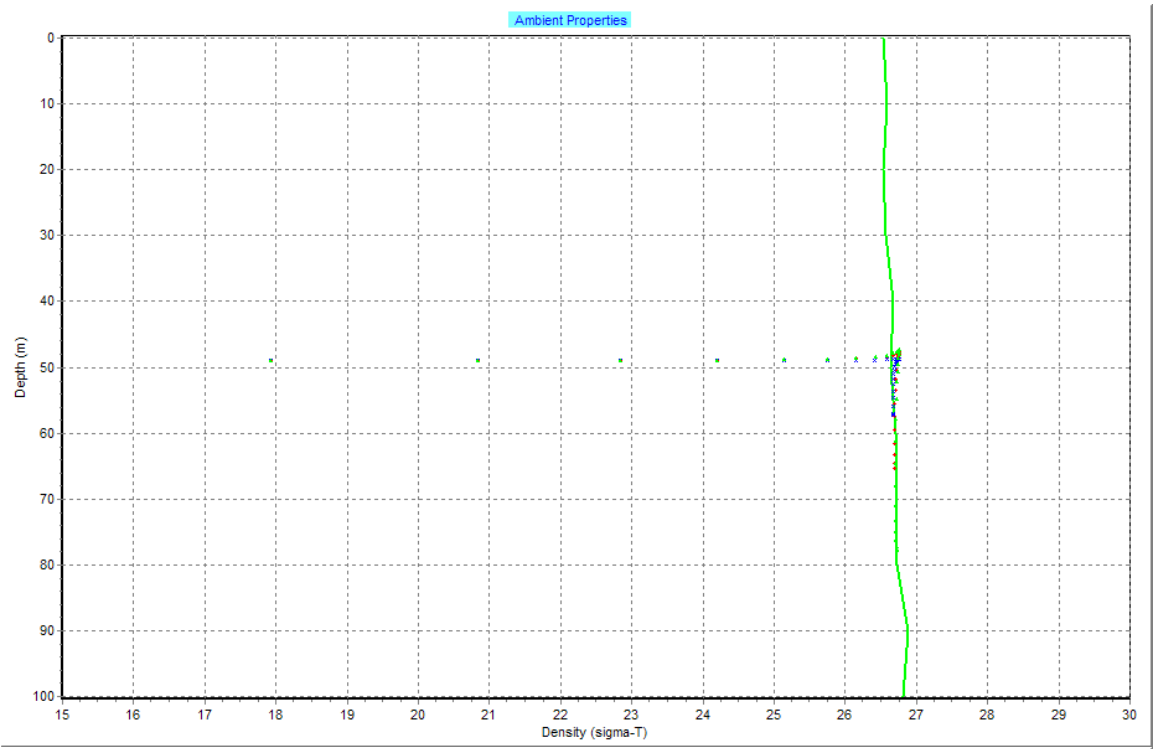
Salinity = 42 psu, Discharge Rate = 56,000 m^3/d

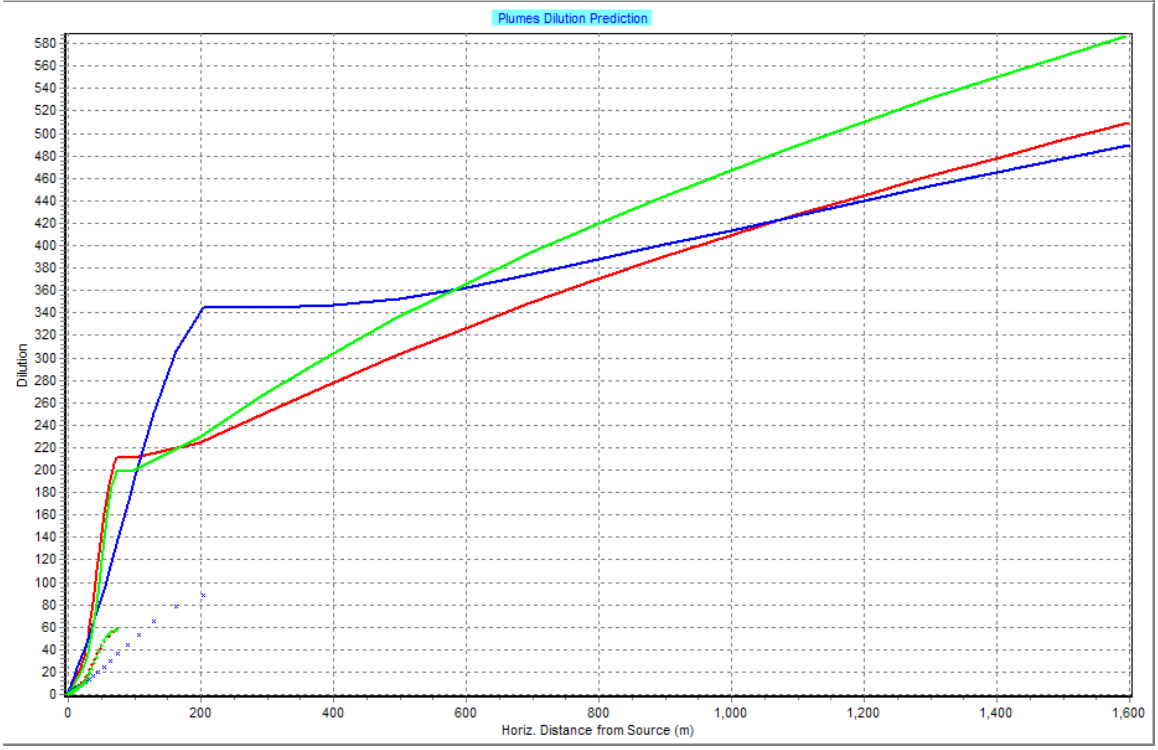
Feb F56 Avg (Red); Feb F56 High (Blue); Feb F56 Low (Green)



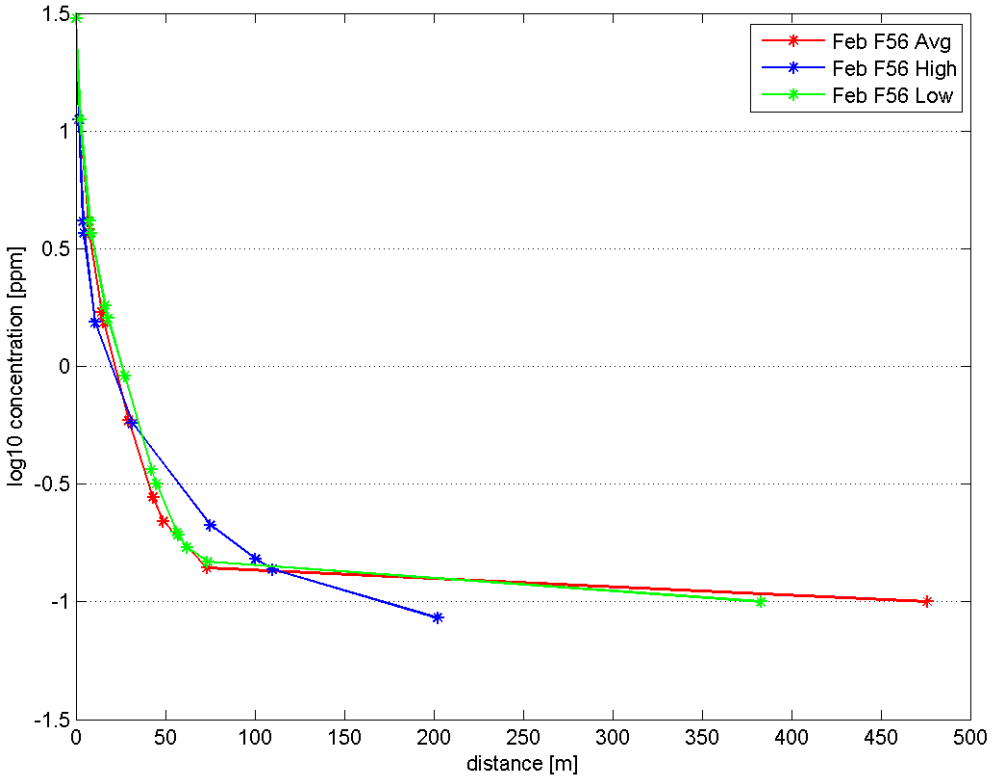


Salinity = 42 psu, Discharge Rate = 56,000 m^3/d
Feb F56 Avg (Red); Feb F56 High (Blue); Feb F56 Low (Green)

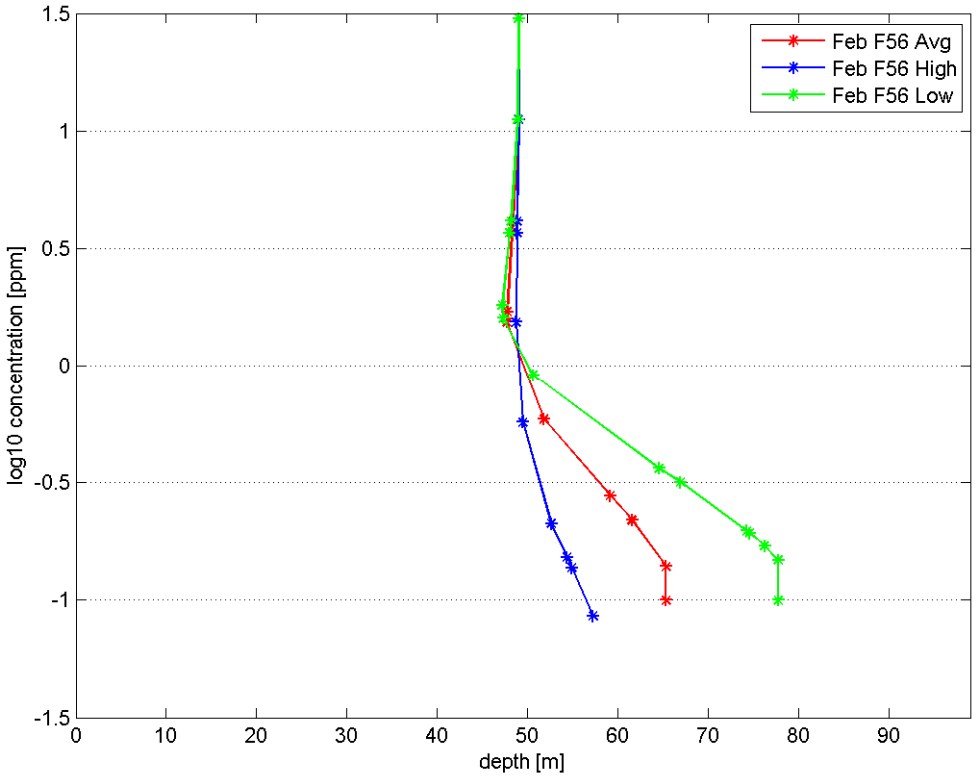




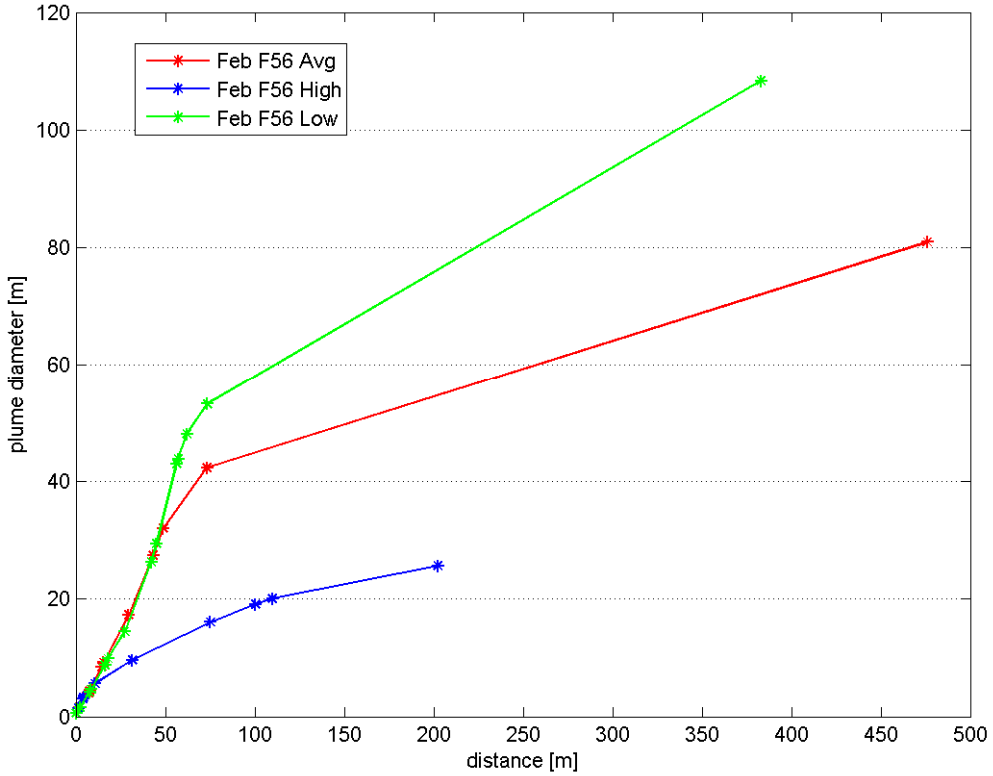
Salinity = 42 psu, Discharge Rate = 56,000 m^3/d
Feb F56 Avg (Red); Feb F56 High (Blue); Feb F56 Low (Green)



Salinity = 42 psu, Discharge Rate = 56,000 m^3/d
Feb F56 Avg (Red); Feb F56 High (Blue); Feb F56 Low (Green)

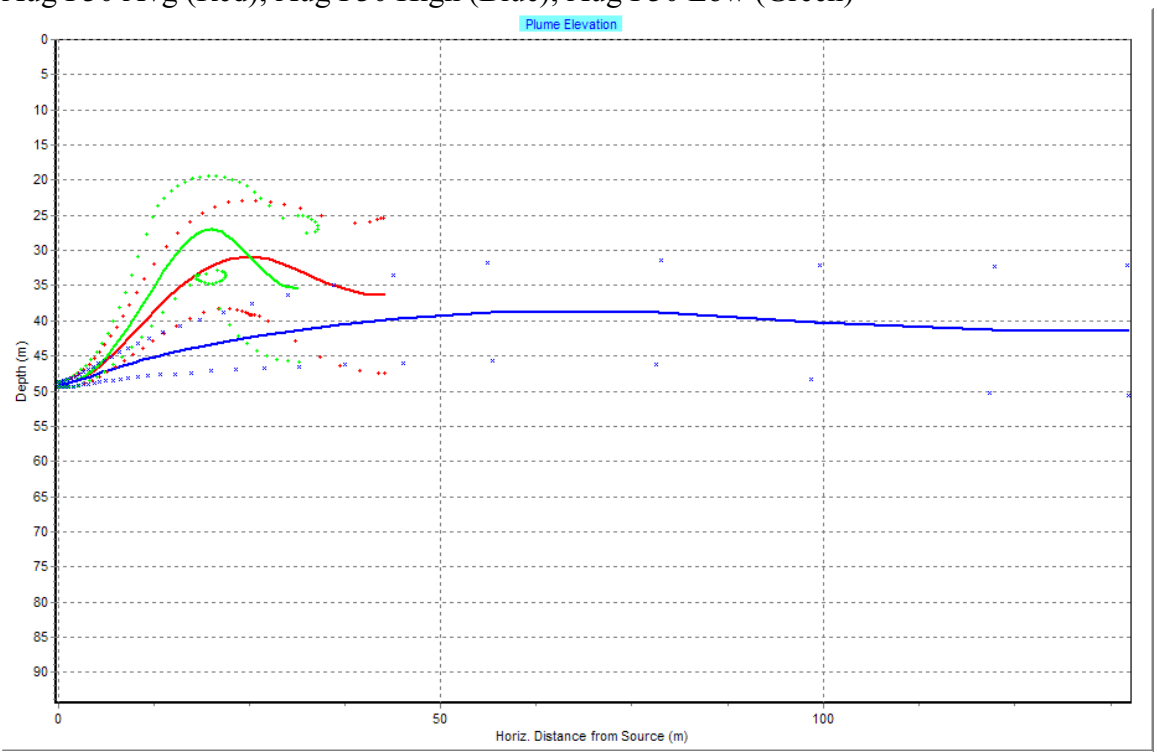


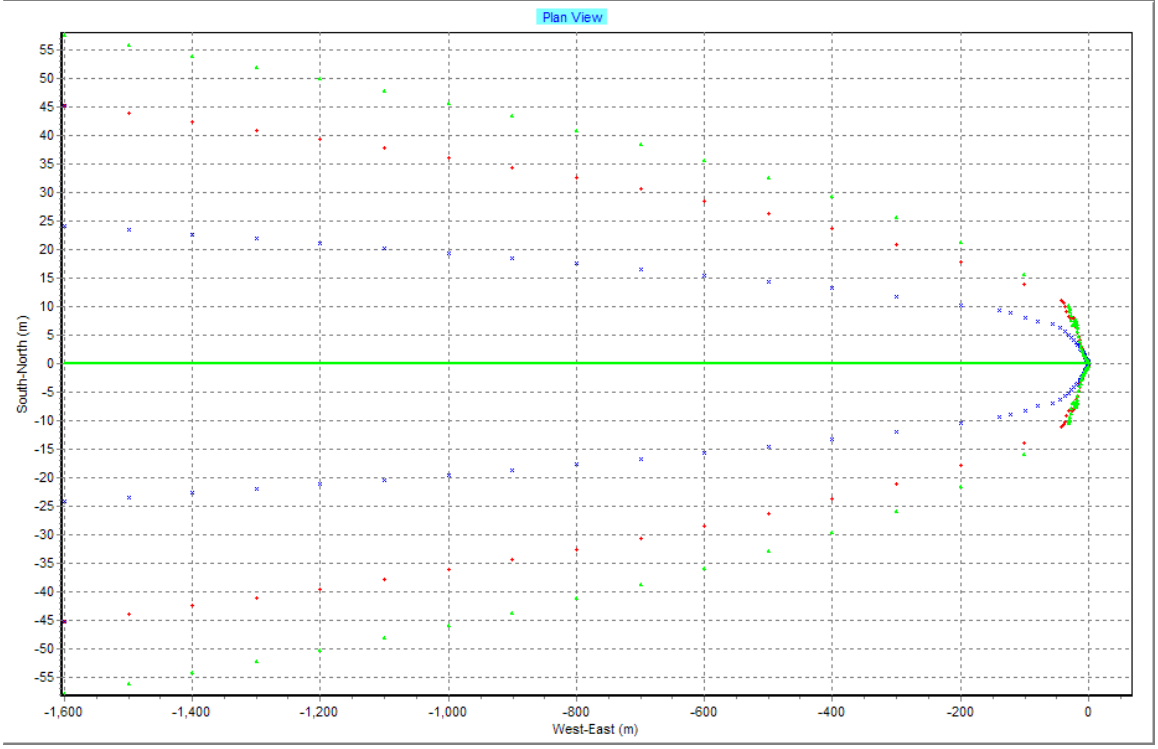
Salinity = 42 psu, Discharge Rate = 56,000 m^3/d
Feb F56 Avg (Red); Feb F56 High (Blue); Feb F56 Low (Green)



Salinity = 32.7 psu, Discharge Rate = 30,000 m^3/d

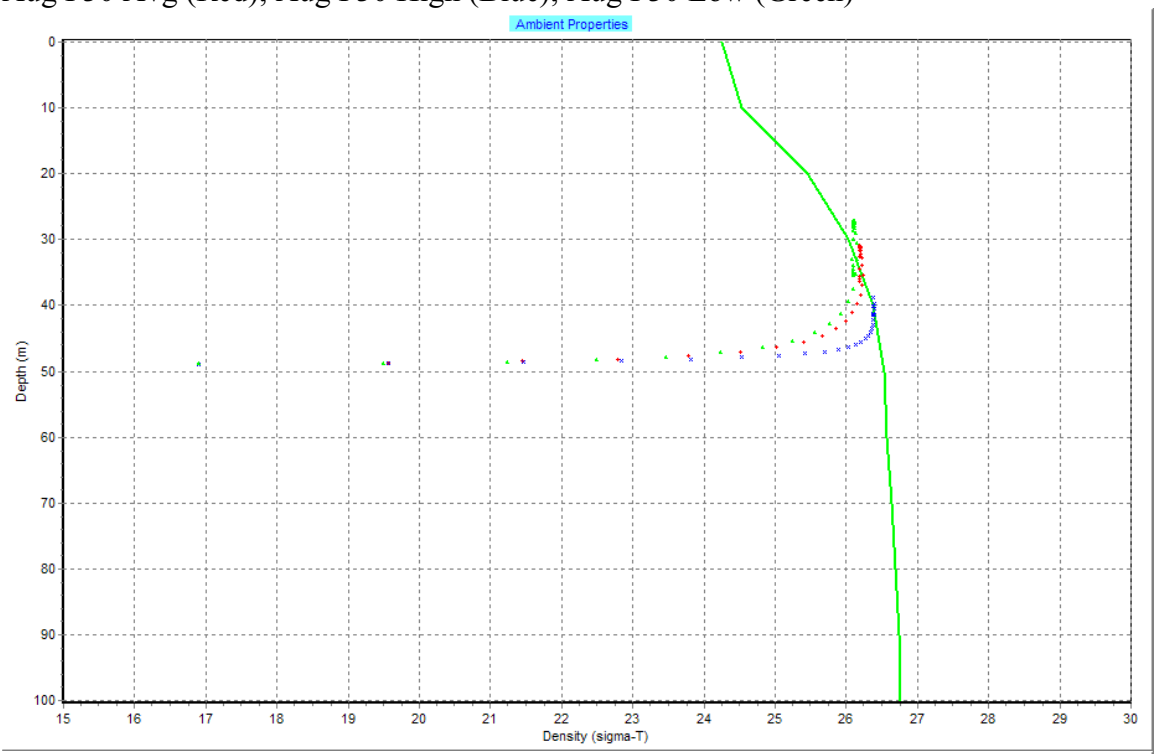
Aug F30 Avg (Red); Aug F30 High (Blue); Aug F30 Low (Green)

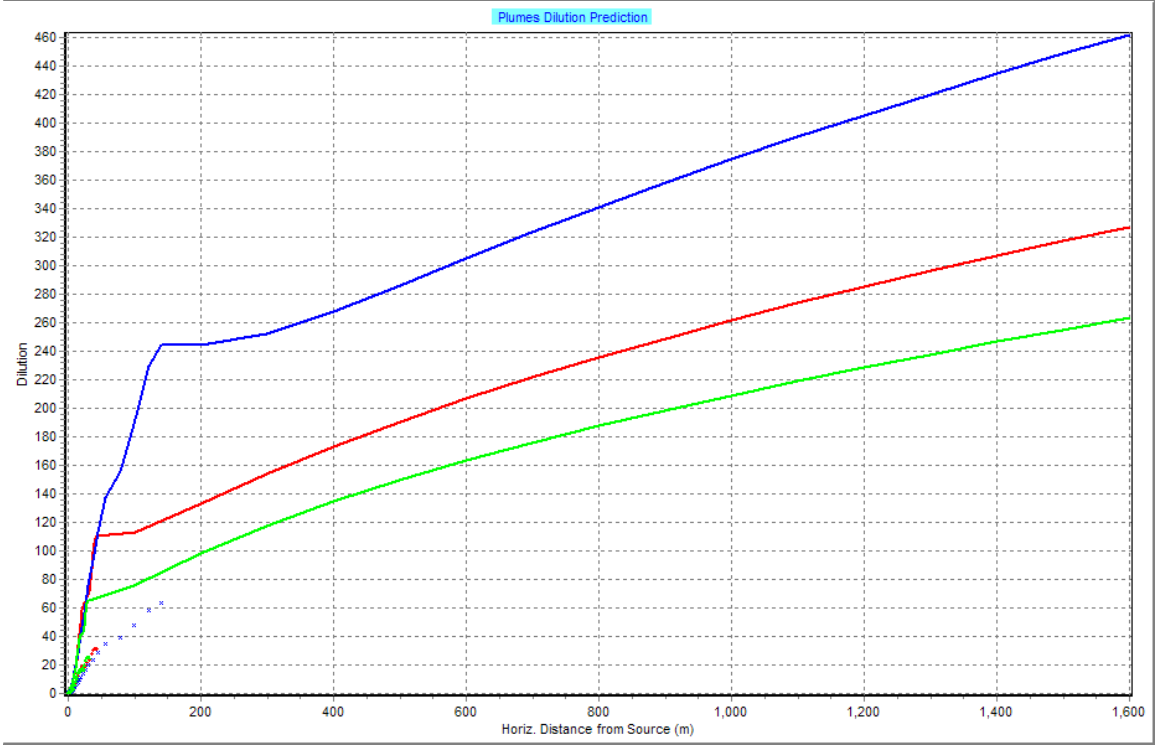




Salinity = 32.7 psu, Discharge Rate = 30,000 m^3/d

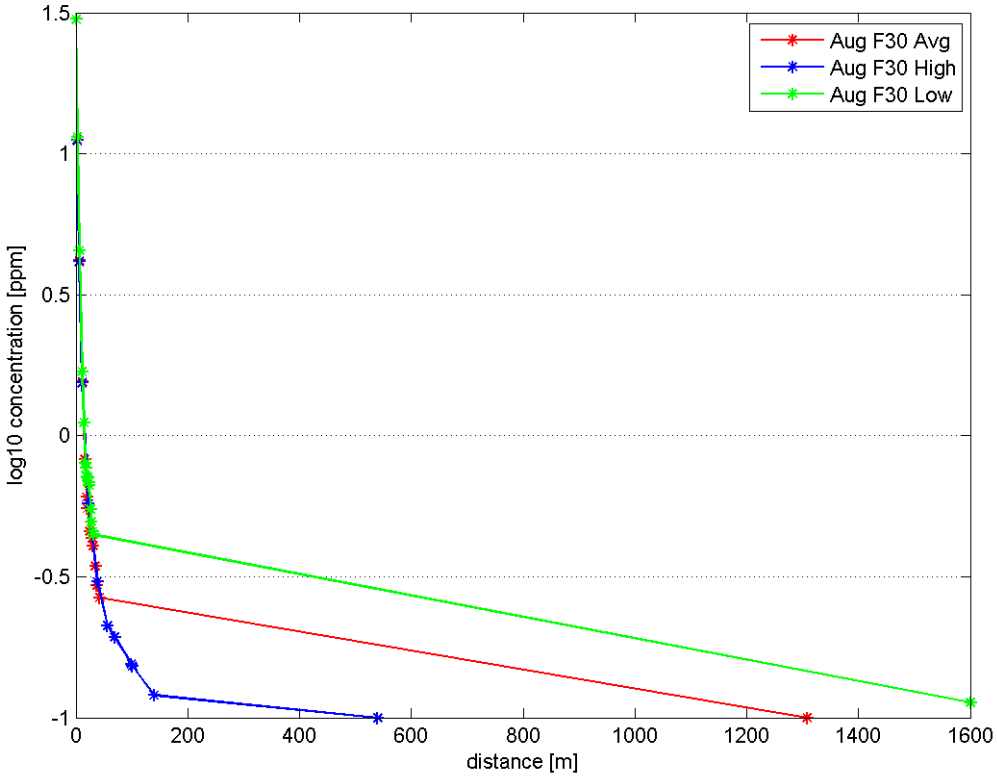
Aug F30 Avg (Red); Aug F30 High (Blue); Aug F30 Low (Green)

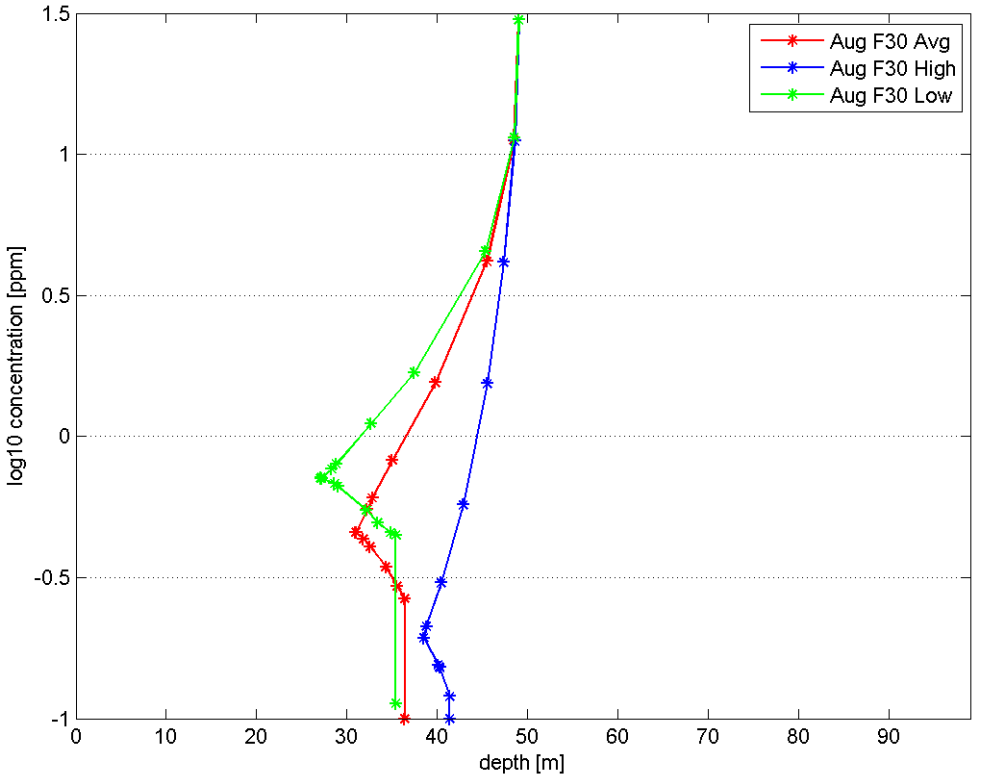




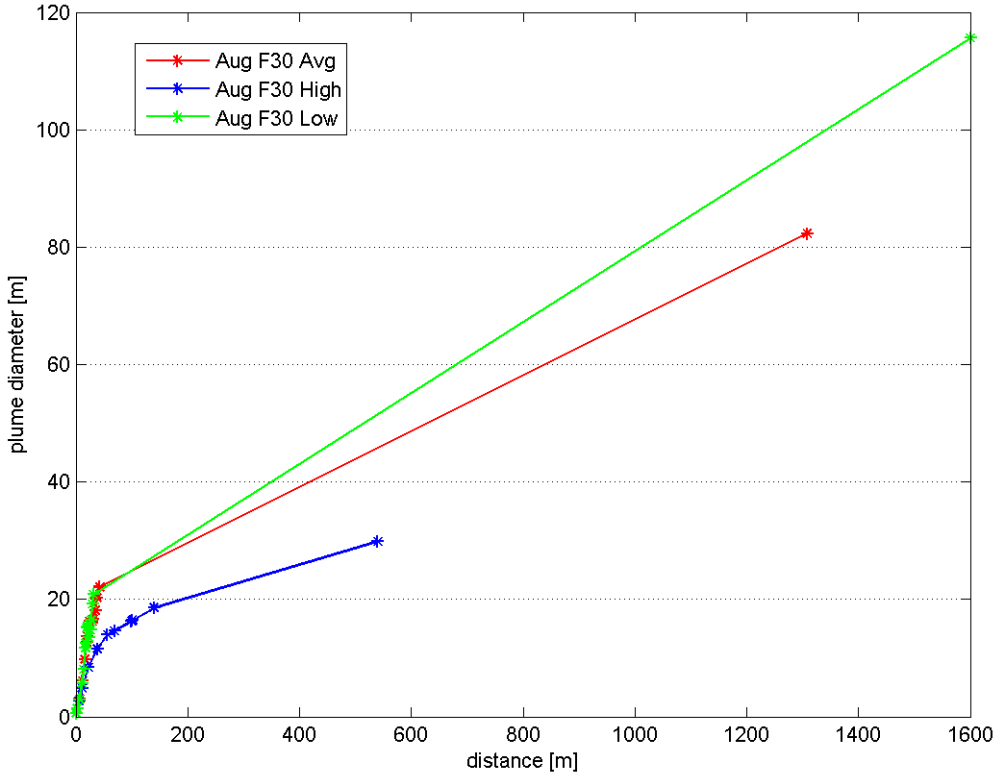
Salinity = 32.7 psu, Discharge Rate = 30,000 m^3/d

Aug F30 Avg (Red); Aug F30 High (Blue); Aug F30 Low (Green)



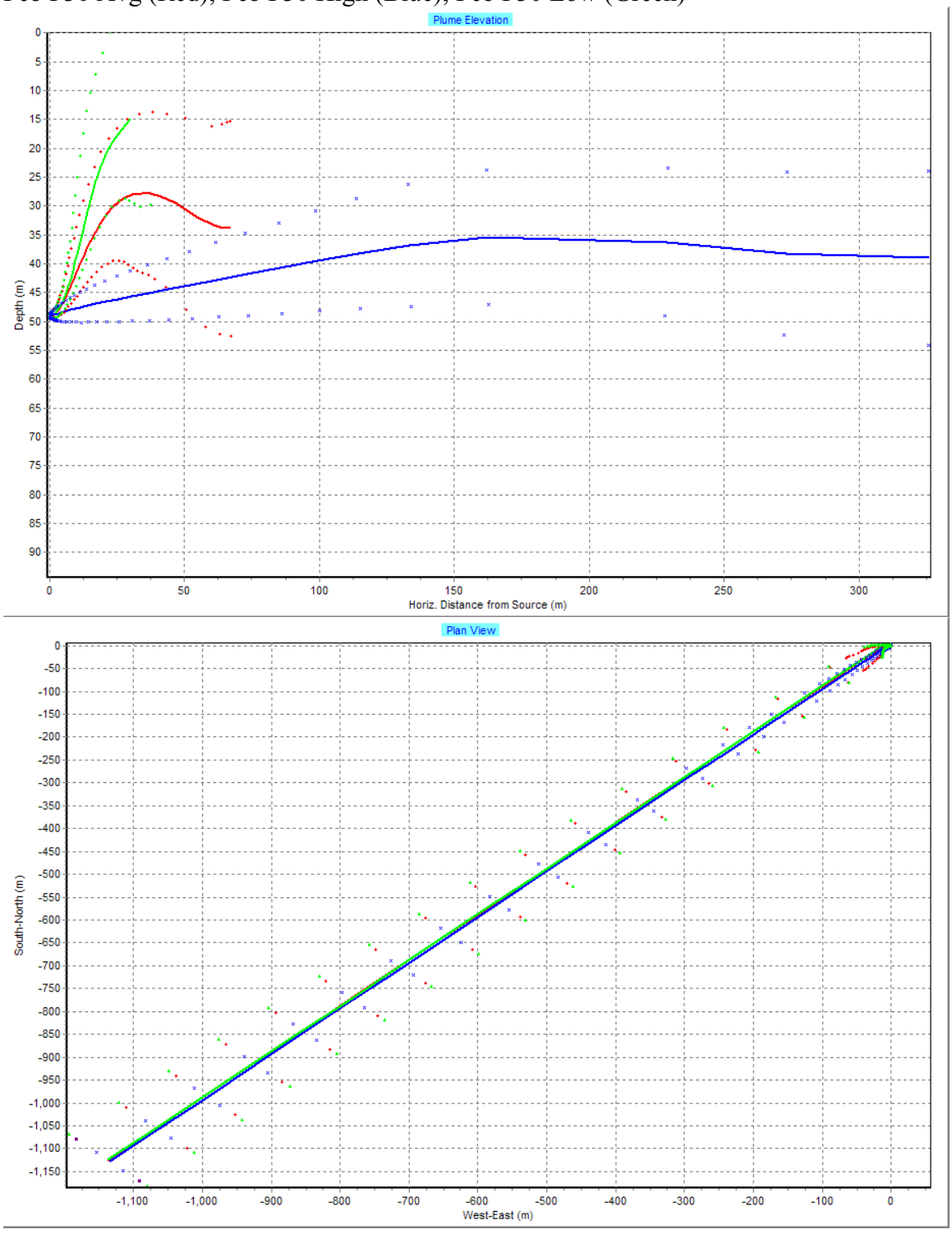


Salinity = 32.7 psu, Discharge Rate = 30,000 m^3/d
Aug F30 Avg (Red); Aug F30 High (Blue); Aug F30 Low (Green)



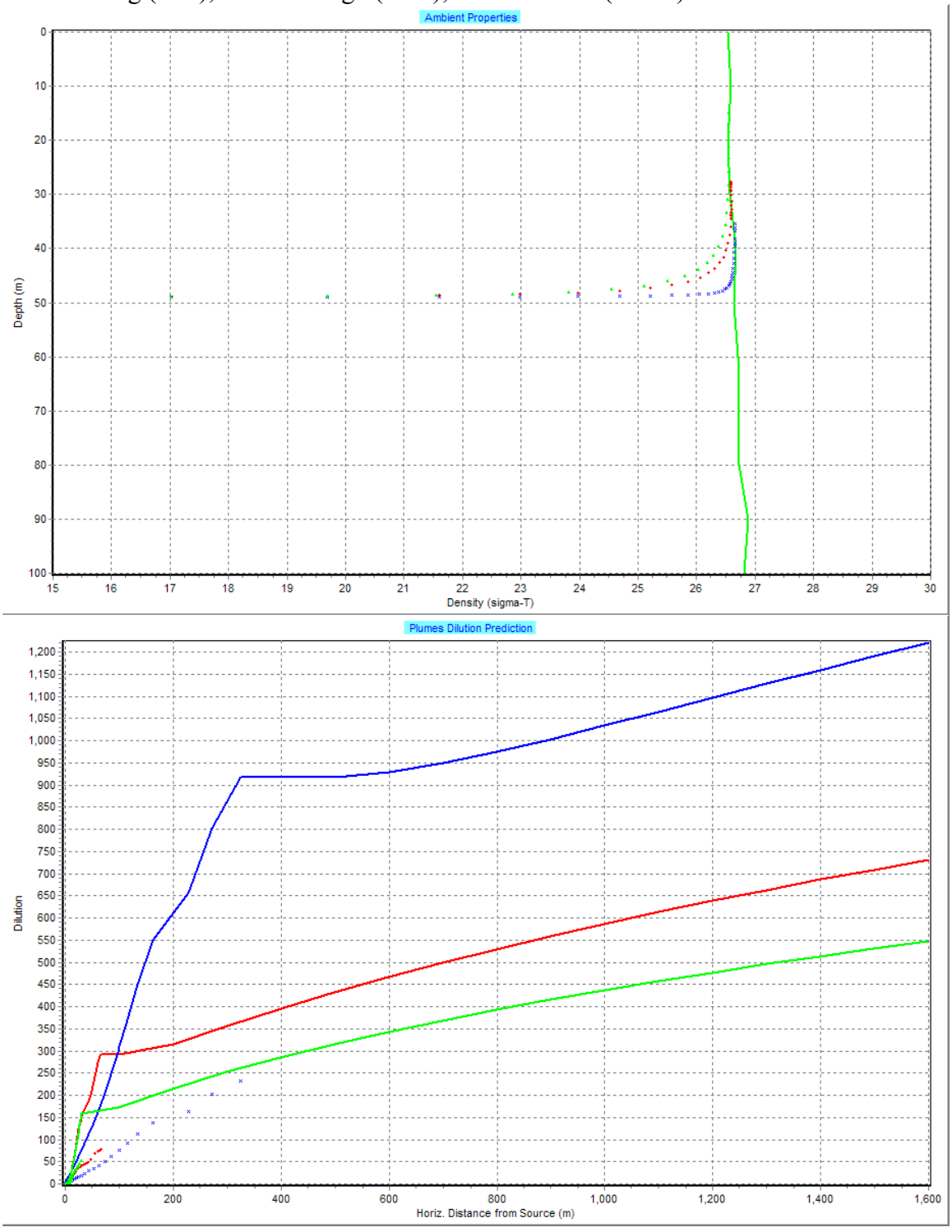
Salinity = 32.7 psu, Discharge Rate = 30,000 m^3/d

Feb F30 Avg (Red); Feb F30 High (Blue); Feb F30 Low (Green)

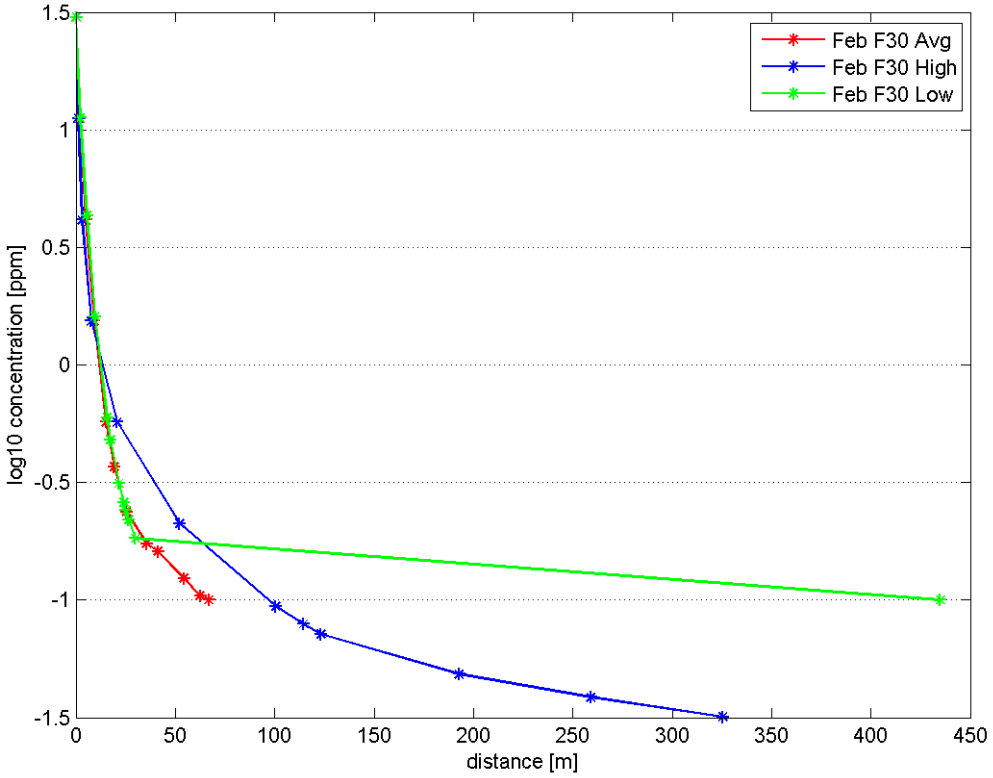


Salinity = 32.7 psu, Discharge Rate = 30,000 m^3/d

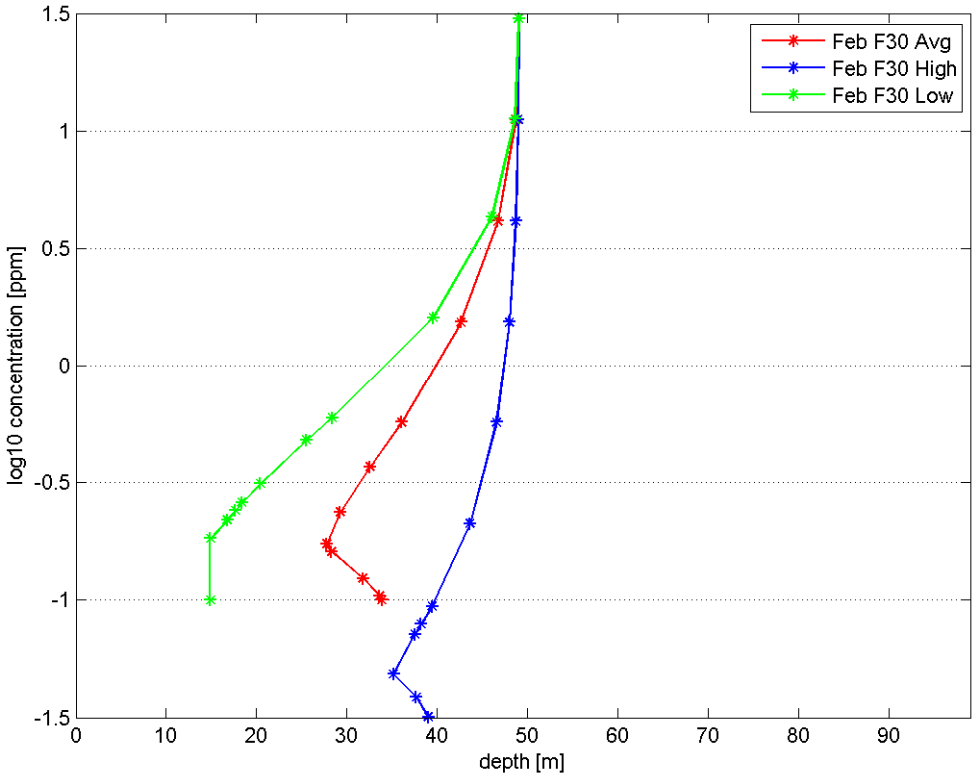
Feb F30 Avg (Red); Feb F30 High (Blue); Feb F30 Low (Green)



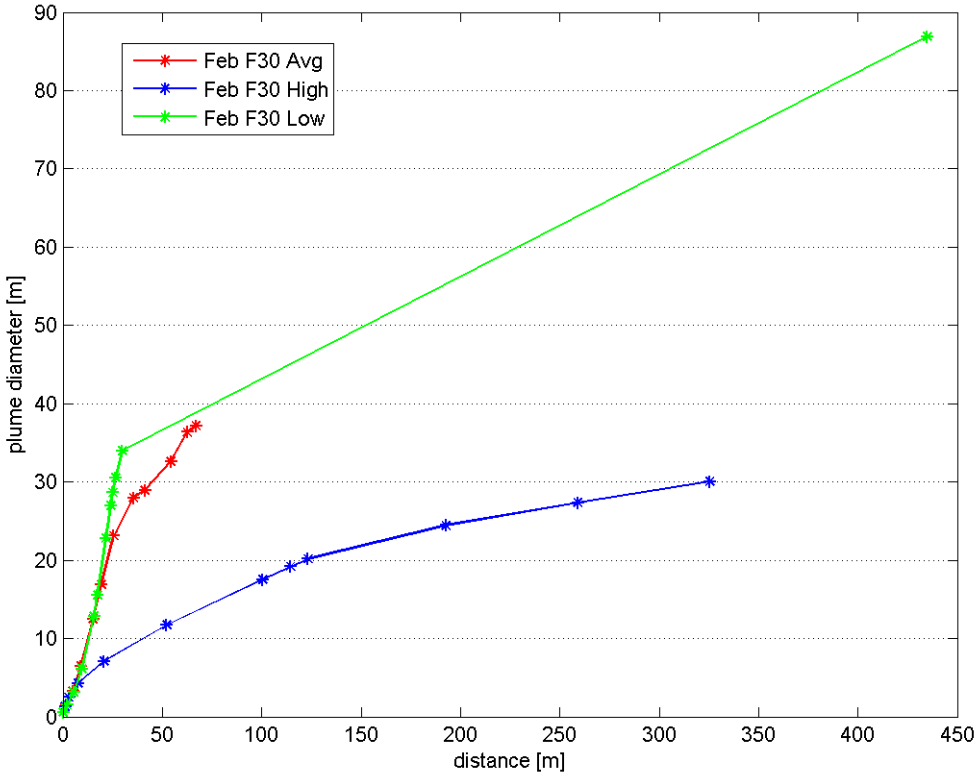
Salinity = 32.7 psu, Discharge Rate = 30,000 m^3/d
Feb F30 Avg (Red); Feb F30 High (Blue); Feb F30 Low (Green)



Salinity = 32.7 psu, Discharge Rate = 30,000 m^3/d
Feb F30 Avg (Red); Feb F30 High (Blue); Feb F30 Low (Green)

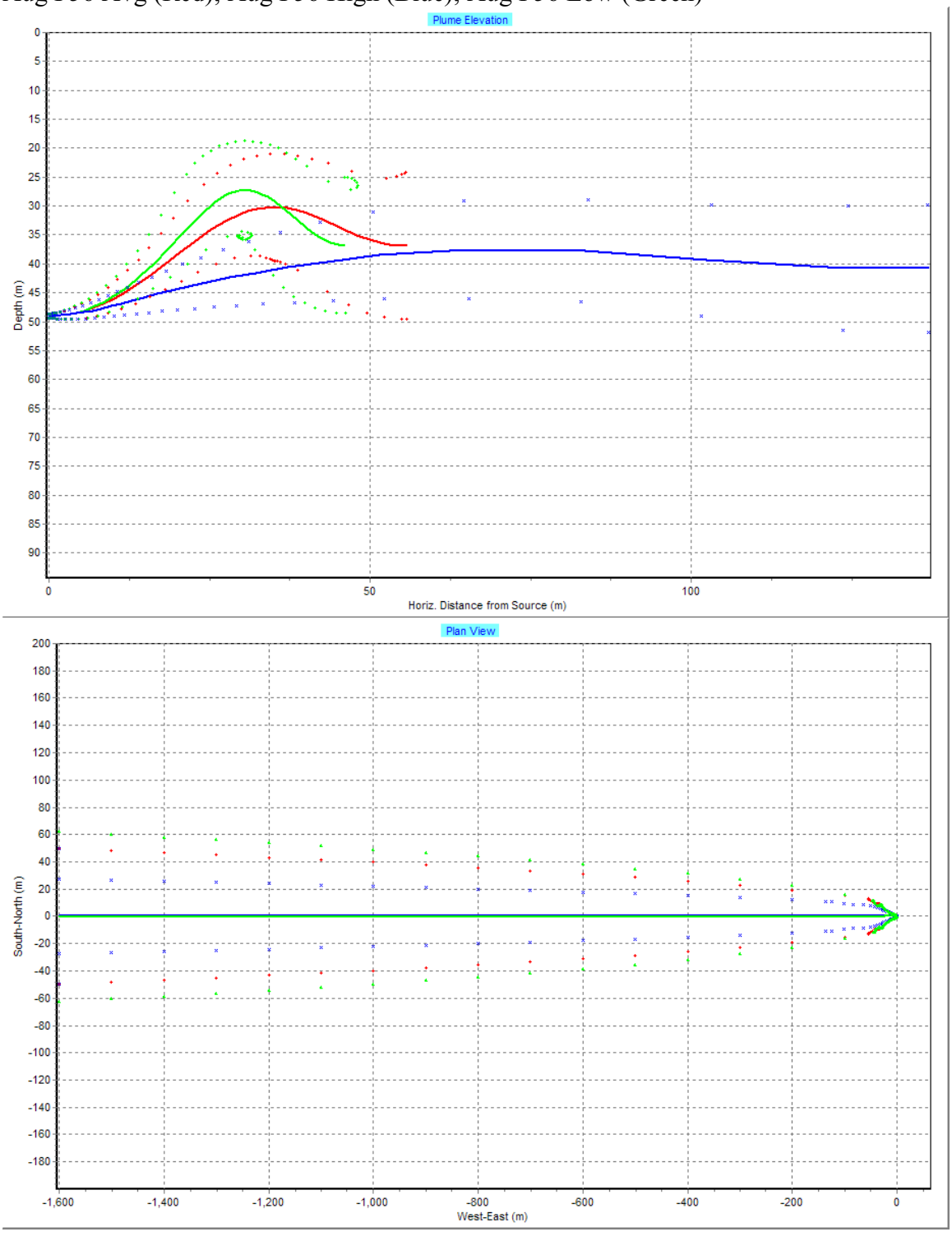


Salinity = 32.7 psu, Discharge Rate = 30,000 m^3/d
Feb F30 Avg (Red); Feb F30 High (Blue); Feb F30 Low (Green)

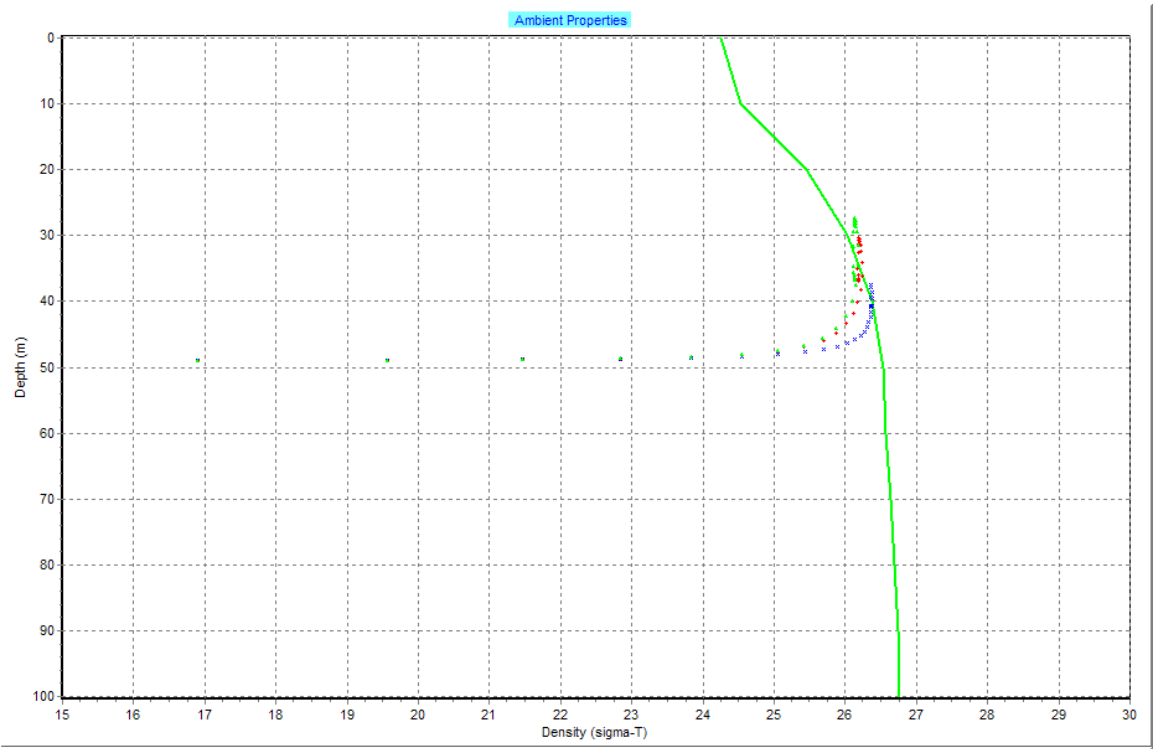


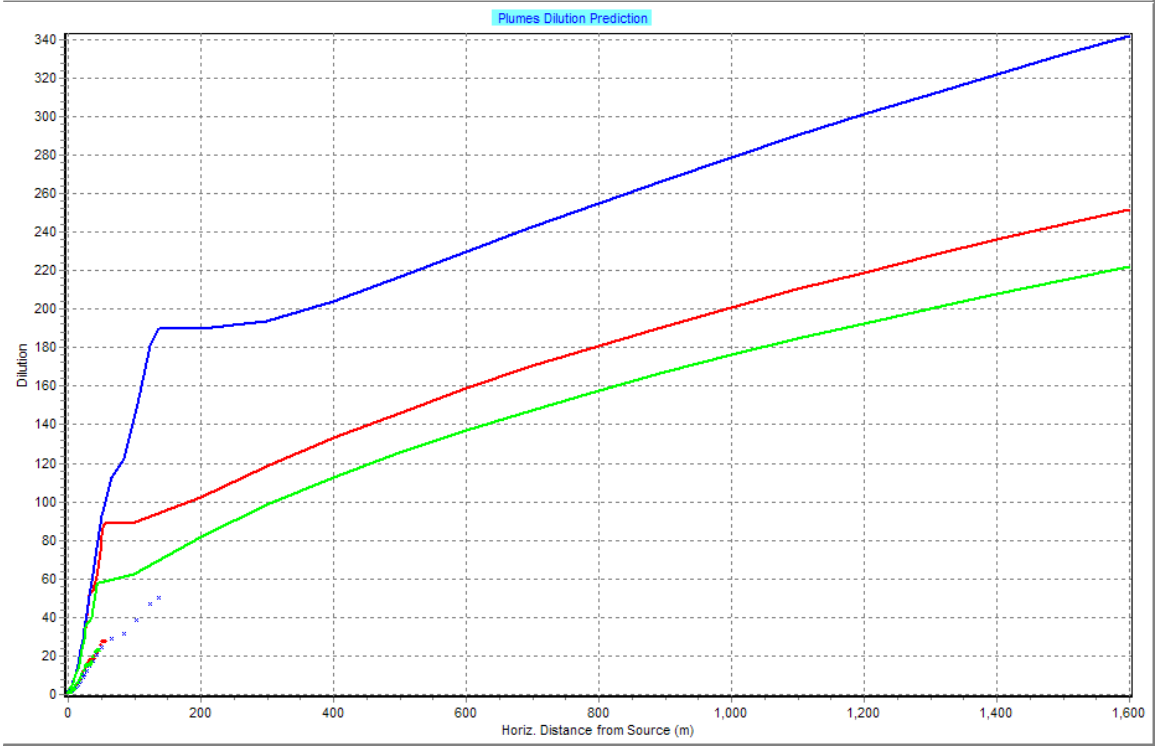
Salinity = 32.7 psu, Discharge Rate = 56,000 m^3/d

Aug F56 Avg (Red); Aug F56 High (Blue); Aug F56 Low (Green)

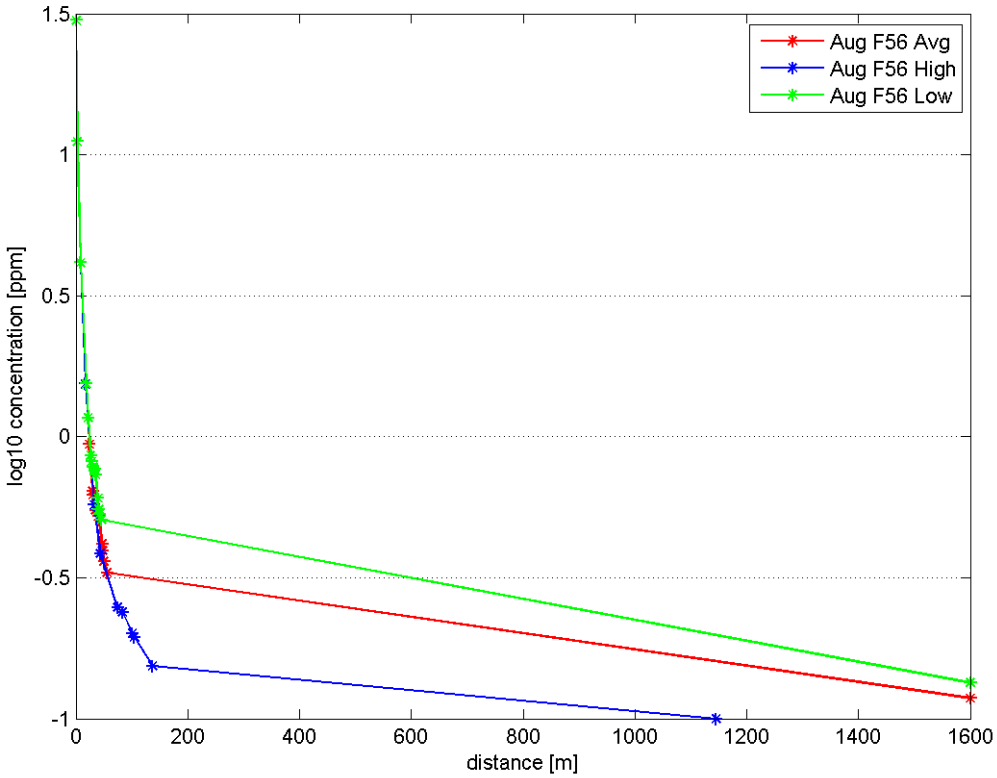


Salinity = 32.7 psu, Discharge Rate = 56,000 m^3/d
Aug F56 Avg (Red); Aug F56 High (Blue); Aug F56 Low (Green)

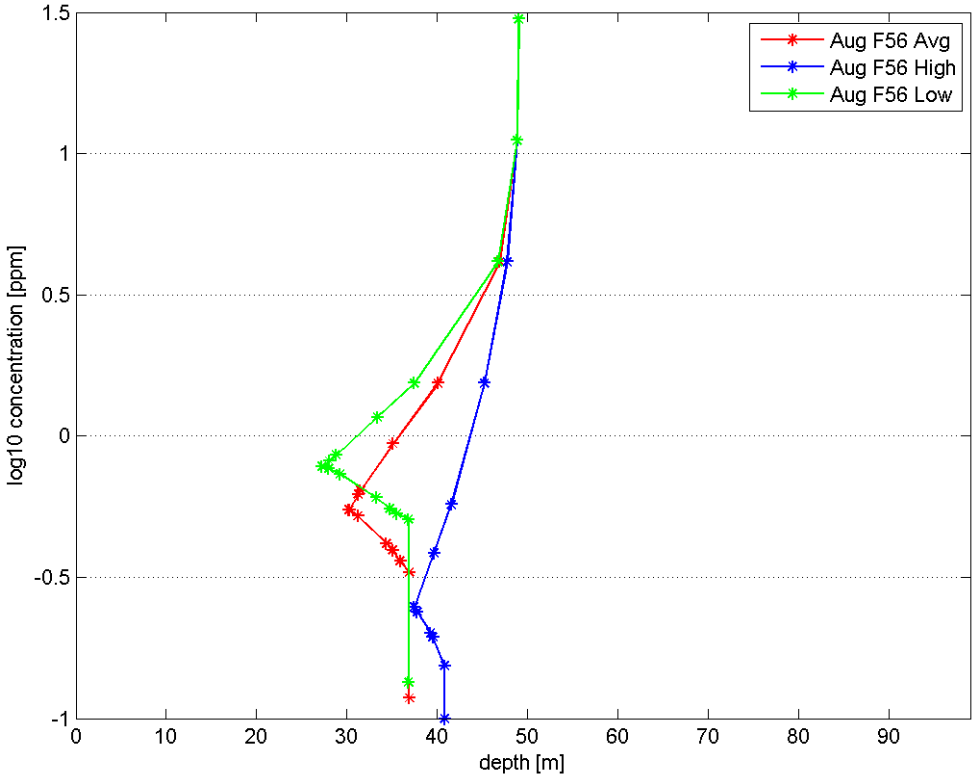




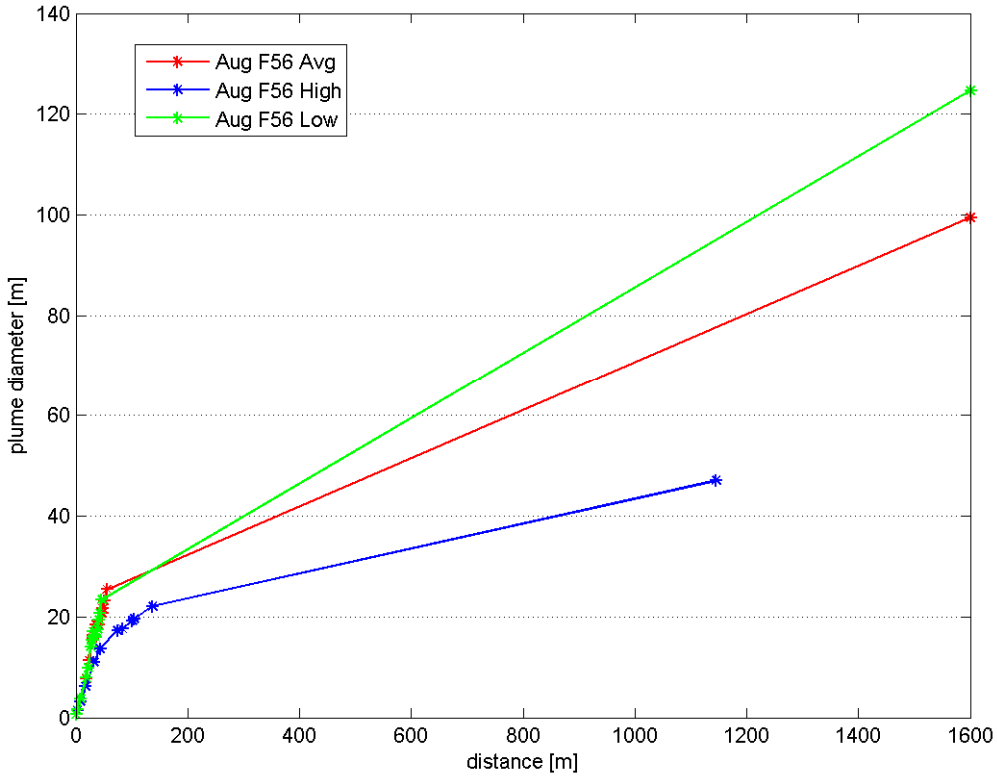
Salinity = 32.7 psu, Discharge Rate = 56,000 m^3/d
Aug F56 Avg (Red); Aug F56 High (Blue); Aug F56 Low (Green)



Salinity = 32.7 psu, Discharge Rate = 56,000 m^3/d
Aug F56 Avg (Red); Aug F56 High (Blue); Aug F56 Low (Green)

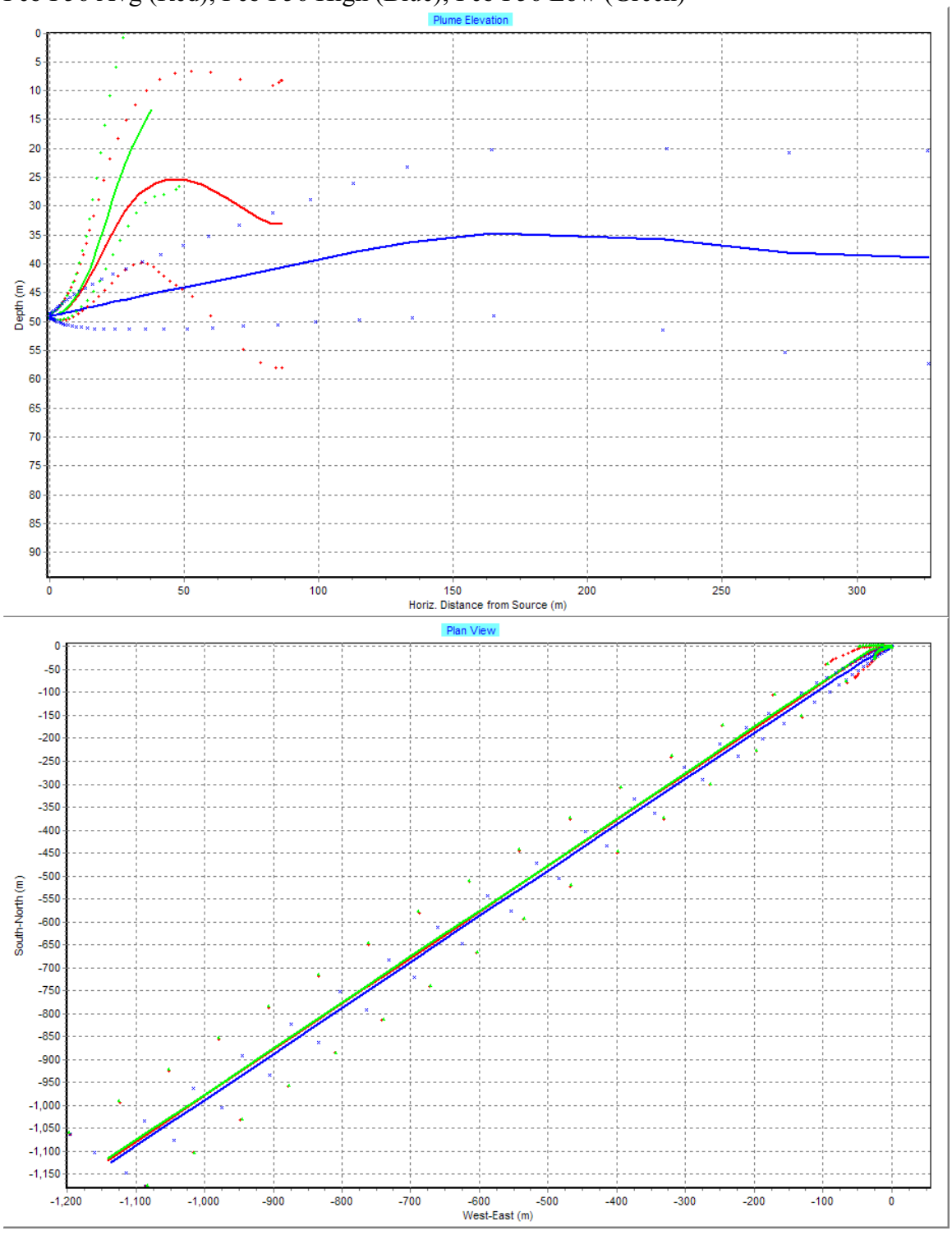


Salinity = 32.7 psu, Discharge Rate = 56,000 m^3/d
Aug F56 Avg (Red); Aug F56 High (Blue); Aug F56 Low (Green)



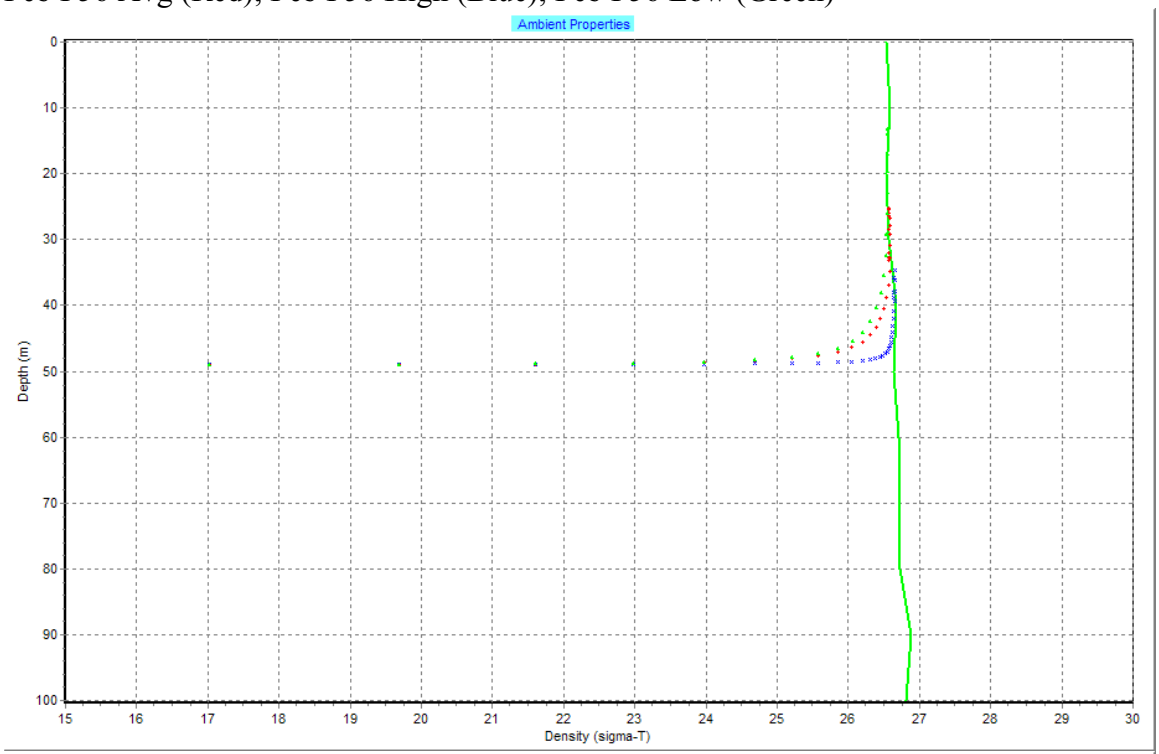
Salinity = 32.7 psu, Discharge Rate = 56,000 m^3/d

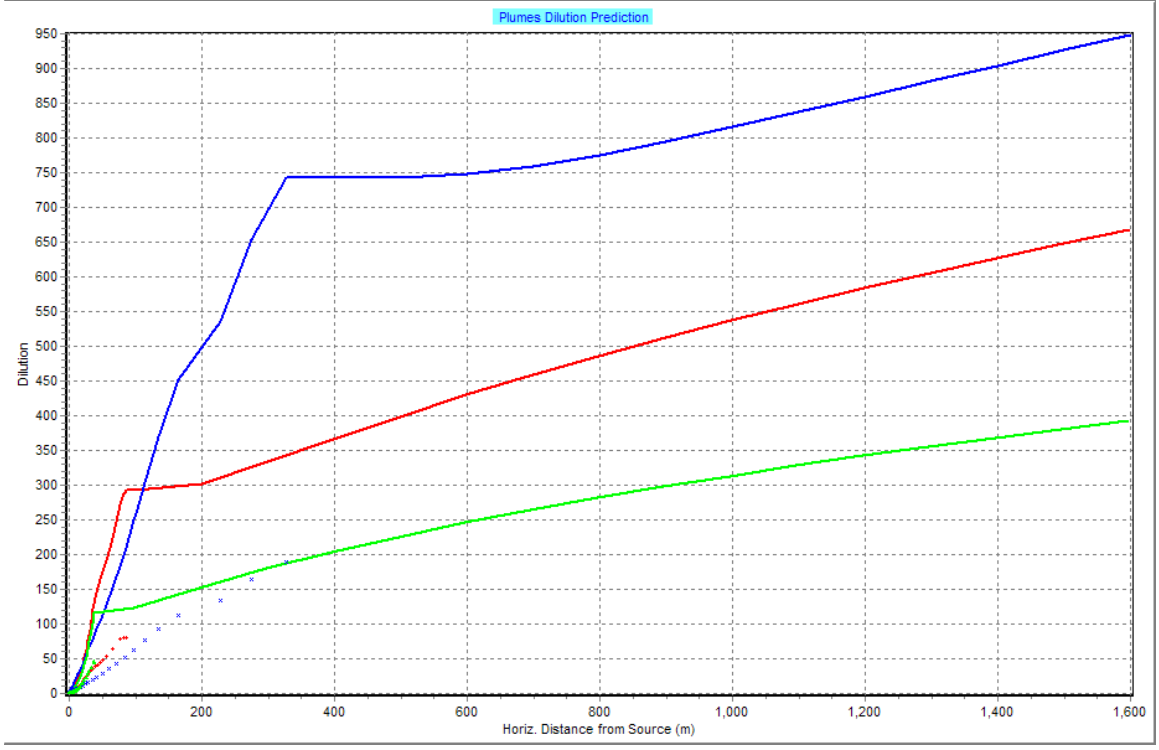
Feb F56 Avg (Red); Feb F56 High (Blue); Feb F56 Low (Green)



Salinity = 32.7 psu, Discharge Rate = 56,000 m^3/d

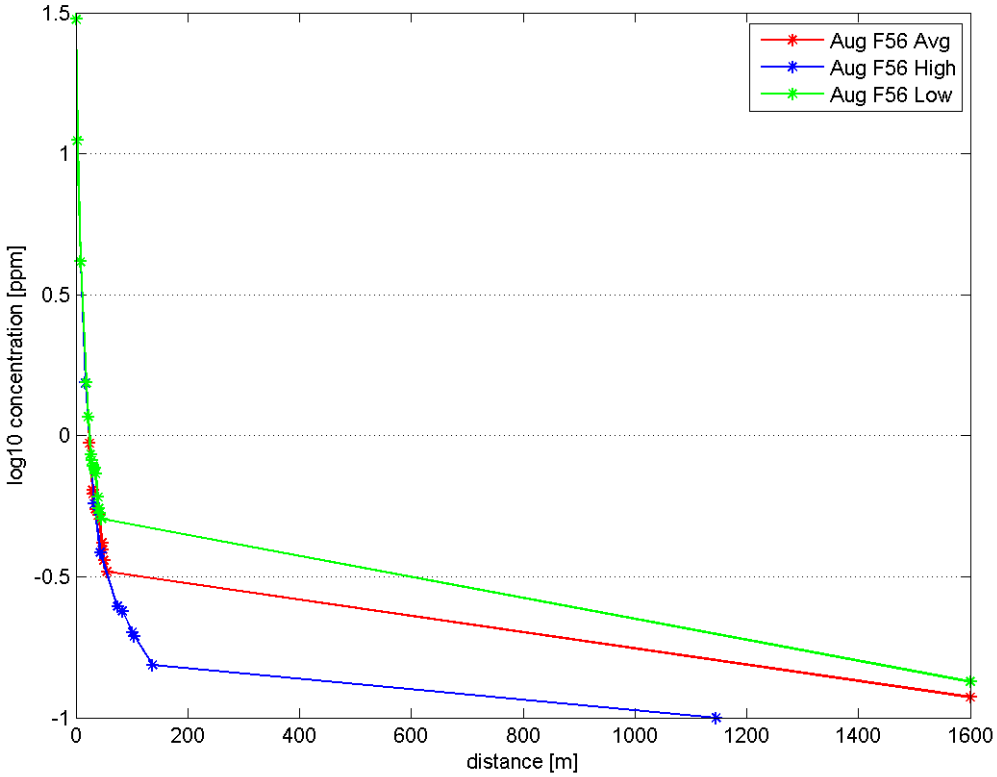
Feb F56 Avg (Red); Feb F56 High (Blue); Feb F56 Low (Green)

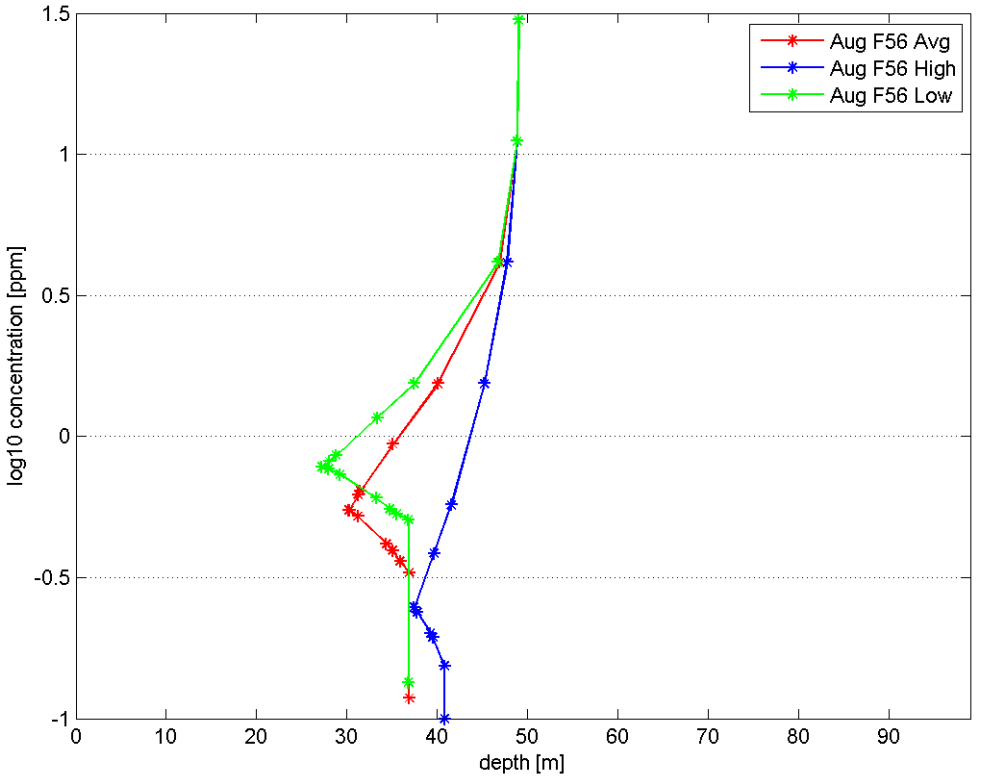




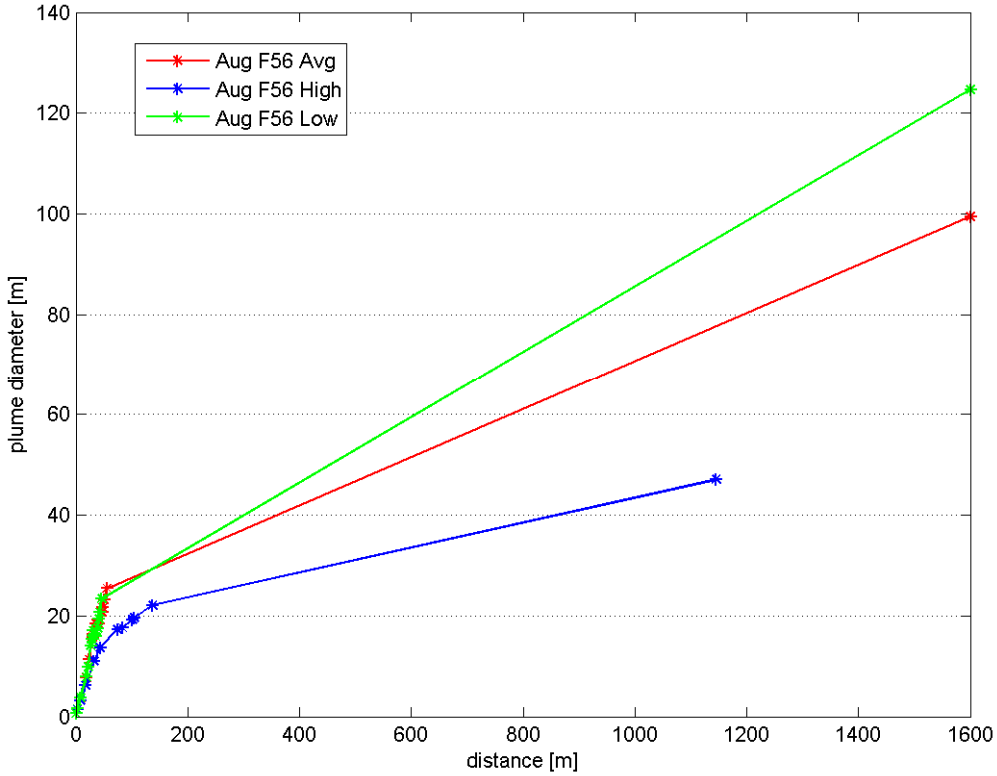
Salinity = 32.7 psu, Discharge Rate = 56,000 m^3/d

Feb F56 Avg (Red); Feb F56 High (Blue); Feb F56 Low (Green)



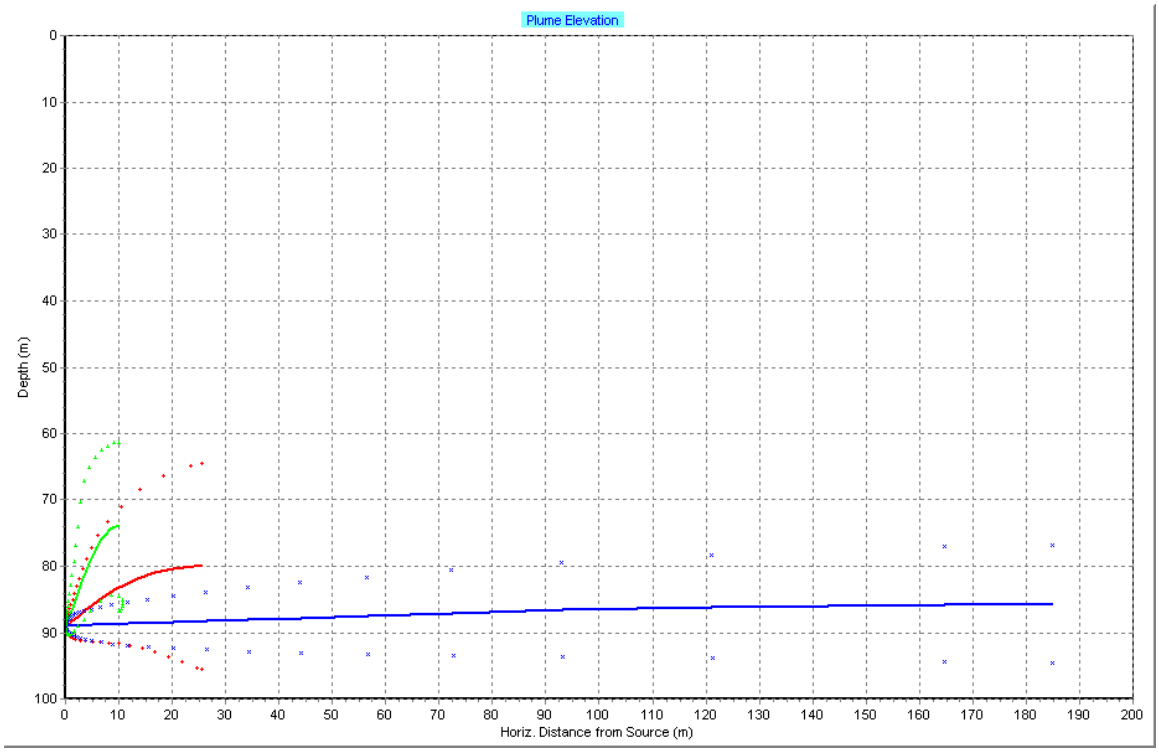


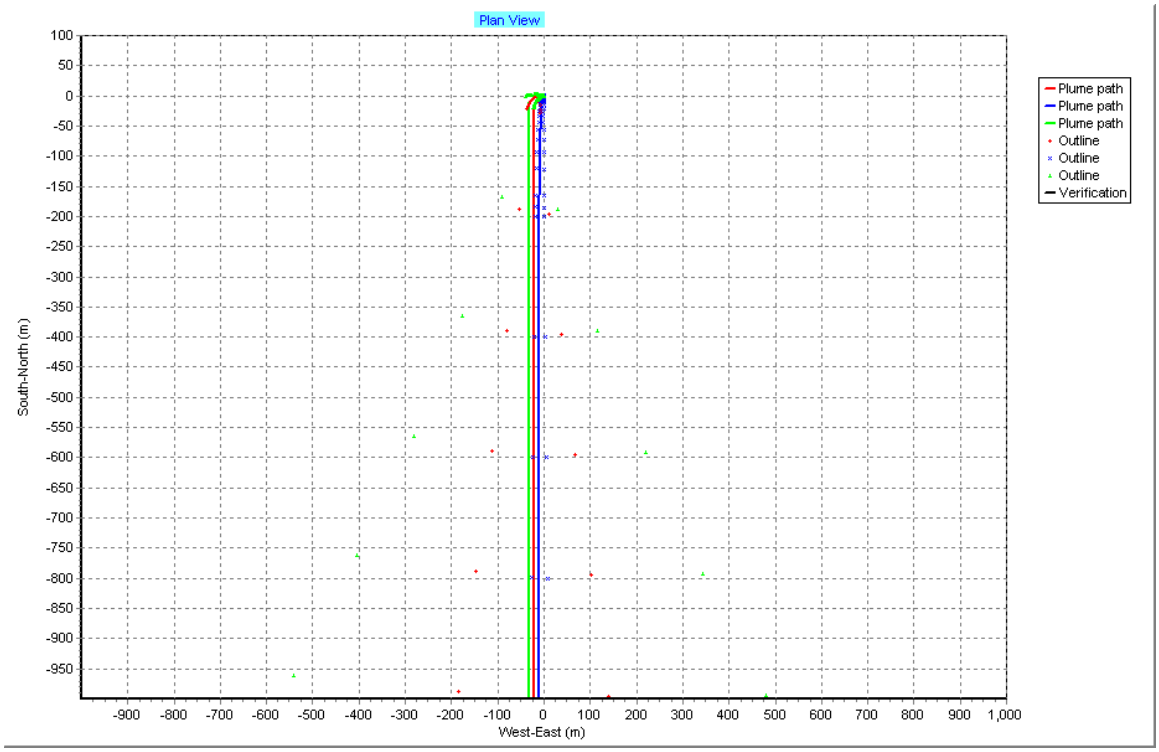
Salinity = 32.7 psu, Discharge Rate = 56,000 m^3/d
Feb F56 Avg (Red); Feb F56 High (Blue); Feb F56 Low (Green)



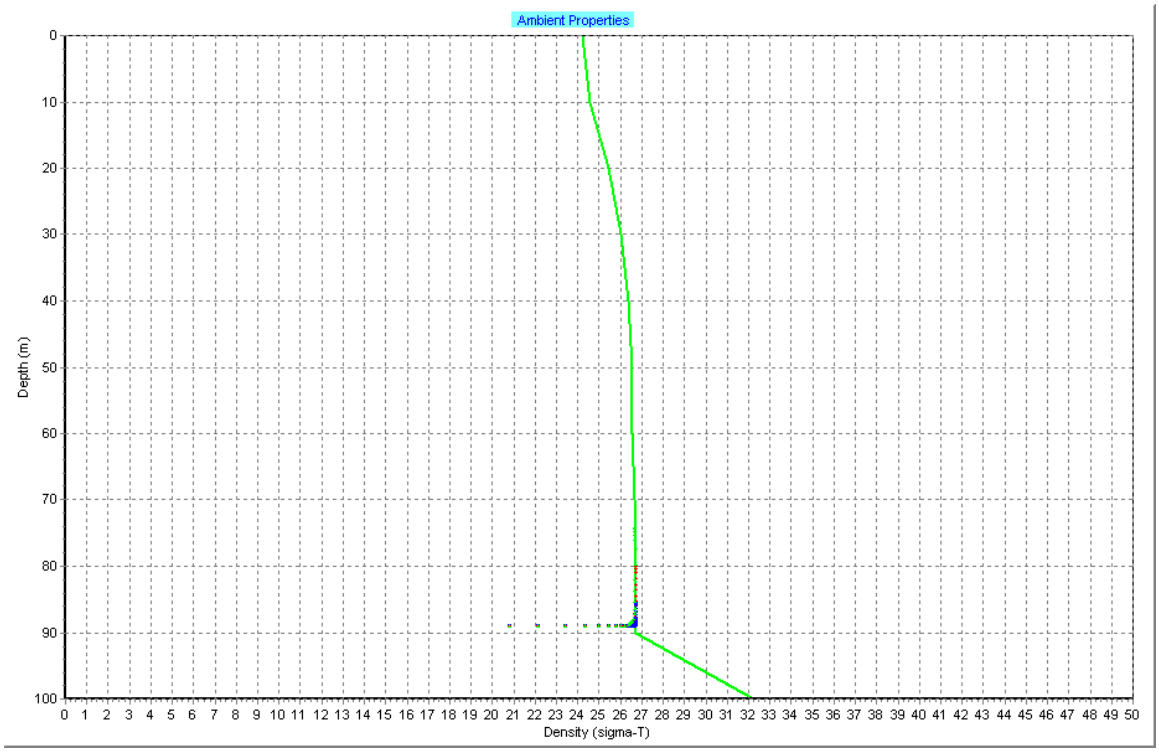
Appendix E
Storage Displacement Water Dispersion Model Results

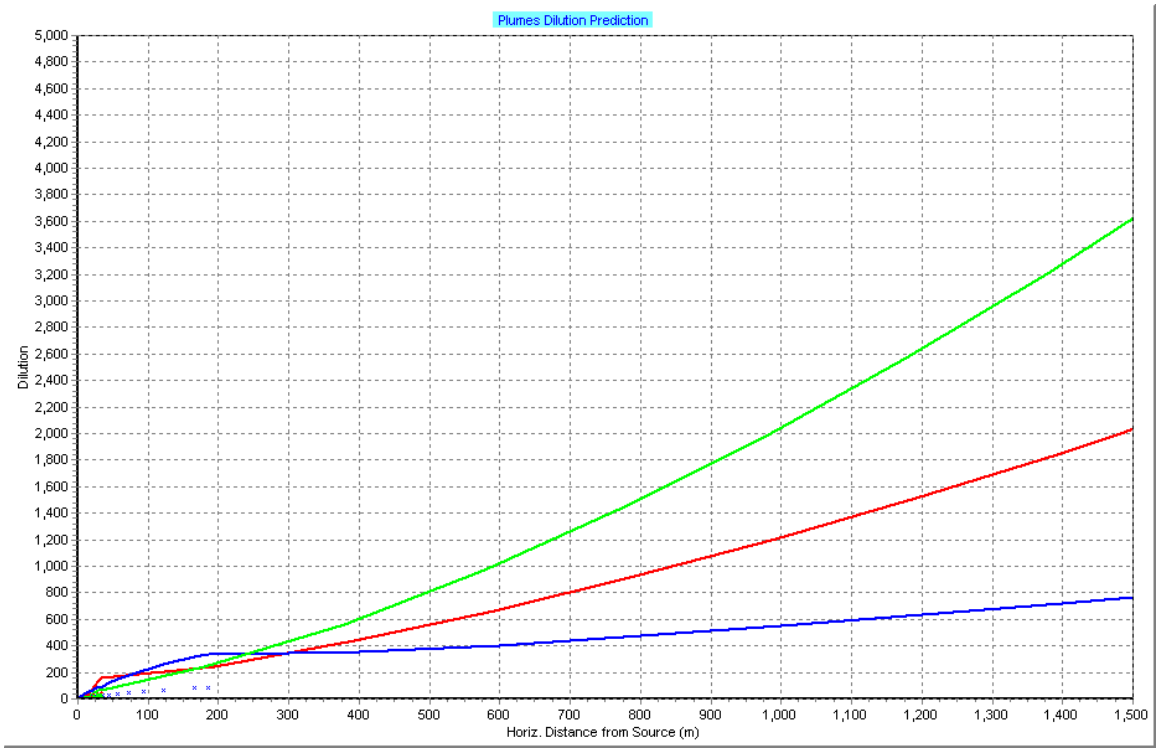
AA (Red); AH (Blue); AL (Green)



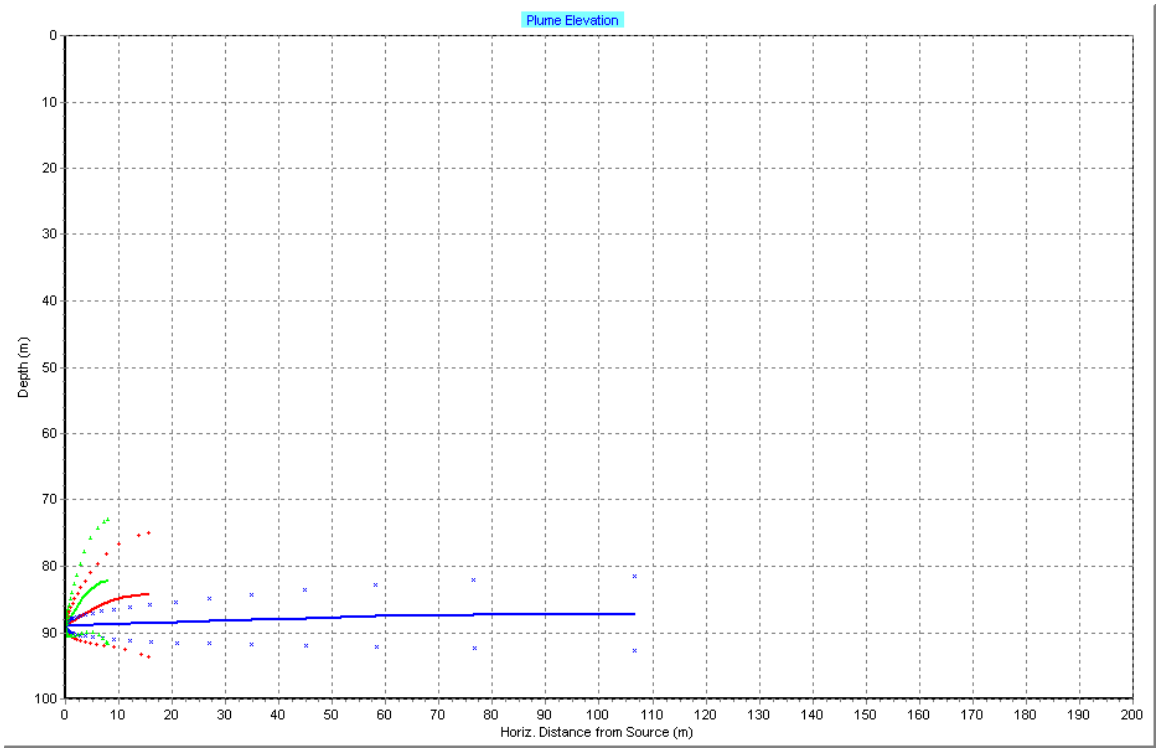


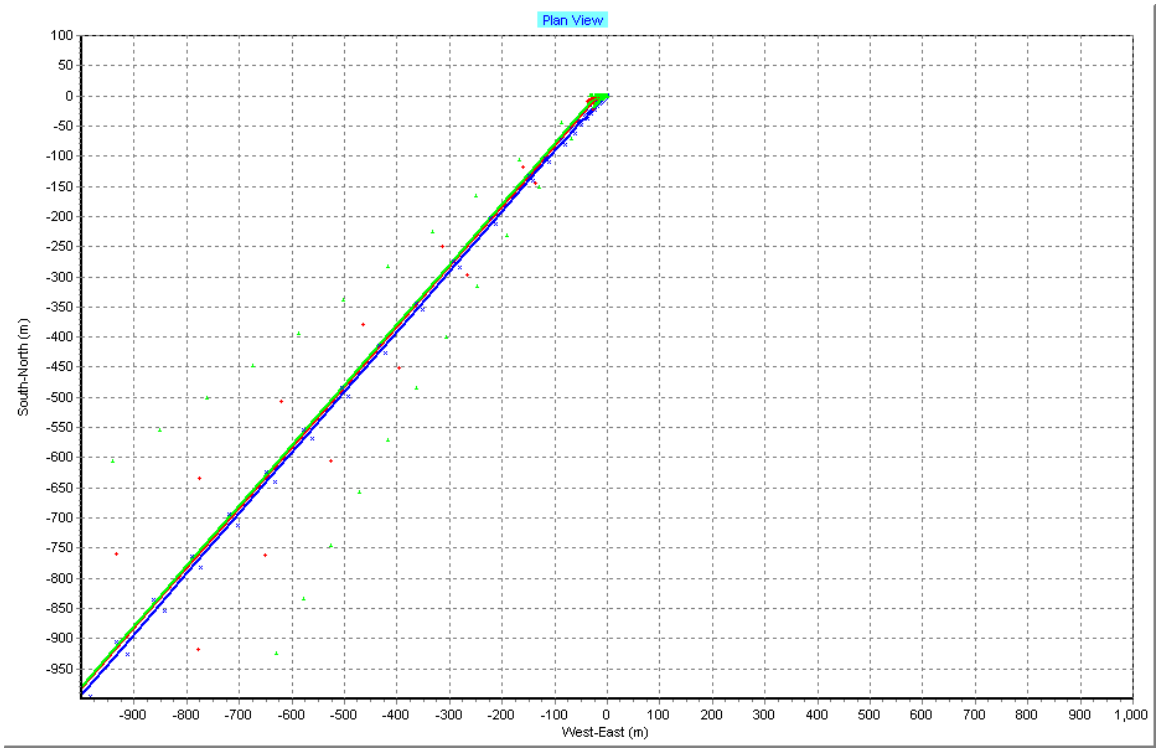
AA (Red); AH (Blue); AL (Green)



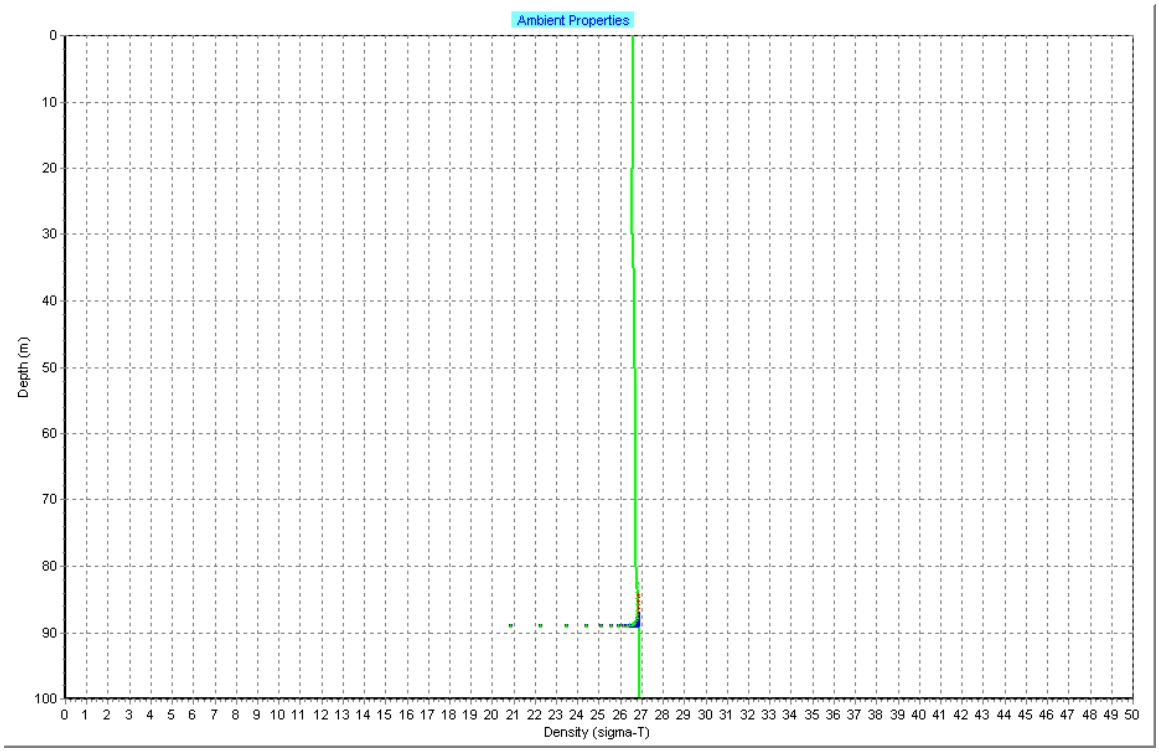


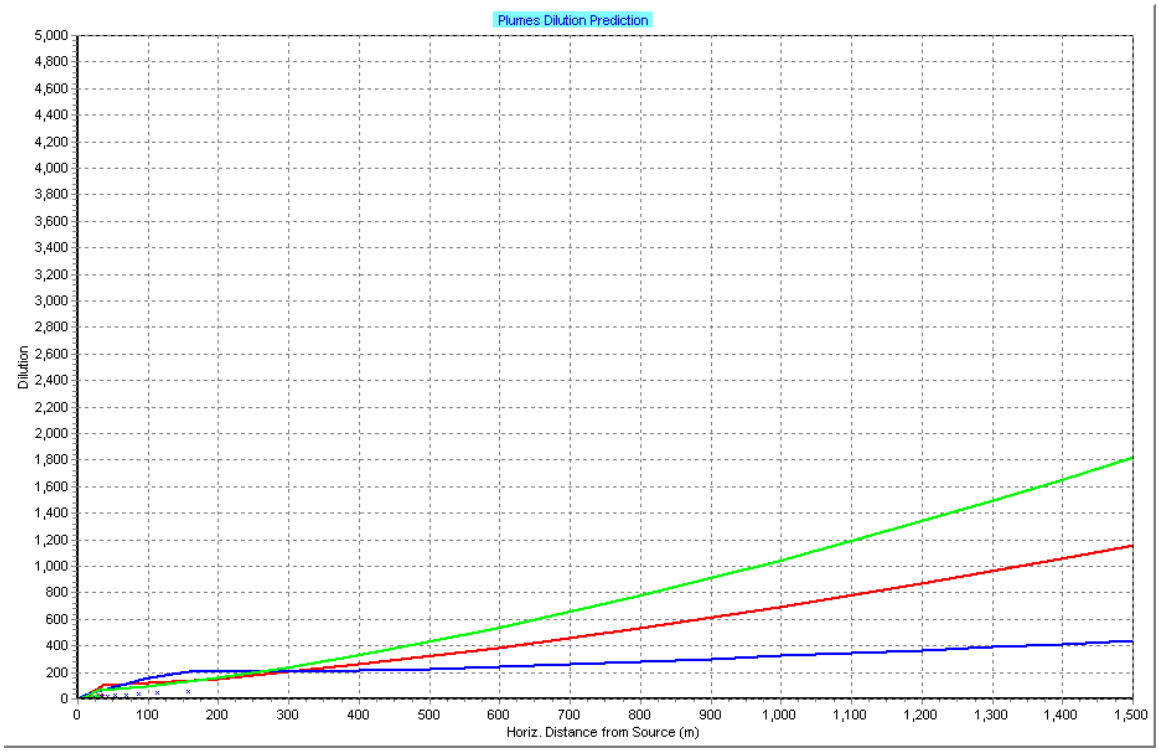
FA (Red); FH (Blue); FL (Green)



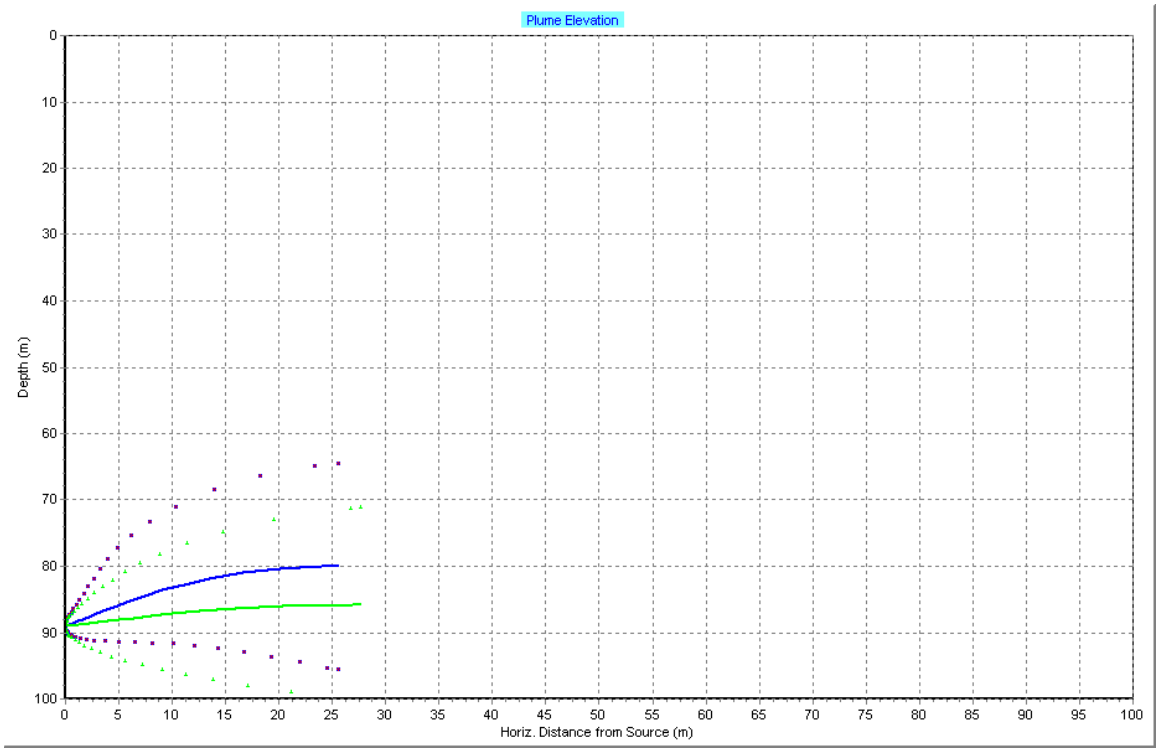


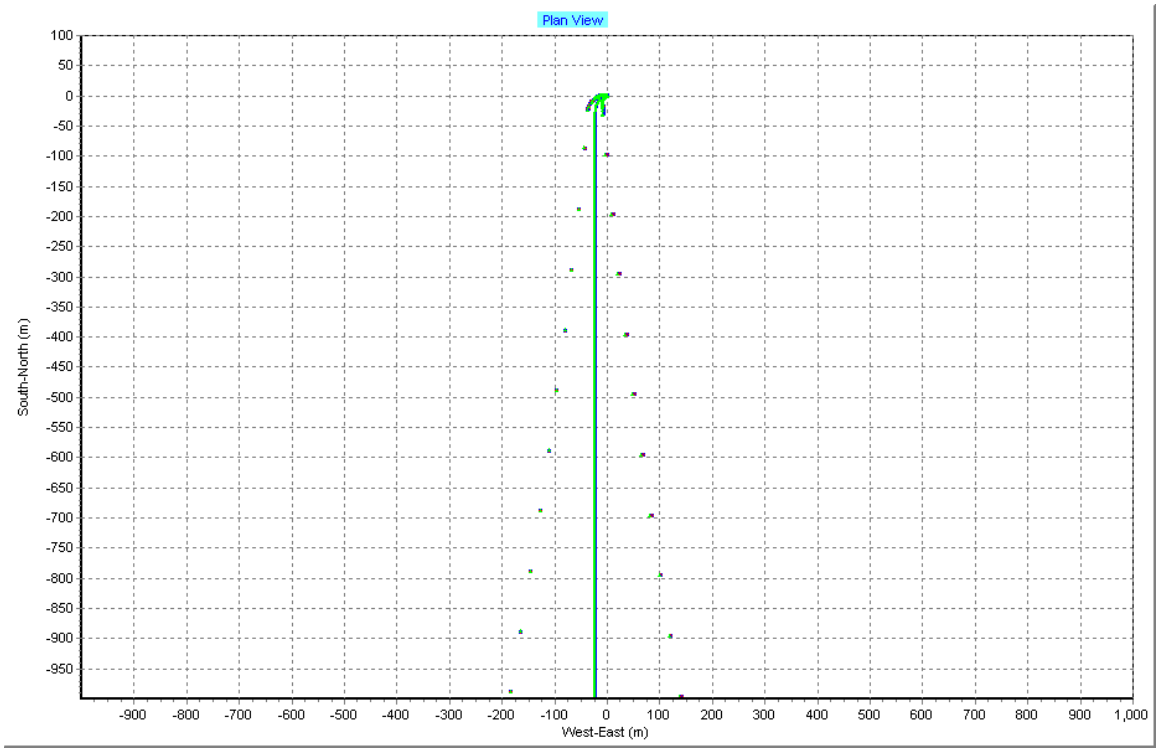
FA (Red); FH (Blue); FL (Green)



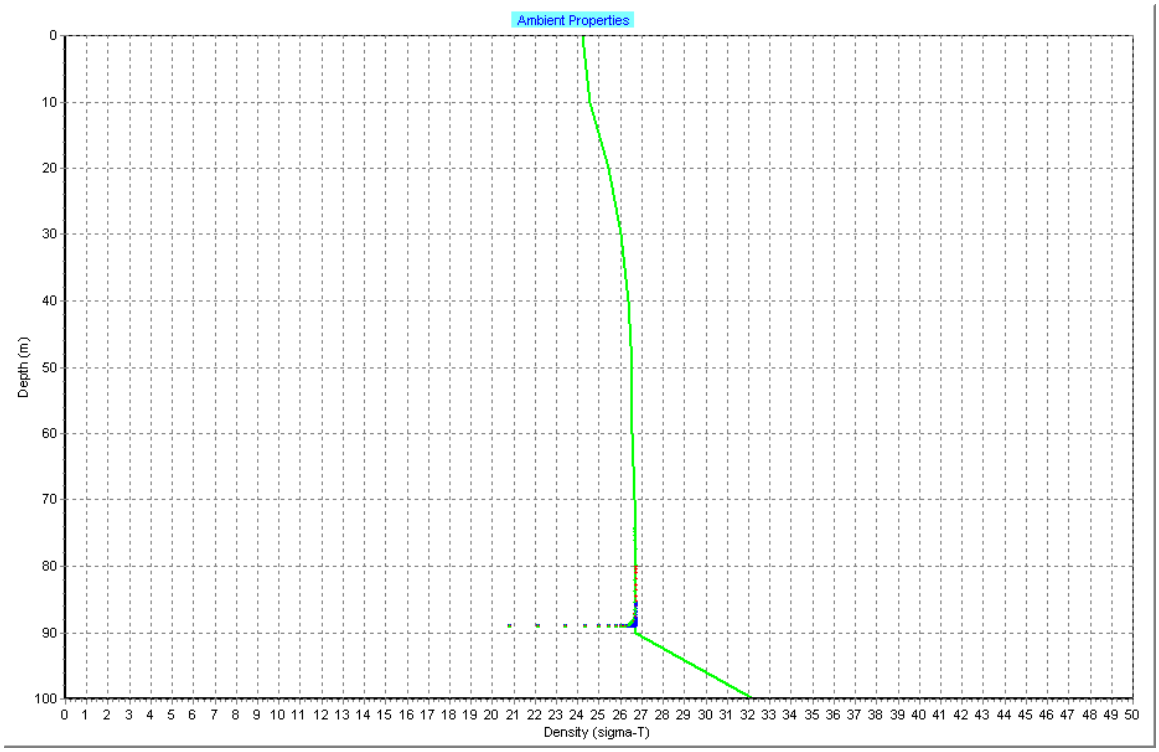


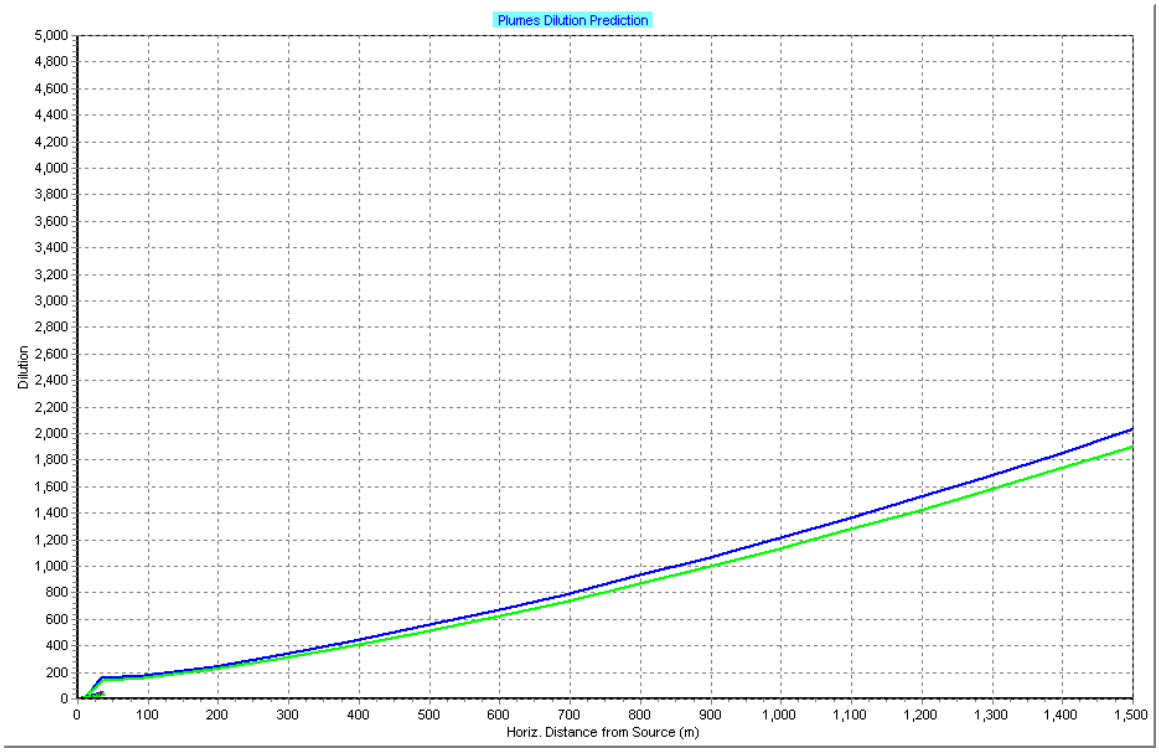
AA (Red); SAE10 (Blue); SAT10 (Green)



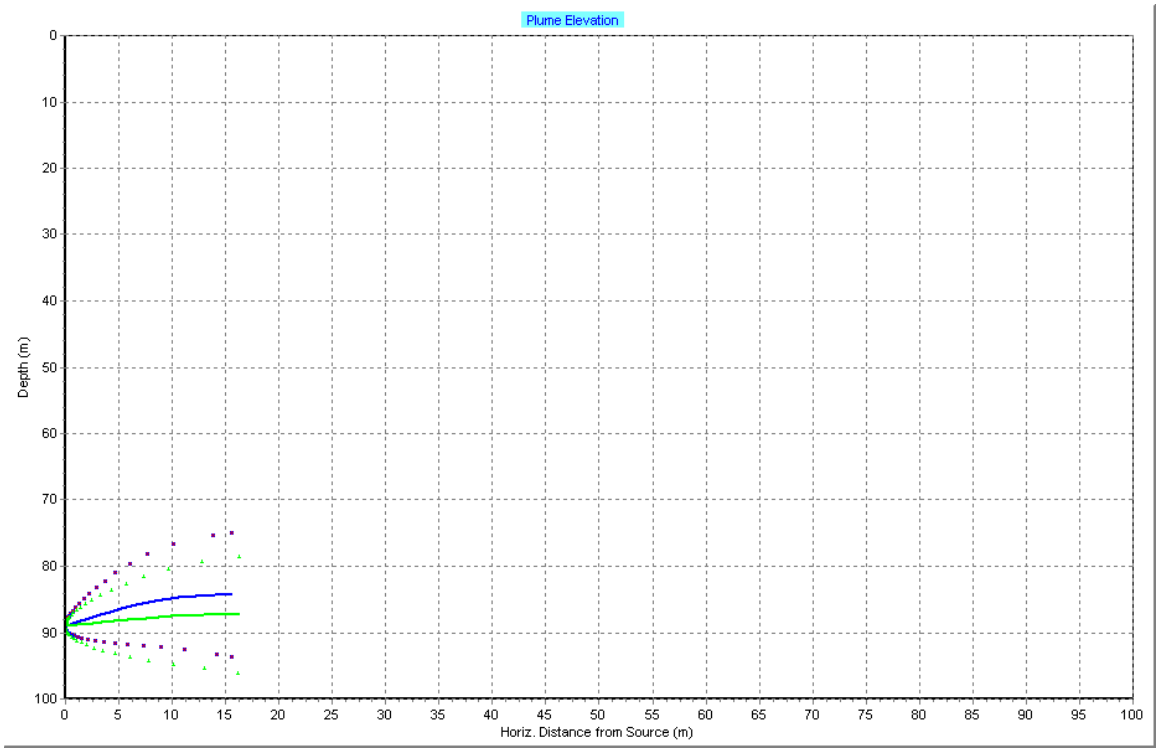


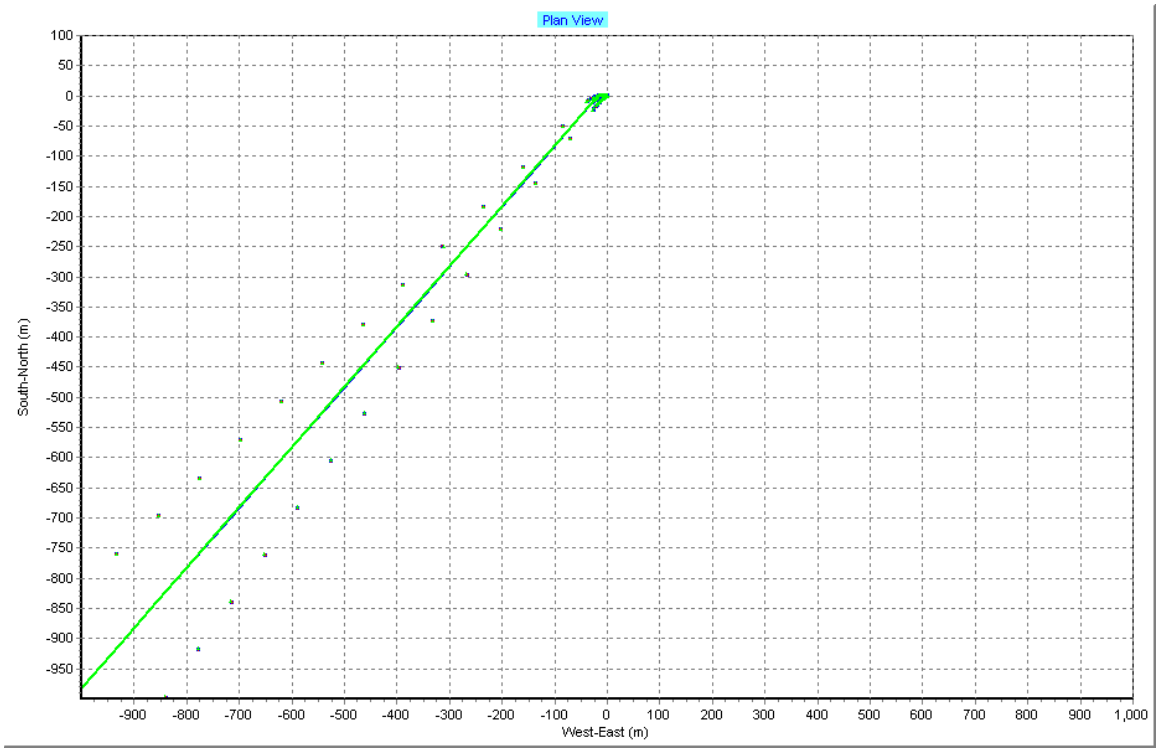
AA (Red); SAE10 (Blue); SAT10 (Green)



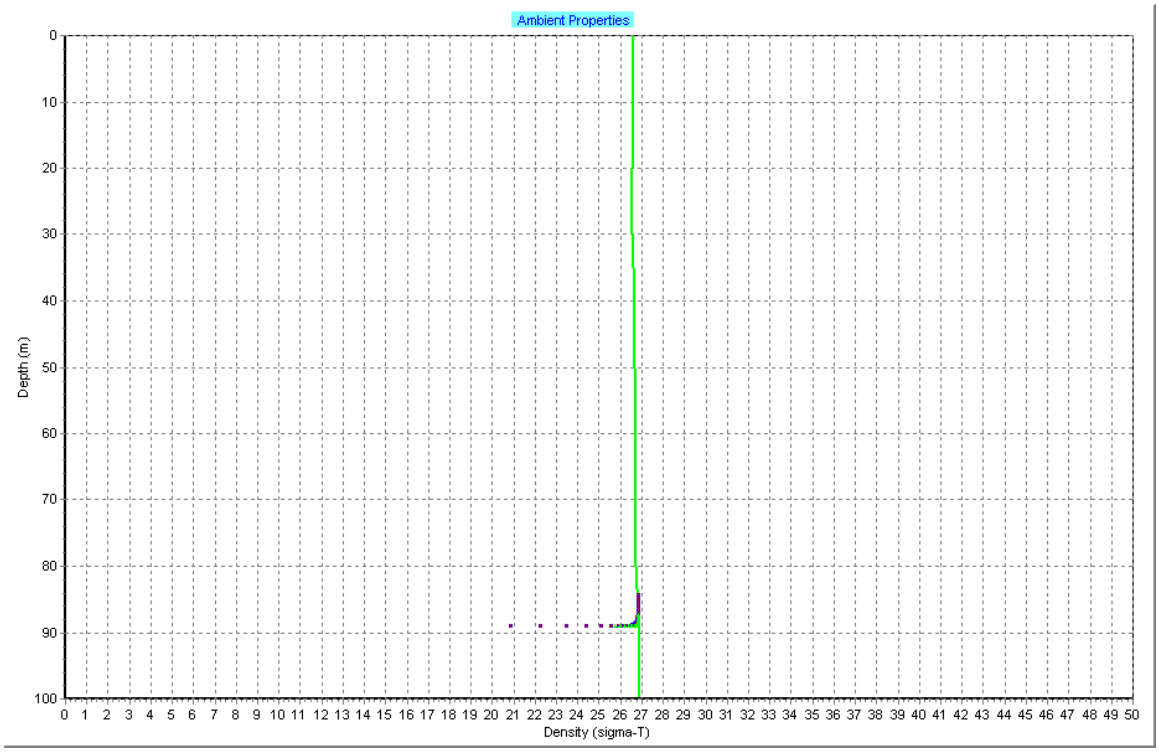


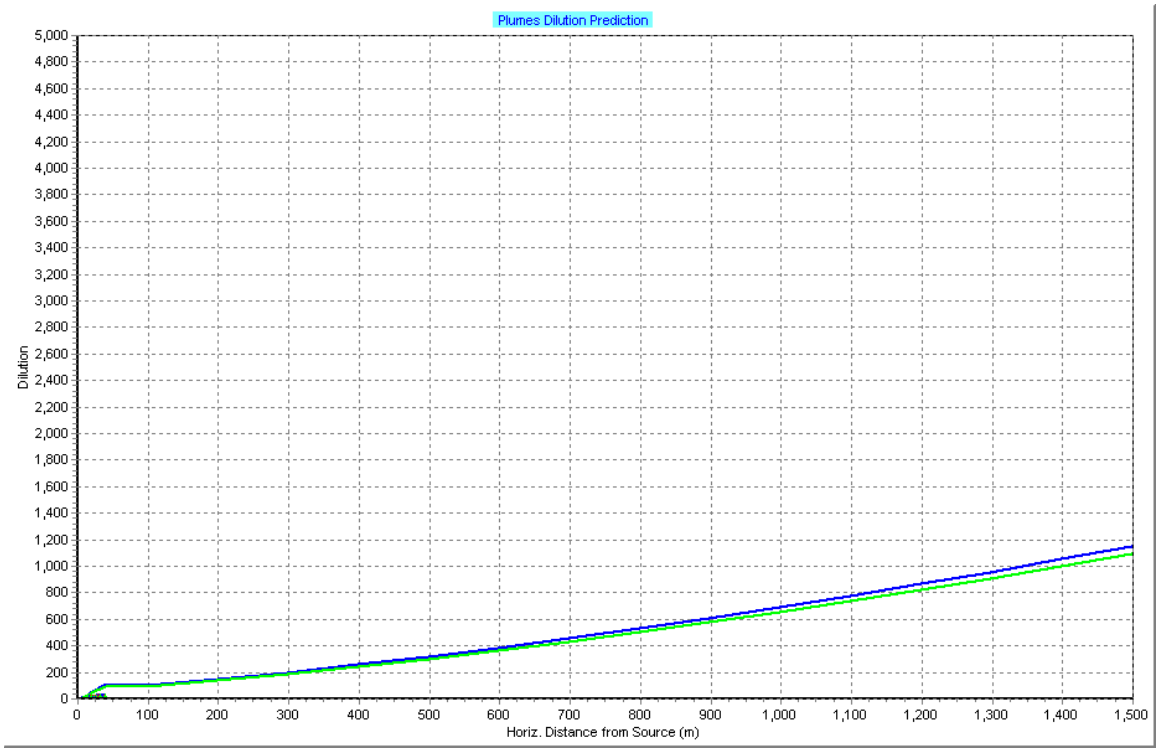
FA (Red); SFE10 (Blue); SFT10 (Green)





FA (Red); SFE10 (Blue); SFT10 (Green)





AL
/ UM3. 11/30/2004 10:11:10 AM
Case 1; ambient file C:\Plumes\AugLow.002.db; Diffuser table record 1: ----------

Ambient Table:

Depth	Amb-cur	Amb-dir	Amb-sal	Amb-tem	Amb-pol	Decay	Far-spd	Far-dir	Disprsn	Density
m	m/s	deg	psu	C	kg/kg	s-1	m/s	deg	m0.67/s2	sigma-T
0.0	0.055	270.0	31.94	11.99	0.0	0.0	0.055	270.0	0.0003	24.24
10.0	0.0553	270.0	32.05	10.83	0.0	0.0	0.0553	270.0	0.0003	24.54
20.0	0.0557	270.0	32.46	6.88	0.0	0.0	0.0557	270.0	0.0003	25.46
30.0	0.056	270.0	32.7	3.49	0.0	0.0	0.056	270.0	0.0003	26.03
40.0	0.0457	270.0	32.89	0.96	0.0	0.0	0.0457	270.0	0.0003	26.38
50.0	0.0353	270.0	33.0	-0.16	0.0	0.0	0.0353	270.0	0.0003	26.53
60.0	0.025	270.0	33.04	-0.39	0.0	0.0	0.025	270.0	0.0003	26.57
70.0	0.025	270.0	33.11	-0.71	0.0	0.0	0.025	270.0	0.0003	26.64
80.0	0.025	270.0	33.17	-0.81	0.0	0.0	0.025	270.0	0.0003	26.69
90.0	0.025	270.0	33.24	-0.62	0.0	0.0	0.025	270.0	0.0003	26.74
100.0	0.025	270.0	40.0	-0.55	0.0	0.0	0.025	270.0	0.0003	32.2

Diffuser table:

P-dia	P-elev	V-angle	H-angle	Ports	AcuteMZ	ChrncMZ	P-depth	Ttl-flo	Eff-sal	Temp	Polutnt
(m)	(m)	(deg)	(deg)	()	(m)	(m)	(m)	(m3/s)	(psu)	(C)	(kg/kg)
0.42	5.0	0.0	180.0	1.0	100.0	1600.0	89.0	0.3	33.15	30.0	15.0

Simulation:
Froude number: 13.5; effluent density (sigma-T) 20.3638335; effluent velocity 2.165(m/s);

Step	Depth (m)	Amb-cur (cm/s)	P-dia (m)	Polutnt (kg/kg)	Dilutn ()	x-posn (m)	y-posn (m)	
0	89.0	2.5	0.42	15.0	1.0	0.0	0.0;	
100	88.68	2.5	2.989	2.07	7.202	-5.619	-0.198;	
194	78.67	2.5	15.9	0.322	46.29	-23.65	-4.863;	trap level;
200	77.28	2.5	17.86	0.286	52.13	-25.13	-5.702;	
209	75.94	2.5	20.54	0.252	59.05	-26.69	-6.696;	begin overlap;
268	74.0	2.5	25.57	0.218	68.42	-31.15	-10.02;	local maximum rise or fall;

4/3 Power Law. Farfield dispersion based on wastefield width of 25.57 m

conc (kg/kg)	dilutn	width (m)	distnce (m)	time (hrs)	(ppm)	(s-1)	(cm/s)	(m0.67/s2)
0.1302	114.8	58.9	100.0	0.748	0.0	0.0	2.5	3.00E-4
6.28E-2	238.3	123.0	200.0	1.859	0.0	0.0	2.5	3.00E-4
3.85E-2	389.7	201.2	300.0	2.97	0.0	0.0	2.5	3.00E-4
2.66E-2	563.8	291.2	400.0	4.081	0.0	0.0	2.5	3.00E-4
1.98E-2	758.2	391.7	500.0	5.192	0.0	0.0	2.5	3.00E-4
1.54E-2	971.0	501.7	600.0	6.303	0.0	0.0	2.5	3.00E-4
1.24E-2	1200.6	620.4	700.0	7.414	0.0	0.0	2.5	3.00E-4
1.03E-2	1446.7	747.1	800.0	8.525	0.0	0.0	2.5	3.00E-4
8.79E-3	1706.9	881.5	900.0	9.636	0.0	0.0	2.5	3.00E-4
7.57E-3	1981.1	1023.2	1000.0	10.75	0.0	0.0	2.5	3.00E-4
6.61E-3	2268.6	1171.6	1100.0	11.86	0.0	0.0	2.5	3.00E-4
5.84E-3	2568.8	1326.7	1200.0	12.97	0.0	0.0	2.5	3.00E-4
5.21E-3	2881.2	1488.0	1300.0	14.08	0.0	0.0	2.5	3.00E-4

							SDW	
4.68E-3	3205.3	1655.4	1400.0	15.19	0.0	0.0	2.5	3.00E-4
4.24E-3	3540.7	1828.6	1500.0	16.3	0.0	0.0	2.5	3.00E-4
3.86E-3	3887.1	2007.5	1600.0	17.41	0.0	0.0	2.5	3.00E-4

count: 16

==========

AA
/ UM3.
Case 2; ambient file C:\Plumes\AugAvg.002.db; Diffuser table record 1: ----------

==========

Ambient Table:

Depth	Amb-cur	Amb-dir	Amb-sal	Amb-tem	Amb-pol	Decay	Far-spd	Far-dir	Disprsn	Density
m	m/s	deg	psu	C	kg/kg	s-1	m/s	deg	m0.67/s2	sigma-T
0.0	0.107	270.0	31.94	11.99	0.0	0.0	0.107	270.0	0.0003	24.24
10.0	0.104	270.0	32.05	10.83	0.0	0.0	0.104	270.0	0.0003	24.54
20.0	0.1	270.0	32.46	6.88	0.0	0.0	0.1	270.0	0.0003	25.46
30.0	0.097	270.0	32.7	3.49	0.0	0.0	0.097	270.0	0.0003	26.03
40.0	0.0853	270.0	32.89	0.96	0.0	0.0	0.0853	270.0	0.0003	26.38
50.0	0.0737	270.0	33.0	-0.16	0.0	0.0	0.0737	270.0	0.0003	26.53
60.0	0.062	270.0	33.04	-0.39	0.0	0.0	0.062	270.0	0.0003	26.57
70.0	0.062	270.0	33.11	-0.71	0.0	0.0	0.062	270.0	0.0003	26.64
80.0	0.062	270.0	33.17	-0.81	0.0	0.0	0.062	270.0	0.0003	26.69
90.0	0.062	270.0	33.24	-0.62	0.0	0.0	0.062	270.0	0.0003	26.74
100.0	0.062	270.0	40.0	-0.55	0.0	0.0	0.062	270.0	0.0003	32.2

Diffuser table:

P-dia	P-elev	V-angle	H-angle	Ports	AcuteMZ	ChrncMZ	P-depth	Ttl-flo	Eff-sal	Temp	Polutnt
(m)	(m)	(deg)	(deg)	()	(m)	(m)	(m)	(m3/s)	(psu)	(C)	(kg/kg)
0.42	5.0	0.0	180.0	1.0	100.0	1600.0	89.0	0.3	33.15	30.0	15.0

Simulation:
Froude number: 13.5; effluent density (sigma-T) 20.3638335; effluent velocity 2.165(m/s);

Step	Depth (m)	Amb-cur (cm/s)	P-dia (m)	Polutnt (kg/kg)	Dilutn ()	x-posn (m)	y-posn (m)	
0	89.0	6.2	0.42	15.0	1.0	0.0	0.0;	
100	88.78	6.2	2.974	2.07	7.202	-4.738	-0.398;	
200	84.45	6.2	15.7	0.286	52.11	-15.8	-7.454;	
225	82.32	6.2	21.55	0.174	85.5	-18.28	-12.24;	trap level;
245	80.67	6.2	27.12	0.119	125.3	-20.3	-18.33;	bottom hit;
264	80.04	6.2	31.01	0.0938	158.9	-22.07	-25.61;	local maximum rise or fall;

4/3 Power Law. Farfield dispersion based on wastefield width of 31.01 m

conc (kg/kg)	dilutn	width (m)	distnce (m)	time (hrs)	(ppm)	(s-1)	(cm/s)	(m0.67/s2)
8.61E-2	173.3	43.84	100.0	0.297	0.0	0.0	6.2	3.00E-4
6.06E-2	246.4	65.83	200.0	0.745	0.0	0.0	6.2	3.00E-4
4.44E-2	336.8	90.62	300.0	1.193	0.0	0.0	6.2	3.00E-4
3.42E-2	437.5	117.9	400.0	1.641	0.0	0.0	6.2	3.00E-4
2.74E-2	547.1	147.5	500.0	2.089	0.0	0.0	6.2	3.00E-4
2.25E-2	664.6	179.2	600.0	2.537	0.0	0.0	6.2	3.00E-4
1.90E-2	789.5	212.9	700.0	2.985	0.0	0.0	6.2	3.00E-4
1.63E-2	921.6	248.5	800.0	3.433	0.0	0.0	6.2	3.00E-4

							SDW	
1.41E-2	1059.9	285.9	900.0	3.881	0.0	0.0	6.2	3.00E-4
1.24E-2	1204.7	325.0	1000.0	4.329	0.0	0.0	6.2	3.00E-4
1.10E-2	1355.6	365.7	1100.0	4.777	0.0	0.0	6.2	3.00E-4
9.91E-3	1512.3	408.0	1200.0	5.225	0.0	0.0	6.2	3.00E-4
8.95E-3	1674.6	451.9	1300.0	5.673	0.0	0.0	6.2	3.00E-4
8.14E-3	1842.4	497.1	1400.0	6.121	0.0	0.0	6.2	3.00E-4
7.44E-3	2015.4	543.8	1500.0	6.569	0.0	0.0	6.2	3.00E-4
6.84E-3	2193.6	591.9	1600.0	7.017	0.0	0.0	6.2	3.00E-4

count: 16

==========

AH
/ UM3.
Case 3; ambient file C:\Plumes\AugHigh.002.db; Diffuser table record 1: ----------

==========

Ambient Table:

Depth	Amb-cur	Amb-dir	Amb-sal	Amb-tem	Amb-pol	Decay	Far-spd	Far-dir	Disprsn	Density
m	m/s	deg	psu	C	kg/kg	s-1	m/s	deg	m0.67/s2	sigma-T
0.0	0.8	270.0	31.94	11.99	0.0	0.0	0.8	270.0	0.0003	24.24
10.0	0.727	270.0	32.05	10.83	0.0	0.0	0.727	270.0	0.0003	24.54
20.0	0.653	270.0	32.46	6.88	0.0	0.0	0.653	270.0	0.0003	25.46
30.0	0.58	270.0	32.7	3.49	0.0	0.0	0.58	270.0	0.0003	26.03
40.0	0.523	270.0	32.89	0.96	0.0	0.0	0.523	270.0	0.0003	26.38
50.0	0.467	270.0	33.0	-0.16	0.0	0.0	0.467	270.0	0.0003	26.53
60.0	0.41	270.0	33.04	-0.39	0.0	0.0	0.41	270.0	0.0003	26.57
70.0	0.41	270.0	33.11	-0.71	0.0	0.0	0.41	270.0	0.0003	26.64
80.0	0.41	270.0	33.17	-0.81	0.0	0.0	0.41	270.0	0.0003	26.69
90.0	0.41	270.0	33.24	-0.62	0.0	0.0	0.41	270.0	0.0003	26.74
100.0	0.41	270.0	40.0	-0.55	0.0	0.0	0.41	270.0	0.0003	32.2

Diffuser table:

P-dia	P-elev	V-angle	H-angle	Ports	AcuteMZ	ChrncMZ	P-depth	Ttl-flo	Eff-sal	Temp	Plutnt
(m)	(m)	(deg)	(deg)	()	(m)	(m)	(m)	(m3/s)	(psu)	(C)	(kg/kg)
0.42	5.0	0.0	180.0	1.0	100.0	1600.0	89.0	0.3	33.15	30.0	15.0

Simulation:

Froude number: 13.5; effluent density (sigma-T) 20.3638335; effluent velocity 2.165(m/s);

Step	Depth (m)	Amb-cur (cm/s)	P-dia (m)	Plutnt (kg/kg)	Dilutn ()	x-posn (m)	y-posn (m)	
0	89.0	41.0	0.42	15.0	1.0	0.0	0.0;	
100	88.98	41.0	2.246	2.324	6.415	-1.68	-0.664;	
200	88.68	41.0	6.469	0.337	44.24	-4.405	-11.64;	
279	86.62	41.0	14.07	0.0705	211.5	-8.134	-90.75;	trap level;
283	86.42	41.0	14.63	0.0651	228.9	-8.366	-100.5;	acute zone;
293	85.95	41.0	16.15	0.0534	279.0	-9.01	-131.9;	bottom hit;
300	85.71	41.0	17.31	0.0465	320.5	-9.579	-164.6;	
303	85.69	41.0	17.83	0.0438	340.1	-9.898	-184.8;	local maximum rise or fall;

4/3 Power Law. Farfield dispersion based on wastefield width of 17.83 m

conc (kg/kg)	dilutn	width (m)	distnce (m)	time (hrs)	(ppm)	(s-1)	(cm/s)	(m0.67/s2)
4.37E-2	340.8	18.17	200.0	0.0101	0.0	0.0	41.0	3.00E-4
4.37E-2	340.9	20.53	300.0	0.0779	0.0	0.0	41.0	3.00E-4

							SDW	
4.24E-2	351.8	22.98	400.0	0.146	0.0	0.0	41.0	3.00E-4
3.99E-2	374.1	25.52	500.0	0.213	0.0	0.0	41.0	3.00E-4
3.70E-2	403.1	28.15	600.0	0.281	0.0	0.0	41.0	3.00E-4
3.42E-2	436.2	30.86	700.0	0.349	0.0	0.0	41.0	3.00E-4
3.16E-2	472.0	33.65	800.0	0.417	0.0	0.0	41.0	3.00E-4
2.93E-2	509.8	36.53	900.0	0.484	0.0	0.0	41.0	3.00E-4
2.72E-2	549.3	39.48	1000.0	0.552	0.0	0.0	41.0	3.00E-4
2.53E-2	590.2	42.51	1100.0	0.62	0.0	0.0	41.0	3.00E-4
2.36E-2	632.2	45.61	1200.0	0.688	0.0	0.0	41.0	3.00E-4
2.21E-2	675.5	48.78	1300.0	0.755	0.0	0.0	41.0	3.00E-4
2.08E-2	719.9	52.02	1400.0	0.823	0.0	0.0	41.0	3.00E-4
1.95E-2	765.3	55.33	1500.0	0.891	0.0	0.0	41.0	3.00E-4
1.84E-2	811.7	58.71	1600.0	0.959	0.0	0.0	41.0	3.00E-4

count: 15

==========

FL
/ UM3. 11/30/2004 10:30:13 AM
Case 1; ambient file C:\Plumes\FebLow.002.db; Diffuser table record 1: ----------

==========

Ambient Table:

Depth	Amb-cur	Amb-dir	Amb-sal	Amb-tem	Amb-pol	Decay	Far-spd	Far-dir	Disprsn	Density
m	m/s	deg	psu	C	kg/kg	s-1	m/s	deg	m0.67/s2	sigma-T
0.0	0.067	225.0	32.99	-0.53	0.0	0.0	0.067	225.0	0.0003	26.53
10.0	0.0633	225.0	33.06	-0.56	0.0	0.0	0.0633	225.0	0.0003	26.59
20.0	0.0597	225.0	32.99	-0.5	0.0	0.0	0.0597	225.0	0.0003	26.53
30.0	0.056	225.0	33.03	-0.47	0.0	0.0	0.056	225.0	0.0003	26.56
40.0	0.054	225.0	33.18	-0.37	0.0	0.0	0.054	225.0	0.0003	26.68
50.0	0.052	225.0	33.12	-0.4	0.0	0.0	0.052	225.0	0.0003	26.63
60.0	0.05	225.0	33.21	-0.28	0.0	0.0	0.05	225.0	0.0003	26.7
70.0	0.05	225.0	33.23	-0.32	0.0	0.0	0.05	225.0	0.0003	26.72
80.0	0.05	225.0	33.24	-0.34	0.0	0.0	0.05	225.0	0.0003	26.73
90.0	0.05	225.0	33.45	-0.18	0.0	0.0	0.05	225.0	0.0003	26.89
100.0	0.05	225.0	33.36	-0.13	0.0	0.0	0.05	225.0	0.0003	26.81

Diffuser table:

P-dia	P-elev	V-angle	H-angle	Ports	AcuteMZ	ChrncMZ	P-depth	Ttl-flo	Eff-sal	Temp	Polutnt
(m)	(m)	(deg)	(deg)	()	(m)	(m)	(m)	(m3/s)	(psu)	(C)	(kg/kg)
0.42	5.0	0.0	180.0	1.0	100.0	1600.0	89.0	0.3	33.3	30.0	15.0

Simulation:
Froude number: 13.48; effluent density (sigma-T) 20.4760849; effluent velocity 2.165(m/s);

Step	Depth (m)	Amb-cur (cm/s)	P-dia (m)	Polutnt (kg/kg)	Dilutn ()	x-posn (m)	y-posn (m)	
0	89.0	5.0	0.42	15.0	1.0	0.0	0.0;	
100	88.74	5.0	2.851	2.07	7.202	-5.276	-0.243;	
185	84.27	5.0	11.95	0.385	38.76	-20.28	-3.811;	trap level;
200	82.96	5.0	15.09	0.287	51.92	-24.2	-5.464;	
225	82.28	5.0	18.66	0.218	68.44	-29.17	-7.927;	local maximum rise or fall;

4/3 Power Law. Farfield dispersion based on wastefield width of 18.66 m

conc	dilutn	width	distnce	time

(kg/kg)	(m)	(m)	(hrs)	(kg/kg)	(s-1)	SDW (cm/s)	(m0.67/s2)
0.16479	90.6	33.46	100.0	0.388	0.0	0.0	5.0 3.00E-4
9.51E-2	157.3	59.16	200.0	0.943	0.0	0.0	5.0 3.00E-4
6.31E-2	237.2	89.33	300.0	1.499	0.0	0.0	5.0 3.00E-4
4.57E-2	327.5	123.4	400.0	2.054	0.0	0.0	5.0 3.00E-4
3.51E-2	427.1	160.9	500.0	2.61	0.0	0.0	5.0 3.00E-4
2.80E-2	535.0	201.6	600.0	3.165	0.0	0.0	5.0 3.00E-4
2.30E-2	650.8	245.3	700.0	3.721	0.0	0.0	5.0 3.00E-4
1.94E-2	774.0	291.7	800.0	4.276	0.0	0.0	5.0 3.00E-4
1.66E-2	904.1	340.7	900.0	4.832	0.0	0.0	5.0 3.00E-4
1.44E-2	1040.7	392.2	1000.0	5.388	0.0	0.0	5.0 3.00E-4
1.26E-2	1183.6	446.1	1100.0	5.943	0.0	0.0	5.0 3.00E-4
1.12E-2	1333.2	502.2	1200.0	6.499	0.0	0.0	5.0 3.00E-4
1.00E-2	1488.0	560.5	1300.0	7.054	0.0	0.0	5.0 3.00E-4
9.10E-3	1648.3	620.9	1400.0	7.61	0.0	0.0	5.0 3.00E-4
8.27E-3	1814.0	683.4	1500.0	8.165	0.0	0.0	5.0 3.00E-4
7.56E-3	1984.9	747.7	1600.0	8.721	0.0	0.0	5.0 3.00E-4

count: 16

==========

FA
/ UM3.
Case 2; ambient file C:\Plumes\FebAvg.002.db; Diffuser table record 1: ----------

==========

Ambient Table:

Depth m	Amb-cur m/s	Amb-dir deg	Amb-sal psu	Amb-tem C	Amb-pol kg/kg	Decay s-1	Far-spd m/s	Far-dir deg	Disprsn m0.67/s2	Density sigma-T
0.0	0.123	225.0	32.99	-0.53	0.0	0.0	0.123	225.0	0.0003	26.53
10.0	0.128	225.0	33.06	-0.56	0.0	0.0	0.128	225.0	0.0003	26.59
20.0	0.134	225.0	32.99	-0.5	0.0	0.0	0.134	225.0	0.0003	26.53
30.0	0.139	225.0	33.03	-0.47	0.0	0.0	0.139	225.0	0.0003	26.56
40.0	0.124	225.0	33.18	-0.37	0.0	0.0	0.124	225.0	0.0003	26.68
50.0	0.109	225.0	33.12	-0.4	0.0	0.0	0.109	225.0	0.0003	26.63
60.0	0.094	225.0	33.21	-0.28	0.0	0.0	0.094	225.0	0.0003	26.7
70.0	0.094	225.0	33.23	-0.32	0.0	0.0	0.094	225.0	0.0003	26.72
80.0	0.094	225.0	33.24	-0.34	0.0	0.0	0.094	225.0	0.0003	26.73
90.0	0.094	225.0	33.45	-0.18	0.0	0.0	0.094	225.0	0.0003	26.89
100.0	0.094	225.0	33.36	-0.13	0.0	0.0	0.094	225.0	0.0003	26.81

Diffuser table:

P-dia (m)	P-elev (m)	V-angle (deg)	H-angle (deg)	Ports ()	AcuteMZ (m)	ChrncMZ (m)	P-depth (m)	Ttl-flo (m3/s)	Eff-sal (psu)	Temp (C)	Polutnt (kg/kg)
0.42	5.0	0.0	180.0	1.0	100.0	1600.0	89.0	0.3	33.3	30.0	15.0

Simulation:
Froude number: 13.48; effluent density (sigma-T) 20.4760849; effluent velocity 2.165(m/s);

Step	Depth (m)	Amb-cur (cm/s)	P-dia (m)	Polutnt (kg/kg)	Dilutn ()	x-posn (m)	y-posn (m)
0	89.0	9.4	0.42	15.0	1.0	0.0	0.0;
100	88.82	9.4	2.735	2.07	7.202	-4.602	-0.368;
200	85.78	9.4	12.48	0.286	52.16	-19.82	-6.625;

 204   85.55   9.4   13.13   0.264   56.46   -20.84   -7.262; trap level;
 234   84.24   9.4   18.73   0.148   100.6   -32.58   -15.56; local maximum rise or fall;

4/3 Power Law. Farfield dispersion based on wastefield width of   18.73 m

conc (kg/kg)	dilutn	width (m)	distnce (m)	time (hrs)	(kg/kg)	(s-1)	(cm/s)	(m0.67/s2)
0.13894	107.3	25.59	100.0	0.189	0.0	0.0	9.4	3.00E-4
0.10084	148.1	37.67	200.0	0.484	0.0	0.0	9.4	3.00E-4
7.49E-2	199.6	51.21	300.0	0.78	0.0	0.0	9.4	3.00E-4
5.82E-2	257.0	66.08	400.0	1.075	0.0	0.0	9.4	3.00E-4
4.69E-2	319.4	82.15	500.0	1.371	0.0	0.0	9.4	3.00E-4
3.88E-2	386.1	99.35	600.0	1.666	0.0	0.0	9.4	3.00E-4
3.28E-2	457.0	117.6	700.0	1.962	0.0	0.0	9.4	3.00E-4
2.82E-2	531.9	136.9	800.0	2.257	0.0	0.0	9.4	3.00E-4
2.46E-2	610.2	157.1	900.0	2.553	0.0	0.0	9.4	3.00E-4
2.17E-2	692.2	178.2	1000.0	2.848	0.0	0.0	9.4	3.00E-4
1.93E-2	777.5	200.1	1100.0	3.144	0.0	0.0	9.4	3.00E-4
1.73E-2	866.1	223.0	1200.0	3.439	0.0	0.0	9.4	3.00E-4
1.56E-2	957.9	246.6	1300.0	3.735	0.0	0.0	9.4	3.00E-4
1.42E-2	1052.6	271.0	1400.0	4.03	0.0	0.0	9.4	3.00E-4
1.30E-2	1150.3	296.1	1500.0	4.326	0.0	0.0	9.4	3.00E-4
1.19E-2	1250.9	322.0	1600.0	4.621	0.0	0.0	9.4	3.00E-4

count: 16

==========

FH
/ UM3.
Case 3; ambient file C:\Plumes\FebHigh.002.db; Diffuser table record 1: ----------

==========

Ambient Table:

Depth m	Amb-cur m/s	Amb-dir deg	Amb-sal psu	Amb-tem C	Amb-pol kg/kg	Decay s-1	Far-spd m/s	Far-dir deg	Disprsn m0.67/s2	Density sigma-T
0.0	0.67	225.0	32.99	-0.53	0.0	0.0	0.67	225.0	0.0003	26.53
10.0	0.693	225.0	33.06	-0.56	0.0	0.0	0.693	225.0	0.0003	26.59
20.0	0.717	225.0	32.99	-0.5	0.0	0.0	0.717	225.0	0.0003	26.53
30.0	0.74	225.0	33.03	-0.47	0.0	0.0	0.74	225.0	0.0003	26.56
40.0	0.7	225.0	33.18	-0.37	0.0	0.0	0.7	225.0	0.0003	26.68
50.0	0.66	225.0	33.12	-0.4	0.0	0.0	0.66	225.0	0.0003	26.63
60.0	0.62	225.0	33.21	-0.28	0.0	0.0	0.62	225.0	0.0003	26.7
70.0	0.62	225.0	33.23	-0.32	0.0	0.0	0.62	225.0	0.0003	26.72
80.0	0.62	225.0	33.24	-0.34	0.0	0.0	0.62	225.0	0.0003	26.73
90.0	0.62	225.0	33.45	-0.18	0.0	0.0	0.62	225.0	0.0003	26.89
100.0	0.62	225.0	33.36	-0.13	0.0	0.0	0.62	225.0	0.0003	26.81

Diffuser table:

P-dia (m)	P-elev (m)	V-angle (deg)	H-angle (deg)	Ports ()	AcuteMZ (m)	ChrncMZ (m)	P-depth (m)	Ttl-flo (m3/s)	Eff-sal (psu)	Temp (C)	Polutnt (kg/kg)
0.42	5.0	0.0	180.0	1.0	100.0	1600.0	89.0	0.3	33.3	30.0	15.0

Simulation:
Froude number: 13.48; effluent density (sigma-T) 20.4760849; effluent velocity   2.165(m/s);

Depth	Amb-cur	P-dia	Polutnt	Dilutn	x-posn	y-posn

```
                                                                SDW
Step      (m)   (cm/s)      (m)  (kg/kg)       ()      (m)      (m)
   0      89.0     62.0     0.42     15.0      1.0      0.0      0.0;
 100     88.98     62.0    1.879      2.07    7.202   -2.297   -0.757;
 200     88.57     62.0    5.586     0.286    52.16   -20.51   -15.93;
 246     87.62     62.0    8.887     0.115    129.7   -59.06   -52.41; trap level;
 256     87.33     62.0    9.822    0.0943    158.1   -75.53   -68.33; acute zone;
 270     87.06     62.0     11.3    0.0715    208.6   -114.8   -106.6; local maximum rise or fall;
4/3 Power Law.  Farfield dispersion based on wastefield width of      11.30 m
    conc  dilutn   width distnce    time
 (kg/kg)            (m)     (m)    (hrs) (kg/kg)   (s-1)  (cm/s)(m0.67/s2)
 7.14E-2   208.8   11.87   200.0  0.0194     0.0     0.0    62.0 3.00E-4
 7.11E-2   209.5   13.21   300.0  0.0642     0.0     0.0    62.0 3.00E-4
 6.90E-2   216.1   14.61   400.0   0.109     0.0     0.0    62.0 3.00E-4
 6.53E-2   228.3   16.05   500.0   0.154     0.0     0.0    62.0 3.00E-4
 6.12E-2   243.9   17.54   600.0   0.199     0.0     0.0    62.0 3.00E-4
 5.70E-2   261.7   19.07   700.0   0.243     0.0     0.0    62.0 3.00E-4
 5.31E-2   280.9   20.64   800.0   0.288     0.0     0.0    62.0 3.00E-4
 4.96E-2   301.3   22.25   900.0   0.333     0.0     0.0    62.0 3.00E-4
 4.63E-2   322.5   23.91  1000.0   0.378     0.0     0.0    62.0 3.00E-4
 4.34E-2   344.5    25.6  1100.0   0.423     0.0     0.0    62.0 3.00E-4
 4.07E-2   367.2   27.33  1200.0   0.467     0.0     0.0    62.0 3.00E-4
 3.83E-2   390.4    29.1  1300.0   0.512     0.0     0.0    62.0 3.00E-4
 3.61E-2   414.2    30.9  1400.0   0.557     0.0     0.0    62.0 3.00E-4
 3.41E-2   438.6   32.74  1500.0   0.602     0.0     0.0    62.0 3.00E-4
 3.23E-2   463.5   34.62  1600.0   0.647     0.0     0.0    62.0 3.00E-4
count: 15
 ;
10:30:24 AM. amb fills: 4
================================================================================================================
SFE10
/ UM3. 12/03/2004 1:53:36 PM
Case 1; ambient file C:\Plumes\FebAvg.002.db; Diffuser table record 1: ---------------------------------
================================================================================================================

Ambient Table:
     Depth   Amb-cur   Amb-dir   Amb-sal   Amb-tem   Amb-pol      Decay   Far-spd   Far-dir   Disprsn   Density
         m       m/s       deg       psu         C     kg/kg       s-1       m/s       deg  m0.67/s2   sigma-T
       0.0     0.123     225.0     32.99     -0.53       0.0       0.0     0.123     225.0    0.0003     26.53
      10.0     0.128     225.0     33.06     -0.56       0.0       0.0     0.128     225.0    0.0003     26.59
      20.0     0.134     225.0     32.99      -0.5       0.0       0.0     0.134     225.0    0.0003     26.53
      30.0     0.139     225.0     33.03     -0.47       0.0       0.0     0.139     225.0    0.0003     26.56
      40.0     0.124     225.0     33.18     -0.37       0.0       0.0     0.124     225.0    0.0003     26.68
      50.0     0.109     225.0     33.12      -0.4       0.0       0.0     0.109     225.0    0.0003     26.63
      60.0     0.094     225.0     33.21     -0.28       0.0       0.0     0.094     225.0    0.0003      26.7
      70.0     0.094     225.0     33.23     -0.32       0.0       0.0     0.094     225.0    0.0003     26.72
      80.0     0.094     225.0     33.24     -0.34       0.0       0.0     0.094     225.0    0.0003     26.73
      90.0     0.094     225.0     33.45     -0.18       0.0       0.0     0.094     225.0    0.0003     26.89
     100.0     0.094     225.0     33.36     -0.13       0.0       0.0     0.094     225.0    0.0003     26.81

Diffuser table:
   P-dia  P-elev V-angle H-angle   Ports AcuteMZ ChrncMZ P-depth Ttl-flo Eff-sal    Temp Polutnt
     (m)     (m)   (deg)   (deg)      ()     (m)     (m)     (m)  (m3/s)   (psu)     (C)   (ppm)
```

```
                                                                SDW
    0.42    10.0     0.0   180.0     1.0   100.0  1600.0    84.0     0.3    33.3    30.0    15.0

Simulation:
Froude number:      13.56; effluent density (sigma-T)  20.4760849; effluent velocity     2.165(m/s);
        Depth  Amb-cur    P-dia  Polutnt   Dilutn   x-posn   y-posn
Step      (m)   (cm/s)      (m)    (ppm)       ()      (m)      (m)
   0      84.0       9.4     0.42     15.0      1.0      0.0      0.0;
 100     83.83       9.4    2.736     2.07    7.202   -4.602   -0.368;
 200     80.92       9.4    12.49    0.286    52.16   -19.98   -6.706;
 203     80.76       9.4    12.98    0.269    55.36   -20.76    -7.19; trap level;
 235     79.41       9.4    19.12    0.143    104.3   -34.34   -16.84; local maximum rise or fall;
4/3 Power Law.  Farfield dispersion based on wastefield width of      19.12 m
    conc  dilutn   width distnce    time
   (ppm)             (m)     (m)    (hrs)   (ppm)   (s-1)  (cm/s)(m0.67/s2)
 0.13501   110.5   25.78   100.0   0.182     0.0     0.0     9.4 3.00E-4
 9.86E-2   151.5   37.89   200.0   0.478     0.0     0.0     9.4 3.00E-4
 7.34E-2   203.8   51.45   300.0   0.773     0.0     0.0     9.4 3.00E-4
 5.71E-2   262.2   66.33   400.0   1.069     0.0     0.0     9.4 3.00E-4
 4.60E-2   325.6   82.43   500.0   1.365     0.0     0.0     9.4 3.00E-4
 3.81E-2   393.5   99.64   600.0    1.66     0.0     0.0     9.4 3.00E-4
 3.22E-2   465.6   117.9   700.0   1.956     0.0     0.0     9.4 3.00E-4
 2.77E-2   541.7   137.2   800.0   2.251     0.0     0.0     9.4 3.00E-4
 2.41E-2   621.4   157.4   900.0   2.547     0.0     0.0     9.4 3.00E-4
 2.13E-2   704.7   178.5  1000.0   2.842     0.0     0.0     9.4 3.00E-4
 1.89E-2   791.4   200.5  1100.0   3.138     0.0     0.0     9.4 3.00E-4
 1.70E-2   881.5   223.4  1200.0   3.433     0.0     0.0     9.4 3.00E-4
 1.53E-2   974.8   247.0  1300.0   3.729     0.0     0.0     9.4 3.00E-4
 1.40E-2  1071.1   271.4  1400.0   4.024     0.0     0.0     9.4 3.00E-4
 1.28E-2  1170.4   296.6  1500.0    4.32     0.0     0.0     9.4 3.00E-4
 1.17E-2  1272.6   322.5  1600.0   4.615     0.0     0.0     9.4 3.00E-4
count: 16
 ;
1:53:40 PM. amb fills: 2
================================================================================================================
SAE10
/ UM3. 12/03/2004 1:56:31 PM
Case 1; ambient file C:\Plumes\AugAvg.002.db; Diffuser table record 1: ---------------------------------
================================================================================================================
Ambient Table:
     Depth   Amb-cur   Amb-dir   Amb-sal   Amb-tem   Amb-pol     Decay   Far-spd   Far-dir   Disprsn   Density
         m       m/s       deg       psu         C     kg/kg       s-1       m/s       deg  m0.67/s2   sigma-T
       0.0     0.107     270.0     31.94     11.99       0.0       0.0     0.107     270.0    0.0003     24.24
      10.0     0.104     270.0     32.05     10.83       0.0       0.0     0.104     270.0    0.0003     24.54
      20.0       0.1     270.0     32.46      6.88       0.0       0.0       0.1     270.0    0.0003     25.46
      30.0     0.097     270.0      32.7      3.49       0.0       0.0     0.097     270.0    0.0003     26.03
      40.0    0.0853     270.0     32.89      0.96       0.0       0.0    0.0853     270.0    0.0003     26.38
      50.0    0.0737     270.0      33.0     -0.16       0.0       0.0    0.0737     270.0    0.0003     26.53
      60.0     0.062     270.0     33.04     -0.39       0.0       0.0     0.062     270.0    0.0003     26.57
      70.0     0.062     270.0     33.11     -0.71       0.0       0.0     0.062     270.0    0.0003     26.64
      80.0     0.062     270.0     33.17     -0.81       0.0       0.0     0.062     270.0    0.0003     26.69
      90.0     0.062     270.0     33.24     -0.62       0.0       0.0     0.062     270.0    0.0003     26.74
     100.0     0.062     270.0      40.0     -0.55       0.0       0.0     0.062     270.0    0.0003      32.2
```

Diffuser table:

P-dia (m)	P-elev (m)	V-angle (deg)	H-angle (deg)	Ports ()	AcuteMZ (m)	ChrncMZ (m)	P-depth (m)	Ttl-flo (m3/s)	Eff-sal (psu)	Temp (C)	Polutnt (ppm)
0.42	10.0	0.0	180.0	1.0	100.0	1600.0	84.0	0.3	33.3	30.0	15.0

Simulation:
Froude number: 13.65; effluent density (sigma-T) 20.4760849; effluent velocity 2.165(m/s);

Step	Depth (m)	Amb-cur (cm/s)	P-dia (m)	Polutnt (ppm)	Dilutn ()	x-posn (m)	y-posn (m)	
0	84.0	6.2	0.42	15.0	1.0	0.0	0.0;	
100	83.79	6.2	2.975	2.07	7.203	-4.739	-0.398;	
200	79.84	6.2	15.85	0.286	52.17	-15.9	-7.547;	
222	78.15	6.2	20.94	0.185	80.65	-18.16	-11.78;	trap level;
260	76.09	6.2	30.26	0.0984	151.6	-22.17	-25.22;	local maximum rise or fall;

4/3 Power Law. Farfield dispersion based on wastefield width of 30.26 m

conc (ppm)	dilutn	width (m)	distnce (m)	time (hrs)	(ppm)	(s-1)	(cm/s)	(m0.67/s2)
8.99E-2	166.0	43.04	100.0	0.298	0.0	0.0	6.2	3.00E-4
6.29E-2	237.4	64.92	200.0	0.746	0.0	0.0	6.2	3.00E-4
4.59E-2	325.5	89.6	300.0	1.194	0.0	0.0	6.2	3.00E-4
3.53E-2	423.7	116.8	400.0	1.642	0.0	0.0	6.2	3.00E-4
2.82E-2	530.6	146.3	500.0	2.09	0.0	0.0	6.2	3.00E-4
2.32E-2	645.1	177.9	600.0	2.538	0.0	0.0	6.2	3.00E-4
1.95E-2	767.1	211.6	700.0	2.986	0.0	0.0	6.2	3.00E-4
1.67E-2	895.9	247.1	800.0	3.434	0.0	0.0	6.2	3.00E-4
1.45E-2	1030.8	284.4	900.0	3.882	0.0	0.0	6.2	3.00E-4
1.27E-2	1172.2	323.5	1000.0	4.33	0.0	0.0	6.2	3.00E-4
1.13E-2	1319.5	364.1	1100.0	4.778	0.0	0.0	6.2	3.00E-4
1.01E-2	1472.5	406.4	1200.0	5.226	0.0	0.0	6.2	3.00E-4
9.19E-3	1631.0	450.1	1300.0	5.674	0.0	0.0	6.2	3.00E-4
8.35E-3	1794.9	495.3	1400.0	6.122	0.0	0.0	6.2	3.00E-4
7.63E-3	1963.9	542.0	1500.0	6.57	0.0	0.0	6.2	3.00E-4
7.01E-3	2137.8	590.0	1600.0	7.018	0.0	0.0	6.2	3.00E-4

count: 16
;
1:56:35 PM. amb fills: 2

==========

SAT10
/ UM3. 12/03/2004 2:15:56 PM
Case 1; ambient file C:\Plumes\AugAvg.002.db; Diffuser table record 1: ----------

==========

Ambient Table:

Depth m	Amb-cur m/s	Amb-dir deg	Amb-sal psu	Amb-tem C	Amb-pol kg/kg	Decay s-1	Far-spd m/s	Far-dir deg	Disprsn m0.67/s2	Density sigma-T
0.0	0.107	270.0	31.94	11.99	0.0	0.0	0.107	270.0	0.0003	24.24
10.0	0.104	270.0	32.05	10.83	0.0	0.0	0.104	270.0	0.0003	24.54
20.0	0.1	270.0	32.46	6.88	0.0	0.0	0.1	270.0	0.0003	25.46
30.0	0.097	270.0	32.7	3.49	0.0	0.0	0.097	270.0	0.0003	26.03
40.0	0.0853	270.0	32.89	0.96	0.0	0.0	0.0853	270.0	0.0003	26.38

							SDW			
50.0	0.0737	270.0	33.0	-0.16	0.0	0.0	0.0737	270.0	0.0003	26.53
60.0	0.062	270.0	33.04	-0.39	0.0	0.0	0.062	270.0	0.0003	26.57
70.0	0.062	270.0	33.11	-0.71	0.0	0.0	0.062	270.0	0.0003	26.64
80.0	0.062	270.0	33.17	-0.81	0.0	0.0	0.062	270.0	0.0003	26.69
90.0	0.062	270.0	33.24	-0.62	0.0	0.0	0.062	270.0	0.0003	26.74
100.0	0.062	270.0	40.0	-0.55	0.0	0.0	0.062	270.0	0.0003	32.2

Diffuser table:

P-dia (m)	P-elev (m)	V-angle (deg)	H-angle (deg)	Ports ()	AcuteMZ (m)	ChrncMZ (m)	P-depth (m)	Ttl-flo (m3/s)	Eff-sal (psu)	Temp (C)	Polutnt (ppm)
0.42	5.0	0.0	180.0	1.0	100.0	1600.0	89.0	0.3	33.15	10.0	15.0

Simulation:

Froude number: 31.18; effluent density (sigma-T) 25.5326347; effluent velocity 2.165(m/s);

Step	Depth (m)	Amb-cur (cm/s)	P-dia (m)	Polutnt (ppm)	Dilutn ()	x-posn (m)	y-posn (m)	
0	89.0	6.2	0.42	15.0	1.0	0.0	0.0;	
100	88.95	6.2	2.988	2.07	7.237	-4.76	-0.4;	
177	88.15	6.2	11.81	0.453	33.06	-13.57	-4.655;	bottom hit;
200	87.51	6.2	16.22	0.29	51.73	-16.41	-8.007;	
223	86.62	6.2	21.49	0.184	81.57	-19.34	-13.5;	trap level;
251	85.72	6.2	29.23	0.105	142.0	-23.77	-27.63;	local maximum rise or fall;

4/3 Power Law. Farfield dispersion based on wastefield width of 29.23 m

conc (ppm)	dilutn	width (m)	distnce (m)	time (hrs)	(ppm)	(s-1)	(cm/s)	(m0.67/s2)
9.68E-2	154.8	41.31	100.0	0.285	0.0	0.0	6.2	3.00E-4
6.72E-2	223.2	62.93	200.0	0.733	0.0	0.0	6.2	3.00E-4
4.87E-2	307.8	87.38	300.0	1.181	0.0	0.0	6.2	3.00E-4
3.73E-2	402.4	114.4	400.0	1.629	0.0	0.0	6.2	3.00E-4
2.97E-2	505.4	143.7	500.0	2.077	0.0	0.0	6.2	3.00E-4
2.44E-2	615.8	175.1	600.0	2.525	0.0	0.0	6.2	3.00E-4
2.04E-2	733.5	208.6	700.0	2.973	0.0	0.0	6.2	3.00E-4
1.75E-2	857.7	244.0	800.0	3.421	0.0	0.0	6.2	3.00E-4
1.51E-2	988.2	281.2	900.0	3.869	0.0	0.0	6.2	3.00E-4
1.33E-2	1124.8	320.0	1000.0	4.317	0.0	0.0	6.2	3.00E-4
1.18E-2	1267.2	360.6	1100.0	4.765	0.0	0.0	6.2	3.00E-4
1.06E-2	1415.1	402.7	1200.0	5.213	0.0	0.0	6.2	3.00E-4
9.56E-3	1568.4	446.3	1300.0	5.661	0.0	0.0	6.2	3.00E-4
8.69E-3	1726.9	491.4	1400.0	6.109	0.0	0.0	6.2	3.00E-4
7.93E-3	1890.3	537.9	1500.0	6.557	0.0	0.0	6.2	3.00E-4
7.29E-3	2058.7	585.8	1600.0	7.005	0.0	0.0	6.2	3.00E-4

count: 16

;

2:15:59 PM. amb fills: 2

==========

SFT10

/ UM3. 12/03/2004 2:18:26 PM

Case 1; ambient file C:\Plumes\FebAvg.002.db; Diffuser table record 1: ----------

==========

Ambient Table:

SDW

Depth	Amb-cur	Amb-dir	Amb-sal	Amb-tem	Amb-pol	Decay	Far-spd	Far-dir	Disprsn	Density
m	m/s	deg	psu	C	kg/kg	s-1	m/s	deg	m0.67/s2	sigma-T
0.0	0.123	225.0	32.99	-0.53	0.0	0.0	0.123	225.0	0.0003	26.53
10.0	0.128	225.0	33.06	-0.56	0.0	0.0	0.128	225.0	0.0003	26.59
20.0	0.134	225.0	32.99	-0.5	0.0	0.0	0.134	225.0	0.0003	26.53
30.0	0.139	225.0	33.03	-0.47	0.0	0.0	0.139	225.0	0.0003	26.56
40.0	0.124	225.0	33.18	-0.37	0.0	0.0	0.124	225.0	0.0003	26.68
50.0	0.109	225.0	33.12	-0.4	0.0	0.0	0.109	225.0	0.0003	26.63
60.0	0.094	225.0	33.21	-0.28	0.0	0.0	0.094	225.0	0.0003	26.7
70.0	0.094	225.0	33.23	-0.32	0.0	0.0	0.094	225.0	0.0003	26.72
80.0	0.094	225.0	33.24	-0.34	0.0	0.0	0.094	225.0	0.0003	26.73
90.0	0.094	225.0	33.45	-0.18	0.0	0.0	0.094	225.0	0.0003	26.89
100.0	0.094	225.0	33.36	-0.13	0.0	0.0	0.094	225.0	0.0003	26.81

Diffuser table:

P-dia	P-elev	V-angle	H-angle	Ports	AcuteMZ	ChrncMZ	P-depth	Ttl-flo	Eff-sal	Temp	Polutnt
(m)	(m)	(deg)	(deg)	()	(m)	(m)	(m)	(m3/s)	(psu)	(C)	(ppm)
0.42	5.0	0.0	180.0	1.0	100.0	1600.0	89.0	0.3	33.3	10.0	15.0

Simulation:

Froude number: 30.89; effluent density (sigma-T) 25.6494597; effluent velocity 2.165(m/s);

Step	Depth (m)	Amb-cur (cm/s)	P-dia (m)	Polutnt (ppm)	Dilutn ()	x-posn (m)	y-posn (m)	
0	89.0	9.4	0.42	15.0	1.0	0.0	0.0;	
100	88.96	9.4	2.746	2.07	7.237	-4.62	-0.369;	
198	87.88	9.4	12.3	0.297	50.39	-21.06	-7.214;	bottom hit;
200	87.83	9.4	12.62	0.286	52.42	-21.7	-7.601;	
202	87.78	9.4	12.94	0.275	54.54	-22.35	-8.008;	trap level;
228	87.28	9.4	17.69	0.164	91.27	-34.26	-16.21;	local maximum rise or fall;

4/3 Power Law. Farfield dispersion based on wastefield width of 17.69 m

conc (ppm)	dilutn	width (m)	distnce (m)	time (hrs)	(ppm)	(s-1)	(cm/s)	(m0.67/s2)
0.1536	97.55	24.24	100.0	0.184	0.0	0.0	9.4	3.00E-4
0.10992	136.3	36.13	200.0	0.479	0.0	0.0	9.4	3.00E-4
8.09E-2	185.3	49.5	300.0	0.775	0.0	0.0	9.4	3.00E-4
6.25E-2	239.9	64.21	400.0	1.07	0.0	0.0	9.4	3.00E-4
5.01E-2	299.3	80.14	500.0	1.366	0.0	0.0	9.4	3.00E-4
4.13E-2	362.9	97.21	600.0	1.661	0.0	0.0	9.4	3.00E-4
3.48E-2	430.6	115.3	700.0	1.957	0.0	0.0	9.4	3.00E-4
2.99E-2	502.0	134.5	800.0	2.252	0.0	0.0	9.4	3.00E-4
2.60E-2	576.9	154.6	900.0	2.548	0.0	0.0	9.4	3.00E-4
2.29E-2	655.2	175.6	1000.0	2.843	0.0	0.0	9.4	3.00E-4
2.04E-2	736.8	197.4	1100.0	3.139	0.0	0.0	9.4	3.00E-4
1.83E-2	821.5	220.2	1200.0	3.434	0.0	0.0	9.4	3.00E-4
1.65E-2	909.3	243.7	1300.0	3.73	0.0	0.0	9.4	3.00E-4
1.50E-2	999.9	268.0	1400.0	4.025	0.0	0.0	9.4	3.00E-4
1.37E-2	1093.4	293.1	1500.0	4.321	0.0	0.0	9.4	3.00E-4
1.26E-2	1189.7	318.9	1600.0	4.616	0.0	0.0		